Methods in Molecular Biology™

VOLUME 106

Receptor Binding Techniques

Edited by

Mary Keen

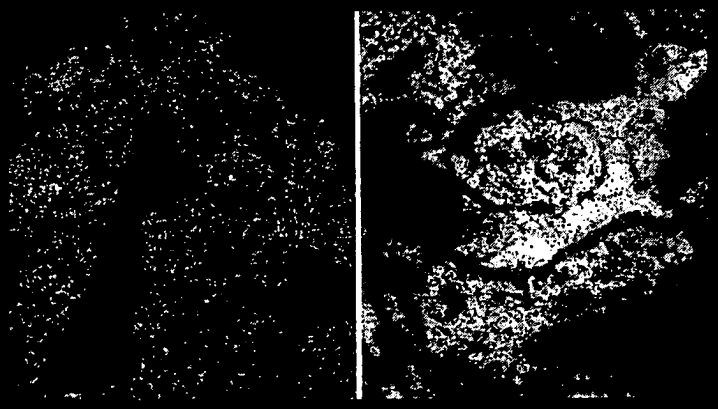

HUMANA PRESS

Receptor Binding Techniques

METHODS IN MOLECULAR BIOLOGY™

John M. Walker, SERIES EDITOR

126. **Developmental Biology Protocols, Vol. II,** edited by *Rocky S. Tuan, 1999*
125. **Developmental Biology Protocols, Vol. I,** edited by *Rocky S. Tuan, 1999*
124. **Protein Kinase Protocols,** edited by *Alastair D. Reith, 1999*
123. **In Situ Hybridization Protocols, 2nd. ed.,** edited by *Ian A. Darby, 1999*
122. **Confocal Microscopy Methods and Protocols,** edited by *Stephen W. Paddock, 1999*
121. **Natural Killer Cell Protocols:** *Cellular and Molecular Methods,* edited by *Kerry S. Campbell and Marco Colonna, 1999*
120. **Eicosanoid Protocols,** edited by *Elias A. Lianos, 1999*
119. **Chromatin Protocols,** edited by *Peter B. Becker, 1999*
118. **RNA–Protein Interaction Protocols,** edited by *Susan R. Haynes, 1999*
117. **Electron Microscopy Methods and Protocols,** edited by *Nasser Hajibagheri, 1999*
116. **Protein Lipidation Protocols,** edited by *Michael H. Gelb, 1999*
115. **Immunocytochemical Methods and Protocols (2nd ed.),** edited by *Lorette C. Javois, 1999*
114. **Calcium Signaling Protocols,** edited by *David Lambert, 1999*
113. **DNA Repair Protocols:** *Eukaryotic Systems,* edited by *Daryl S. Henderson, 1999*
112. **2-D Proteome Analysis Protocols,** edited by *Andrew J. Link 1999*
111. **Plant Cell Culture Protocols,** edited by *Robert Hall, 1999*
110. **Lipoprotein Protocols,** edited by *Jose M. Ordovas, 1998*
109. **Lipase and Phospholipase Protocols,** edited by *Mark H. Doolittle and Karen Reue, 1999*
108. **Free Radical and Antioxidant Protocols,** edited by *Donald Armstrong, 1998*
107. **Cytochrome P450 Protocols,** edited by *Ian R. Phillips and Elizabeth A. Shephard, 1998*
106. **Receptor Binding Techniques,** edited by *Mary Keen, 1999*
105. **Phospholipid Signaling Protocols,** edited by *Ian M. Bird, 1998*
104. **Mycoplasma Protocols,** edited by *Roger J. Miles and Robin A. J. Nicholas, 1998*
103. ***Pichia* Protocols,** edited by *David R. Higgins and James M. Cregg, 1998*
102. **Bioluminescence Methods and Protocols,** edited by *Robert A. LaRossa, 1998*
101. **Mycobacteria Protocols,** edited by *Tanya Parish and Neil G. Stoker, 1998*
100. **Nitric Oxide Protocols,** edited by *Michael A. Titheradge, 1998*
99. **Human Cytokines and Cytokine Receptors,** edited by *Reno Debets, 1998*
98. **Forensic DNA Profiling Protocols,** edited by *Patrick J. Lincoln and James M. Thomson, 1998*
97. **Molecular Embryology:** *Methods and Protocols,* edited by *Paul T. Sharpe, 1998*
96. **Adhesion Proteins Protocols,** edited by *Elisabetta Dejana, 1998*
95. **DNA Topology and DNA Topoisomerases:** *II. Enzymology and Topoisomerase Targetted Drugs,* edited by *Mary-Ann Bjornsti, 1998*
94. **DNA Topology and DNA Topoisomerases:** *I. DNA Topology and Enzyme Purification,* edited by *Mary-Ann Bjornsti, 1998*
93. **Protein Phosphatase Protocols,** edited by *John W. Ludlow, 1997*
92. **PCR in Bioanalysis,** edited by *Stephen Meltzer, 1997*
91. **Flow Cytometry Protocols,** edited by *Mark J. Jaroszeski, 1998*
90. **Drug–DNA Interactions:** *Methods, Case Studies, and Protocols,* edited by *Keith R. Fox, 1997*
89. **Retinoid Protocols,** edited by *Christopher Redfern, 1997*
88. **Protein Targeting Protocols,** edited by *Roger A. Clegg, 1997*
87. **Combinatorial Peptide Library Protocols,** edited by *Shmuel Cabilly, 1998*
86. **RNA Isolation and Characterization Protocols,** edited by *Ralph Rapley, 1997*
85. **Differential Display Methods and Protocols,** edited by *Peng Liang and Arthur B. Pardee, 1997*
84. **Transmembrane Signaling Protocols,** edited by *Dafna Bar-Sagi, 1998*
83. **Receptor Signal Transduction Protocols,** edited by *R. A. J. Challiss, 1997*
82. **Arabadopsis Protocols,** edited by *José M Martinez-Zapater and Julio Salinas, 1997*
81. **Plant Virology Protocols,** edited by *Gary D. Foster, 1997*
80. **Immunochemical Protocols (2nd ed.),** edited by *John Pound, 1997*
79. **Polyamine Protocols,** edited by *David M. L. Morgan,* 1997
78. **Antibacterial Peptide Protocols,** edited by *William M. Shafer,* 1997
77. **Protein Synthesis:** *Methods and Protocols,* edited by *Robin Martin, 1997*
76. **Glycoanalysis Protocols,** edited by *Elizabeth F. Hounsel, 1997*
75. **Basic Cell Culture Protocols,** edited by *Jeffrey W. Pollard and John M. Walker, 1997*
74. **Ribozyme Protocols,** edited by *Philip C. Turner, 1997*
73. **Neuropeptide Protocols,** edited by *G. Brent Irvine and Carvell H. Williams, 1997*
72. **Neurotransmitter Methods,** edited by *Richard C. Rayne, 1997*
71. **PRINS and *In Situ* PCR Protocols,** edited by *John R. Gosden, 1997*
70. **Sequence Data Analysis Guidebook,** edited by *Simon R. Swindell, 1997*
69. **cDNA Library Protocols,** edited by *Ian G. Cowell and Caroline A. Austin, 1997*
68. **Gene Isolation and Mapping Protocols,** edited by *Jacqueline Boultwood, 1997*
67. **PCR Cloning Protocols:** *From Molecular Cloning to Genetic Engineering,* edited by *Bruce A. White, 1996*
66. **Epitope Mapping Protocols,** edited by *Glenn E. Morris, 1996*
65. **PCR Sequencing Protocols,** edited by *Ralph Rapley, 1996*
64. **Protein Sequencing Protocols,** edited by *Bryan J. Smith, 1996*
63. **Recombinant Proteins:** *Detection and Isolation Protocols,*

METHODS IN MOLECULAR BIOLOGY™

Receptor Binding Techniques

Edited by

Mary Keen

The Medical School,
University of Birmingham,
Birmingham, UK

Humana Press  **Totowa, New Jersey**

999 Riverview Drive, Suite 208
Totowa, New Jersey 07512

This publication is printed on acid-free paper. ♾
ANSI Z39.48-1984 (American Standards Institute) Permanence of Paper for Printed Library Materials.

Cover illustration: Fig. 1A, B from Chapter 7, "Autoradiography of Peptide Receptors" by John Wharton and David A. Walsh.

Cover design by Patricia F. Cleary.

For additional copies, pricing for bulk purchases, and/or information about other Humana titles, contact Humana at the above address or at any of the following numbers: Tel: 973-256-1699; Fax: 973-256-8341; E-mail: humana@humanapr.com, or visit our Website at www.humanapress.com

Printed in the United States of America. 10 9 8 7 6 5 4 3 2 1

Preface

Radioligand binding is essentially a very simple technique, applicable to a wide range of preparations. It can of course be used to study many different types of receptors, but can also be adapted to investigate a variety of nonreceptor proteins, such as enzymes and uptake sites. The basic technique allows the affinity of drugs for the receptor of interest to be determined very easily, and the speed and precision of binding have led to its widespread use as a primary screen in drug discovery programs. It also allows receptor number to be measured and the kinetics of the receptor–ligand interaction to be determined, parameters not readily accessible by any other means. Receptor distribution can be studied in great detail using the technique of autoradiography; radioligand binding provides the most sensitive technique for dissecting allosteric interactions between ligands and receptors, and even between receptors and effector molecules, such as G proteins. Moreover, by allowing receptors to be identified in the absence of any measurable response, binding is a prerequisite for receptor solubilization and purification studies. It is even possible to measure ligand receptor interactions in vivo, using positron emission tomography and other powerful techniques.

Receptor Binding Techniques provides detailed experimental protocols for the measurement of binding to various receptor and nonreceptor sites in a range of preparations, including solubilized receptors, membrane preparations, whole cells, autoradiography, and PET and SPECT analysis in living human subjects. It also contains several more general chapters, in which the problems inherent in the binding technique are explicitly discussed, to help the reader avoid common pitfalls in the design of their own experiments.

The authors and I hope that *Receptor Binding Techniques* will prove useful both to researchers new to the field of radioligand binding as well as more experienced workers. The protocols can of course be used as step-by-step "recipes." However, they may also be used as examples of good practice, providing ideas for how the strategies described might be applied to another system. The range of techniques described in the book also serves as an illustration of how the basic binding technique can be adapted and applied in many different situations, and perhaps also as an inspiration for the development of new techniques.

I have enjoyed putting *Receptor Binding Techniques* together and hope that you will enjoy reading it. I am grateful to the series editor, John Walker, for inviting me to edit this volume and for all his help and advice. And I would like to express my sincere thanks to all the authors for their excellent contributions.

***Mary Keen,* PHD**

Contents

Contributors

NICHOLAS M. BARNES • *Department of Pharmacology, The Medical School, University of Birmingham, Birmingham, UK*

CHRISTOPHER P. BERRIE • *Department of Cell Biology and Oncology, Istituto di Ricerche Farmacologiche "Mario Negri Sud," Consorzio Mario Negri Sud, Chieti, Italy*

RACHEL BRUTON • *Department of Medicine, University of Birmingham, Edgbaston, Birmingham, UK*

STEPHANIE FLETCHER • *Department of Pharmacology, The Medical School, University of Birmingham, Edgbaston, Birmingham, UK*

ALAN HUDSON • *Psychopharmacology Unit, School of Medical Sciences, University of Bristol, UK*

EDWARD C. HULME • *Division of Physical Biochemistry, National Institute for Medical Research, London, UK*

MARY KEEN • *Department of Pharmacology, The Medical School, University of Birmingham, Edgbaston, Birmingham, UK*

JENNIFER A. KOENIG • *Department of Pharmacology and Glaxo Institute of Applied Pharmacology, University of Cambridge, Cambridge, UK*

SEBASTIAN LAZARENO • *MRC Collaborative Centre, London, UK*

ANNE LINGFORD-HUGHES • *Department of Psychological Medicine, Institute of Psychiatry, London, UK*

LISA A. LIONE • *Psychopharmacology Unit, School of Medical Sciences, University of Bristol, UK*

ANDREA MALIZIA • *MRC Cyclotron Unit, Hammersmith Hospital, London, UK*

JAQUELINE K. MILLER • *Janssen-Cilag, Sandton, South Africa*

RACHEL M. C. PARKER • *Neurobiology Program, The Garvan Institute of Medical Research, Sydney, Australia*

MICHELLE QUME • *Department of Pharmacology, The Medical School, University of Birmingham, Edgbaston, Birmingham, UK*

DAVID A. WALSH • *Rheumatology Unit, University of Nottingham, City Hospital, Nottingham, UK*

JOHN WHARTON • *Department of Histochemistry, Imperial College of Science and Technology, Hammersmith Hospital, London, UK*

I

INTRODUCTION

NO TEXT

EMPTY PAGE

1

Overview of Ligand-Receptor Binding Techniques

Michelle Qume

1. Introduction

The aim of this chapter is to give a general overview of techniques employed in the process of ligand-receptor binding. The theoretical aspects of the ligand-receptor interactions and mathematical aspects of binding are not detailed here. These are considered in Chapter 9, and there are also very readable chapters in **refs.** *1* and *2*. The techniques referred to use radioligands in the study of the central nervous system, but many are applicable to work outside this field, for example, GABA binding in the periphery *(3)* as well as nonradioligands such as fluorescent and enzyme-linked antibodies.

The first question to be asked is, "What do I want to measure?" This is a function of the following questions. "What receptor?" "Where is the receptor?" "What ligand?" "What sort of results am I interested in?" "Do I have the time for techniques requiring exposure times of weeks, or do I need an answer now?" Other queries regarding the amount of tissue available, and so forth, are all components of the decision of which technique to use.

2. Basic Radioligand Binding Theory

The basic theory behind radioligand binding is that receptor [R] plus ligand [L] bind reversibly to produce a bound receptor-ligand complex [RL] with free ligand remaining. It is this complex that is measured with radioligand binding, whether in simple total and nonspecific analysis or in the more complicated saturation and competition binding assays. There are many papers detailing the mathematical models involved in this and other more complicated processes, but they are beyond this chapter. For further details, the reader is referred to Chapter 9.

From: *Methods in Molecular Biology, Vol. 106: Receptor Binding Techniques*
Edited by: Mary Keen © Humana Press Inc., Totowa, NJ

It is important to consider that radioligand binding measures the amount of the ligand binding to a binding site under the given conditions (i.e., including endogenous ligands, displacing drugs and modulators, etc.). Binding should have the same tissue distribution as the receptor, be linear with respect to protein concentration, be saturable, reversible, reproducible, and stereoselective (*4*), but this does not necessarily imply functionality of these binding sites, and so data (e.g., affinity) obtained with these methods should be correlated with pharmacological or functional studies (*see* Chapter 10).

Specific binding is defined as the mathematical difference between total binding and nonspecific binding (NSB), carried out under the same conditions in the presence of excess, saturating displacing agent, a ligand with binding specificity for the receptor.

3. Basic Radioligand Binding Techniques

Radioligand binding can be considered to fall into two main categories: homogenate/cell binding and autoradiography (or section binding).

3.1. Homogenate/Cell Binding

This technique can be very useful for kinetic analysis, detailed receptor characterization, and as a screening procedure for new ligands. It tends to involve less time than autoradiography, allowing a variety of conditions and samples to be processed. This type of assay may be applied to a wide variety of preparations, from isolated whole cells down to membrane and solubilized preparations.

Following the preparation of the tissue, often involving homogenization, centrifugation (*see* **Subheading 4.1.**), and preincubation to remove endogenous ligands and so forth (*see* **Subheading 5.**), the basic principle involves radioligand incubation performed within tubes (*see* **Subheading 6.6.**). Following termination of the reaction by separation of bound and free radioligand (*see* **Subheading 7.**), the particulate matter containing the bound ligand may be washed, if necessary. If a tritiated ligand is used, the particulate matter may be solubilized overnight, followed by liquid scintillation counting of the sample; iodinated ligands may be counted directly in a gamma counter (*see* **Subheading 8.1.**).

A drawback with this technique is that the only information obtained is the radioactive content of the tissue; so if, for example, a whole brain homogenate were used, no differentiation could be made of separate areas of the brain or heterogeneity in binding within the structure, whereas with autoradiography, binding within the thalamic nuclei, hippocampal areas, and layers of the cerebellum may be determined (e.g., the comparison of $GABA_A$ and $GABA_B$ receptor distribution in **ref. *5***). Obviously, various brain areas may be dissected

out for homogenization, but then the amount of tissue available is an important factor, comparing the size of the cortex with the hypothalamus, for example.

3.2. Autoradiography

Autoradiography is the localization of a radiolabel within a solid specimen, usually a thin section, by placing the specimen against a layer of detector material *(6)*. The radioactive decay occurring within the sample emits radiation particles, causing changes within the detection system that are then amplified to produce a detectable signal. Most autoradiographical experiments use a photographic detection system, and the resultant image relates to the distribution and quantity of the bound radiolabel. According to the techniques involved, autoradiography may produce images detectable at the macroscopic to electron-microscopic levels. Macroscopic detection using premounted emulsion (radiosensitive film) is useful for general mapping of binding sites, whereas microscopic techniques using emulsion-dipped cover slips may be used for the resolution of small brain nuclei or spinal cord laminae. The image produced allows spatial quantification by densitometric analysis (film) or grain counting (cover slips), allowing different areas within the same section to be analyzed.

Another method of producing an image is available, using wet apposition. This technique requires prior histological fixation and defatting of the tissue, and the sections are dipped directly into emulsion. The technique is interesting but time-consuming and rather specialized and will not be discussed. For further information the reader is referred to **ref. *7***.

The sample of interest may be a whole animal or a section of tissue, perhaps from pretreated or previously lesioned animals. Following perfusion fixation, if required, the specimen is frozen and subsequently sectioned and stored on microscope slides (*see* **Subheading 4.2.**). These sections are then subjected to preincubation to remove endogenous ligands, etc. (*see* **Subheading 5.**), followed by incubation with the ligand (*see* **Subheading 6.7.**). The ligand is removed from the section, which is then washed and thoroughly dried (*see* **Subheading 7.2.**), following which the slides are exposed to the detection system (*see* **Subheading 8.2.**).

One of the most important drawbacks involved in this technique is the amount of time involved in careful preparation of the tissue, which is often more involved than binding, from requiring a method of sectioning frozen tissue through to the prolonged exposure times that are required to allow reasonable detection—most techniques involve weeks, but exposure times of months and even years have been reported! Furthermore, quantification of the images produced requires considerable attention and dedicated equipment, usually computer-based and rather expensive (*see* **Subheading 8.2.5.**).

Instead of putting the sections down onto film for exposure, it is possible to assess the total radioactivity content by liquid scintillation or gamma counting, depending on the radioisotope species. Although the only information obtained is the radioactive content, this can be useful in determining if the experiment has worked (i.e., if specific binding is present, which is useful for parameter setting: varying incubation and wash times, and so forth) and in estimating the exposure times required, as low levels of activity will require more prolonged exposure. Apart from this, liquid scintillation counting of autoradiograms seems a long drawn-out process if the only information required is specific binding—in this instance, cell or homogenate binding tends to be a preferable technique.

In vivo autoradiography is a useful technique for the evaluation of drug distribution, uptake, metabolism, receptor occupancy, and binding modulation ***(8)*** in particular tissues and differs somewhat from the standard protocol. The radioligand is administered to the live animal, and following the time period required, the animal is anaesthetized and rapidly frozen, e.g., in hexane cooled to –75°C. Sections are then cut at the appropriate levels of interest. Following freeze-drying of the sections, they are apposed to the detection system, exposed for the relevant time period and then developed. Obviously, when interpreting the results obtained from this technique, care must be taken, as normal physiological and biochemical factors such as metabolism and the presence of endogenous ligands are at play in an *in vivo* situation.

Autoradiography may also be performed on cell cultures grown on cover slips. The labeling technique is essentially the same as conventional autoradiography, although fixing of the cell culture is usually desirable (*see* **ref. *9***).

To reiterate, autoradiography tends to be a more time-consuming process compared with homogenate/cell binding, restricting the number of samples/conditions that can be assayed in a day. However, homogenate/cell binding will not provide data on distribution within the sample. The choice of technique will be determined by the information required by the worker. Homogenate/cell binding may be used as a preliminary indication of receptor populations, followed by more detailed structural analysis with autoradiography.

4. Tissue Preparation

As touched on previously, a wide range of preparations may be used, depending on the technique employed.

Tissues for radioligand binding studies are generally removed from freshly sacrificed animals with exceptions, including *post mortem* human (*see* **Subheading 4.3.** and Chapter 12) and abattoir samples, cell lines, and cell cultures. Anesthesia should generally be avoided if possible (although this is not possible with techniques involving fix perfusion), as this may have an effect on

the receptor of interest. Cervical dislocation or decapitation (with or without prior stunning) are acceptable methods, depending on the species involved and subject to the appropriate regulatory approval.

4.1. Tissue Preparation for Homogenate/Cell Binding

Tissues for this technique tend not to be fixed, as histological preservation is not required. Following preparation of the tissue, samples may be washed to remove endogenous ligands by resuspension and centrifugation; this is especially important for the determination of GABA binding in crude synaptic membranes (*see* Chapter 2).

4.1.1. Isolated Whole Cell Preparations

Primary cell culture, cell lines, and mechanically acutely dissociated cells may be used effectively. Enzymatic dissociation may be used although this may lead to cleavage of receptors *(9)*. Methods of producing these preparations are numerous and depend on the type of cell of interest (*see* Chapter 6).

4.1.2. Membrane Preparations

There are many membrane preparations in use, ranging from crude synaptosome fractions, through washed, lysed, and gradient-centrifuged fractions, to very specific purified membrane preparations. It obviously depends on the location and abundance of the binding site as to which fraction is used. As a general guide, locating binding from crude homogenates through to P_3 pellets is a good beginning; a brief method for production of these fractions is described in Chapter 2.

4.1.3. Soluble Receptors

These may be cytoplasmic soluble receptors or solubilized membrane receptors. For further details on these preparations, the reader is refered to Chapters 4 and 5.

4.2. Tissue Preparation for Autoradiography

Tissues for this may be either fixed with gluteraldehyde and/or formaldehyde or unfixed. Although fixation provides a better histological preservation, many fixing compounds are crosslinking agents and may react with receptors, affecting their binding characteristics.

4.2.1. Tissue Fixation

Tissues may be fixed by whole animal perfusion fixation using 0.05% gluteraldehyde or 0.1% formaldehyde in ice-cold phosphate buffered saline

introduced by cardiac puncture under suitable anesthesia, or else small blocks may be lightly fixed for 10 min in 0.1% formaldehyde/ice-cold phosphate buffered saline.

4.2.2. Tissue Removal

When removing the tissue, especially that requiring the prior removal of bone, e.g., brain and spinal cord, care should be taken not to damage or squash the tissue. Fixed tissues are less delicate than unfixed, but nevertheless both are delicate. Removal of surrounding meninges, blood clots, and any animal fur that may have fallen onto the tissue (damping the fur before dissection may prevent this) is necessary to prevent damage on sectioning. Although autoradiography may be performed on slightly damaged tissues, sections with rips and tears are not aesthetically pleasing—though bear in mind that only one perfect section needs to be published!

4.2.3. Tissue Cooling and Storage

Once the tissue has been removed from the animal and fixed as necessary, it is frozen. From previous experience, brains are normally placed straight into isopentane cooled to approx −55°C with liquid nitrogen for approx 2 min. Other techniques involve cryoprotection with 7% sucrose/0.1*M* phosphate buffer, pH 7.4 ***(10)***, freezing with powdered dry ice and putting the tissue directly into storage at −80°C. Once the tissue has been frozen, the tissue may be sectioned straight away; however storage, for a few weeks (−80°C) is often more convenient.

4.2.4. Tissue Sectioning

Tissues may be surrounded in an embedding medium such as OCT (Tissue Tek, Miles Labs., Elhart, IN) or carboxymethyl cellulose (Sigma-Aldrich, Poole, Dorset, U.K.) prior to sectioning. Using a cryostat, 10–20 μm sections are routinely cut and the sections normally thaw mounted onto clean or even acid-washed glass microscope slides. To increase section adhesion properties, the microscope slides may be gelatin-subbed, poly-l-lysine-coated, Vectabond-treated (Vector Labs., Peterborough, U.K.), or electrostatically charged (Superfrost plus, BDH, Merck Ltd., Lutterworth, Leicestershire, U.K.). Specific methods for slide coatings are detailed in **ref.** ***11*** although pretreated slides are commercially available (e.g., BDH). More than one section may be mounted on each slide, bearing in mind (1) that the whole slide will subsequently be treated at one time and the sections thus subjected to identical conditions, and (2) that different binding conditions should be performed on adjacent tissue sections. Multiple mounting is useful for the preparation of specimen duplicates/triplicates, but not for holding specific and nonspecific

sections together. Sections are allowed to dry at room temperature for about 30 min before being refrozen for subsequent autoradiography, preferably within 1 mo.

4.3. Human Samples

There has been a lot of interest in the use of human tissue, both post mortem and biopsy samples, from control and diseased patients (e.g., Alzheimer's disease, Prion diseases, and AIDS). It is very important when working with human tissues that zealous safety procedures be carried out (e.g., gloves, eye protection, and protective clothing). The use of safety cabinets is especially important when carrying out procedures such as homogenization, which may produce aerosols. Disinfection of all surfaces and equipment is necessary, as is very careful disposal of contaminated waste. These safety procedures should also be used when handling other tissues of hazardous nature.

Studies involving human samples have inherent problems (*see* Chapter 12), often stemming from the heterogeneity of the population (e.g., age, gender, previous drug history, presence of disease, and mode of death) as well as possible *post mortem* influences such as *post mortem* delay and storage techniques, for which some adequate control should be attempted. There may also be difficulties in obtaining samples, including the requirement for ethical approval in studies involving tissue from live patients, as well as the need for collaborating with tissue banks and pathologists for stored and *post mortem* tissue.

5. Preincubation

Many radioligand binding techniques involve a preincubation or washing step. The samples are preincubated in buffer (*see* **Subheading 6.3.** for details on buffer composition) to remove endogenous ligand or previously administered drugs. Sometimes the buffer alone is not sufficient to induce dissociation of the ligand, and other procedures may be incorporated, such as adding guanine nucleotides *(11)*. Buffer used, time, temperature, volume, and number of preincubations are all variables within this step and require careful thought and investigation when setting up new assays or troubleshooting.

Preincubation for homogenate/cell binding normally involves suspending samples in buffer and subsequent centrifugation. Autoradiographical preincubation is carried out with the slides in racks, placed within beakers of buffer.

6. Incubation with Ligand

During this phase, the radioligand is introduced in buffer in the absence or presence of displacing agents, modulators, or other drugs of interest, and binds (ideally) to the receptors, allowing an equilibrium to be reached between bound and free ligand. There are many variables within this incubation.

6.1. Choice of Radioligand

The choice of radioligand used depends on a number of factors; this is not an exhaustive list.

6.1.1. Ligand

The ligand requires a selective recognition of the receptor or subtype to be assayed, although using agents to displace the ligand from other binding sites may be used (*see* Chapter 2). Antagonist use is preferred, as agonist-receptor interactions tend to be influenced more by cations, pH, and the presence of nucleotides ***(4)***. The affinity of the ligand is very important, as dissociation rates have a bearing on the incubation time and the subsequent separation technique employed (*see* **Subheading 7.**). In general, the dissociation of the ligand from the receptor should not be so fast that the ligand-receptor complex dissociates before it can be measured nor too slow, leading to problems in achieving equilibrium ***(4)***.

6.1.2. Radioisotope

The radioisotope will need sufficient specific activity to allow accurate detection of low levels of binding. Tritium is probably the most common isotope used. It may be incorporated into the ligand molecule by either direct synthesis or catalytic tritium exchange with hydrogen. Tritiated ligands behave identically to the unlabeled compound and have long radiochemical half-lives (about 12.5 yr). Iodinated ligands (^{125}I) may also be used; they tend to have a higher specific activity than ^{3}H-ligands. However, as iodine is not normally an endogenous atom within the ligand structure, the ^{125}I is usually a replacement or additional atom, possibly altering the biological activity of the ligand. The radiochemical half-life of iodine is only 60 d, reducing the shelf life of these ligands. Other radioisotopes such as ^{32}P and ^{35}S are occasionally used, but ^{3}H and ^{125}I are by far the most common. Many radioligands are commercially available. **Reference *12*** discusses methods of "in house" radiolabeling.

6.1.3. Radioligand

The radioligand must be soluble and stable within the incubation medium, both enzymatically and chemically; the use of antioxidants or enzyme inhibitors may therefore be required. Purity of the radioligand may need to be determined, especially with custom synthesis ***(13)***. Proper storage of radioligands is crucial; the addition of free radical scavenging solvents or storage at low temperatures may be required. Manufacturers' data sheets detail the storage methods required for commercially available ligands. Safety is a very important

aspect when dealing with radioligands, and extreme care should be taken at all times with their use. This includes proper labeling, protective equipment (gloves, eye protection) and adequate disposal and decontamination techniques. Cost is also a very important factor in determining the choice of radioligand, as is the presence of the equipment necessary to accurately detect the decay.

6.2. Choice of Displacing Agent for Assessment of Nonspecific Binding

Nonspecific binding assessments may include true binding to other components of the tissue (e.g., enzymes and uptake sites), binding to nonbiological materials (e.g., filters, test tubes), and also free ligand that has not washed away *(13)*. The chosen displacer should bind with high specificity to the receptor, but it is preferable that it not be the same compound as the radioligand. The displacing agent is ideally used in concentrations of 100 X its K_D, or 100 X the highest concentration of radioligand used, whichever is the greater *(4)*.

6.3. Choice of Buffer

HEPES (10–20 m*M*), Tris-HCl (10–170 m*M*) or phosphate buffers (30 m*M*) tend to be used for radioligand binding *(11)*, depending on the receptor type. The ionic strength of the buffer can be important with respect to the receptor-ligand interaction *(14)*.

Ion composition is also important; for example, Na^+ ions will inhibit agonist and promote antagonist binding to opioid receptors *(15)*, Mg^{2+} ions may be added to buffers to promote agonist binding to G-protein coupled receptors, and $GABA_B$ binding is dependent on Ca^{2+} (*see* Chapter 2). However, buffers containing heavy metal ions may lead to reactions with sulphydryl groups in the receptor, reducing binding activity.

The pH of the buffer is important, as changes in pH may have effects on the ionization of groups within the receptor or on the ligand, affecting receptor ligand interactions, influencing both the equilibrium binding constant and the kinetic rate constants.

The presence of enzyme inhibitors (e.g., trypsin and acetylcholinesterase inhibitors) in a buffer may be useful in reducing degradation of receptors or ligands; these inhibitors may also be added to the preincubation buffer. Care is needed with the use of these compounds, as there is evidence that they may also inhibit specific ligand binding. Chelating agents such as EDTA and EGTA may also be added to buffers to inhibit the action of metalloproteases and calcium-activated proteases, although caution should be exercised, as these may alter ligand interactions (e.g., the Ca^{2+} dependence of GABA binding to

$GABA_B$ sites), often by removing regulatory metal cations. See **refs.** *11* and *14* for further details on the use of proteolysis inhibitors.

To reduce the presence of endogenous ligand, enzymes such as adenosine deaminase may be included in the buffer, although care should be taken to ensure that the radioligand used is not subject to metabolism by the enzyme.

6.4. Assay Temperature

It is possible to reduce the degradation of ligand and/or receptor by performing the assay at a low incubation temperature (e.g., 4°C), even though this may increase the incubation time required for binding equilibrium to occur.

6.5. Incubation Time

Equilibrium binding may be used to determine ligand affinity and total receptor number, as well as to allow investigation of receptor homogeneity and allosteric regulation of ligand binding *(4)*. At equilibrium, the rates of formation and dissociation of the ligand-receptor complex are equal, leading to a constant concentration of the ligand-receptor complex. Association experiments wherein the specific binding of radioligand to receptor is assessed at time points after addition of the radiolabel may be used to determine equilibrium binding time. It is important to also consider that the lower the radioligand concentrations, the longer it will take to achieve equilibrium; this may lead to internalization of ligand and/or receptors in whole cell preparations *(4)* or receptor degradation.

6.6. Homogenate Binding Incubation

The pellet produced following the final centrifugation step needs to be resuspended in buffer to give an appropriate protein concentration for the assay, allowing sufficient volume for the number of tubes required and an excess to be retained for subsequent protein determination. Protein concentration may be determined using the methods of Lowry *(16)* or Bradford *(17)*, both of which are available as ready-made kits [BDH, Merck Ltd.) and Pierce and Warriner (U.K.) Ltd. (Chester, U.K.)]. It is wise to retain some binding buffer for inclusion as a blank in the protein assay, as some buffers (e.g., Tris) may cause interference.

The suspension is then added to a series of tubes setup containing the radioligand incubation medium with the various inclusions necessary for nonspecific determination and any other compounds necessary for the assay: displacing agents, and so forth. It is useful for these prepared tubes to be at the temperature required for the assay. When determining the various components and volumes to be added to the tubes, it is preferable to ensure that most of the volume (approx 750 µL in a 1000 µL assay) is made up from the protein sus-

pension; this allows an adequate mixing of the various components on adding this large volume. Assays carried out in uncapped tubes for later filtration are not easily vortexed; often one has to use only a strong rocking motion. Assays carried out in capped tubes (e.g., Eppendorf tubes for centrifugation assays) do not have such a problem. For ease of use, reproducibility, and speed, I also try to ensure that the volumes of components added are dispensable using a repeater pipet (e.g., Eppendorf multipipet 4780), especially for the addition of the protein suspension. It is important that the tubes are set-up and ready to use as soon as the pellet is resuspended or the membrane preparation thawed, as leaving the suspension lying on the bench may lead to degradation of the receptor or production of endogenous ligand (e.g., GABA) and possible association of this ligand with the receptor.

If the assay is performed in microcentrifuge tubes, they should be of good quality, so that the lids do not become loose. This leads to spillages and possible contamination. A more detailed discussion on microcentrifuge tubes is given in Chapter 2.

6.7. Incubation Prior to Autoradiography

When varying the incubation medium, for the determination of nonspecific binding or the effect of compounds on binding, adjacent sections should be used for each of the conditions, hence ensuring that variability within the tissue because of different structures, and the like, is minimized between conditions. Racks of slides may be immersed in incubation medium as with the preincubation and washing stages. However, this is often a very expensive method. It is cheaper to use either Coplin jars or plastic slide boxes that allow the slide to be placed on end (section end down), and only use sufficient incubation medium to cover the section. With forward planning and thought, the sections could be mounted on the slides as close to the bottom as possible, allowing for rack placement, thus requiring the minimum amount of incubation medium. With both of these immersion methods, it may be possible, if one is very careful, to reuse the incubation medium for another batch of slides, assuming that the amount of medium and ligand lost from the total is negligible; estimation of the radioactive content of the incubation medium between batches is necessary.

Instead of immersion of the slide in the incubation medium, it is possible to cover only the section. After preincubation, excess buffer is removed from the slide with tissue, the slides placed horizontal, and the incubation medium very carefully pipeted over the section; 100 µL is more than sufficient for a whole rat brain section. It is very important to make sure that the slides are completely horizontal, as the buffer pool may otherwise move, causing the section to be incompletely covered. The area designated for autoradiography should therefore be checked to ensure that fluid does not slide. Using a glass sheet or

perspex box may be helpful, as these may be slightly elevated at one side using pipet tips. This procedure tends to use even less medium and therefore radioligand, minimizing expense; however, the major drawback with this is that each slide is treated individually, minimizing the number of samples that can be processed. The samples need to be staggered, as it takes time to apply the medium. After the appropriate time has elapsed, the medium is aspirated off, again treating the samples separately. With assays involving a short incubation time, this can create problems—it is very easy to pipet the medium onto the section every 30 s, but if the incubation time is 20 min, only 40 sections can be incubated before the first section has completed its incubation and requires aspiration. Pipeting, aspirating, and washing sections every 30 s requires a skilled person! Obviously, in this example, for the less experienced, batches of only 40 sections can be used, or again with forethought and planning, perhaps three sections can be mounted on each slide—staggering the incubation at 1-min intervals per slide, dealing with pipeting 300 µL over the slide, and subsequent aspiration and washing is not as hectic with this routine. For techniques requiring a longer incubation time, these logistical problems are reduced, but evaporation of the medium may occur; this may be minimized if the incubating slides are kept in a lidded chamber kept humid by the inclusion of a tissue soaked in buffer.

"Blank controls" should be included to detect background radiation and any chemography, a sensitization response in the emulsion crystals not produced by radiation *(6)*. For these, the sections are treated exactly the same as the assay sections except that they are not exposed to the radiolabeled ligand.

6.8. Estimation of Radioactive Content of Incubation Medium

With all of these techniques, it is important to estimate the actual amount of radioligand present. Following good laboratory practice, this estimation would occur as soon as the medium is made; however, with very routine assays, and because of the constraints on time and equipment, aliquots of the incubation medium, the same volume as that in the binding or drop autoradiography assays, or a known amount for the immersion autoradiography are reserved for later counting. When incubation media are being reused for the immersion autoradiographical method, aliquots should be taken and radioactive content estimated at the beginning and end of each incubation.

7. Separation of Bound from Free Ligand

Following incubation of the sample with the radioligand, the bound ligand needs to be separated from the free, and the bound complex washed to reduce any residual free ligand remaining. This is a very important step, as overzealous separation may lead to dissociation of the bound ligand, resulting in an

underestimate of receptors. Conversely, lack of adequate washing may lead to an overestimate. The rate of dissociation of the ligand-receptor complex is the major factor when choosing a separation technique. Rapidly dissociating complexes will require a separation technique that minimizes the amount of dissociation. In theory, allowable separation times, including the washing step, may be calculated using the radioligand dissociation constant, K_D. This technique is discussed in **ref. *13***.

Particulate receptor binding assays are directly suitable for separation by centrifugation and filtration. For solubilized receptor preparations, separation may be by dialysis, gel filtration (*see* Chapter 5) or by adsorption/precipitation followed by centrifugation. They may also be filtered through polyethylenimine-coated filters (*see* Chapter 4) or through untreated filters following precipitation with polyethylene glycol ***(18)***. The main separation techniques are outlined below.

7.1. Separation of Bound from Free Ligand in Homogenate/Cell Binding

7.1.1. Filtration

Vacuum filtration is a very widely used method of separating bound from free ligand. The particulate matter containing the bound ligand remains on the filter (by adhesion properties rather than by sieving), which can then be briefly washed and the radioactivity present determined following overnight incubation in an emulsifying liquid scintillant (e.g., Optiphase safe, LKB, Leicestershire, U.K.) to extract radioactivity from the filter. It is possible to filter samples "by hand" using, for example, the Millipore 1225 sampling manifold, treating each individual sample separately; this is very useful for kinetic experiments. Alternatively, there are many commercially available filtration systems that will efficiently filter and wash many samples at the same time, reducing variability (e.g., the Brandel or Skatron Cell Harvesters).

The wash buffer used should be ice-cold to reduce dissociation and is ideally the same as that used in the assay, maintaining ionic strength and species. However, as large volumes of wash buffer are required, it may be possible to use a cheaper saline substitute or even tap water. Using both the individual method and some of the automated systems, it is possible to choose whether to or not dilute the sample before filtration and also to vary the volume and number of washes of the filters. Increasing the volume of wash and/or the number of washes decreases nonspecific binding, but may also lead to dissociation of the bound ligand.

This technique only works efficiently for those ligands with a dissociation binding constant (K_D) of 10^{-8} *M* or less, as excessive dissociation of bound

ligand is likely to occur during the washing step with lower affinity ligands *(13)*. Another disadvantage of this technique is the nonspecific binding of the ligand to the filters; this may not be a problem with high levels of binding, but can lead to difficulties in samples with low receptor binding. The testing of various filters with the possible use of antiadsorbants such as pretreatment with 0.05–0.5% polyethyleneimine may reduce this to an acceptable level. The protein binding capacity of filters is limited, and increasing the tissue in the preparation may lead to nonlinear increases in binding, inefficient washing, and possible clogging and overflow of the filtration systems.

7.1.2. Centrifugation

A common alternative method is centrifugation, in which the bound ligand remains with the particulate matter in the resultant pellet. If the binding is performed in 1.5 mL microcentrifuge tubes, a bench-top centrifuge can be used (11,000–15,000*g* for approx 5 min); these have the advantage of having faster run up and down speeds compared to the larger centrifuges, as well as being able to centrifuge many samples at once. The ability to centrifuge at 4°C can be useful in some experiments; microcentifuges that are not temperature-controlled may be used in a cold room. The free ligand contained in the supernatant may then be tipped out or aspirated off with a vacuum/water pump attached to a Pasteur pipet. The interface between the pellet and the supernatant must then be surface-washed; this is accomplished by rapidly but carefully either dipping the whole tube into ice-cold distilled water or buffer, or else by adding about 1 mL of the same fluid followed by quickly aspirating. The wash buffer should be in contact with the pellet for as little time as possible, but the procedure carried out gently enough to prevent disturbing the pellet. Any remaining fluid may be blotted from the surface of the pellet with paper tissue.

This method is very useful for low-affinity ligands or where nonspecific binding to filters is too high for filtration. Unfortunately, each sample has to be manually handled, which substantially cuts down the number of samples in a batch—although batches may be staggered. Due to the inefficient washing technique available, nonspecific binding does tend to be higher; further washing of the pellet, including repetition of the centrifugation, lowers this, but defeats the object of centrifuging as a method of separation when the dissociation rate is rapid. Use of an appropriate buffer is important: pellets become "fluffy" and difficult to work with in phosphate buffers. If very small amounts of tissue are used, a problem can occur, as washing and aspiration may disturb the pellet; the use of tubes with conical bottoms will help with this problem.

7.1.3. Dialysis

This technique is useful for ligands with rapid dissociation rates and may be used for soluble receptor preparations, especially plasma proteins. The receptor and buffer are separated by a semipermeable membrane in small dialysis cells, allowing equilibration of radioligands of a small molecular weight. From the quantification of the free ligand in the buffer area and the free and bound ligand in the receptor area, an estimate of the bound ligand may be made. This technique has disadvantages in that as a result of the low affinities of the ligands used for this technique, large amounts of protein are required to produce an adequate signal. This method is not the most accurate one, as specific binding tends to be less than 10% of total radioligand concentration, allowing only about a 20% increase in the radioactive content of the receptor area as compared with the buffer area *(13)*. Nonspecific binding of the ligand to the dialysis membrane is also a factor in this method. This technique of separation is very much slower than the other methods, impeding the number of samples that may be processed.

7.1.4. Gel Filtration

This is a method suited to solubilized receptors. Filtration may be carried out by passing the receptor preparation through a column whereby bound ligand is separated from free and subsequently quantified (nonequilibrium). It is also possible to carry out equilibrium gel-filtration, in which the receptor preparation is loaded onto a column equlibrated with radioligand and eluted with a buffer containing radioligand. In both techniques, fractions are collected and the radioactive content analyzed. This is a farily time-consuming process, requiring preparation and subsequent regeneration of elution columns. Detailed protocols can be found in Chapter 5 and **ref. *19***.

7.1.5. Precipitation

Solubilized receptors may be precipitated by the addition of compounds such as polyethylene glycol or ammonium sulphate. This is followed by centrifugation or filtration to separate the precipitated complex. This technique requires that both the precipitation and isolation of the precipitated complex is rapid enough to minimize dissociation of the ligand.

7.1.6. Adsorption

This is a technique widely used in radioimmunoassay, adapted to allow the quantification of bound ligand in soluble receptor studies. The free ligand is selectively adsorbed to an inert medium such as talc or activated charcoal,

which is then isolated by centrifugation and the bound ligand in the supernatant analyzed. It is possible to coat the adsorbant with dextran or albumin to increase its selectivity for the small, free ligand molecules. As with all of the previous methods, the separation time must be as rapid as possible to prevent excessive dissociation of the ligand-receptor complex.

7.2. Separation of Bound from Free Ligand in Autoradiography

For separation of the free ligand in autoradiography, the choices are simple: If the drop method is employed, the buffer surrounding the section is aspirated off. Vacuum or water pumps connected to a glass Pasteur pipet are much more efficient for the aspiration than is a pipet on its own. If the tank method is used, the incubation medium is removed by putting the sections into fresh buffer. Following removal of the excess radioligand incubation buffer, one to three washes may be carried out by placing the slides in fresh buffer. Wash times should be optimized to maximize the specific-to-nonspecific binding ratio. The sections are then dipped in distilled water to remove salts, aspirated, and left to dry, often overnight. The use of low-temperature washes and/or rapidly drying the sections under a stream of cold air, e.g., a hair dryer, may minimize diffusion of the ligand. Note that if the sections are to be scintillation-counted, they do not necessarily need to be dried (*see* **Subheading 8.2.**).

8. Development and Quantification of Binding

Following separation of the bound from the free ligand, some form of quantification of the radioactive content of the sample must be determined. Homogenate cell binding samples need to be counted, whereas dried sections for autoradiographical analysis need to be applied to film or cover slips and subsequently developed.

With dialysis, gel filtration, and absorption, a fluid phase is used for analysis; these may be counted directly, with the use of scintillant as necessary. Following filtration or centrifugation, further processing may be required prior to radiometric determination.

8.1. Preparation of Filters and Pelleted Tissue for Radioactive Counting

In scintillation counting, the energy from β-particles emitted from tritiated compounds is converted into photons by the scintillator. The photons may then be detected by the scintillation counter. Liquid scintillation cocktails are most commonly used, although solid-phase scintillation is available and may be useful for estimating the radioactive content of filters. Gamma emitters such as ^{125}I allow direct determination of the radioactive content of the filter or pellet without the need for scintillator or solubilization.

8.1.1. Filters

Following careful removal from the filtration system, filters may be air-dried for approx 1/2 h before being placed in vials. Single circular filters may be placed directly into the vials and left to dry; 5 mL scintillation vials are routinely used as they only require approx 3 mL scintillation fluid compared to the 10 mL of scintillant needed for 20 mL vials. The scintillation cocktail (e.g., Optiphase safe, LKB) is added to the vial, vortexed, and the samples left overnight to allow extraction of the radioactivity by the scintillant. Radioactive counting is then carried out.

8.1.2. Pelleted Tissues

When tritiated ligands are used, the scintillation cocktail must have access to the bound ligand in order for radioactive to be determined—hence the pellet requires solubilization. Following the washing procedure, a solubilizer [e.g., 400 µL Soluene-350 (Canberra Packard, Pangbourne, Hertfordshire, U.K.)] is added, vortexed, and the samples left overnight. If necessary, this may be hastened by warming. To neutralize the Soluene, 400 µL of 0.2*M* HCl is added. Following vortexing, the cap is cut off the tube and the tube and contents inverted into a 20 mL scintillation vial. Scintillation cocktail (10 mL) is added, the sample revortexed, and the tritium content estimated. Alternatively, an aliquot of the digested material may be removed and placed into a scintillation vial; in this case, 5 mL tubes may be used, with the subsequent reduction in scintillation fluid used.

8.2. Autoradiographical Development and Quantification

8.2.1. Apposition and Exposure of Sections

Autoradiograms are generated by exposing the *thoroughly* dry labeled sections to photographic emulsion, on coated film or cover slips. **Reference *6*** covers the theory behind emulsions and explains the factors governing the choice of film and emulsion, including radioisotope used, sensitivity required, and presence of an antiscratch layer.

If the sections are going to be used for radiometric counting instead of production of autoradiograms, sections may be wiped or scraped off the slides before they are dry and placed into a scintillation vial and counted with scintillator, as necessary. An alternative is to wait until the sections are dry and cut the glass slide with a diamond pen, placing the glass and section within a scintillation vial followed by counting.

When apposing sections for macroscopic autoradiography, lightproof cassettes are used, which give an even pressure over the film and are designed to hold the film and slide securely. Once the sections are dry, the slides are

mounted onto a card with double-sided tape; excess slide around the sections may be cut away with a diamond pen to maximize the number of sections apposed. The card is labeled to identify the slides, then carefully placed into the cassette, ensuring that movement of the slides within the cassette is negligible. Radiolabeled standards (*see* **Subheading 8.2.2.**) are also placed or glued onto mounted slides, thus keeping the standards at the same level as the sections. In a dark room under safelight conditions, the film is placed carefully onto the sections, with the emulsion-coated side facing the sections. The cassette is then closed, labeled adequately and placed in a cool dry place, sometimes even at –70°C. The cassette may be stored within a plastic bag containing silica gel, which should be checked periodically, if the exposure time is prolonged. Care must be taken not to scratch the film; it should be handled only at the edges and it should be stored away from high-energy emitting sources. Further instructions, such as which side of the film is emulsion-coated on single-sided films, storage conditions, etc., are supplied with the film.

Glass cover slips for microscopic autoradiography need to be coated with nuclear emulsions before application to tissue sections. They may be prepared and used right away or else stored at 4°C for several weeks, although they must be brought up to dark room temperature before use. Under safelight conditions, the cover slips are glued squarely onto the top of the slides, using a drop of strong adhesive at the top end of the slide. Once dry, the assemblies are clamped together, either singly or separated by paper "spacers." These are then placed in a labeled, lightproof box with silica gel and stored at 4°C until development. Standards, both brain paste and polymers, may be attached to slides and similarly applied to cover slips.

8.2.2. Standards

Standards are used to enable quantification of the autoradiogram on analysis. Two types are commonly used, tissue paste and plastic-impregnated standards. Brain paste standards are generally prepared by the investigator, by mixing varying amounts of radioisotope with brain paste, which is then placed in a mold and sectioned in a cryostat. Plastic-impregnated standards are available for ^{125}I, ^{14}C, and ^{3}H from Amersham (Little Chalfont, Buckinghamshire, U.K.). Both types of standards have their drawbacks, but the plastic form seems more robust and uniform. For further details on standards, the reader is referred to **ref. *20*** and the literature supplied by the manufacturers.

Autoradiographical data is often normalized to allow expression of radioactivity per unit weight, correlating with that obtained from homogenate binding experiments. However, this simply assumes that all regions within a tissue have the same protein content, which in brain, for example, is not the case. Care should therefore be taken in interpreting data as allowances will not be made

for changes in protein within tissues because of different regions, the effect of experimental procedures, or developmental ages. Some workers therefore prefer autoradiographical data to be expressed as radioactivity per unit area unless true protein concentrations are known *(20)*.

8.2.3. Development and Fixation of Autoradiograms

Following application of the section to the emulsion, the latent image contained within it is made visible. For development and further processing, such as histology, when using cover-slipped sections, the cover slip and slide are held apart with spacers, allowing the section and autoradiograph image to be reunited following developing and staining. Following development, the film/cover slips are rinsed in a stop bath (commonly distilled water, although 0.2% acetic acid in water may be used for films). Fixation solubilizes remaining silver bromide crystals, leaving behind the metallic silver. The manufacturers of films and emulsions supply detailed instructions on developing their product, which may or may not be suitable for processing in an automatic processor. Care should be taken to ensure the emulsion is uppermost if the film does not have an antiscratch layer. Chapter 12 details a method of developing and fixing autoradiographic films.

8.2.4. Histological Staining of Sections

Histological staining allows the identification of tissue structures within the section. There are many staining procedures available, depending on the structures to be visualized. The sections remaining from macroscopic autoradiography readily lend themselves to further processing. However, when staining sections from cover-slip-generated autoradiograms, allowance must be made for the emulsion layer on the coverslip, with great care taken not to disrupt this. To prevent a clearing agent such as xylene from dissolving the strong adhesive joining the slide and cover-slip, the sections are best stained on end, with the glued edge uppermost. **References *6*** and ***7*** provide suitable staining protocols. Following staining, the spacer is removed and the slide and coverslip may then be "glued" together with a mounting agent such as DPX.

8.2.5. Quantification of Autoradiograms

Manual visual graticule grain counting of the autoradiograms is the simplest and cheapest method available and requires little specialized equipment. However, this is extremely time-consuming and tedious! Films are often analyzed by densitometry, ultimately expressing the film optical density as tissue radioactivity by reference to known standards. Cover slips are analyzed by grain counting, expressing data as number of silver grains per unit area, or by reference to standards as tissue radioactivity.

Many user-friendly computerized digital image analysis systems are available (e.g., Microcomputer Imaging Device, MCID, Imaging Research, Ont., Canada) to analyze both films and cover slips. These systems often allow the data to be exported and therefore available for further manipulation on spreadsheet and statistical packages. The images may also be digitized with or without color enhancement, allowing easy production of figures.

Both grain counting and densitometric analysis have inherent difficulties, including image resolution, tissue quenching, and efficiency. For more detailed reviews see **refs. *6*, *7*,** and ***20***.

Systems are currently evolving that allow imaging of radioisotopes without the need for photographic emulsions (e.g., Micro and Beta Imagers, Biospace Mesures, Paris, France). Such systems promise shorter exposure times (hours rather than days), increased sensitivity for ^3H compared to film, increased spatial resolution, real-time accumulation of data, and double-labeling detection. The major drawback with this seems to be the low number of samples that can be measured at one time.

9. Mathematical Analysis of Binding

Radioligand binding data is usually reported as specific binding (total minus nonspecific binding, NSB). Homogenate binding may be expressed as radioactivity bound per unit weight, e.g., fmol/mg protein, whereas autoradiographical data may be radioactivity bound per unit weight or area (*see* **Subheading 8.2.2.**). Analysis of radioligand binding data is covered in Chapter 9 of this volume and in **refs. *4*** and ***14***.

Acknowledgments

The author gratefully acknowledges Profs. N. G. Bowery and D. M. Bowen in whose departments the techniques were developed.

References

1. Hulme, E. C. (ed.) (1992) *Receptor-Ligand Interactions*, Oxford University Press, New York.
2. Wharton, J. and Polak, J. M. (eds.) (1993) *Receptor Autoradiography Principles and Practice*, Oxford University Press, New York.
3. Erdo, S. L. and Bowery, N. G. (eds.) (1986) *GABAergic Mechanisms in the Mammalian Periphery*, Raven, New York.
4. Keen, M. and MacDermot, J. (1993) Analysis of receptors by radioligand binding, in *Receptor Autoradiography, Principles and Practice* (Wharton, J. and Polak, J. M., eds.), Oxford University Press, New York, pp. 23–55.
5. Bowery, N. G., Hudson, A. L., and Price, G. W. (1987) $GABA_A$ and $GABA_B$ receptor site distribution in the rat central nervous system. *Neuroscience* **20,** 365–383.

6. Baker, J. R. J. (1989) *Autoradiography: A Comprehensive Overview*, Oxford University Press, New York.
7. Hudson, A. L. (1993) Autoradiographic techniques, in *Receptor Autoradiography, Principles and Practice* (Wharton, J. and Polak, J. M., eds.), Oxford University Press, New York, pp. 57–77.
8. Seeger, T. F. and Pert, A. (1985) Arcuate nucleus stimulation: induction of naloxone reversible analgesia with concomitant localization of opiate release using *in vivo* autoradiography. *Soc. Neurosci. Abs.* **15,** 1068.
9. Hulme, E. C. and Buckley, N. J. (1992) Receptor preparations for binding studies, in *Receptor-Ligand Interactions* (Hulme, E. C., ed.), Oxford University Press, New York, pp. 177–212.
10. Turner, A. J. and Bachelard, H. S. (eds.) (1987) *Neurochemistry: A Practical Approach*, IRL, Washington and Oxford, U.K.
11. Wharton, J., Walsh, D. A., Rutherford, A. D., Knock, G. A., and Polak, J. M. (1993) *In vitro* autoradiographic localization and characterization of binding sites, in *Receptor Autoradiography, Principles and Practice* (Wharton, J. and Polak, J. M., eds.), Oxford University Press, New York, pp. 79–102.
12. McFarthing, K. (1992) Selection and synthesis of receptor-specific radioligands, in *Receptor-Ligand Interactions* (Hulme, E. C., ed.), Oxford University Press, New York, pp. 1–18.
13. Bennett, J. P. Jr. and Yamamura, H. I. (1985) Neurotransmitter, hormone, or drug receptor binding methods, in *Neurotransmitter Receptor Binding* (Yamamura, H. I., Enna, S. J. and Kuhar, M. J., eds.), Raven, New Jersey, pp. 61–89.
14. Hulme, E. C. and Birdsall, N. J. M. (1992) Strategy and tactics in receptor-binding studies, in *Receptor-Ligand Interactions* (Hulme, E. C., ed.), Oxford University Press, New York, pp. 63–176.
15. Slater, P. and Cross, A. J. (1991) Receptors for opiod peptides in brain, in *Neuropeptide Technology: Gene Expression and Neuropeptide Receptors. Methods in Neurosciences*, vol. 5 (Conn, P. M., ed.), Academic, San Diego, CA, pp. 459–478.
16. Lowry, O. H. (1951) Protein measurement with Folin's phenol reagent. *J. Biol. Chem.* **193,** 265–273.
17. Bradford, M. M. (1976) A rapid and sensitive method for the quantification of microgram quantities of protein utilising the principle of protein-dye binding. *Anal. Biochem.* **72,** 248–254.
18. Wang, J.-X., Yamamura, H. I., Wang, W., and Roeske, W. R. (1992) The use of the filtration technique in *in vitro* radioligand binding assays for membrane-bound and solubilized receptors, in *Receptor-Ligand Interactions* (Hulme, E. C., ed.), Oxford University Press, New York, pp. 213–234.
19. Hulme, E. C. (1992) Gel-filtration assays for solubilized receptors, in *Receptor-Ligand Interactions* (Hulme, E. C. ed.), Oxford University Press, New York, pp. 255–263.
20. Baskin, D. G. (1993) Quantitative analysis of radioligand binding autoradiographs, in *Receptor Autoradiography, Principles and Practice* (Wharton, J. and Polak, J. M., eds.), Oxford University Press, New York, pp. 107–133.

NO TEXT

EMPTY PAGE

II

Radioligand Binding in Different Preparations

2

[^{3}H]-GABA Binding to $GABA_A$ and $GABA_B$ Sites on Rat Brain Crude Synaptic Membranes

Rachel Bruton and Michelle Qume

1. Introduction

GABA (γ-aminobutyric acid) is the main inhibitory neurotransmitter in the central nervous system and acts on three pharmacologically distinct receptors: $GABA_A$, $GABA_B$, and $GABA_C$. $GABA_A$ receptors are pharmacologically defined on the basis of antagonism by bicuculline and insensitivity to the GABA-analog baclofen, whereas $GABA_B$ receptors are stimulated by baclofen and are insensitive to bicuculline; $GABA_C$ receptors are insensitive to both *(1)*.

$GABA_A$ is the most prevalent of the receptors in the mammalian central nervous system (CNS). It is a ligand-gated ion channel that can be allosterically modulated by both benzodiazepines and barbiturates. The transmembrane ion channel is opened by the binding of two agonist molecules, which allows an influx of chloride ions. This results in a decrease of the depolarizing effects of an excitatory input, thereby depressing excitability *(2)*. $GABA_B$ is a metabotropic receptor, belonging to the family of guanine nucleotide binding protein (G protein) coupled receptors that are coupled to the activation of second messenger pathways. The inhibitory action of $GABA_B$ receptor activation is mediated by an increase in potassium conductivity and/or a decrease in calcium conductivity within the neurone *(3)*. Functional $GABA_C$ receptors seem to be restricted to the retina and structurally resemble the $GABA_A$ receptor *(1)* and thus should perhaps be designated as a subgroup of the $GABA_A$ receptor class *(4)*.

The therapeutic benefits of $GABA_A$ and $GABA_B$ receptor ligands have been well documented [*see (5)* and *(3)*, respectively], and the technique of radioligand binding to crude synaptic membranes is a convenient method by

From: *Methods in Molecular Biology, Vol. 106: Receptor Binding Techniques*
Edited by: Mary Keen © Humana Press Inc., Totowa, NJ

which to assess the properties of potential GABA receptor modulators, both by direct assay and by evaluation of the long-term effects of drugs on GABA receptors following animal pretreatment *(6)*.

This chapter describes the preparation of crude synaptic membranes using the method of Zukin et al. *(7)*, which is a modification of that of Gray and Whittaker *(8)*. This preparation must be thoroughly washed in order to remove endogenous GABA and other possible inhibitory substances that would otherwise interfere with the radioligand binding assay *(9)*. It is also important to use the membranes immediately after the final wash steps to prevent *de novo* GABA synthesis and tissue degradation, both of which will reduce [^{3}H]-GABA binding.

The radioligand binding assay described here is based on the method of Hill and Bowery *(10)* and allows determination of both $GABA_A$ and $GABA_B$ binding sites within the same assay using the same radioligand, [^{3}H]-GABA. 1–5 n*M* [^{3}H]-GABA is routinely used for determination of binding, 3 n*M* [^{3}H]-GABA is suitable for use in displacement binding assays, with, for example, 0–100 μ*M* (–) baclofen *(11)*. As GABA has a low affinity for both $GABA_A$ and $GABA_B$ receptors *(1)*, the centrifugation radioligand binding technique is the most appropriate method, (*see* Chapter 1). To determine binding to $GABA_A$ sites only, an excess (100 μ*M*) of the $GABA_B$ agonist (–) baclofen is incorporated, whereas $GABA_B$ receptors are studied using 40 μ*M* isoguvacine (a $GABA_A$ receptor agonist) to block binding to the $GABA_A$ sites. Nonspecific (NS) $GABA_A$ binding is defined by the addition of 100 μ*M* isoguvacine, whereas nonspecific $GABA_B$ binding is defined using 100 μ*M* baclofen. Specific binding is defined as the difference between total and NS binding and is typically approx 30–60% of total binding. Example values for $GABA_A$ and $GABA_B$ binding using this technique in whole rat brain, labeled with 5 n*M* [^{3}H]-GABA, are 807 and 218 fmol/mg protein, respectively *(6)*.

2. Materials

1. One (or more) adult rat.
2. 0.32*M* sucrose (BDH, Merck Ltd., Lutterworth, Leicestershire, U.K.): 35 mL per whole rat brain. This may be prepared the day before and stored in the refrigerator; however, we prefer to make it up on the day of the assay, using previously cooled distilled water.
3. Binding buffer: 50 m*M* Tris-HCl, 2.5 m*M* $CaCl_2$, pH 7.4 (Sigma-Aldrich Co. Ltd., Poole, Dorset, U.K.) prepared in liter quantities and stored at 4°C. (*see* **Note 1**).
4. Ice-cold distilled water.
5. [^{3}H]-GABA, specific activity (70–100) Ci/mmol (NEN Life Science, Hounslow, U.K.), in binding buffer. This should be diluted from stock just before the assay.

6. (–) Baclofen (Research Biochemicals Int., Semat Technical (U.K.) Ltd., St. Albans, Hertfordshire, U.K.): 1 m*M* in binding buffer. For ease, (–) baclofen may be made up as a stock solution of 1 mg/mL in distilled water and stored in appropriate aliquots at –80°C for 2–4 mo.
7. Isoguvacine (Research Biochemicals Int.: 1 m*M* and 400 μ*M* in binding buffer. Isoguvacine may be made up as a stock solution of 1 mg/mL in distilled water and stored in appropriate aliquots at –80°C for 2–4 mo.
8. Tissue solubilizer such as Soluene-350 (Canberra Packard, Pangbourne, Hertfordshire, U.K.)
9. 0.2 *M* HCl stored at room temperature.
10. Scintillation fluid e.g., Optiphase Safe (LKB Scintillation Products, FSA Laboratory Supplies, Leicestershire, U.K.).
11. Standard dissection equipment, including large and small scissors, scalpel or blade, curved forceps, and small spatula (e.g., BDH, Merck Ltd.).
12. Ice bucket and ice.
13. Absorbent paper, about 5-cm square (e.g., paper toweling, filter paper).
14. 50-mL glass homogenizer with PTFE pestle and overhead stirrer motor capable of 600 r.p.m. (e.g., IKA models). Both are available from BDH, Merck Ltd.
15. Screw-top centrifuge tubes (50 mL) capable of withstanding 48,000*g* [e.g., Beckman polyallomer centrifuge tubes, Beckman Instruments (U.K.) Ltd., High Wycombe, Buckinghamshire, U.K.], three per brain sample, although two can be used if you wash the first after use.
16. Temperature-controlled ultracentrifuge, capable of centrifuging at 48,000*g* and maintaining a temperature of 4°C, e.g., Beckman J2-21M/E centrifuge [Beckman Instruments (U.K.)].
17. Vortex mixer (e.g., BDH, Merck Ltd.).
18. 5-mL scintillation vial (e.g., BDH, Merck Ltd.).
19. 1.5-mL microcentrifuge tubes (*see* **Note 2**), e.g., Eppendorf (BDH, Merck Ltd.).
20. Repeater pipet (e.g., Eppendorf multipipet 4780, BDH, Merck Ltd.) and tips appropriate to dispense 50, 100, and 750 μL.
21. Bench-top microcentrifuge (e.g., Eppendorf 5415C, BDH, Merck Ltd.,) centrifuging at 11,000–13,000*g*.
22. Vacuum pump (electrical or water).
23. Short-tipped Pasteur pipet.
24. Scintillation counter (e.g., Tri Carb 1500 TR, Canberra Packard, Pangbourne, Berkshire, U.K.)].
25. Protein assay reagents, e.g., Bradford assay *(12)*, available as a commercial kit [Pierce and Warriner (U.K.) Ltd., Chester, U.K.].

3. Methods

Although the incubations are performed at room temperature, at other times the tissue/homogenate must be kept on ice to minimize degradation.

3.1. Preparation of Crude Synaptic Membranes

1. The adult rat should be sacrificed according to Home Office regulations, for example, stunning followed by cervical dislocation/decapitation or straight decapitation, depending on license. Anesthesia of the rat may lead to alterations in binding, such as benzodiazepine and barbiturate modulation of $GABA_A$ receptors *(13)*.
2. Place the head on ice. Trim excess tissue from neck, up to the base of the skull, with a pair of large scissors. Using a scalpel or blade, make an midline skin incision along the top of the skull (from between the eyes to the base of the skull is more than enough) and pull this back to expose the bone. With the points of the small scissors make two lateral cuts in the bone at the base of the skull to enable this "flap" to be removed with forceps. The small scissors may then be used to carefully cut up the side (or midline, depending on preference) of the skull, removing the bone covering the top of the brain with forceps. Again, using the small scissors, make a midline cut through the nasal sinuses and remove this bone. With the small spatula, carefully scoop out the brain onto sucrose-soaked absorbent paper (paper toweling is suitable) placed on ice, severing the cranial nerves with either the spatula or small scissors. Rinse the brain with sucrose, removing any remaining blood, hair, meningeal or bone fragments and place in the glass homogenizer.
3. Homogenize (*see* **Note 3**) the rat brain in 15 vols (25 mL) of ice-cold sucrose (*see* **Note 4**), maximum setting of stirrer (about 600 r.p.m.) 10 up/down strokes (about 30 s). This produces a smooth, creamy homogenate.
4. Pour into 50-mL screw-top centrifuge tube.
5. Centrifuge the homogenate at 1000*g* for 10 min at 4°C. (*see* **Note 5**).
6. Carefully pour the supernatant (S_1) into a fresh centrifuge tube and centrifuge at 20,000*g* for 20 min at 4°C. Discard the pellet (P_1) remaining in the original centrifuge tube, and wash the tube if only two are available.
7. Discard the supernatant and resuspend the pellet (P_2) in 25 mL ice-cold distilled water and centrifuge at 8,000*g* for 20 min at 4°C, producing a bilayer pellet (*see* **Note 5**).
8. Remove the supernatant along with the soft upper layer of the pellet (*see* **Note 6**) and centrifuge at 48,000*g* for 20 min at 4°C. Discard the lower pellet.
9. Discard the supernatant.
10. Wash the pellet by resuspending in 25 mL ice-cold distilled water, transfer to homogenizer, and homogenize as in **step 3**. Return to centrifuge tube and centrifuge at 48,000*g* for 20 min at 4°C.
11. Discard the supernatant.
12. Repeat washing steps 10 and 11 twice more.
13. Resuspend the final pellet in 4 mL ice-cold distilled water, and pour into a 5-mL scintillation vial (*see* **Note 7**).
14. Store at −80°C for at least 18 h prior to use (*see* **Note 8**).

Table 1
Volumes of Solutions (µL) Required for Preparation of Tubes for $GABA_A$ and $GABA_B$ Binding

Stock Solution	Stock Conc.	Final Conc.	$GABA_A$ Total	$GABA_A$ NS	$GABA_A$ Test	$GABA_B$ Total	$GABA_B$ NS	$GABA_B$ Test	Notes
[³H]-GABA	100 n*M*	5 n*M*	50	50	50	50	50	50	
(-) Baclofen	1 m*M*	100 µ*M*	100	100	100	—	—	—	Block $GABA_B$ sites
Isoguvacine	400 µ*M*	40 µ*M*	—	—	—	100	100	100	Block $GABA_A$ sites
(-) Baclofen	1 m*M*	100 µ*M*	—	—	—	—	100	—	
Isoguvacine	1 m*M*	100 µ*M*	—	100	—	—	—	—	
Buffer			100	—	—	100	—	—	To make up volume if required
Test Drug	*x* µ*M*	*x* µ*M*/10	—	—	100	—	—	100	
Membranes			750	750	750	750	750	750	
Total Volume	—	—	1000	1000	1000	1000	1000	1000	

3.2. Washing the Crude Synaptic Membranes

See **Notes 9** and **10**.

1. Thaw the membranes at room temperature (approx 15 min).
2. Wash the membrane pellet by resuspending in 30 mL ice-cold distilled water and centrifuging for 10 min at 9000*g* at 4°C.
3. Discard the supernatant.
4. Repeat steps 2 and 3 twice more.
5. Resuspend the pellet in 25 mL binding buffer and incubate at room temperature for 45 min before centrifuging for 10 min at 9000*g* at 4°C.
6. Discard the supernatant.
7. Repeat wash steps 5 and 6 twice more (decreasing the incubation time to 15 min) before resuspending the final pellet in an appropriate volume of ice-cold binding buffer to obtain a membrane preparation with a protein concentration of approximately 0.6–1.2 mg/mL. One whole rat brain should yield enough tissue for about 40 tubes (34 mL).
8. Use the membranes immediately for the radioligand binding assay, but save a small amount of each preparation for later determination of protein content (*see* **Note 11**).

3.3. Radioligand Binding Assay

1. Each assay condition is determined in triplicate.
2. Perform the assay in 1.5-mL microcentrifuge tubes prepared as detailed in **Table 1** (*see* **Notes 2, 12–14**). The amount of [³H]-GABA added to the assay should be determined by adding 50-µL aliquots into scintillation vials along with 10 mL of the scintillation cocktail, followed by beta counting.

3. Finally, add 750 µL of freshly washed membranes (this will give a final concentration of 0.5–1 mg protein/tube), vortex, and incubate at room temperature for 10 min.
4. Terminate the reaction by centrifuging in a microcentrifuge at 11,000–13,000*g* for 4 min.
5. Carefully aspirate off the supernatant (*see* **Note 15**) and rapidly but gently dip the microcentrifuge into ice-cold distilled water (*see* **Note 16**), filling the tube. Aspirate rapidly and repeat this wash, being careful not to dislodge the pellet. Any remaining droplets may be blotted with tissue paper.
6. Add 100 µL Soluene to the pellet, vortex, and leave to solubilize overnight at room temperature (*see* **Note 17**).
7. Following solubilization, vortex the samples, checking that the tissue has been solubilized, and neutralize the Soluene by adding 400 µL 0.2*M* HCl.
8. Cut off the top of the microcentrifuge tube with scissors (*see* **Note 18**) and invert both the tube and contents into a 20-mL scintillation vial. Leaving the tubes in the vials, add 10 mL scintillation fluid (*see* **Note 19**).
9. Count the samples in a beta scintillation counter over an appropriate counting period (e.g., 3 min).

4. Notes

1. $GABA_B$ binding has been shown to have an absolute dependence on divalent cations *(9)* with maximal [^{3}H]-GABA binding to $GABA_B$ sites in the presence of 2.5 m*M* $CaCl_2$. Enna and Snyder *(14)* reported that $GABA_A$ binding, however, has been reported to be independent of either Ca^{2+} or Mg^{2+}. For this reason, the buffer contains 2.5 m*M* $CaCl_2$ and is suitable for the determination of both binding sites.
2. 1.5-mL microcentrifuge tubes are routinely used for this type of assay, although it is important that a few points are noted. Good-quality tubes should be used—some of the cheaper products have occasionally had lids that either break off in use or do not provide a good seal. It is especially important that the lids are secured to avoid loss of the sample and contamination of both equipment and other samples. For very hazardous samples, "Safe-lock" Eppendorf microcentrifuge tubes (BDH, Merck Ltd.) may be used. The tubes should be of the clear variety, and when labeled, only the lids should be written on; the tubes themselves are placed into the scintillation vials, so colored tubes and dye from writing on the sides may interfere with accurate counting of the samples. Tubes with as tapered a bottom as possible should also be used, as this will make the final pellet more defined, allowing easier aspiration of the supernatant and less disruption of the pellet (important if the pellet is very small).
3. Great care should be exercised when homogenizing: Gloves (possibly even leather) and eye protection should be worn, and ensure that hair and clothes sleeves do not come into contact with the rotating part of the tissue stirrer. Hold the glass homogenizer by the sides, not underneath (which could cause glass to

be driven into your hand on the down stroke if the homogenizer were to break), and carefully but smoothly move this up and down the pestle. Apart from breaking the homogenizer, excess speed and force on the down stroke may cause the homogenate to spray out of the top. On the up stroke, do not pull the homogenizer down hard, which may produce empty areas, as this may lead to foaming and denaturation of the tissue; a gentle movement should be used.

4. If specific brain areas are required (or neonatal/immature rats are required), the volume of sucrose and subsequent buffers may be modified to compensate for the reduced tissue.
5. The pellet produced (P_1) is the crude nuclear fraction, enriched in cell nuclei, unbroken cells, and brain microvessels. Centrifuging the supernatant (S_1, the crude membrane fraction, enriched in myelin, synaptosomes, and mitochondria) produces the P_2 pellet and the S_2 supernatant. Following hypotonic shock (to lyse nerve endings) and further centrifugation of the P_2 pellet, the pellet becomes a bilayer. The brownish, lower layer of the bilayer is the mitochondrial and myelin fraction, whereas the combined supernatant and upper layer are the crude synaptic fraction rich in synaptic membranes. This crude synaptic fraction then undergoes further resuspension and centrifugation to wash the membranes, reducing endogenous ligand content, which enhances binding. Further centrifugation of the S_2 fraction for 60 min, 100,000*g* produces the crude microsomal fraction, P_3.
6. With care, the supernatant may be gently poured into the fresh tube, and the "buffy coat," the soft upper layer, may be collected by *gently* pouring approx 1 mL of the supernatant back and very gently rocking before returning it to the supernatant tube; doing this three times is adequate. If preferred, a wide-bore Pasteur pipet may be used instead to remove both the supernatant and upper layer. It is very important that whichever method is used that it is carried out as carefully as possible so as not to disturb the remaining pellet and contaminate the membranes with the lower mitochondrial fraction.
7. The pellet itself may be frozen directly in the centrifuge tube, although resuspending prior to freezing is useful, as centrifuge tubes may be in short supply.
8. Bowery et al. ***(9)*** observed that freezing and thawing the membrane preparation, prior to binding, produced a significant increase of 109% in the amount of [^{3}H]-GABA specifically bound to $GABA_B$ sites when compared with fresh tissue. This finding was also observed when $GABA_A$ binding sites were studied ***(15)***. It is thought that freezing and thawing before the final centrifugation steps (*see* **Subheading 3.2.**) allow the removal of proteins and/or phospholipids present in the membrane preparation that impair the binding of [^{3}H]-GABA ***(9)*** as replacement of the supernatant following freeze-thawing and centrifugation reduces binding ***(16)***. The prepared membranes may be stored (–80°C) for a few weeks prior to assay.
9. This is done on the day of the radioligand binding assay to remove compounds that impair binding and is not a separate procedure; the actual assay should be initiated immediately after final resuspension of the membranes.

10. While the membranes are thawing and washing (approx 3–4 h in total), begin to think about preparing the tubes and drugs for the radioligand binding experiment so that the membranes may be added as soon as they are prepared.
11. Analysis of protein content may be carried out either on the same day or the samples frozen for later determination. Bradford *(12)* assays are suitable, with reference to bovine serum albumin standards.
12. If different samples are to be used, ensure that the assay tubes are laid out to provide fast and easy access to those requiring the same membrane suspension. The incubation time is relatively short and time should not be wasted. Also make sure that only the number of samples that can be terminated at one time are initiated in one batch—otherwise stagger them; 5 min is usually adequate.
13. The volumes of solutions being added may be altered to suit the investigator, although for rapidity, volumes that can be dispensed with a repeater pipet are useful. The solutions are added in this order to reduce contamination of pipet tips. It is preferable to add the final membrane preparation in as large a volume as possible in order to aid initial mixing before vortexing.
14. Although tritium is only a low-energy beta emitter, it is still important to follow normal safety procedures, particularly as tritium cannot be monitored directly, and any spillages are more difficult to detect.
15. A vacuum pump (electrical or water) attached to a Pasteur pipet (short-tipped) is the most efficient method.
16. Distilled water may be added using a pipet, but this method is faster and results in less disruption of the tissue pellet.
17. To speed up solubilization, samples may be incubated in a warm (not hot) oven. Wear suitable gloves and eye protection when handling Soluene and preferably work in a fume hood.
18. For quickness, the tube hinges may be cut following vortexing with Soluene, leaving the lids on but ready to be removed quickly the next day. It is not recommended that the caps be pulled off as this may spill the contents.
19. The safety procedures involved with scintillation fluid should be followed, which normally means suitable gloves, eye protection, and the use of a fume hood.

Acknowledgments

The authors gratefully acknowledge Prof. N. G. Bowery, in whose laboratories the techniques were developed.

References

1. Johnston, G. A. R. (1996) $GABA_C$ receptors: relatively simple transmitter-gated ion channels. *Trends Pharmacol. Sci.* **17,** 319–323.
2. Schofield, P. R., Darlison, M. G., Fujita, N., Burt, D. R., Stephenson, F. A., Rodriguez, H., Rhee, L. M., Ramachandran, J., Reale, V., Glencorse, T. A., Seeburg, P. H., and Barnard, E. A. (1987) Sequence and functional expression of the $GABA_A$ receptor shows a ligand-gated receptor super-family. *Nature* **328,** 221–227.

3. Bowery, N. G. (1993) $GABA_B$ receptor pharmacology. *Ann. Rev. Pharmacol. Toxicol.* **33,** 109–114.
4. Bowery, N. G. and Brown, D. A. (1997) The cloning of $GABA_B$ receptors. *Nature* **386,** 223–224.
5. Krogsgaard-Larsen, P., Frolund, B., and Ebert, B. (1997) $GABA_A$ receptor agonists, partial agonists, and antagonists, in *The GABA Receptors* (Enna, S. J. and Bowery, N. G., eds.), Humana, Totowa, NJ, pp. 37–81.
6. Qume, M., Bowery, N. G., and Fowler, L. J. (1995) The effect of 2-, 8- and 21-day treatment with GABA-T inhibitors on $GABA_A$, $GABA_B$ and flunitrazepam binding to rat crude synaptic membranes. *Br. J. Pharmacol.* **116,** 391P.
7. Zukin, S. R., Young, A. B., and Snyder, S. H. (1974) Gamma-aminobutyric acid binding receptor sites in rat central nervous system. *Proc. Natl. Acad. Sci. USA* **71,** 4802–4807.
8. Gray, E. G. and Whittaker, V. P. (1962) The isolation of nerve endings from brain: an electron microscopic study of cell fragments derived from homogenisation and centrifugation. *J. Ant.* **96,** 79–88.
9. Bowery, N. G., Hill, D. R., and Hudson, A. L. (1983) Characteristics of $GABA_B$ receptor binding sites on rat whole brain synaptic membranes. *Br. J. Pharmacol.* **78,** 191–206.
10. Hill, D. R. and Bowery, N. G. (1981) [^{3}H]-baclofen and [^{3}H]-GABA bind to bicuculline-insensitive $GABA_B$ sites in rat brain. *Nature* **290,** 149–152.
11. Knott, C., Maguire, J. J., and Bowery, N. G. (1993) Age-related sensitivity to pertussis toxin-mediated reduction in $GABA_B$ receptor binding in rat brain. *Mol. Brain Res.* **18,** 353–357.
12. Bradford, M. M. (1976) A rapid and sensitive method for the quantification of microgram quantities of protein utilising the principle of protein-dye binding. *Anal. Biochem.* **72,** 248–254.
13. Wong, E. H. F. (1989) Modulation of $GABA_A$ receptors in the mammalian brain, in *GABA: Basic Research and Clinical Applications* (Bowery, N. G. and Nistico, G., eds.), Pythagora, Rome–Milan, pp. 135–151.
14. Enna, S. J. and Snyder, S. H. (1977). Influences of ions, enzymes, and detergents on γ-aminobutyric acid-receptor binding in synaptic membranes of rat brain. *Mol. Pharmacol.* **13,** 442–453.
15. Enna, S. J. and Snyder, S. H. (1975) Properties of γ-aminobutyric acid (GABA) receptor binding in rat brain synaptic membrane fractions. *Brain Res.* **100,** 81–97.
16. Toffano, G., Guidotti, A., and Costa, E. (1978) Purification of an endogenous protein inhibitor of the high affinity binding of γ-aminobutyric acid to synaptic membranes of rat brain. *Proc. Natl. Acad. Sci. USA* **75,** 4024–4028.

3

Characterization of Imidazoline Receptors by Radioligand Binding

Alan L. Hudson and Lisa A. Lione

1. Introduction

Imidazoline receptors are divided into two main types, known as I_1- and I_2-receptors, and whereas I_1 receptors appear to play a role in control of blood pressure, I_2 receptor mediated functions are still unclear *(1)*.

While it is possible to study the physiology of I_1 receptors, they are difficult to label and identify in binding studies because of a lack of selective high-affinity radioligands. For example, most binding studies use [^{3}H]clonidine, [^{3}H]-*p*-aminoclonidine, or an iodinated derivative, [^{125}I]-*p*-aminoclonidine, for receptor binding studies, although recently [^{3}H]moxonidine has been described as a semiselective I_1 radioligand (*see* **ref. 2**). All these radioligands show a degree of affinity for α_2-adrenoceptors, an artifact that must be masked to allow proper identification of I_1 receptors. In addition, I_1 receptors are thought to be highly localized to the lateral reticular nucleus of the brain stem, so obtaining enough tissue for binding assays can be difficult. In fact, much of the reported work concerning I_1 receptor binding assays has been performed on cow brain, a tissue that is not now readily available because of Bovine Sponciform Encephalopathy (BSE) in cattle. However, I_1 receptor binding has also been found on NG108-15 cells, chromaffin cells, and PC12 cells *(2)*, and in this chapter these cell lines will be used. There are many protocols reported for I_1 binding studies (*see* **refs. 2** and *3*), from which our protocol has been adapted. However, it should be noted that I_1 receptor binding can prove to be illusive—the amount of specific binding being variable. The signal transduction for I_1-receptor-mediated events is thought to involve prostaglandin release via a coupling to phospholipase C to generate diacylglycerol *(4)*; agmatine is proposed as the endogenous ligand *(5)*.

From: *Methods in Molecular Biology, Vol. 106: Receptor Binding Techniques*
Edited by: Mary Keen © Humana Press Inc., Totowa, NJ

In contrast to I_1 receptors, I_2 sites are extremely easy to label and identify in a range of tissues and species (**Table 1**), especially following the introduction of radiolabeled drugs demonstrating high affinity and selectivity for this site. For several years, researchers have utilized [^{3}H]idazoxan to identify I_2 receptors, both in binding studies and autoradiography *(6)*. However, like [^{3}H]clonidine, [^{3}H]idazoxan has high affinity for α_2-adrenoceptors, so experiments must be performed in the presence of a drug such as the α_2-adrenoceptor antagonist rauwolscine, which will mask the adrenoceptor component of binding, which allows proper characterization of I_2 receptors. The introduction of new ligands such as [^{3}H]2-BFI (2-(2-benzofuranyl)-2-imidazoline) and [^{3}H]RS-45041-190 (4-chloro-2-(imidazolin-2yl)isoindolene) obviates the need for adrenoceptor masking as they are highly selective and demonstrate very high affinity for I_2 site receptors.

Recent studies have now subdivided I_2 receptors into I_{2A} and I_{2B} based on their sensitivity to amiloride, with I_{2A} being amiloride-sensitive; again the functional consequence of this heterogeneity is unknown. Fortunately, selective radioligands such as [^{3}H]2-BFI are now commercially available (*see* **Table 1**), which facilitate the labeling of both subtypes of these receptors *(7)*. There is also a photoaffinity ligand, 2-(3-azido-4-^{125}I-iodophenoxy)methyl-imidazoline, which can be used to permanently label I_2 receptors for molecular studies *(8)*. I_2 receptors are widespread in brain and peripheral tissues, and although their function is not clear, a substantial population of these sites is located on the enzyme monoamine oxidase *(9)*. In brain, at least, I_2 receptors facilitate a decrease in monoamine turnover and may play a role in depression; indeed the density of I_2 receptors is changed in a wide range of brain disorders (**Table 1**), including Alzheimer's disease, opioid dependence, and depression *(10)*. Again, agmatine is the proposed endogenous ligand for these receptors, although many reports find this amino acid to have low affinity at the I_2 site. The signal transduction pathway for I_2 receptors is unknown, although the proposed link with monoamine oxidase may negate the need for a signal transduction pathway for these novel sites.

There is good evidence for another population of imidazoline receptors that are linked to a potassium channel. These imidazoline receptors, sometimes termed "atypical" imidazoline receptors, play a role in the regulation insulin secretion *(11)*. They demonstrate low affinity for [^{3}H]clonidine and [^{3}H]2-BFI but show some degree of affinity for [^{3}H]RX821002 (2-methoxy-idazoxan). Overall, they are difficult to study in the context of binding studies, with high nanomolar concentrations of the [^{3}H]RX821002 required for their study *(11)*. The protocols shown here, therefore, focus on the study of I_1 and I_2 receptors.

Table 1
Some of the General Characteristics of I_1 and I_2 Receptors

	I_1 RECEPTORS	I_2 RECEPTORS
Radioligands	[^{3}H]clonidine[a] [^{3}H]-*p*-aminoclonidine[a] [^{125}I]-*p*-aminoclonidine[a] [^{3}H]moxonidine	[^{3}H]idazoxan[a] [^{3}H]2-BFI[a] [^{3}H]RS-45041-190 [^{125}I]AMIPI[a]
Source of receptors	Bovine brainstem Bovine adrenal medulla NG108-15 cells PC12 cells Human platelets	Rat brain, kidney, liver, adipocytes Rabbit brain, kidney, liver Guinea pig brain
Signal transduction	Coupled to phospholipase C	Monoamine oxidase linked
Function	Modulation of blood pressure, clonidine and moxonidine are agonists Increase water and Na^+ secretion in kidney	Unclear: modulation of monoamine turnover in brain Central receptor density increased in Alzheimer's, but decreased in Huntington's patients and morphine addicts Inhibition of Na^+ uptake in rat kidney

[a] Denotes commercial availability.

2. Materials

2.1. I_1 Receptor Studies

1. HEPES buffered sucrose: 50 m*M* HEPES buffered sucrose, pH 7.4 at 4°C, containing the protease inhibitors (1,10)-phenanthroline (100 μ*M*) and phenylmethylsulfonyl fluoride (50 μ*M*), allowing 20 vol/gm of tissue for the homogenization. The protease inhibitors should be added just before use.
2. Assay buffer: 50 m*M* Tris-HCl, pH 7.7, containing 5 m*M* EDTA, 5 m*M* EGTA, and 5 m*M* $MgCl_2$ (*see* **Note 1**).
3. Radioligand: [^{3}H]-*p*-amino clonidine (40–60 Ci m mol) is available from NEN Research Products (Hounslow, UK), stored in ethanol under nitrogen at –70°C, and diluted in water or assay buffer immediately before use.
4. Rauwolscine (Research Biochemicals Inc./Sigma-Aldrich Ltd., Poole, UK).
5. Moxonidine (Solvay Duphar, Bruxelles, The Netherlands).
6. Cirazoline (Tocris Cookson, Langford, Bristol, UK).

7. Coomassie plus protein assay kit (Pierce & Warriner Ltd., Chester, UK).
8. Polyethyleneimine (PEI; Aldrich/Sigma-Aldrich).
9. Glass-glass hand-held homogenizer.
10. Ultracentrifuge and tubes suitable for spinning at 48,000*g* at 4°C.
11. Whatman GF/B filters.
12. Cell harvester (e.g., Brandel).

2.2. I_2 Receptor Studies

1. Tris-HCl buffered sucrose: 50 m*M* Tris-HCl buffered 0.32 *M* sucrose, pH 7.4 at 4°C, allowing 10 vol/gm of tissue.
2. Assay buffer: 50 m*M* Tris HCl, 1 m*M* $MgCl_2$, pH 7.4 (*see* **Note 1**).
3. Radioligand: [^{3}H]2-BFI (45 Ci mmol^{-1}) and [^{3}H]idazoxan (58 Ci mmol^{-1}) are obtained from Amersham, (Little Chalfont, UK) and stored at 4°C and –20°C, respectively.
4. Idazoxan (SIGMA, UK).
5. BU224, (2-(4,5-dihyroimidaz-2-yl)-quinoline; Tocris Cookson).
6. Polyethyleneimine (PEI; Aldrich).
7. Motor-driven Teflon-glass homogenizer.
8. Ultracentrifuge and tubes suitable for spinning at 48,000*g* at 4°C.
9. Whatman GF/B filters.
10. Cell harvester (e.g., Brandel).

3. Methods

3.1. Membrane Preparation

3.1.1. For I_1 Receptors

1. Gently homogenize bovine adrenomedullary chromaffin cells in 20 vol (w/v) of ice-cold HEPES buffered sucrose by 10 strokes in a glass-glass hand-held homogenizer.
2. Centrifuge the homogenate at 1000*g* for 5 min at 4°C to remove nuclei and debris.
3. Resuspend the pellets (P1) in 20 mL of ice-cold HEPES buffered sucrose and recentrifuge at 1000*g* for 5 min.
4. Pool the resultant supernatants and recentrifuge at 48,000*g* for 18 min at 4°C.
5. Discard the supernatants. Resuspend each pellet (P2) in 10–25 vol of assay buffer and spin at 48,000*g* for 18 min at 4°C.
6. Wash the pellets three more times by repeated centrifugation at 48,000*g* for 18 min at 4°C.
7. Flash freeze the dried pellets in liquid nitrogen and store at –70°C until use.
8. Prior to radioligand binding studies, thaw the membrane pellets and resuspend in 40 mL of assay buffer at 25°C.

3.1.2. For I_2 Receptors

1. Sacrifice male Wistar rats (240–300 g) by stunning followed by decapitation. One rat brain will provide enough tissue for approx 72 tubes.

2. Immediately remove the whole brains over ice and homogenize in 10 vol (w/v) of ice-cold Tris-HCl buffered sucrose using a motor-driven Teflon-glass homogenizer.
3. Centrifuge the homogenate at 1000*g* for 10 min at 4°C.
4. Pool the resultant supernatants and recentrifuge at 31,000*g* for 20 min at 4°C.
5. Discard the supernatants. Resuspend each pellet in 10 vol of assay buffer and spin at 32,000*g* for 20 min at 4°C.
6. Wash the pellets twice by repeated centrifugation at 32,000*g* for 20 min at 4°C. The final pellets can be stored at −70°C until use.
7. Prior to radioligand binding studies, thaw the membrane pellets and wash them three to four more times by resuspension in 10 vol of assay buffer and repeated centrifugation at 32,000*g* for 20 min.
8. For the assay, resuspend the pellets in assay buffer to give 100–250 µg of protein in 400 µL of suspension.

3.2. Radioligand Binding Assays

3.2.1. Saturation Binding Studies to Determine Receptor Density (B_{max})n (see **Note 2**)

1. Prepare the tritiated ligands at 10X the final concentration required in the assay tube so that 50 µL is added in a final assay volume of 500 µL. For the concentrations and assay layout, *see* **Table 2**.
2. A range of concentrations of [^{3}H]2-BFI, [^{3}H]idazoxan, and [^{3}H]-*p*-aminoclonidine are added in a volume of 50 µL. Make up the latter two ligands in the presence of 50 µ*M* rauwolscine to preclude binding to α_2-adrenoceptors, yielding a final concentration of 5 µ*M* rauwolscine in the assay tube.
3. Start the assay by the addition of 400 µL well-mixed freshly resuspended membrane preparation, to give a final volume in each tube of 500 µL.
4. Each sample should be prepared in triplicate. Specific binding is defined at each free radioligand concentration with either 10 µ*M* idazoxan, BU224, or moxonidine, respectively (*see* **Notes 3** and **4**).
5. Incubate the tubes to equilibrium (40 min at 25°C).
6. Terminate all assays by rapid filtration through presoaked Whatman GF/B filters on a vacuum-assisted cell harvester (Brandel).
   a. For [^{3}H]2-BFI and [^{3}H]idazoxan I_2 receptor binding assays, Whatman filters are presoaked with 0.5% PEI for 5 min at 4°C prior to filtration. Once the tube contents have been sucked through onto the filters, the tubes are then flushed twice with ice-cold assay buffer, which is then aspirated through the filters to constitute the two washes.
   b. For [^{3}H]-*p*-aminoclonidine I_1 receptor binding assays, Whatman filters are presoaked with 0.5% PEI for 4–16 h at 4°C prior to filtration, followed by four rinses with ice-cold assay buffer (as **step 6a**).
7. Dry the filters and punch them out into scintillation vials.

Table 2
Typical Plan for a Saturation Binding Assay to Determine Receptor Density

Tube no.	[^{3}H]ligand (final conc.[a], n*M*) 50 µL	Nonspecific (µL) of 100 µ*M*	Blank buffer (µL)	Membrane (µL)
1–3	0.001	0	50	400
4–6	0.001	50	0	400
7–9	0.003	0	50	400
10–12	0.003	50	0	400
13–15	0.005	0	50	400
16–18	0.005	50	0	400
19–21	0.01	0	50	400
22–24	0.01	50	0	400
25–27	0.03	0	50	400
28–30	0.03	50	0	400
31–33	0.05	0	50	400
34–36	0.05	50	0	400
37–39	0.1	0	50	400
40–42	0.1	50	0	400
43–45	0.3	0	50	400
46–48	0.3	50	0	400
49–51	0.5	0	50	400
52–54	0.5	50	0	400
55–57	1.0	0	50	400
58–60	1.0	50	0	400
61–63	3.0	0	50	400
64–66	3.0	50	0	400
67–69	5.0	0	50	400
70–72	5.0	50	0	400

[a]Note: The stocks of radioligand and cold displacing drug are prepared at ten times their final concentration so that the final concentration is correct. We suggest that the solutions be added in the above order so that the addition of membrane starts the binding assay. For a simple saturation curve where only one-site is present, it is possible to determine a Bmax from eight concentrations

8. Bound radioactivity is determined by liquid scintillation counting, after allowing the filters to mix with 3-mL scintillation fluid overnight.

3.2.2. Competition Studies

Competition binding studies are carried out under similar conditions to saturation experiments.

1. The ability of various drugs to displace a fixed concentration of tritiated ligand (e.g., 1-n*M* [^{3}H]2-BFI) binding at equilibrium (40 min at 25°C) is assessed by the

Table 3
Typical Plan for a Competition Binding Assay

Tube no.	[^{3}H]ligand (final conc., 0.5 n*M*) µL	Nonspecific or Test ligand (n*M*) 50 µL	Blank buffer (µL)	Membrane (µL)
1–3 Total	50	0	50	400
4–6 Non-spec	50	10	0	400
7–9	50	0.01	0	400
10–12	50	0.03	0	400
13–15	50	0.1	0	400
16–18	50	0.3	0	400
19–21	50	1.0	0	400
22–24	50	3.0	0	400
25–27	50	10	0	400
28–30	50	30	0	400
31–33	50	100	0	400
34–36	50	300	0	400
37–39	50	1000	0	400
40–42	50	3000	0	400
43–45	50	10000	0	400
46–48	50	100000	0	400

use of at least 10 concentrations of a test drug, ranging between 0.01 n*M* and 0.1 m*M* in a final volume of 500 µL (*see* **Table 3**). Therefore, stock solutions are prepared by serial dilution at concentrations 10X those that are finally required, and 50 µL is then added to the assay tubes.

2. Similarly, add 50 µL of the tritiated ligand to each tube, having previously prepared this ligand at 10X the final concentration required.
3. Specific binding is defined in the second triplicate of tubes, using 50 µL of a relatively high concentration (100 µ*M*) of a drug reported as selective for the given receptor, to yield a final concentration of 10 µ*M* (*see* **Subheading 3.2.1.**). Ascorbate (0.05%) is often included in the assay buffer for competition studies, using drugs such as noradrenaline to prevent their degradation.
4. Assays are terminated in a identical fashion as described for the saturation assays (*see* **Subheading 3.2.1.**), and the filters and their bound contents are counted in a scintillation counter.
5. Concentration points are usually performed in triplicate, although a rough screening procedure may utilize duplicate tubes in the first instance.

3.3. Analysis of Results

Results from the saturation and competition binding studies are analyzed by computer-assisted iterative nonlinear regression curve fitting procedures (i.e.,

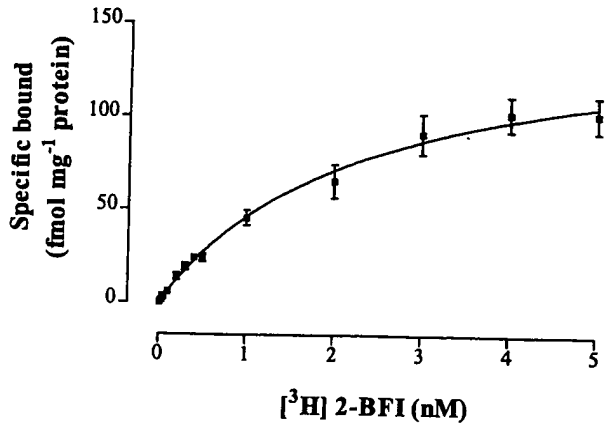

Fig. 1. A saturation binding curve for [^{3}H]2BFI binding to I_2 receptors in rat whole brain membranes showing specific binding (fmol mg protein^{-1}, *y*-axis) plotted vs the concentration of tritiated ligand (n*M*, *x*-axis).

GraphPAD Prism, version 2.01, running on a PC. This is capable of fitting data to a one- or two-site model of binding.

3.3.1. Saturation Studies

1. Deduct the nonspecific disintegrations per minute (dpm) from the total at each concentration of hot ligand, to give specific binding in dpm.
2. The dpm are then converted to femtomole per milligram of protein and Prism can then fit the points to a saturation curve (**Fig. 1**). The program obviously determines the maximal binding capacity (B_{max}) and also the equilibrium dissociation constant (K_D) for the radioligand, a constant that is equal to the concentration of ligand at which half of the total number of receptors are occupied (**Fig. 1**).

3.3.2. Competition Assays

1. Deduct the nonspecific component of binding from the total (to yield the total specific component of binding) and also from all the other displacement points.
2. The dpm remaining for each displacement point can then be expressed as a percentage of the total specific component and these data are then fitted by the software program (**Fig. 2**).
3. The concentration of drug displacing 50% specific binding (IC_{50}) is converted to the inhibitory constant (K_i) by the equation of Cheng and Prusof *(12)* where $K_i = IC_{50} / (1 + L / K_D)$, where *L* is the radioligand concentration. Given the K_D of the hot ligand allows the K_i to be automatically determined by the software program.
4. All displacement curves are usually initially analyzed assuming a one-site model of binding. Displacement curves with Hill coefficients significantly less than

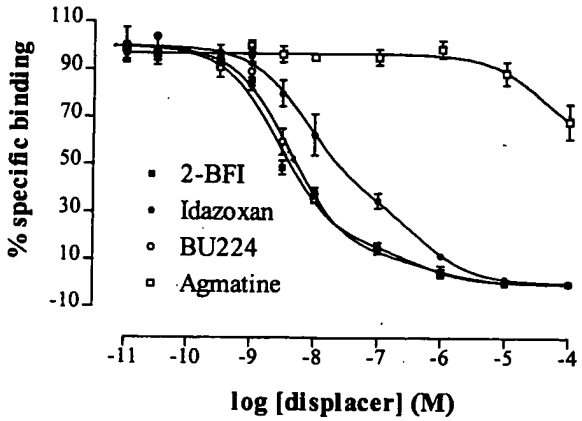

Fig. 2. Competition binding curves for several imidazoline ligands and agmatine displacing a fixed concentration (1 n*M*) of [^{3}H]2BFI from I_2 receptors in rat whole brain membranes. It is interesting to note that agmatine, the putative endogenous ligand displays very low affinity, while the other compounds show biphasic displacement curves indicating the existence of subpopulations of I_2 receptors in this tissue.

unity are reanalyzed assuming a two-site model of high- and low-affinity binding (*see* **Fig. 2**).

5. The *F* test is then used to statistically analyze whether the applicable displacement curve fits significantly better to a two-site model as opposed to a one-site model. The differential *F* value is derived from the equation:

$$F = \frac{(SS_1 - SS_2) / (d.f._1 - d.f._2)}{SS_2 / (d.f._2)}$$

where *SS* and *d.f.* are the residual sum of the squares and degrees of freedom, respectively, associated with the models of fit being compared ($_1$ = one-site model, $_2$ = two-site model). The two-site model is assumed to be a better fit than the one-site model if the *F* value has a $p < 0.05$.

3.4. Protein Determination

The protein content of the membrane preparations is determined with Coomassie blue and bovine serum albumin (0–1 mg/mL in assay buffer) as the standard, using the method of Bradford *(7)*.

1. For a quick method, add 50 µL of blank buffer, standard or membrane preparation, to 1 mL of Coomassie blue reagent in a microcuvet.
2. Mix and read at 595 nm in a spectrophotometer, using the blank as zero.
3. Analyze the standard curve and unknown protein values by computer-assisted linear-regression curve-fitting procedures (GraphPAD Prism, version 2.01).

4. Notes

1. For a binding assay, it is useful to prepare 5 L of buffer, adjust the pH accordingly, and remove approx 1 L for washing the pellet, diluting the hot ligand and unlabeled drugs. The remaining 4 L for the washes needed to terminate the assay is placed in a refrigerator to cool; however, the pH of many buffers is temperature-dependent, so the pH should be rechecked and adjusted prior to use.
2. The density or B_{max} of imidazoline receptors will, of course, vary with species, tissue, and the homogenate preparation, but as a guide, expect the density to fall in the range of 25 to 200 fmol/mg protein. As mentioned in the introduction, I_1 receptor binding can be illusive, and the investigator may wish to consult **ref. *3***, which contains further useful hints for optimizing receptor binding assays. In contrast, using [^{3}H]2BFI to label I_2 receptors is almost infallible and therefore makes a good first step in familiarizing the investigator with imidazoline receptor binding assays in general.
3. This chapter has featured just a few imidazoline compounds that may be used to define the nonspecific component of binding. There are many drugs that are imidazolines, imidazoles, imidazolidines, or contain a guanidino group, which show affinity for I_1 receptors, I_2 receptors, or both. However, what is clear is that there are many more compounds containing an imidazoline or related moiety that have little if any affinity for these receptors. Cirazoline displays good affinity for both I_1 and I_2 sites and could be used to define the specific component of binding in either assay and, unlike moxonidine, is available from commercial sources.
4. Agmatine or decarboxylated arginine is the proposed putative endogenous ligand for imidazoline receptors; therefore, one would quite rightly ask why agmatine is not used to define the specific component of both I_1 and I_2 receptor binding? For reasons that are still unclear, several groups including ours find agmatine to have negligible affinity for I_2 receptors. It is possible that very subtle factors are required for agmatine to recognize the I_2 receptor, factors that are removed during the membrane preparation process. Whatever the actual reason, it is preferable at present to use a high saturating concentration of an imidazoline compound or drug to define the specific component of binding.
5. The rapid expansion of the World Wide Web has led to an excellent site known as "The imidazoline receptor resource page" (http://www.mmcc.monash.edu.au:80/phimr/ireceptor/). This site provides a comprehensive source of information on new ligands, binding techniques, and various other postings of relevance to the field of imidazoline receptors. This resource is compiled by Dr. I. Musgrave, Prince Henry's Institute of Medical Research, Melbourne, Australia.

Acknowledgments

A. Hudson is a Wellcome Research Fellow and L. Lione is currently engaged as a postdoctoral research assistant in the Psychopharmacology Unit, University of Bristol, U.K. We gratefully acknowledge The Wellcome Trust for financial support.

References

1. Bousquet, P. (1997). Imidazoline receptors. *Neurochem Int.* **30,** 3–7.
2. Ernsberger, P., Graves, M. E., Graff, L. M., Zakieh, N., Nguyen, P., Collins, L. A., Westbrooks, K. L., and Johnson, G. G. (1995) I_1-Imidazoline receptors. *New York Acad. Sci.* **763,** 22–42.
3. Ernsberger, P., Piletz, J. E., Graff, L. M., and Graves, M. E. (1995) Optimization of radioligand binding assays for I_1-imidazoline sites. *New York Acad. Sci.* **763,** 163–168.
4. Separovic, D., Kester, M., and Ernsberger, P. (1996) Coupling of I_1-imidazoline receptors to diacylglyceride accumulation in PC12 rat pheochromocytoma cells. *Mol. Pharmacol.* **49,** 668–675.
5. Li, G., Regunathan, S., Barrow, C. J., Eshragi, J., Cooper, R., and Reis, D. J. (1994) Agmatine: an endogenous clonidine displacing substance in the brain. *Science* **263,** 966–969.
6. Mallard, N. J., Hudson, A. L., and Nutt, D. J. (1992) Characterisation and autoradiographical localisation of non-adrenoceptor idazoxan binding sites in the rat brain. *Br. J. Pharmacol.* **106,** 1019–1027.
7. Lione, L. A., Nutt, D. J., and Hudson, A. L. (1996) [^{3}H]2-(2-Benzofuranyl)-2-imidazoline: a new selective high affinity radioligand for the study of rabbit brain imidazoline I_2 receptors. *Eur. J. Pharmacol.* **304,** 221–229.
8. Lanier, S. M., Ivkovic, B., Singh, I., Neumeyer, J. L., and Bakthavachalam, V. (1993) Visualisation of multiple imidazoline/guainidium-receptive sites. *J. Biol. Chem.* **268,** 16,047–16,051.
9. Parini, A., Moudanos, C. G., Pizzinat, N., and Lanier, S. M. (1996) The elusive family of imidazoline binding sites. *Trends Pharmacol. Sci.* **17,** 13–16.
10. Sastre, M. and García-Sevilla, J. A. (1997) Densities of I_2-imidazoline receptors, α_2-adrenoceptors and monoamine oxidase in brains of suicide victims. *Neurochem. Int.* **30,** 63–72.
11. Morgan, N. G., Chan, S. L., Brown, C. A., and Efthymia, T. (1995) Characterisation of the imidazoline binding site involved in regulation of insulin secretion. *New York Acad. Sci.* **763,** 361–373.
12. Cheng, Y. C. and Pru, W. H. (1973) Relationship between the inhibition constant (K_i) and the concentration of inhibitor which causes 50% inhibition (IC_{50}) of an enzymatic reaction. *Biochem. Pharmacol.* **22,** 3099–3108.

4

Radioligand Binding to Solubilized 5-HT_3 Receptors

Stephanie Fletcher and Nicholas M. Barnes

1. Introduction

Most receptors, apart from those for steroid and thyroid hormones, are transmembrane glycoproteins and are generally expressed by tissues in relatively low quantities. Exceptions include the nicotinic acetylcholine receptor in *Torpedo* electric organs and the rhodopsin receptor in the retina, in which the abundance of these receptors aided their characterization much earlier than other receptors.

Solubilization of a receptor is an essential prerequisite for purification. The use of various detergents for the solubilization of receptors has been well documented *(1,2)*. Like membrane phospholipids, detergents are amphipathic; that is, they have a hydrophilic "head" and a hydrophobic "tail." Detergent molecules "slot" into the membrane, causing lysis, and the constituents of the cell are solubilized in the form of detergent–lipid–protein complexes. These complexes are then further solubilized to give detergent-lipid complexes and detergent-protein complexes, and the solubilized material may be isolated by centrifugation. The critical micellular concentration (CMC) of a detergent is the concentration at which detergent monomers form clusters or micelles. Solubilization of protein (e.g., receptors) is thought to begin to occur at or near the CMC for most detergents. As the concentration of detergent is increased, the amount of protein solubilized also increases, but above a certain point, there is no further increase in receptor yield. This may be owing to denaturation of the receptor protein by the detergent, or removal of essential lipids.

Transmembrane receptors can be divided into three main groups: receptors with a single transmembrane segment (e.g., tyrosine kinase-linked receptors such as the insulin, EGF, and PDGF receptors), ligand-gated ion channels (e.g., nicotinic acetylcholine receptor, $GABA_A$ receptor, 5-HT_3 receptor), and recep-

From: *Methods in Molecular Biology, Vol. 106: Receptor Binding Techniques*
Edited by: Mary Keen © Humana Press Inc., Totowa, NJ

tors coupled to G proteins (e.g., β-adrenoreceptor). Receptors belonging to the first group may be solubilized with nonionic detergents such as Triton X-100 and octyl glucoside *(3,4)*, which bind preferentially to the hydrophobic transmembrane domain, whereas the ligand-binding activity and tyrosine kinase domains remain intact. The nondenaturing, zwitterionic detergent CHAPS has also been used successfully *(4)*. Triton X-100 and CHAPS have been used for the solubilization of ligand-gated ion channels *(5–7)*; these receptors can also be solubilized with the anionic bile salt detergents sodium cholate or deoxycholate *(7–9; see* **Note 1**). The ligand-binding activity of G protein-linked receptors is labile in the presence of most detergents, possibly partly owing to the fact that the hydrophobic transmembrane domains are likely to participate in ligand binding for this family of receptors. Digitonin is the best established detergent for solubilizing receptors belonging to this family *(10,11)*, although it is expensive and not readily soluble in water (*see* **ref. *2* Note 2,** Chapter 5). CHAPS and sodium cholate have also been effective (*12,13*, *see* **Notes 1** and **3**). **Table 1** documents the properties of some detergents used commonly for receptor solubilization. The choice of detergent depends not only on the type of receptor, but also on its cellular enviroment. One criterion for selection is that a suitable detergent will show little inhibition of radioligand binding at concentrations above its CMC (*see* **Note 4**).

Radioligand binding can provide a great deal of information about solubilized receptor preparations. Data from saturation binding experiments allow the determination of the affinity and the concentration of binding sites for a given ligand. It is often important to demonstrate that the solubilized species retains the same pharmacological characteristics as the native receptor by comparing the pharmacological profiles obtained in a series of competition assays using structurally different compounds. However, the technique of solubilization has inherent problems for binding studies. The detergent used in the solubilization process may interfere with the ligand binding activity of a receptor. In particular, cofactors may be lost in the solubilization process (e.g., for G protein-coupled receptors). This chapter documents the problems that may be encountered when experimenting with solubilized receptor preparations, and some of the strategies applied to overcome these difficulties, using the solubilization of the 5-HT_3 receptor from homogenates of pig cerebral cortex as an example.

2. Materials

2.1. Preparation of Brain Homogenate

1. Radioligand binding buffer: 25 m*M* Tris-HCl to pH 7.4. At least 100 mL of buffer should be prepared for each individual membrane preparation, and cooled to 4°C before use. It can be stored for up to 2 d at 4°C.

Table 1
Detergents Commonly Used for Receptor Solubilization[a]

Detergent	Micellular weight (Da)	Molecular weight (g)	CMC (m*M*)[b]	Types of receptor solubilized[c]	Head group	Notes
Triton X-100	90,000	625	0.2–0.9	Groups 1,2	Non-ionic	Hydrophobic. High mol wt & low CMC impedes removal by dialysis. High A_{280nm}. Interferes with Lowry protein assay. Micellular wt changes with temp.
Octyl glucoside	8000	292	20–25	Groups 1,2	Non-ionic	Can form hydrogen bonds.
Cholate	900–1800	431	3–15	Groups 1,2,3	Anionic	Rigid structure. May precipitate with metal ions. Increased ionic strength markedly decreases CMC. Inhibits adenylate cyclase.
Deoxycholate	1700–4200	415	1–6	Groups 1,2	Anionic	May precipitate with metal ions. Inhibits adenylate cyclase. Precipitates in the cold.
CHAPS	6200	615	3–10	Groups 1,2,3	Zwitterionic	Increased salt conc. reduces CMC.
Digitonin	70,000	1229	—	Group 3	Non-ionic	Complexes specifically with cholesterol and can solubilize cholesterol containing membranes. Not dialyzable. Expensive. Not readily soluble (*see* **Note 2**).

[a] Data from **refs. *1*** and ***2***.
[b] This varies according to the concentration of NaCl (*see* **ref. *1***).
[c] Group 1 = receptors with a single transmembrane segment (e.g., tyrosine kinase-linked receptors)
Group 2 = ligand gated ion channels (e.g., nicotinic acetylcholine receptor)
Group 3 = receptors coupled to G proteins (e.g., β-adrenoreceptor)

2. Source of receptors: we used pig cerebral cortex. 1.5 g wet wt of tissue is needed for each individual membrane preparation.
3. Cold room: for dissection of tissue.
4. Scalpel.
5. Insulated ice box and ice.
6. Polytron blender, or similar.
7. Refrigerated centrifuge, rotor and tubes. We used an 8 × 50 mL (JA-20) rotor for initial solubilization experiments, and a 6 × 250 mL (JA-14) rotor to scale up the process for purification.

2.2. Evaluation of Suitable Detergents for Solubilization Using Radioligand Binding

1. Radioligand binding buffer: 25 m*M* Tris-HCl, pH 7.4. At least 2l of buffer, plus 1l for each radioligand binding experiment, should be prepared and cooled to 4°C before use. It can be stored for up to 2 d at 4°C.
2. A range of detergents: e.g., Triton X-100, CHAPS, octyl glucoside (Sigma, Poole, Dorset, U.K. *see* **Subheading 1.** and **Table 1**). Detergents that have been used successfully for similar applications should provide a good starting point.
3. [^{3}H]-(S)-Zacopride (78 Ci/mmol, Amersham, Buckinghamshire, U.K.). This should be stored at −20°C, and diluted in radioligand binding buffer just before use.
4. Ondansetron (GR38032F; Glaxo-Wellcome, Stevenage, UK). A stock solution of 4×10^{-3} *M* in distilled water should be prepared and stored at −20°C for up to 3 mo. The stock solution should be diluted with radioligand binding buffer before use.
5. Glass test tubes: We have found that plastic tubes, although more convenient, do not give good results, probably owing to adhesion of the membrane preparation, drugs, or detergents to the test tube wall.
6. Brandel Cell Harvester.
7. Whatman GF/B filter paper.
8. Polyethyleneimine (PEI; Sigma, Poole, Dorset, U.K.). A 10% (v/v) stock solution in distilled water will last for up to one yr at room temperature.
9. 5 ml scintillation vials.
10. Scintillation fluid (Ecoscint A, National Diagnostics, Hull, UK).
11. Liquid scintillation spectrophotometer.

2.3. Determining the Optimum Concentration of Detergent to Solubilize the Receptor

2.3.1. Solubilization

1. Solubilization buffer (buffer A): 25 m*M* Tris-HCl, 2 m*M* EDTA, pH 7.4 cooled to 4°C. This can be stored for up to 2 d at 4°C. Just before use, a cocktail of protease inhibitors should be added; we used 0.2 m*M* PMSF (50 m*M* stock solution in methanol stable at 4°C for up to 6 mo), 20 μg/ml bacitracin (50 mg/mL

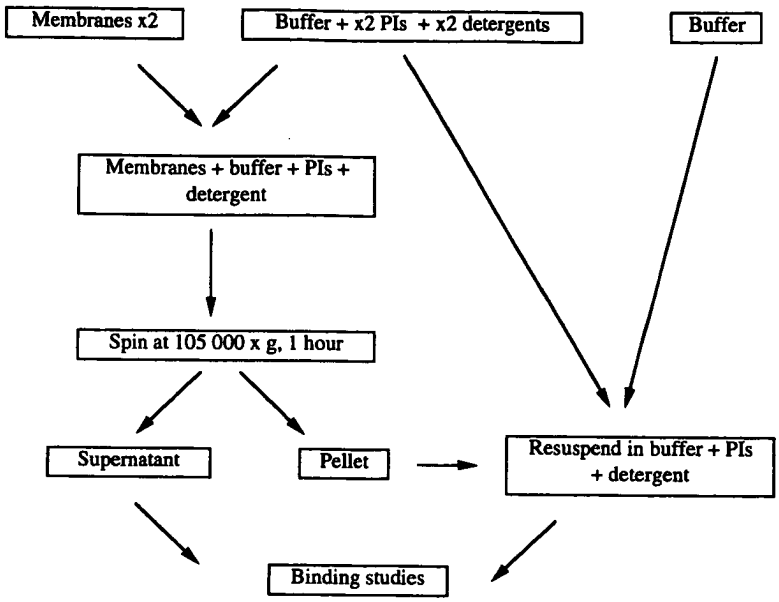

Fig. 1. Procedure for solubilizing receptors.

stock solution stable at 4°C for up to 4 wk), and 20 µg/mL soybean trypsin inhibitor (50 mg mL^{-1} stock solution stable at –20°C for up to 3 mo). The concentrations of the protease inhibitors and EDTA given here are double the final concentrations used in solubilization. (*See* **Subheading 3.3.1.** and **Fig. 1**). All the protease inhibitors were obtained from Sigma, Poole, Dorset, U.K. (*see* **Notes 5, 6, Table 2**).

2. A refrigerated ultracentrifuge capable of reaching at least 100,000g (e.g., Beckman L-60 ultracentrifuge), tubes and rotor. We used an 12 × 10 mL (70 Ti) capacity rotor for initial solubilization experiments, and a 10 × 26 mL (55.2 Ti) rotor to scale up the process for purification.
3. A tube rotator is very useful, but not essential. We used a "homemade" version, but several commercial makes are available.

2.3.2. *Radioligand Binding*

Requirements as in **Subheading 2.2.**

2.3.3. *Protein Estimation*

1. Protein quantifying reagent: BioRad Bradford method or DC (detergent compatible) reagents. We used the BioRad Bradford method reagent. A good review of protein counting methods is available in a companion volume to this series (Methods in Molecular Biology Vol. 32, Ch 1–3; *see also* **ref. *14*** and **Note 7**).

Table 2
Protease Inhibitors Used in Solubilization Studies[a]

Inhibitor	Class of Protease	Working Concentration	Notes
Aprotinin	kallikrein	1–10 µg/mL	Antibiotic. Soluble in water at 5 mg/mL. Store at 4°C.
Bacitracin	nonspecific	10–100 µg/mL	Antibiotic. 50 mg/mL stock in water stable for 2–4 wk at 4°C.
Chymostatin	chymotrypsin, papain	1–10 µg/mL	Antibiotic. 10m*M* or 10 mg/mL stock in DMSO stable for months at –20°C. Can also be dissolved in glacial acetic acid.
EDTA	metalloproteases, Ca^{2+} dep SH proteases	1–10 m*M*	Will not dissolve in buffers <~ pH = 8, but does not precipitate out as pH is lowered.
Leupeptin	serine and SH proteases	1–10 µg/mL	Antibiotic. 10 m*M* stock in water/buffer stable for 1 week at 4°C, 1 month at –20°C.
Pepstatin A	aspartic proteases	1–10 µg/mL	Antibiotic. 10 mg/mL stock will dissolve in ethanol but may require heating.
PMSF	serine proteases	0.1–1 m*M*	Toxic. Insoluble in water—dissolve (50 m*M* stock) in iso-propanol or (m)ethanol. Short half life—add immediately before use. Stable for months at ~ 4°C, can also store dilute stock at –20°C. Cysteine protease activity reversible by reduced thiols.
Trypsin inhibitor	trypsin	10–500 µg/mL	Protein. 50 mg/mL stock in water stable for weeks at –20°C.

[a] Data from **refs. *2,26***.

2. Disposable plastic cuvettes.
3. Spectrophotometer: set at 595 nm.

2.4. Improving the Yield of Solubilized Receptor

1. Salt: KCl, NaCl, or ammonium sulphate.
2. Phospholipids: phosphatidylcholine or asolectin.
3. Glycerol.

2.5. Characterization of the Solubilized Receptor Preparation

1. A range of structurally unrelated 5-HT_3 ligands, both agonists and antagonists, is required, e.g., granisetron (HCl; SmithKline Beecham, Harlow, Essex, U.K.),

5-HT (bimaleate; Sigma, Poole, Dorset, U.K.), *meta*-chlorophenylbiguanide (mCPBG; HCl; Research Biochemicals Inc., Natick, MA), ondansetron (hydrochloride dihydrate; Glaxo-Wellcome, Stevenage, U.K.), phenylbiguanide (PBG; Aldrich, Gillingham, Dorset, U.K.), tropisetron (ICS 205-930; Sandoz, Basle, Switzerland), (S)-zacopride (HCl; Delalande, Paris, France).

2. Radioligand binding requirements as in **Subheading 2.2.**

3. Methods

3.1. Preparation of Brain Homogenate

1. Pig brain tissue, obtained within 30 min of death, should be transported over ice.
2. Dissect the tissues in a cold (4°C) room, and store them at −80°C (in plastic bags kept in an airtight box) within 2 h of death.
3. Label 8 × 50 ml centrifuge tubes, and cool them on ice.
4. Gently thaw brain tissues over ice or in a cold room (just enough so that they may be cut easily by a clean scalpel blade) and homogenize 1.5 g of each tissue in 15 mL of ice-cold radioligand-binding buffer (25 m*M* Tris, pH 7.4) using a Polytron blender at full power for 10 s. The container holding the tissue (we found that the centrifuge tubes were the most convenient) should be held in a beaker of ice and water during the homogenization to keep the tissue cold. The blender should be cleaned with buffer or distilled water between each individual membrane preparation.
4. Add an extra 15 mL of buffer, and centrifuge the homogenate at 25,000*g* for 10 min, 4°C (*see* **Note 8**).
5. Discard the supernatant. Resuspend the pellet in 15 mL of Tris buffer using the blender at half power for 4 s, add another 15 mL of buffer, and centrifuge the homogenate at 25,000g for 10 min, 4°C. This step should be repeated at least twice for effective washing of the homogenate.
6. The pellet should be finally resuspended in 3.0 mL (for binding studies) or 1.5 mL (for solubilization studies) of buffer using the blender at half power (i.e., at a concentration of 500 or 1000 mg/mL wet weight, *see* **Note 9**).
7. The homogenate can be stored at −80°C for up to 3 wks. We have found that freshly prepared homogenates give increased levels of receptor binding, but it must be remembered that experimental procedures should be kept consistent for comparable results.

3.2. Evaluation of Suitable Detergents for Solubilization Using Radioligand Binding

1. Prepare a dilution series of each detergent up to and above the CMC of the detergent (e.g., 0–2 % Triton X-100 (= 0 - 110 × CMC), remembering that in this particular assay the detergent will be diluted 1:4 (see **step 4**) (*see* **Notes 10–12**). Detergent:protein (w/w) ratios covering a range of 10:1 to 0.1:1 should be examined. Commonly used ratios are 1:1 and 2–3:1 ***(15)***. A good reference source for the CMC of several detergents can be found in **refs.** ***1,15***; *see also* **Table 1.**

Table 3
Preparation of Brain Homogenate

Tube	Memb. prep.[a]	Buffer	Competing Agent	[^{3}H][b]	Comments
1–3	250 µL	250 µL	0 µL	500 µL	Total binding
4–6	"	0 µL	250 µL detergent at conc. A	"	
7–9	"	"	250 µL detergent at conc. B	"	
			etc		
43–45	"	"	250 µL of 10 µ*M* ondansetron[c]	"	Non-specific
46–48	0 µL	500 µL	0 µL	"	Filter blanks[d]

[a]Membrane preparation @ 100 mg mL^{-1} wet wt.
[b][^{3}H]-(S)-Zacopride to give a *final* concentration of 1 n*M*.
[c]Ondansetron to give a *final* concentration of 10 µ*M*.
[d]*See* **Note 13**.

2. Perform a competition binding assay using these detergents. First, cool a rack of 48 test tubes on ice, and allow a stock solution of ondansetron and any frozen membrane preparations to defrost.
3. Dilute the stock solution of ondansetron and the membrane preparation(s) appropriately in radioligand binding buffer. Ondansetron should be diluted to give a *final* concentration of 10 µ*M* i.e., the actual concentration needed is 4×10^{-5} *M*. At least 1 mL of diluted ondansetron is required per assay. The membrane preparation should be diluted to ~ 100 mg/mL wet wt, and kept on ice.
4. Each test tube, in triplicate, should contain the following (*see* **Table 3**).
   The buffer, detergent, and ondansetron should be added to the tubes first (*see* **Note 12**). Then the radioligand, [^{3}H]-(S)-zacopride, should be diluted appropriately in buffer to give a *final* concentration of 1 n*M* (i.e., the actual concentration is 2 n*M*) and added to each tube, and the membrane preparation added last of all to initiate binding (*see* **Note 14**).
5. Incubate the rack of tubes in a shaking waterbath at 37°C, for 1 h (this is sufficient for equilibrium of the radioligand binding to be acheived).
6. At least half an hour before the incubation is due to end, soak a Whatman GF/B filter paper (one for each rack of tubes) in ice-cold 0.3% PEI (10% stock diluted in radioligand binding buffer) at 4°C (i.e., in a cold room). (*See* **Note 15**.)
7. Ten minutes before the incubation is due to end, run at least 1L of ice-cold radioligand binding buffer through the Brandel Cell Harvester. Place the Harvester buffer bottle in a bucket of ice water to keep the buffer cold.

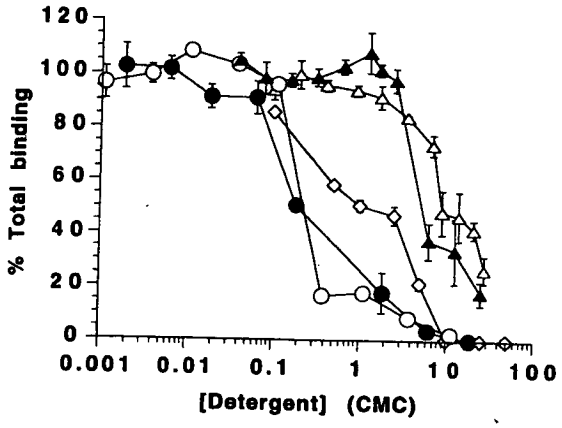

Fig. 2. Inhibition of [^{3}H]-(S)-zacopride binding to membrane bound 5-HT$_3$ receptors originating from pig cerebral cortex by various detergents; ● CHAPS, △ Triton X-100, ◇ deoxycholate, ○ octyl glucoside, ▲ GENAPOL. The final protein concentration (0.95–1.44 mg/mL) was constant for each experiment. Data represents mean ± SEM, n = 3.

The detergents with high CMC values (<1 m*M*; CHAPS, 3-5 m*M*; octyl glucoside, 19–25 m*M*; deoxycholate, 1–4 m*M*) markedly inhibited [^{3}H]-(S)-zacopride binding at concentrations below and around their CMC. The non-ionic detergent Triton X-100 (CMC ~0.25 m*M*) exhibited the least inhbition of [^{3}H]-(S)-zacopride binding above its CMC, and it was decided to use this detergent for further studies.

8. Place the presoaked filter paper in the Harvester.
9. Remove the rack of tubes from the waterbath, and *immediately* use the Harvester to suck the contents of the tubes through the filter paper, using 2 washes of 4 s each.
10. Using a pair of tweezers, transfer the filter paper circles (one for each tube) to small scintillation vials. Add 3.5 mL of scintillation fluid to each vial. Label the vials on the lids (*not* on the sides of the vials), and let stand overnight.
11. Vortex the vials, and then measure the radioactivity bound to the filters by using a liquid scintillation counter, set to read [^{3}H] dpm, with 2 min counting cycles.
12. From these results, determine which detergent shows the least inhibition of radioligand binding at concentrations above its CMC (*see* **Note 16, Fig. 2**).

3.3. Determining the Optimum Concentration of Detergent to Solubilize the Receptor

3.3.1. Solubilization

1. Prepare 500 mL of buffer (25 m*M* Tris, pH 7.4) containing protease inhibitors (*see* **Subheading 2.3.1., Note 6, Table 2**) at twice the final concentration required and cool to 4°C (buffer A).

2. Make up a solution of your chosen detergent at twice the final maximum concentration required e.g., 4% Triton X-100 to give a final concentration of 2%, in buffer A (*see* **Notes 10–12, Fig. 1**). Serially dilute this with buffer A to give a range of (double) concentrations of detergent.
3. Cool 4–8 ultracentrifuge tubes in ice. In each tube, mix ~2 mL of membrane homogenates (at double the concentration used in binding studies) with an equal volume of buffer A containing × 2 detergent (*see* **Note 17**).
4. Leave the tubes on a rotator at 4°C for 1 h. If no tube rotator is available, the tubes can be manually inverted a few times every 10–15 min. Excessive agitation should be avoided since foam formation is associated with the denaturation of proteins *(16)*.
5. Centrifuge the tubes at 105,000g for 1 h at 4°C. The supernatant contains the solubilized receptor. Carefully remove the supernatant for binding studies. Resuspend the pellet in buffer containing 1X protease inhibitors and detergent (dilute the solutions already made up with "normal" (25 m*M* Tris HCl, pH 7.4) buffer, *see* **Fig. 1**) for use in binding studies. This should ensure that any influence of detergent or protease inhibitors on radioligand binding will be equivalent in both preparations.

3.3.2. Radioligand Binding

1. Perform binding assays to determine the total and nonspecific binding in the supernatant and pellet at each detergent concentration (*see* **Subheading 3.2., steps 2–11**). Each test tube, in triplicate, should contain the following (added in the same order as in **Subheading 3.2.**, *see* **Table 4**).

3.3.3. Protein Estimation

1. Using a protein counting method, estimate the amount of protein in these supernatants and pellets. Determine which concentration of detergent gives the best solubilized receptor yield (*see* **Notes 7** and **18**), both in terms of % total (specific) binding of the "original," nonsolubilized receptor preparation, and as receptor density (fmol/mg protein, **Fig. 4,** *see* **Note 19**).

3.4. Improving the Yield of Solubilized Receptor

High ionic strength reduces electrostatic interactions between membrane components, and thus may increase yield. Therefore, the presence of salt (0.1–0.5 *M* KCl or up to 2.5 *M* NaCl) or ammonium sulphate (up to 800 m*M*) may increase the amount of receptor solubilized. They can easily be included in the solubilization buffer, but initially, their inhibition of radioligand binding should be investigated, as in **Subheading 3.2.** (*see* **Notes 20** and **21**). We found that the presence of NaCl (0.25–2 *M*) in the solubilization buffer had no significant effect on the yield of Triton X-100 solubilized 5-HT_3 receptor *(6)*, although at higher concentrations (1.5–2 *M*) there was a significant decrease in the specific binding (approx 50% of specific binding in the absence of salt).

Table 4
Radioligand Binding

Tube	Receptor Preparation	Buffer	Competing agent	[^{3}H][a]	Comments
1–3	75 µL memb. prep.[c]	225 µL	0 µL	300 µL	Total
4–6	"	75 µL	150 µL of 10 µ*M* OND[b]	"	Nonspecific
7–9	150 µL supernatant A[d]	150 µL	0 µL	"	Total
10–12	"	0 µL	150 µL of 10 µ*M* OND		Nonspecific
13–15	150 µL pellet A	150 µL	0 µL	"	Total
16–18	"	0 µL	150 µL of 10 µ*M* OND	"	Nonspecific
19–21	150 µL supernatant B	150 µL	0 µL	"	Total
22–24	"	0 µL	150 µL of 10 µ*M* OND		Nonspecific
25–27	150 µL pellet B	150 µL	0 µL	"	Total
28–30	"	0 µL	150 µL of 10 µ*M* OND	"	Nonspecific
			etc		
43–45	0 µL	300 µL	0 µL	"	Filter blank
46–48	"	300 µL +detergent[e]		"	Filter blank

[a] [^{3}H]-(S)-Zacopride to give a *final* concentration of 1 n*M*.
[b] Ondansetron (OND) to give a *final* concentration of 10 µ*M*.
[c] Needed to determine % yield. *See* **Figs. 3** and **4**.
[c] In general, a greater volume of solubilized receptor compared to membrane homogenates will be required to provide a comparable level of binding. *See* **Note 18**.
[e] *See* **Note 13**.

However, this contrasts with data for the same detergent solubilizing the 5-HT$_3$ receptor from a cell line *(5)* and may reflect a difference in receptor enviroment. Ammonium sulphate (200–800 m*M*) was found to inhibit [^{3}H]-(S)-zacopride binding, and did not improve the yield of Triton X-100 solubilized 5-HT$_3$ receptor. This contrasts with results obtained using sodium cholate to solubilize the 5-HT$_3$ receptor from rabbit tissue *(17)*.

The presence of exogenous phospholipids, e.g., phosphatidylcholine (0-1%), asolectin (0–2%) and/or glycerol (0–50% v/v, both pre- and postsolubilization), may stabilize the solubilized receptor in the absence of membranes, and thus increase yield (*see* **Note 1**). Again, they can be easily included in the solubilization buffer, but must be investigated as to their inhibition of radioligand binding. We found that glycerol (5–20%) and phosphatidylcholine (0.15–1%)

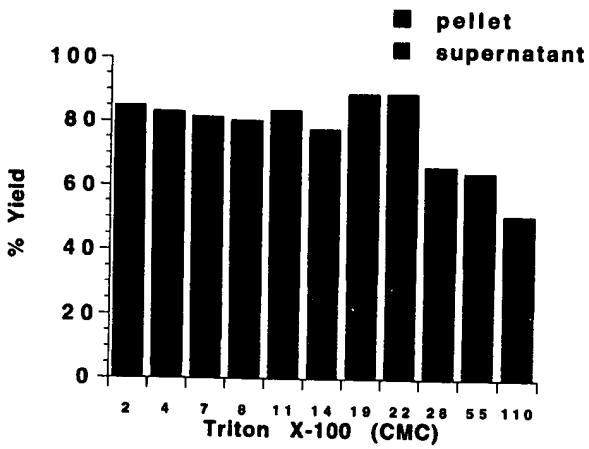

Fig. 3. Binding of [^{3}H]-(S)-zacopride to the supernatants and pellets obtained during Triton X-100 solubilization of the 5-HT$_3$ receptor from homogenates of pig cerebral cortex, calculated as a percentage of the binding present in the homogenate preparation pre-solubilization (mean ± SEM, n = 2–13). The pellets were resuspended in an equal volume of solubilization buffer containing the appropriate concentration of Triton X-100 before assessing 5-HT$_3$ receptor levels by radioligand binding. It can be seen that Triton X-100, at a concentration of 22 times its CMC, gave the best yield of solubilized 5-HT$_3$ receptor in the supernatant. It is also apparent that at higher concentrations of Triton X-100 the total % yield decreases, this is probably owing to increasing inhibition of [^{3}H]-(S)-zacopride binding by the detergent.

inhibited [^{3}H]-(S)-zacopride binding to the 5-HT$_3$ receptor, and did not improve the yield of Triton X-100 solubilized 5-HT$_3$ receptor. Glycerol also has an advantage in that it is a nonspecific protease inhibitor at moderate concentrations (20% w/v, **ref. *18***). However, the presence of glycerol affects both the viscosity and the density of the medium and may therefore change the behavior of the preparation in the centrifuge or on chromatography columns.

3.5. Characterization of the Solubilized Receptor Preparation and Criteria for Receptor Identification

Once the optimum detergent and conditions for solubilization have been determined, the solubilized receptor preparation can be characterized using radioligand binding studies, as in **Subheading 3.2., steps 2–11**. For competition studies, test tubes, in triplicate, should contain the following (*see* **Table 5**).

For saturation studies, test tubes, in triplicate, should contain the following (*see* **Table 6**).

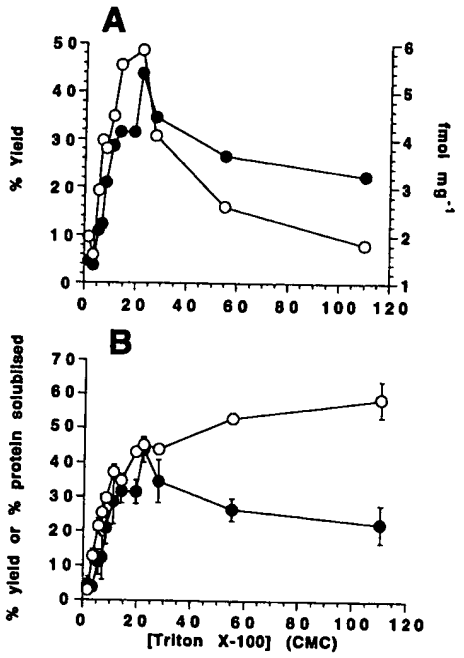

Fig. 4. Determining the optimum concentration of Triton X-100 to solubilize 5-HT_3 receptors from homogenates of pig cerebral cortex. (**A**) Although the density of solubilized 5-HT_3 receptor (○, fmol mg^{-1}, assessed by [^{3}H]-(S)-zacopride (1 n*M*) binding) was comparable when using Triton X-100 at concentrations of 14 × (0.25 %) and 22 × (0.4 %) its CMC, it can be seen that Triton X-100 at a concentration of 22 × its CMC gave the best yield (●, calculated as a % of the specific binding of the non-solubilized receptor preparation). Data represents mean ± SEM, n = 3–13. (**B**) Effect of Triton X-100 concentration on the yield (●, calculated as a % of the binding of the homogenate preparation pre-solubilization) of solubilized 5-HT_3 receptors and total protein (○) from pig cerebral cortex membranes. As the concentration of detergent was increased, the amount of protein solubilised also increased, but above 0.4% Triton X-100 (22 × CMC) there was no further increase in receptor yield. Figure redrawn from **ref. *6***.

Several criteria can be investigated when assessing the integrity of a solubilized receptor by radioligand binding, including the affinity of ligands, the number of receptor sites, reversibility (i.e., competition by a nonradiolabeled ligand) and stereospecificity. For example, the functional state of the solubilized $GABA_A$ receptor has been defined as the preservation in detergent solution of the ligand-binding properties and the corresponding allosteric interactions between these sites *(7)*.

Table 5
Solubilized Recepter Preparation Characterized Using Radioligand Binding Studies

Tube	Solubilized Receptor	Buffer	Competing Agent	[^{3}H][a]	Comments
1–3	150 µL	150 µL	0 µL	300 µL	Total binding
4–6	"	0 µL	150 µL drug at conc. A	"	
7–9	"	"	150 µL drug at conc. B	"	
			etc		
43–45	"	"	150 µL of 10 µ*M* ondansetron[b]	"	Non-specific
46–48	0 µL	300 µL	0 µL	"	Filter blanks[c]

[a] [^{3}H]-(S)-Zacopride to give a *final* concentration of 1 n*M*.
[b] Ondansetron to give a *final* concentration of 10 µ*M*, *see* **Note 22**.
[c] *See* **Note 13**.

Table 6
Saturation Studies

Tube	Solubilized Receptor	Buffer	Competing Agent	[^{3}H]	Comments
1–3	150 µL	150 µL	0 µL	300 µL at conc. A	Total binding
4–6	"	0 µL	150 µL of 10 µ*M* OND[a]	"	Nonspecific
7–9	"	150 µL	0 µL	300 µL at conc. B	Total binding
10–12		0 µL	150 µL of 10 µ*M* OND		Nonspecific
			etc		
46–48	0 µL	300 µL	0 µL	"	Filter blanks[b]

[a] Ondansetron (OND) to give a *final* concentration of 10 µ*M*.
[b] *See* **Note 13**.

Solubilization may change the affinity of the receptor for ligand(s), or it may change the number of detected binding sites. We found that solubilization of the 5-HT_3 receptor from pig brain did not alter the affinity of our radioligand, [^{3}H]-(S)-zacopride, (K_d = 1.62 ± 0.35 and 1.57 ± 0.53 n*M*, mean ± SEM, n = 6, for the membrane bound and solubilized receptor preparations respectively), but a decrease in the density of receptor in the solubilized receptor preparation was detected (B_{max} = 21 ± 4 fmol/mg compared with 54 ± 6 fmol/mg for the membrane bound receptor, mean ± SEM, n = 6, **Fig. 5**). Presumably, this reflects a more efficient solubilization of non-5-HT_3 receptor protein relative to 5-HT_3 receptor protein. Despite extensive "optimization" experiments, we were unable to improve the density of 5-HT_3 receptors in the solubilized receptor preparation. However, the pharmacological profile of the solubilized 5-HT_3 receptor preparation was comparable to that of the receptor sites in crude homogenates (the correlation coefficient between the pKi values of structur-

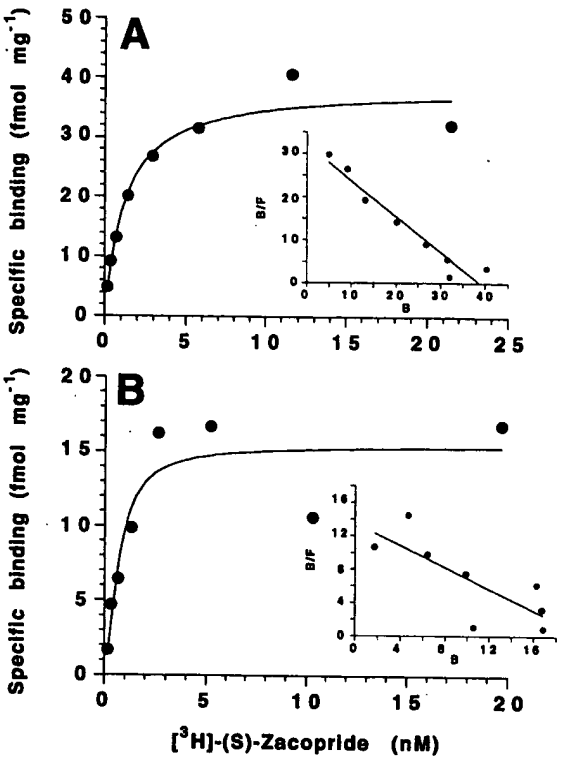

Fig. 5. Representative saturation data for [^{3}H]-(S)-zacopride (0.2–32.2 n*M*) binding to (**A**) membrane bound and (**B**) solubilized (Triton X-100, 0.4 %) 5-HT$_3$ receptor preparations originating from pig cerebral cortex. Values represent the specific binding calculated from triplicate determinations of total and non-specific binding (defined by the presence of ondansetron, 10 μ*M*). Inset: subsequently derived Scatchard plot (B, specifically bound radioligand (fmol mg^{-1} protein); B/F, specifically bound radioligand/free concentration of radioligand (fmol mg^{-1} protein/n*M*)). Adapted from **ref. *29***.

ally unrelated compounds competing for [^{3}H]-(S)-zacopride binding in the membrane bound and solubilised 5-HT$_3$ receptor preparations was r = 0.99, *see* **Figs. 6** and **7**).

The detergent may interact with the ligand (e.g., **ref. *19***), giving the appearance of a high capacity, low affinity binding site, or it may interact with the receptor itself, either directly at the binding site (steric hindrance), or by modulating binding through a change in the conformation of the protein or lipid surroundings. In particular, excess concentrations of detergent may displace lipids essential to maintain a native conformation of the receptor ***(8)***. This may

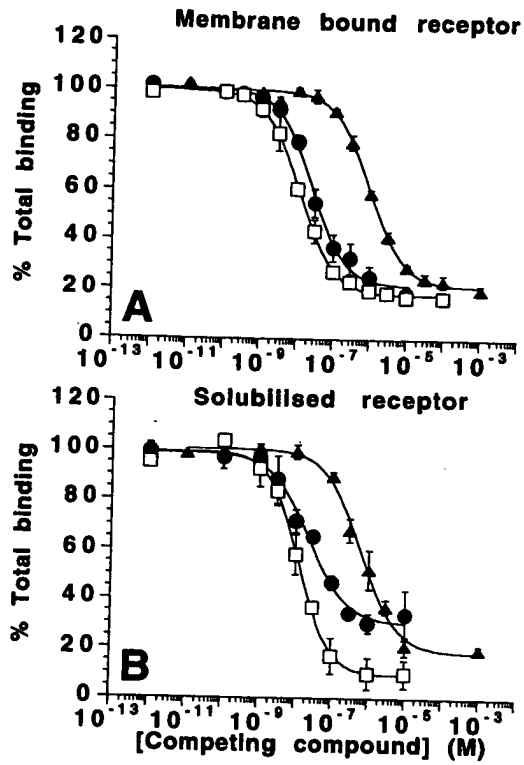

Fig. 6. Representative examples of three 5-HT_3 receptor ligands (● ondansetron, □ mCPBG, ▲ 5-HT.) competing for [^{3}H]-(S)-zacopride (~1 n*M*) binding in membrane bound and solubilized (Triton X-100, 0.4 %) 5-HT_3 receptor preparations from pig cerebral cortex. Data represents the mean ± SEM, n = 3.

explain the apparent decrease in total binding (supernatant + pellet) of the 5-HT_3 receptor at higher detergent concentrations (**Fig. 3**). Direct interaction of ligand and detergent in the absence of receptor can be shown by gel filtration, giving a peak of labeled ligand at the mol wt of the detergent micelle *(18)*. Some detergent-receptor effects may be reversed by dilution of the detergent (*see* **Note 18, Fig. 8**). The number of binding sites available at different detergent concentrations may also differ *(3)*, whereas at higher concentrations, the detergent may be acting in a similar manner to membrane lipids by shielding and reducing the number of available sites.

4. Notes

1. For ligand-gated ion channels, the addition of exogenous phospholipids, either derived from the tissue from which the receptor is solubilized, or from an exog-

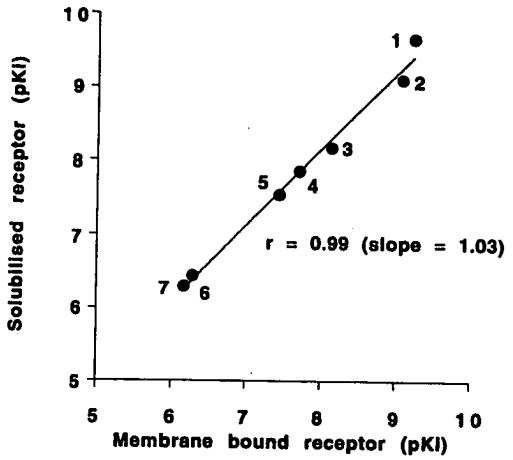

Fig. 7. Correlation of the affinity (pKi) of several compounds for the [^{3}H]-(S)-zacopride labeled 5-HT$_3$ receptor in homogenates of pig cerebral cortex and in solubilized (Triton X-100, 0.4 %) 5-HT$_3$ receptor preparations. Numbered compounds are: 1 granisetron, 2 (S)-zacopride, 3 mCPBG, 4 ondansetron, 5 tropisetron, 6 5-HT, 7 phenylbiguanide. Data from **ref. *6***.

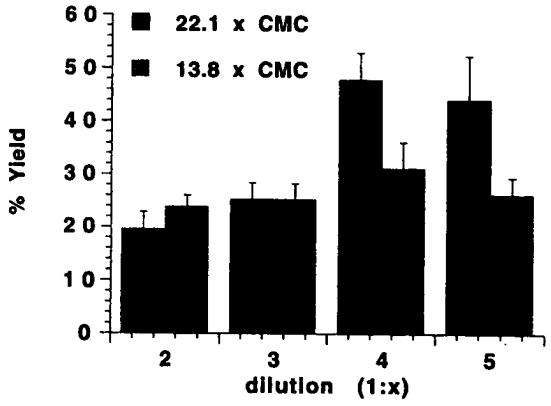

Fig. 8. 5-HT$_3$ receptors were solubilized from homogenates of pig cerebral cortex using two different concentrations of Triton X-100. 150 µL of solubilized receptor preparation was diluted in the binding assay in a total volume of 750 µL (1:5 dilution), 600 µL (1:4), 450 µL (1:3) or 300 µL (1:2). The binding of [^{3}H]-(S)-zacopride to the soluibilzed receptor preparation at each dilution was calculated as a percentage yield of the binding present in the homogenate receptor preparation pre-solubilization (mean ± SEM, n=3). It can be seen that dilution of the solubilized receptor preparations 1:4 or 1:5 produces an increase in % yield, by reversal of some of the inhbition of [^{3}H]-(S)-zacopride binding.

enous source (e.g., phosphatidylcholine, soybean lipids ("asolectin"), is often necessary to preserve full functionality, in particular for reconstitution of the ion channel, and to maintain any allosteric properties of the receptor *(7,8,9)*. Cholesterol may also be utilized to maintain functional integrity of the receptor *(20)*. For solubilization of G protein-coupled receptors, maintenance of the lipid enviroment of the receptor protein can also be very important (*13,21*, note also **ref. *22***). Hydrophobic detergents such as Triton X-100 and Thesit extract relatively high levels of protein relative to lipid *(15)*.

2. To use digitonin, an aqueous suspension of 2% should be prepared using distilled water, boiled for 5–10 min, allowed to cool and any precipitate filtered off. Precipitation will continue for up to a week. Digitonin remains in solution better when used in combination with sodium cholate (e.g., 10:1 ratio).
3. Bile salt detergents (cholate or deoxycholate) inhibit adenylate cyclase *(23)*; therefore, other detergents such as CHAPS would be more suitable if the transduction system associated with such a receptor is to be examined subsequently. It has also been reported that the 5-HT_3 receptor is not stable in bile salt detergents e.g. > 80% of deoxycholate solubilized 5-HT_3 receptor activity was lost after overnight storage at 4°C *(24)*, and ~50% of sodium cholate solubilized 5-HT_3 receptor-binding activity was lost during 1 d at 4°C *(17)*. The stability of the receptor in detergent for long periods is an essential prerequisite for time-consuming procedures such as purification.
4. Nonionic or zwitterionic detergents should preferentially be used for subsequent charge-based procedures such as ion exchange chromatography or electrophoresis.
5. In choosing a buffer for solubilization, the buffer used for radioligand binding studies on the native receptor is a good starting point. If this buffer contains divalent cations (e.g., Krebs buffer), however, it may be advisable to leave these out as they will activate proteases—there are numerous buffers available that do not contain divalent cations (e.g., Tris, HEPES, and so forth). However, if divalent cations are essential for the assay, detergents that scavenge these should not be used. For example, detergents containing carboxylate anions (e.g., EMPIGEN, N-lauryl sarcosinate, some bile salts) form insoluble precipitates with divalent cations. Most receptors have an optimum pH for ligand-binding reactions, that, when possible, should be utilized in the buffer. Since electrostatic interactions between membrane components are a major intermolecular force, the ionic strength of the buffer is extremely important. If strict control of ionic strength is required, detergents that have a net charge should not be used. Where possible, high ionic strength conditions should be employed to dissociate components held together by electrostatic forces (e.g., 0.1–0.5 M KCl or 0.25–2 M NaCl). It is also possible to achieve high ionic strength by using elevated buffer concentrations. Phosphate is more efficient than Tris as a solubilization buffer *(18)*, and is capable of solubilizing some membrane proteins when used alone at relatively high concentrations *(25)*. It should be noted that anionic detergents are soluble only at a pH greater than that of the pKa of their ionizable group, conversely cationic detergents are soluble only at a pH smaller than their pKa.

6. A problem often encountered in solubilization studies is the liberation of endogenous proteases that occurs following lysis of the membrane and the increased surface area of membrane proteins available to proteases. Low temperatures and a cocktail of protease inhibitors that cover the various classes of proteases is used to prevent hydrolysis of receptors (e.g., PMSF inhibits serine proteases, EDTA or EGTA inhibits Ca^{2+} activated proteases and metalloproteases. Bacitracin is a general protease inhibitor). A table of commonly used protease inhibitors and their working concentrations is given in **Table 2**. A good review of proteolysis is available in **ref. *26***. Protease inhibitors, especially PMSF, lose their activity within hours at room temperature; consequently, it is best to add these just before use. Protein or peptide inhibitors such as the antibiotic bacitracin should not be used if the solubilized receptor is to be microsequenced following purification studies.
7. Several detergents interfere with commonly used protein assays. This can be overcome by precipitating the protein from the detergent solution. Most proteins will be precipitated by addition of 4 vol of acetone (or ethanol) and 1 vol of distilled water, or by addition of 10% trichloroacetic acid, at 4°C. The precipitate may be encouraged by centrifuging in a microcentrifuge for 5 min, and any remaining acetone left to evaporate for a few minutes after the supernatant has been discarded. UV spectroscopy at 280 nm can also be used to determine protein concentration ***(14)***, but this requires between 0.05 and 2 mg of relatively pure protein, and detergents such as Triton X-100 interfere with UV measurements in this region, although nonabsorbing analogs are available. We have found that Triton X-100 at concentrations of > 0.1% interferes with the BioRad Bradford Method protein assay, but dilution of the solubilized receptor 1:10 with buffer (to bring the protein concentration into the range covered by the standards) removed this problem.
8. The actual length of time in the centrifuge may need to be increased to give a full 10 min spin at 25000*g*; we found that our centrifuge took 2 min to accelerate to 25000*g* so we used a spin time of 12 min.
9. A protein concentration of 1–10 mg/mL (100–500 mg/mL wet wt tissue) is suitable for an initial solubilization experiment. If the protein concentration is too small, significant losses can occur owing to surface adsorption ***(16)***. In general, the procedure usually employed for the preparation of membrane/cell homogenates can be followed; however, it is useful to make these receptor preparations twice as concentrated as usual, so that in the solubilization procedure they can be diluted with an equal vol of solubilization buffer containing double concentrations of detergent and protease inhibitors (**Fig. 1**). To determine the optimum detergent:protein ratio for solubilizing a particular protein, the protein concentration should ideally be kept constant from experiment to experiment while varying the detergent concentration.
10. Detergents such as Triton X-100, which are supplied as a liquid, are viscous and difficult to measure out by pipet in the normal way. We have found that cutting the end off a 5 mL pipet tip enables us to pipet out such detergents, rinsing the tip with buffer afterwards. Alternatively, these detergents can be weighed out.

11. Detergents which are difficult to dissolve in aqueous buffer may be helped by gently heating the solution to ~ 80°C. (N.B. cool before use).
12. Solutions of detergents are difficult to pipet out normally, as they are very "bubbly." We suggest using the reverse pipet technique; depressing the push button all the way to the second stop, draw solution up slowly, and deliver the required volume by gently depressing the push button to the first stop only. It is a good idea to gently wipe the tip with a tissue after drawing the solution up, and to wipe the tip on the side of the test tube to avoid drop formation after pipeting the solution out.
13. We have noticed that the presence of detergent alters the amount of radioligand binding to the filter paper; therefore, appropriate concentrations should always be included in the filter blanks.
14. The actual volumes used can be increased or decreased by a constant factor if required, but the concentration of the membrane preparation must be altered by the same factor e.g., from 100 mg/mL to 500 mg/mL if using 50 µL of membrane preparation rather than 250 µL.
15. PEI coats filter papers with a negative charge, which encourages the binding of proteins. It is used to help trap solubilized receptor on the filter when separating the bound and unbound radioligand. The use of charged detergents may interfere with this. Some solubilized receptors have been reported to pass through GF/B glass fiber filters, so alternative separation methods may be required. Three possibilities include precipitation of the receptor with polyethylene glycol (PEG) followed by filtration, filtration through ion exchange filters, and charcoal absorption *(27)*.
16. Some high CMC detergents, such as CHAPS and octyl glucoside, are only successful in solubilizing receptors at concentrations below their CMC *(18)*. If it is suspected that these detergents would be successful in solubilizing a particular receptor, it would be advisable to compare the yields obtained with several detergent at one particular concentration (e.g., 0.1%). If such a high CMC detergent appeared to be giving better or comparable yields to another detergent previously demonstrated to show the least inhibition of radioligand binding at a concentration above its CMC, it would be worthwhile investigating further the ability of the high CMC detergent to solubilize the receptor at various concentrations below its CMC.
17. The microcentrifuge tubes should be free of defects, as they may implode under pressure, particularly if not full.
18. Dilution of the detergent in the solubilized receptor preparation may give an apparent increase in the binding of the radioligand to the receptor by reversing some of the inhibition of binding caused by the detergent. For example, we have found that, when Triton X-100 was present at concentrations of 0.4%, dilution of 150 µL of solubilized 5-HT_3 receptor preparation in a total volume of 600 µL (1:4 dilution) as opposed to a total volume of 300 µL (1:2 dilution) or 450 µL (1:3 dilution) gave an increase in the level of [^{3}H]-(S)-zacopride binding, and thus a greater yield (**Fig. 8**).

19. The specific activity of [^{3}H]-(S)-zacopride used was 78 Ci mmol^{-1}. 1 Ci = 2.2×10^{12} dpm; therefore, 1 fmol gives 173.16 dpm.
20. Ammonium sulphate (500 m*M*) has also been found to inhibit CHAPS-solubilized adenylate cyclase activity *(23)*.
21. The presence of salt is known to decrease the CMC of charged detergents, such as SDS (28), since it reduces the repulsion between the charged headgroups, allowing micelles to form at lower concentrations. Furthermore, it has recently been shown that there is a significant reduction in CMC with increasing salt concentration for the zwitterionic detergent CHAPS (28). This is significant given that CHAPS is effective at solubilizing receptors at concentrations below its CMC (*see* **Note 16, ref. *18***).
22. We have found that the specific binding determined as a percentage of the total binding can vary for each solubilized receptor preparation; however, the use of ondansetron as a reference compound to determine nonspecific binding means that the results from such experiments are still comparable.

References

1. Neugebauer, J. (1992) A guide to the properties and uses of detergents in biology and biochemistry. Calbiochem-Novabiochem Corporation, CA, pp. 1–62.
2. Haga, T., Haga, K., and Hulme, E. C. (1990) Receptor Biochemistry: A Practical Approach (Hulme, E. C., ed). IRL Press, Oxford, UK, pp. 1–50.
3. Gould, R. J., Ginsberg, B. H., and Spector, A. A. (1981) Effects of octyl β-glucoside on insulin binding to solubilized membrane receptors. *Biochemistry* **20,** 6776–6781.
4. Liscia, D. S., Alhadi, T., and Vonderhaar, B. K. (1981) Solubilization of active prolactin receptors by a nondenaturing zwitterionic detergent. *J. Biol. Chem.* **257,** 9401–9405.
5. Boess, F. G., Lummis, S. C. R., and Martin, I. L. (1992) Molecular properties of 5-hydroxytryptamine$_3$ receptor type binding sites purified from NG108-15 cells. *J. Neurochem.* **59,** 1692–1701.
6. Fletcher, S. and Barnes, N. M. (1997) Purification of 5-hydroxytryptamine$_3$ receptors from pig brain. *Br. J. Pharmacol.* **122,** 655–662.
7. Stephenson, F. A. (1988) Understanding the GABA$_A$ receptor: a chemically gated ion channel. *Biochem. J.* **249,** 21–32.
8. Anholt, R., Lindstrom, J., and Monttal, M. (1981) Stabilization of acetylcholine receptor channels by lipids in cholate solution and during reconstitution in vesicles. *J. Biol. Chem.* **356,** 4377–4387.
9. McCarthy, M. P. and Moore, M. A. (1992) Effects of lipids and detergents on the conformation of the nicotinic acetylcholine receptor from *Torpedo californica*. *J. Biol. Chem.* **267,** 7655–7663.
10. Caron, M. G. and Lefkowitz, R. J. (1976) Solubilization and characterisation of the beta-adrenergic receptor binding sites of frog erythrocytes. *J. Biol. Chem.* **251,** 2374–2384.
11. Zweig, A., Siegel, M. I., Egan, R. W., Clark, M. A., Shorr, R. G. L., and West, R. E. (1992) Characterization of a digitonin-solubilized bovine brain H3 histamine

receptor coupled to a guanine nucleotide-binding protein. *J. Neurochem.* **59,** 1661–1666.

12. Simonds, W. F., Koski, G., Streaty, R. A., Hjelmeland, L. M., and Klee, W. A. (1980) Solubilization of active opioid receptors. *Proc. Natl. Acad. Sci. USA* **77,** 4623–4627.
13. Balen, P., Kimura, K., and Sidhu, A. (1994) Specific phospholipid requirements for the solubilization and reconstitution of D-1 dopamine receptors from striatal membranes. *Biochem.* **33,** 1539–1544.
14. Dunn, M. J. (1989) Protein Purification Methods, A Practical Approach (Harris, E. L. V. and Angal, S., eds). IRL Press, Oxford, UK, pp. 10–16.
15. Bannerjee, P., Joo, J. B., Buse, J. T., and Dawson, G. (1995) Differential solubilization of lipids along with membrane proteins by different classes of detergents. *Chem & Physics of Lipids* **77,** 65–78.
16. Hjelmeland, L. (1990) Solubilization of native membrane-proteins. *Methods in Enzymology* **182,** 253–264.
17. Gordon, J. C., Sarbin, N. S., Barefoot, D. S., and Pinkus, L. M. (1990) Solubilization of a 5-HT_3 binding site from rabbit small bowel muscularis membranes. *Eur. J. Pharmacol.* **188,** 313–319.
18. Hjelmeland, L. M. and Chrambach, A. (1984) Membranes, Detergents and Receptor Solubilization (Venter, J. C. and Harrison, L. C., eds). Alan R. Liss, New York, pp. 35–46.
19. Shiu, R. P. C. and Friesen, H. G. (1974) Solubilization and purification of a prolactin receptor from the rabbit mammary gland. *J. Biol. Chem.* **249,** 7902–7911.
20. Criado, M., Eibl, H., and Barrantes, F. J. (1982) Effects of lipids on acetylcholine receptor. Essential need of cholesterol for maintenance of agonist-induced state transitions in lipid vesicles. *Biochem.* **21,** 3622–3629.
21. Rinken, A. (1995) Subtype-specific changes in ligand binding properties after solubilization of muscarinic receptors from baculovirus-infecetd Sf9 insect cell membranes. *J. Pharm. Exp. Ther.* **272,** 8–14.
22. Houston, D. B. and Howlett, A. C. (1993) Solubilization of the cannabinoid receptor from rat brain and its functional interaction with guanine nucleotide-binding proteins. *Mol. Pharm.* **43,** 17–22.
23. Bitoni, A. J., Moss, J., Hjelmeland, L., and Vaughan, M. (1982) Resolution and activity of adenylate cyclase compounds in a zwitterionic cholate derivative. *Biochem.* **21,** 3650–3653.
24. McKernan, R. M., Quirk, K., Jackson, R. G., and Ragan, C. I. (1990) Solubilisation of the 5-hydroxytryptamine receptor from pooled rat cortical and hippocampal membranes. *J. Neurochem.* **54,** 924–930.
25. Dey, A. C., Sheilagh, R., Rimsay, R. L., and Senciall, I. R. (1981) A simple procedure for the solubilization of NADH-cytochrome b_5 reductase. *Anal. Biochem.* **110,** 373.
26. Beynon, R. J. (1990) Protein Purification Methods, A Practical Approach (Harris, E. L. V. and Angal, S., eds)., IRL Press, Oxford, UK, pp. 40–50.

27. Janssen, M. J., Stegeman, M., Ensing, K., and Zeeuw, R. A. (1996) Solubilized benzodiazepine receptors for use in receptor assays. Journal of Pharmaceutical and *Biomed. Anal.* **14,** 989–996.
28. Chattopadhay, A. and Harikumar, K. G. (1996) Dependence of critical micellular concentration of a zwitterionic detergent on ionic strength: implications in receptor solubilization. *FEBS Letts* **391,** 199–202.
29. Fletcher, S. and Barnes, N. M. (1996) Distribution and characterisation of the [^{3}H]-(S)-zacopride labelled 5-HT_3 receptor in pig forebrain. *Brain Res.* **729,** 281–284.

5

Solubilized Muscarinic Acetylcholine Receptors from the Rat Myocardium: Pharmacological and Hydrodynamic Characterization

Christopher P. Berrie and Mary Keen

1. Introduction

The vast majority of receptors are membrane proteins, so solubilization is an essential prerequisite for purification of these receptors. If the receptor can be solubilized without destroying its characteristic ability to bind specific ligands, it is possible to use the powerful tool of affinity chromatography in the purification procedure. Furthermore, investigation of the pharmacological and hydrodynamic characteristics of solubilized receptors can, in itself, yield useful information about receptor function, particularly regarding the role of accessory proteins and/or membrane lipids in ligand binding.

During the early 1970s, many different systems were devised for the purification of membrane proteins and active membrane complexes *(1)*. However, because of their low abundance and sensitivity to denaturation by detergents, it was only in the late 1970s that cell surface neurotransmitter and hormone receptors began to be successfully solubilized *(2)*.

The fundamental problem in all attempts to solubilize neurotransmitter and hormone receptors is that of choice of detergent. The suitability of a particular detergent system for solubilization of a particular membrane protein depends on the ability of the detergent to displace membrane lipid from hydrophobic domains of the protein without disrupting any protein/protein, protein/lipid, or intramolecular interactions that are essential to the active conformation of that protein. Thus, denaturing detergents, such as SDS, are extremely efficient at removing proteins from membranes, but will also disrupt the tertiary and secondary structures of the protein molecule. Furthermore, the degree of such dis-

From: *Methods in Molecular Biology, Vol. 106: Receptor Binding Techniques*
Edited by: Mary Keen © Humana Press Inc., Totowa, NJ

ruptive effects is also highly dependent on the precise solubilization conditions employed, including detergent:protein ratio, temperature, and length of the solubilization incubation *(1)*. Unfortunately, there is no way of predicting which detergent system (if any) will allow solubilization of a particular receptor in its active conformation. The only way to develop a solubilization strategy is by trial and error (*see* Chapter 4).

In the case of the muscarinic acetylcholine receptor, retention of ligand binding activity has been demonstrated in a variety of detergent systems, including Lubrol PX, CHAPS, lysophosphatidylcholine, cholate, and digitonin *(2,3)*. This chapter describes the methods used to solubilize muscarinic receptor from the rat myocardium using digitonin. This procedure typically results in the recovery of 30–40% of the membrane receptors in the solubilized preparation, with the remainder being retained undenatured in the membrane *(4)*. An interesting characteristic of muscarinic receptors solubilized from the heart is that these receptors retain their ability to couple to guanine nucleotide-binding (G) proteins. This chapter describes how the receptor-G protein interaction can be studied pharmacologically, by determining the effect of guanine nucleotides on agonist binding, and hydrodynamically, by examining the behavior of receptors in sucrose density gradient centrifugation. Further methods for studying receptor-G protein complexes in solution can be found in **ref. *5***.

2. Materials

2.1. Myocardial Membrane Preparation

1. HEPES buffer: 20 m*M* HEPES, adjusted to pH 7.5 by the addition of NaOH. This buffer may be prepared in liter quantities and stored at 4°C.
2. KCl/PPi solution: 3*M* potassium chloride, 250 m*M* disodium pyrophosphate, stored at 4°C.
3. Refrigerated centrifuge, rotor, and tubes, suitable for performing high-speed centrifugation of reasonably large volumes. We found an 8 × 50-mL capacity rotor to be most useful.
4. HEPES/10 m*M* EDTA: 20 m*M* HEPES, 10 m*M* EDTA, adjusted to pH 7.5 by the addition of NaOH. This buffer may be prepared in liter quantities and stored at 4°C.
5. HEPES/0.1 m*M* EDTA: 20 m*M* HEPES, 0.1 m*M* EDTA, adjusted to pH 7.5 by the addition of NaOH. This buffer may be prepared in liter quantities and stored at 4°C.

2.2. Digitonin Solubilization

1. HEPES/Mg^{2+}: 20 m*M* HEPES, 5 m*M* $MgCl_2$, adjusted to pH 7.5 by the addition of NaOH. This buffer may be prepared in liter quantities and stored at 4°C.
2. Digitonin stock solution: digitonin (Wako Fine Chemicals, Osaka, Japan) as a 10% or 4% (w:v) solution in HEPES/Mg^{2+} (*see* **Note 1**). This solution may be prepared in 10–20 mL quantities and stored at 4°C for several days.

2.3. Radioligand Binding

1. [^{3}H]-oxotremorine-M (Amersham, International, Little Chalfont, UK): The undiluted stock solution should be stored at –20°C and diluted in HEPES/Mg^{2+} as required, just before use.
2. GppNHp: guanylylimidodiphosphate (Sigma, Poole, U.K.) is routinely prepared as a 10 m*M* solution in HEPES/Mg^{2+} just before use. Any remaining solution may be stored at –20°C for use on another occasion.
3. [^{3}H]-NMS: Undiluted [^{3}H]-N-methyscopolamine (Amersham) stock solution should be stored at –20°C and diluted in HEPES/Mg^{2+} as required, just before use.
4. QNB (3-quinuclidinylbenzilate): In the studies described here, QNB (at a final concentration of 1 μM) was routinely used to define nonspecific binding (*see* **Note 2**). It was synthesized by B. Peck (National Institute for Medical Research, London, U.K.) and was stored at 4°C as a 10 m*M* stock solution in 50% ethanol/water (v/v). The preparation of this stock solution requires time, continuous stirring, and gentle heating to coax the QNB into solution.
5. Atropine (Sigma, Poole, UK): is much more readily available than QNB and can be used to define nonspecific binding, using a final concentration of 1 μM (*see* **Note 2**). Stock solutions of atropine can be stored at 4°C for up to 1 wk if they are prepared in H_2O; they are much less stable in buffer.
6. Oxotremorine-M: synthesized by B. Peck.
7. Cold room: Many of these procedures need to be performed at 4°C in a cold room or cabinet.

2.4 Separation of Bound Radioligand from Free Radioligand

1. Gel filtration columns; plastic columns with a small internal diameter and a volume of 4–6 mL. We used demountable columns from Konte, cut down to half-length, giving an internal volume of approx 5 mL and plugged with disks of sintered glass.
2. Sephadex G50M resin (Pharmacia, Uppsala, Sweden).
3. Scintillant: any water-miscible scintillant, such as Liquiscint (National Diagnostics) or Ecoscint (National Diagnostics).

2.5. Sucrose Density Gradient Centrifugation

1. 5% sucrose solution: 5% sucrose (w:v) in HEPES/Mg^{2+}, containing 0.2% digitonin and radioligand as appropriate, prepared just before use and kept on ice.
2. 20% sucrose solution: 20% sucrose (w:v) in HEPES/Mg^{2+}, containing 0.2% digitonin and radioligand as appropriate, prepared just before use and kept on ice.
3. Small gradient maker with minimal "dead" volume (i.e., as small a volume as possible between the two chambers).
4. Peristaltic pump, such as the P1 from Pharmacia (Uppsala, Sweden).
5. Ultracentrifuge and a small swing-out rotor, such as the Beckman SW 42.1.
6. Standards: 1 mg/mL of each of β-galactosidase, catalase, and lactate dehydrogenase (all available from Sigma) in 0.5–1 mL distilled H_2O. Dialyse this solution against HEPES/Mg^{2+} for several hours prior to sucrose gradient centrifugation in order to remove ammonium sulphate.

7. Fraction collector, such as the Frac 100 from Pharmacia.
8. UV/visible spectrophotometer, linked to a pen recorder so that change in absorbance with time can be recorded.
9. 10 m*M* *ortho*-nitrophenyl-β-galactopyranoside (Sigma) in 100 m*M* citrate buffer, pH 5.5, prepared just before use. The citrate buffer may be made in liter quantities and stored at 4°C.
10. 500 m*M* Na_2CO_3 (Sigma), prepared in liter quantities and stored at 4°C.
11. 20 m*M* H_2O_2 in 10 m*M* sodium phosphate buffer, pH 7.4, prepared fresh before use. The phosphate buffer may be prepared in liter quantities and stored at 4°C.
12. 1 m*M* NAD/100 m*M* lactic acid (Sigma) in 100 m*M* Tris-HCl, pH 9.0, prepared fresh before use. The Tris buffer may be prepared in liter quantities and stored at 4°C.

3. Methods

3.1. Myocardial Membrane Preparation

In the experiments described here, hearts were obtained from rats (Wistar or Sprague Dawley) killed by stunning and decapitation. Unless otherwise stated, all of the procedures for the preparation of myocardial membranes are performed at ice-bath temperatures.

1. Remove the ribs to expose the heart, then cut the aorta and perfuse the ventricles by injecting 1–2 mL ice-cold HEPES buffer. This procedure washes much of the blood out of the heart.
2. Excise the whole heart, trimming off excess blood vessels, and place in a preweighed beaker (*see* **Note 3**). Weigh the heart and add 9 vols (i.e., 9 mL for every 1 g heart tissue) ice-cold HEPES buffer .
3. Using a small, sharp pair of scissors, roughly chop the heart tissue into small lumps.
4. Homogenize the tissue using a Sorvall Omnimixer (setting 3, for 15 s), a Polytron (setting 5, 3 X 15 s bursts, cooling on ice between bursts), or similar.
5. Pour this crude homogenate into a Potter-Elvehjem (glass/Teflon) homogenizer and homogenize further with 10 up-and-down strokes with the pestle rotating at a speed of approx 500 rpm.
6. Filter the homogenate through a double layer of cheesecloth to remove any remaining lumps of tissue.
7. Supplement this crude homogenate with 0.8 vol (i.e., 0.8 mL for every 1 mL of homogenate) KCl/PP_i solution (*see* **Note 4**).
8. Mix rapidly and centrifuge at 140,000*g* for 50 min at 4°C.
9. Discard the supernatant and resuspend the pellet in HEPES/10 m*M* EDTA to a volume equivalent to the original 1:10 tissue dilution, using 10 up-and-down strokes of the Potter-Elvehjem homogenizer.
10. Stir on ice for 30 min (*see* **Note 5**), then centrifugation at 100,000*g* for 30 min at 4°C.

11. Resuspend the resulting pellet in HEPES/0.1 m*M* EDTA as described in **step 9**, and centrifuge once more as described in **step 10**.
12. Repeat **step 11** (*see* **Note 6**).
13. Pour off the supernatant and freeze the pellet rapidly in a mixture of dry ice and methanol. These heart membranes can then be stored at −20°C until required (*see* **Notes 7–9**).

3.2. Solubilization

Unless otherwise stated, all parts of the solubilization procedure are carried out at ice-bath temperatures.

1. Thaw the frozen heart membranes and resuspend in HEPES/Mg^{2+} to a protein concentration of 4–5 mg/mL. In practice, this corresponds to a dilution of 1:10 original wet wt:vol for these heart membranes (*see* **Note 10**).
2. Supplement the membrane suspension with digitonin stock solution to give a final digitonin concentration of 1% (*see* **Notes 11** and **12**).
3. Stir on ice for 15 min.
4. Centrifuge at 140,000*g* for 30 min at 4°C. The resulting supernatant is used as the solubilized myocardial muscarinic receptor preparation (*see* **Notes 13** and **14**).

3.3. Radioligand Binding

Exposure to muscarinic ligands can be performed either before (prelabeling) or after (postlabeling) solubilization. Postlabeling experiments allow pharmacological characterization of the solubilized receptor. However, prelabeling experiments tend to give better recoveries of receptors, especially of receptor-G protein complexes, because the receptor or the complex is stabilized by the binding of the ligand (*see* **Notes 15** and **16**). Thus prelabeling may be especially useful for hydrodynamic characterization of receptors.

3.3.1. Prelabeling G Protein Coupled and Uncoupled Forms of the Myocardial Muscarinic Receptor

1. Thaw the frozen heart membranes and resuspend in HEPES/Mg^{2+} to a protein concentration of 4–5 mg/mL (*see* **Note 10**).
2. To label receptor-G protein complexes, add [^{3}H]-oxotremorine-M to this membrane suspension to a concentration of 10 n*M* (*see* **Note 17**).
3. Alternatively, to label uncoupled receptors, add GppNHp and [^{3}H]-NMS to this membrane suspension to concentrations of 100 μ*M* and 10 n*M*, respectively (*see* **Note 18**).
4. Incubate the membranes with the radioligands for 2 h at 4°C to allow equilibrium to be closely approached (*see* **Notes 19** and **20**).
5. Supplement this prelabeled membrane suspension with digitonin and proceed as described in **Subheading 3.2., steps 2–4**.

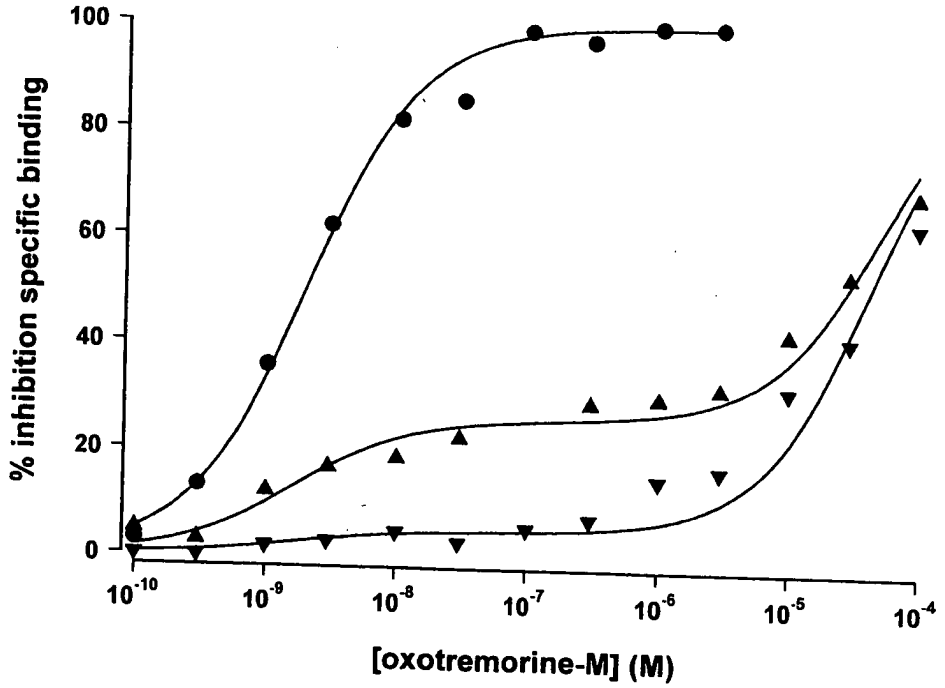

Fig. 1. The binding of oxotermorine-M to the solubilized myocardium of the rat. Inhibition of the specific binding of 0.8 n*M* [^{3}H]-oxotremorine-M (circles) or 0.8 n*M* [^{3}H]-NMS (triangles) by oxotremorine-M. Binding was measured in the absence (●,▲) or presence (▼) of 100 μ*M* GppNHp. Data are the mean of two determinations from a single, representative experiment. The solid lines represent the best fit of a one- (circles) or two- (triangles) site model of binding to the data (*see* **Note 24**).

3.3.2. Postlabeling the Solubilized Myocardial Muscarinic Receptor

1. Prepare the solubilized receptor preparation as described in **Subheading 3.2.** (*see* **Note 21**).
2. Working in a cold room at 4°C (*see* **Note 22**), pipet 250 μL aliquots of the solubilized preparation into 1.5 mL microcentrifuge ("Eppendorf") tubes containing 10 μL of radioligand alone, 10 μL of radioligand in the presence of 10 μL QNB or atropine to define nonspecific binding (*see* **Note 2**), or 10 μL of radioligand plus 10 μL unlabeled ligand, as appropriate for competition binding assays (*see* **Note 23**). Additional components such as GppNHp can be added in the same way.

   Figure 1 shows the results of a competition binding experiment in which the solubilized myocardial preparation was exposed to a range of concentrations of unlabeled oxotremorine-M (10^{-10}–10^{-4}M) in the presence of either 0.8 n*M* [^{3}H]-oxotremorine-M or 0.8 n*M* [^{3}H]-NMS; inhibition of [^{3}H]-NMS binding was determined in the absence and presence of 100 μ*M* GppNHp (*see* **Note 24**).

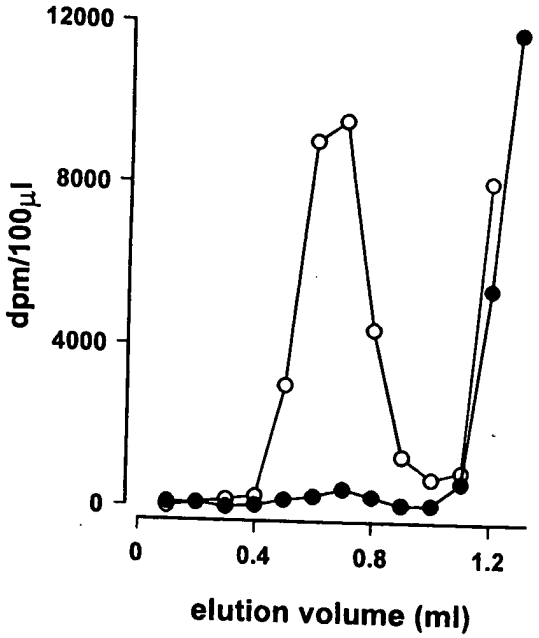

Fig. 2. Separation of bound [^{3}H]-NMS from free [^{3}H]-NMS by gel filtration. Solubilized muscarinic receptors were incubated with 10 n*M* [^{3}H]-NMS as described in **Subheading 3.3.1.**, in the absence (○) or presence (●) of 2 µ*M* QNB, to define nonspecific binding. Aliquots (100 µL) of each incubation mixture were then applied to 2 mL columns of Sephadex G50M, as described in **Subheading 3.4.2.**, and eluted with 100 µL aliquots of HEPES/Mg^{2+} buffer. The early peak, which is suppressed in the presence of QNB, represents receptor-bound [^{3}H]-NMS. The much larger peak of free [^{3}H]-NMS is just starting to come through in the later fractions.

3. Cap the tubes and mix, using a vortex mixer. Leave the samples at 4°C for at least 18 h to enable equilibrium to be approached (*see* **Note 25**).
4. Separate bound radioligand from free radioligand as described in **Subheading 3.4.**

3.4. Separation of Bound Radioligand from Free Radioligand

In the experiments described here, bound radioligand was separated from free radioligand by gel filtration on small columns of Sephadex G50M, whereby the receptors (and thus bound radioligand) are eluted in the void volume, the free ligand being retarded within the gel (**Fig. 2**; *see* **Note 26**).

3.4.1. Preparation and Care of the Gel Filtration Columns

1. Swell the Sephadex G50M resin in distilled H_2O for at least 1 h, then rinse in several changes of distilled H_2O.

2. Allow the resin to settle in a measuring cylinder and adjust the volume of water over the resin so that there are equal volumes of each.
3. Suspend the resin in the water by gentle shaking, tip into a beaker, and keep suspended by using a magnetic stirrer.
4. Pipette 4 mL aliquots of this "slurry" into suitable columns (*see* **Subheading 2.4.**). The water will run out, leaving a 2 mL bed of gel in the column (*see* **Notes 27** and **28**).
5. Before use, equilibrate the columns with HEPES/Mg^{2+} and cool them to 4°C (*see* **Notes 29** and **30**).
6. After elution and collection of the bound radioligand (*see* **Subheading 3.4.2.**), the columns can be washed with two column volumes (i.e., 4 mL) of HEPES/Mg^{2+} and stored for future use (*see* **Note 31**).

3.4.2. Gel Filtration of Samples

1. Working in a cold room to slow down dissociation of ligand from the receptor, place a gel filtration column in a suitable scintillation vial, preparing two columns for each sample to be assayed (*see* **Note 32**).
2. Pipet 100 µL of sample onto each of two columns, being careful to avoid disturbing the gel bed.
3. As soon as the sample has run into the columns, apply 100 µL HEPES/Mg^{2+} to wash the sample into the gel. When that has run into the columns, apply 700 µL HEPES/Mg^{2+}, collecting the 900 µL of eluate in the vial.
4. Remove the columns from the vials and regenerate as described in **Subheading 3.4.1.**
5. Remove the vials from the cold room. Add a suitable water-miscible scintillant and determine the bound radioactivity by liquid scintillation counting.

3.5. Sucrose Density Gradient Centrifugation

1. Add 2.25 mL of 20% and 5% sucrose solutions (*see* **Subheading 2.5.**) to each side of a small gradient maker and pump 4.5 mL sucrose gradients (*see* **Note 33**) into centrifuge tubes held securely in a rack and immersed in ice. During the pouring of the gradients, the outlet tube from the peristaltic pump should be kept just above the level of the forming gradient, and gradually raised as the gradient is poured (*see* **Note 34**).
2. Mix 50 µL of the internal standards (*see* **Subheading 2.5.**) with 450 µL of the solubilized preparation, which can be prelabeled, postlabeled, or unlabeled. Pump this mixture carefully onto the top of the gradient. When using labeled preparations, it is necessary to include the radioligand throughout the gradient to minimize dissociation from the receptor (*see* **Note 35**).
3. Centrifuge immediately in a swing-out rotor at 100,000*g* for 19 h at 0°C (*see* **Note 36**). At the end of the spin, the rotor should be allowed to coast to a halt, as the use of the brake may disrupt the gradients.
4. Remove the tubes from the rotor and place carefully in racks immersed in ice. Working in a cold room, carefully insert a thin piece of stainless steel tube

attached to a peristaltic pump into the gradient until it rests on the bottom of the centrifuge tube (*see* **Note 37**). Pump the gradient out from the bottom of the tube at a rate of 12.5 mL/h, collecting 250 µL fractions in suitable tubes.

5. Assay the fractions for the receptor, by measuring bound radioactivity as described in **Subheading 3.4.** Assaying a single 100 µL aliquot from each 250 µL fraction should leave ample sample for the assay of the internal standards.
6. Assay for β-galactosidase (15.93 $S_{20,w}$, *see* **Note 38**): Add a 10 µL aliquot of each fraction to 500 µL 10 m*M* *ortho*-nitrophenyl-β-galactopyranoside in 100 m*M* citrate buffer, pH 5.5 (*see* **Subheading 2.5.**) and incubate for 15 min at 30°C. Add 500 µL 500 m*M* Na_2CO_3 to stop the reaction; a yellow color will develop. Quantify the enzyme activity by measuring the absorbance of the sample at 430 nm (*see* **Note 39**).
7. Assay for catalase (11.3 $S_{20,w}$, *see* **Note 38**): Mix a 20 µL aliquot of each fraction with 2 mL 20 m*M* H_2O_2 in 10 m*M* sodium phosphate buffer, pH 7.4. Immediately place the sample in a spectrophotometer; the enzyme activity is assessed by the initial rate of the change of absorbance at 230 nm (*see* **Note 39**).
8. Assay for lactate dehydrogenase (7.3 $S_{20,w}$, *see* **Note 38**): Mix a 50 µL aliquot of each fraction with 2 mL 1 m*M* NAD/100 m*M* lactic acid, in 100 m*M* Tris-HCl, pH 9.0. Immediately place the sample in a spectrophotometer; the enzyme activity is assessed by the initial rate of the change of absorbance at 340 nm (*see* **Note 39**).
9. Plot amount of radioactivity bound and enzyme activity against fraction number. It helps the comparison of the receptor and standard peaks if values are normalized to a percentage of the maximum ("peak") value. Representative gradients obtained for myocardial muscarinic receptors labeled with [^{3}H]-NMS and [^{3}H]-oxotremorine-M are shown in **Fig. 3** (*see* **Note 40**).

4. Notes

1. Digitonin is a naturally occurring plant glycoside, with commercial preparations being extracted from the foxglove, *Digitalis purpura*. These have been shown to contain more or less equal amounts of two glycosides, digitonin and gitonin, and a number of other minor components ***(6)***. It is probable that the notorious variations in solubility and effects of digitonin obtained from different commercial sources (or even batch-to-batch variations from the same source) is a result of the different proportions of digitonin and gitonin in these "digitonin" preparations. Furthermore, there appears to be an optimal digitonin:gitonin ratio (3:2) for the solubilization of stable muscarinic binding sites ***(6)***. The digitonin obtained from Wako was usually soluble enough to allow the preparation of 10% stock solutions. However, with some batches of digitonin from the same supplier, it was only possible to obtain 4% stock solutions.
2. As QNB is not available very readily, it may be much more convenient to use atropine or another muscarinic antagonist to define nonspecific binding. There is a theoretical advantage to using QNB rather than atropine to define the nonspecific binding of [^{3}H]-NMS; NMS and atropine are structurally rather similar and thus are more likely to bind to the same nonreceptor sites than dissimilar ligands,

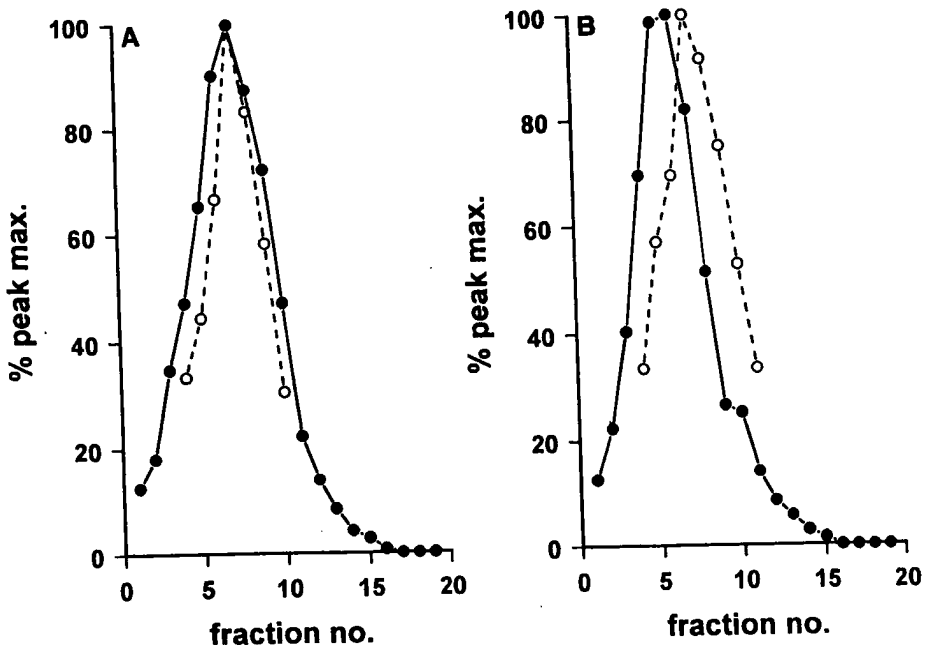

Fig. 3. Sucrose density gradient centrifugation of solubilized muscarinic receptors from the rat myocardium. The solubilized receptors were labeled with **(A)** 7 n*M* [^{3}H]-NMS or **(B)** 10 n*M* [^{3}H]-oxotremorine-M as described in **Subheading 3.3.1.** Solid circles (●) represent bound radioligand, open circles (○) represent catalase activity, included as an internal standard. Data are the means of two independent determinations from a single, representative experiment (*see* **Note 40**).

such as QNB. However, there is, in practice, no problem in using atropine in this way.

3. Excess fluid (blood and HEPES buffer) can be removed before weighing the heart by "dabbing" on a piece of filter paper, with the atria and cut blood vessels facing down.
4. This KCl/PP_i pretreatment removes many of the proteins loosely associated with the heart cell membranes. It improves the specific:nonspecific binding ratio for muscarinic ligands binding to the heart membranes by about twofold, without a significant loss in the total number of binding sites. Furthermore, it appears to improve the stability of the preparation both in storage and after solubilization.
5. This EDTA pretreatment slightly but significantly enhances the affinity of [^{3}H]-oxotremorine-M for the myocardial muscarinic receptor *(7)*.
6. The two washing steps in the low concentration of EDTA are required to reduce the EDTA concentration sufficiently to enable the Mg^{2+}-dependent interaction of the receptor with the G protein to be observed in subsequent experiments.

7. Freezing and storing the pellets in the bottom of the centrifuge tubes in which they were prepared is most convenient but requires a large stock of tubes. It is possible to resuspend the pellets at this stage and freeze aliquots of the resulting suspension.
8. There should be no change in the binding properties of this frozen membrane fraction over a period of 1 to 2 mo at −20°C. For more prolonged storage, it may be advisable to store the membranes at −70°C.
9. Membranes may be prepared from other tissues (e.g., brain regions, lachrymal gland, etc.) by the same procedure, with the omission of the KCl/PP_i pretreatment step.
10. In order to obtain approx 5 mg protein /mL from other membrane preparations, medulla/pons and lachrymal gland membranes need to be resuspended to 1:10 original wet w/v, whereas membranes from rat cerebral cortex need to be resuspended to 1:20 original wet w/v.
11. It is more convenient to use a digitonin concentration of 0.8% when using a 4% stock solution. This makes little or no difference to the recovery of solubilized receptors.
12. This protein-to-detergent ratio works well for the solubilization of muscarinic receptors, giving a yield of about 30%. For other receptors, the best detergent and solubilization protocol needs to be determined empirically, that is, by trial and error.
13. The fact that binding activity remains in the supernatant following high-speed centrifugation suggests that the receptor has been solubilized and is used to routinely "define" solubilized receptors. However, it is possible for membrane associated receptors to remain in the supernatant if fragments of membrane are sufficiently small, particularly if the solution is dense—containing glycerol, for example. Therefore, when devising a new solubilization procedure, it is necessary to check that receptors in the high-speed supernatant are actually solubilized, for example by looking at the behavior of the binding sites in gel filtration or sucrose density gradient centrifugation or by examining the supernatant with an electron microscopy.
14. The solubilized preparation is reasonably stable and can be stored overnight at 4°C. However, it is probably better to use it at once, especially as binding assays or hydrodynamic characterization may take several days. It is wise to supplement the preparation with protease inhibitors if it is to be subject to particularly lengthy procedures (e.g., purification).
15. Some solubilized receptors (e.g., V_1 vasopressin receptors) cannot be postlabeled, either because they are denatured during solubilization in the absence of ligand or because the interaction of the detergent with the receptor occludes the ligand binding site.
16. It is possible to recover muscarinic receptor-G protein complexes from myocardial membranes solubilized in the absence of ligand, although the abundance of these complexes is improved by prelabeling with agonist (e.g., [^{3}H]-oxotremorine-M). However, in most other tissues, it is necessary to prelabel with agonist to obtain solubilized receptor-G protein complexes.

17. Agonists such as [^{3}H]-oxotremorine-M induce the formation of receptor-G protein complexes and stabilize them. They bind with higher affinity to these complexes than to uncoupled receptors, such that low concentrations of labeled agonists bind preferentially to the complexed form of the receptor.
18. Guanine nucleotides such as GTP, or its nonhydrolyzable analog GppNHp, disrupt receptor-G protein complexes. Moreover, antagonist ligands such as [^{3}H]-NMS do not distinguish receptor-G protein complexes from uncoupled receptors.
19. If necessary, the progress of the radioligand binding to the membranes can be monitored by dilution of an aliquot of the incubation in 5–10 vol ice-cold 20 m*M* NaHEPES, pH 7.5, followed by immediate microcentrifugation at 4°C and scintillation counting of the resultant pellet *(8)*.
20. As with radioligand binding studies of the solubilized myocardial receptor (**Subheading 3.3.2.**), the nonspecific binding of these radioligands can be determined in parallel incubations that include 1 μ*M* QNB or atropine.
21. In the case of the myocardial preparation, the solubilized supernatant can usually be used undiluted. However, it is sometimes necessary to dilute the supernatant with HEPES/Mg^{2+} containing 1% digitonin to reduce the receptor concentration and thus avoid excessive depletion of ligands. Depletion occurs when the free ligand concentration is significantly affected by "loss" of ligand when it binds to the receptor and is a particular problem when investigating the binding of low concentrations of high-affinity ligands to preparations with a high receptor density.
22. The stability of the solubilized muscarinic receptor is improved at low temperatures. However, the kinetics of ligand binding are also slowed. This is coupled with a slowing of binding kinetics, which occurs as a consequence of solubilization and necessitates very long incubations in order for equilibrium to be approached (*see* **Note 25**). Binding is more rapid at 30°C. However, there appears to be a selective instability of the M_1 receptor subtype at the higher temperature, whereby these receptors are lost during the course of the assay *(9)*.
23. Just as in membrane binding assays, both direct binding assays (in which the total and nonspecific binding of a range of radioligand concentrations is measured) and competition binding assays (in which the binding of an unlabeled ligand is measured as its ability to inhibit the specific binding of a low, fixed concentration of radioligand) can be performed on the solubilized preparations.
24. The data in **Fig. 1** shows the inhibition of [^{3}H]-NMS and [^{3}H]-oxotremorine-M binding by unlabeled oxotremorine-M. Inhibition of [^{3}H]-NMS binding in the absence of GppNHp is markedly biphasic; oxotremorine-M binds to a subpopulation of [^{3}H]-NMS labeled sites with a high affinity (receptor-G protein complexes) and with a lower affinity to the remainder of sites (uncoupled receptors). The difference in agonist affinity between these two populations of sites is enhanced in the solubilized preparation, mainly as a result of a decrease in the affinity of the low affinity, "uncoupled" site on solubilization. In the presence of GppNHp, the curve for inhibition of [^{3}H]-NMS binding by oxotremorine-M is shifted markedly to the right and loses much of its biphasic character. This is consistent with conversion of high-affinity, receptor-G protein complexes to low-affinity, uncoupled

receptors in the presence of the guanine nucleotide. When oxotremorine-M binding is measured by its ability to inhibit the binding of [^{3}H]-oxotremorine-M, the competition curve appears monophasic and of high affinity, because the low concentration of [^{3}H]-oxotremorine-M used binds selectively to the high-affinity sites.

25. The slow binding kinetics in the solubilized preparation have already been mentioned (*see* **Note 22**). Approach to equilibrium may be slowed still further in competition binding experiments, especially if the high-affinity radioactive tracer ligands bind more rapidly than the competing ligands, which are often of lower affinity. To try to get around this problem, the data shown in **Fig. 1** were obtained by preincubating the solubilized preparation in the presence of the unlabeled ligand for 24 h, followed by the addition of the radioligand for a further 20 h.
26. Various other separation procedures can be used in binding assays with solubilized (or soluble) receptors. Of these, the most useful are probably charcoal adsorption or filtration, using glass fiber filters that have been pretreated with polyethyleneimine (*see* Chapter 4).
27. It is useful to mark the top of the gel bed with a line on the outside of the column. All columns lose some gel during use and will need to be repoured when the level drops noticeably or if nonspecific binding starts to increase, suggesting recovery of free ligand in the "bound" fraction.
28. The number of columns required depends on the number of samples to be assayed and on the frequency with which these assays are to be performed. Two columns are required per sample, plus a few spares. If these assays are to be routine, it is useful to have two full sets of columns, so that one set can be in use while the others are being washed or repoured.
29. Columns are equilibrated with the buffer by running at least 4 mL (2 column vol) of cold buffer through the columns just before use. The simplest way to do this is to gently fill each column with buffer from a wash bottle; let this run through and then repeat. If the columns are stored at room temperature, ensure that cold buffer is running through the columns as they are moved into and out of the cold room to minimize the formation of bubbles within the gel bed.
30. There is no need to include digitonin in the equilibration or elution buffer if the samples contain 0.8–1% digitonin. However, if the detergent concentration is less than this (e.g., during purification of the receptor), 0.2% digitonin should be included in these buffers.
31. The columns may be washed and stored at room temperature or at 4°C. These small columns do not dry out if their tips are in fluid and they can be conveniently stored standing in beakers. To minimize microbial growth during storage, it helps to wash the columns with 2 vol of distilled H_2O prior to storage, including 0.01% sodium azide if they are to be left for more than a few days. Any columns that do dry out during storage will need to be repoured.
32. The columns will stand in 10 mL vials, supported in a suitable rack or box. Large vials are probably better than small, as the accumulation of eluted fluid around the tip of the column will slow down the elution and increase dissociation of the ligand from the receptor.

33. When preparing small sucrose gradients, there can be two major practical problems. The first of these is the introduction of an air bubble in the connecting tap tube, and the other is the possible rush of the heavier mixture into the chamber containing the lighter mixture when the tap is opened (or vice versa) if not prepared carefully enough. Both of these problems can be avoided in the following way. With the connecting tap and the exit tube to the peristaltic pump both closed, pour 2.25 mL of the 20% sucrose solution into the first (exit) chamber. Tip the gradient former with the empty chamber uppermost, and open the connecting tap just enough to allow the connecting tube to fill on both sides of the tap with this mixture. Close the connecting tap. With the gradient former still slightly tipped, introduce 2.25 mL of the 5% sucrose solution slowly into the second chamber, while returning the gradient former to the vertical. Introduce a small magnetic "flea" or a spatula mounted in an overhead stirrer into the exit chamber, and check that the levels of liquid in the two chambers are the same; here a few drops of either mixture may need to be added. Start the magnetic/overhead stirrer, then switch on the peristaltic pump at a pumping speed of around 25 mL/h, opening the connecting tap slowly at first. There should be minimal initial mixing of the contents of the two chambers, thus allowing the formation of very reproducible gradients.
34. The gradients are reasonably stable and can be stored overnight at 4°C before use if necessary.
35. In the experiments described here (**Fig. 3**), the preparation was labeled with 5–10 n*M* [^{3}H]-NMS or [^{3}H]-oxotremorine-M, but it is sufficient to include 1 n*M* radioligand in the gradient.
36. This centrifugation step may conveniently be performed overnight.
37. Thread the steel tube through a cork before inserting it into the gradient, then support the cork with a clamp once the tube is in place.
38. $S_{20,w}$ is the sedimentation coefficient of the standards and this information can be used in the calculation of various hydrodynamic parameters (see **ref. 5**). However, the main use of the standards is to allow for comparisons between individual gradients.
39. After the addition of the Na_2CO_3, samples can be stored on ice for up to 1 h before measuring the absorbance.
40. **Figure 3** shows sucrose density gradients obtained with solubilized muscarinic receptors from myocardium labeled after solubilization with 7 n*M* [^{3}H]-NMS or 10 n*M* [^{3}H]-oxotremorine-M. The peak of [^{3}H]-NMS binding activity is much wider than the standard catalase peak, suggesting heterogeneity in the hydrodynamic properties of the [^{3}H]-NMS-labeled sites. In contrast, the width of the [^{3}H]-oxotremorine-M peak is very similar to that of the standard, suggesting that these sites are more homogeneous. The apparent sedimentation coefficient of the [^{3}H]-oxotremorine-M peak is greater than that of catalase and of the majority of the [^{3}H]-NMS labeled sites. These findings are consistent with the selective labeling by [^{3}H]-oxotremorine-M of a subpopulation of the sites recognized by [^{3}H]-NMS. This subpopulation of sites appears "bigger" than the majority of the receptor population because they represent receptor-G protein complexes.

Acknowledgments

The authors gratefully acknowledge Drs. E. C. Hulme and N. J. M. Birdsall of the Division of Physical Biochemistry, National Institute for Medical Research, Mill Hill, London, NW7 1AA, U.K., in whose laboratories these studies took place.

References

1. Helenius, A. and Simons, K. (1975) Solubilization of membranes by detergents. *Biochim. Biophys. Acta* **415,** 29–79.
2. Hulme, E. C., Berrie, C. P., Haga, T., Birdsall, N. J. M., Burgen, A. S. V., and Stockton, J. M. (1983) Solubilization and molecular characterisation of muscarinic acetylcholine receptors. *J. Recep. Res.* **3,** 301–311.
3. Berrie, C. P., Birdsall, N. J. M., Haga, K., Haga, T., and Hulme, E. C. (1984) Hydrodynamic properties of muscarinic acetylcholine receptors from rat forebrain. *Br. J. Pharmacol.* **82,** 839–851.
4. Berrie, C. P., Birdsall, N. J. M., Hulme, E. C., Keen, M., and Stockton, J. M. (1984) Solubilization and characterisation of guanine nucleotide-sensitive muscarinic agonist binding sites from rat myocardium. *Br. J. Pharmacol.* **82,** 853–861.
5. Poyner, D. (1990) Receptor-G-protein complexes in solution, in: *Receptor-Effector Coupling: A Practical Approach* (Hulme, E. C., ed.), Oxford University Press, pp. 31–58.
6. Repke, H. and Matthies, H. (1980) Solubilized muscarinic receptors. *Brain Res. Bull.* **5,** 703–709.
7. Hulme, E. C., Berrie, C. P., Birdsall, N. J. M., Jameson, M., and Stockton, J. M. (1983) Regulation of muscarinic agonist binding by cations and guanine nucleotides. *Eur. J. Pharmacol.* **94,** 59–72.
8. Berrie, C. P., Birdsall, N. J. M., Burgen, A. S. V., and Hulme, E. C. (1979) Guanine nucleotides modulate muscarinic receptor binding in the heart. *Biochem. Biophys. Res. Comm.* **87,** 1000–1005.
9. Berrie, C. P., Birdsall, N. J. M., Hulme, E. C., Keen, M., Stockton, J. M., and Wheatley, M. (1986) Muscarinic receptor subclasses: the binding properties of the soluble receptor binding sites. *Trends Pharmacol. Sci.* **7 (Suppl.),** 1–6.

6

Radioligand Binding in Intact Cells

Jennifer A. Koenig

1. Introduction

Radioligand binding to plasma membranes or complete cell homogenates has been widely used to characterize the binding interactions between a large number of receptors and ligands (*see* Chapters 1–3). These experiments are generally performed under conditions that optimize the data obtained but are usually nonphysiological. It is difficult to compare the binding affinity obtained for a radioligand to cell membranes, in a low ionic strength buffer that contains no divalent cations, with functional assays performed under near-physiological conditions. However, there are a number of complicating factors that must be considered when using intact cells. The aim of this chapter is to describe the additional factors that must be taken into consideration when measuring radioligand binding in intact cells.

The complications arising from using intact cells rather than membranes for radioligand binding studies fall into four main categories:

1. the effects of various inorganic ions on binding affinity,
2. guanine nucleotide sensitivity,
3. hydrophobic or hydrophilic nature of the radioligand, and
4. subcellular location of receptors and agonist-induced internalization and recycling.

Many of these factors vary between receptors and even between receptor subtypes, so there are no hard-and-fast rules. I will use as examples muscarinic acetylcholine receptors and somatostatin receptors, both of which belong to the G protein-coupled receptor superfamily. Ligands available for muscarinic receptors include cell-impermeant and cell-permeant antagonists, as well as agonists, whereas somatostatin receptor binding is limited to peptide agonists.

From: *Methods in Molecular Biology, Vol. 106: Receptor Binding Techniques*
Edited by: Mary Keen © Humana Press Inc., Totowa, NJ

1.1. Ion and Guanine Nucleotide Sensitivity

High-affinity binding of agonists to G protein-coupled receptors relies on the formation of a receptor-G protein complex *(1–2)*. Dissociation of this complex by either salt and/or guanine nucleotides (GTP, or the nonhydrolyzable analogs GppNHp or GTPγS) leads to a marked reduction in agonist binding affinity (*see* **Fig. 1**). In contrast, binding of antagonists is considerably less sensitive. Since intact cells have high levels of GTP, the practical consequence of this is that the measured form of the receptor is usually predominantly the low-affinity form. There are some examples where binding of agonists directly to intact cells is possible *(4)*. However, in many cases (e.g., the somatostatin receptor) this low-affinity form is not measurable by direct radioligand binding assays *(5)*, and it is more common to measure agonist affinity in intact cells by displacement of antagonist binding. It is theoretically possible to measure high-affinity agonist binding in intact cells by depleting GTP levels *(6)* or by using permeabilized cells *(2,7)*.

Permeabilized cells may be an attractive compromise between membrane preparations and intact cells, depending on the nature of the experiments. Different membrane preparation protocols may disrupt the G protein complement of the cell, so experiments studying receptor-G protein coupling using permeabilized cells may be more appropriate (*see* **ref. 2** for example). However, permeabilization often reduces the ability of cells to remain adherent, and this is particularly true of neuronal cell cultures.

1.2. Internalization and Recycling of Receptors

Agonist activation of G protein-coupled receptors and growth factor tyrosine kinase receptors results in a rapid redistribution of receptors from the plasma membrane to an intracellular compartment [*see (3)* for review]. Internalization is thought to occur by interaction of the receptor with clathrin-coated pits, caveolae, or both, depending on the cell type. The intracellular compartment responsible is generally thought to be a tubulo-vesicular endosomal compartment. Once internalized, most G protein-coupled receptors are thought to recycle back to the cell surface *(8)*, although this has not really been investigated with many peptide hormone receptors.

The practical consequences of these processes for radioligand binding studies in intact cells are obviously different for agonist and antagonist ligands, since antagonists are thought not to initiate internalization. Measuring only surface receptors is quite straightforward if a membrane-impermeant antagonist radioligand is available (e.g., [^{3}H]-N-methyl-scopolamine for muscarinic receptors, *see* **Subheading 3.1.**). Measuring total (i.e., both surface and internal) receptors is more complicated. Membrane-permeant antagonist ligands

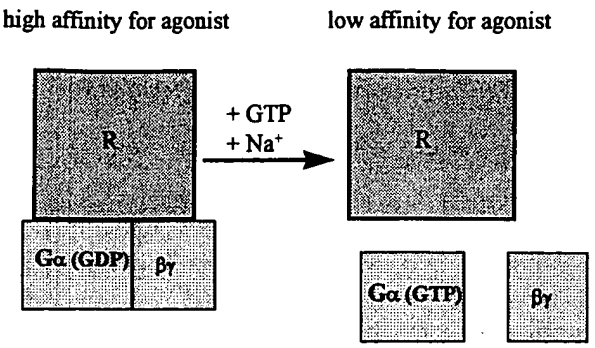

Fig. 1. The binding affinity of agonist radioligands depends on association of receptors with G proteins *(1–3)*.

have been used, such as [^{3}H]-scopolamine or [^{3}H]-quinuclidinyl benzilate, for muscarinic receptors *(9)*. It is important, though, to be certain that displacing ligands have equal access to, and equal affinity for, internal receptors. I have found that such membrane-permeant ligands are not equally able to label internal as well as surface receptors, perhaps because the endosomal compartment is at low pH (< 5.5), and radioligands often have lower affinity at low pH *(8)*.

Binding of agonist radioligands in intact cells may result in internalization of the ligand in addition to binding at the surface. This has really only been demonstrated for high-affinity ligands—usually [^{125}I]-labeled peptides. It is commonly assumed that lower affinity agonists are more likely to dissociate than they are to internalize. The internalized ligand can be measured by a stringent acid wash after incubation in order to dissociate all of the surface ligand. The ability of the acid wash to dissociate the radioligand from surface receptors should be demonstrated using membrane binding studies *(5)*, since it is known that some peptides show almost irreversible binding [e.g., endothelin *(10)*]. For some radioligands, a pH 5.0 wash is sufficient [e.g., somatostatin, *(5)*], whereas for others, more drastic conditions are necessary [e.g., epidermal growth factor, *(11)*]. It is important to be aware that agonist radioligands can recycle back to the extracellular medium so that the amount of ligand that has accumulated inside the cell is a balance between the rate of internalization and the rate of recycling *(5)*.

Even antagonist binding at 37°C can be complicated by internalization, since the basal turnover rate of receptors becomes significant with longer incubation times of over 1 h, *(8,9)*. Internalization and recycling of both receptors and radioligands can be significantly reduced by depletion of ATP and/or tempera-

tures below 16°C, *(5,12)*. Another approach is to prevent internalization by treatment with concanavalin A, phenylarsine oxide, or hyperosmolar sucrose, or by depletion of intracellular potassium. The mechanism of action of concanavalin A is unknown, and although it works efficiently in preventing internalization of some receptors [e.g., β-adrenergic receptors, *(13)*], it is less effective at preventing muscarinic receptor internalization, decreasing the internalization rate constant by half *(13a)*. Phenylarsine oxide has a multiplicity of actions because of its interaction with disulfide bonds, including depletion of ATP and effects on phosphatases *(14)*. It has been used successfully in a number of reports *(4,14)*, but we have had variable results; the most reliable effect seems to be decreased adherence of cells to plastic surfaces. Hyperosmolar sucrose and potassium depletion are thought to prevent formation of clathrin-coated pits *(15)*: their effects on caveolin-dependent internalization is unclear. Hyperosmolar sucrose is effective and straightforward, preventing internalization of a number of receptor types *(5,16,17)*. None of these methods for preventing internalization of receptors is specific and many affect other aspects of cellular function, including the functional response. This may limit the ability to compare binding data obtained in this way with data from functional studies.

Efforts have been made to develop mathematical approaches to enable estimates of affinity in intact cells by accounting for internalization of receptors. This was done for the epidermal growth factor receptor where recycling was thought to be negligible *(18)*. Although mathematical descriptions of G protein-coupled receptor internalization and recycling have been described *(8)*, determining affinity in addition to internalization and recycling parameters is at present too complex.

There are two main experimental formats for radioligand binding in intact cells: using cells in suspension or cells adherent to multiwell plates. For assays in cell suspension, an experimental setup similar to membrane binding assays can be used: i.e., filtration through glass-fiber filters using a cell harvester (*see* Chapters 1 and 3). This format is often easier for large assays. However, it has been reported that internalization and recycling of receptors can be dependent on the structure of the cytoskeleton, which will obviously change dramatically in the transition from adherent to suspension. I will therefore concentrate in this chapter on using cells adherent to multiwell plates. Indeed, for smaller assays, a multiwell plate format can be quicker and easier. Two main procedures will be described. The first describes antagonist binding to muscarinic acetylcholine receptors on intact cells adherent to multiwell plates. The second describes binding and internalization of radiolabeled somatostatin agonist ligands.

2. Materials

2.1. Materials Common to Both Subheadings 3.1. *and* 3.2.

1. Thermostatically controlled water bath.
2. 24-well multiwell plates.
3. Polylysine-L-lysine (25 µg/well; Sigma, Poole, Dorset, UK).
4. Vacuum line for removing liquid from multiwell plates.
5. PBS-Ca,Mg: phosphate buffered saline containing 0.9 m*M* $CaCl_2$ and 0.5 m*M* $MgCl_2$ or medium (e.g., DMEM) buffered with HEPES. Powdered medium is relatively inexpensive and convenient for making large quantities.
6. 0.5% Triton-X-100 in water.
7. PBS-EDTA (1 m*M*), PBS-Trypsin (0.5 mg/mL) EDTA (1 m*M*) or Versene to detach cells for counting.
8. Hemocytometer or Coulter counter.

2.2. Additional Materials Required for Subheading 3.1.

1. [^{3}H]-N-methylscopolamine, specific activity 80–85 Ci/mmol from Amersham (Little Chalfont, Bucks, UK) or NEN (Sheverage, Herts, UK). Keep stock frozen in aliquots (200 n*M*, –20°C), dilute into incubation medium (PBS-Ca,Mg or HEPES-buffered DMEM).
2. NMA: N-methylatropine (Sigma): used to define nonspecific binding. Make stock solution 10^{-2} *M* in water and keep at 0–4°C.
3. Scintillant: Optiphase Safe or a similar scintillant that is water miscible at a scintillant:water volume ratio of 1:8.

2.3. Additional Materials Required for Subheading 3.2.

1. [^{125}I]-somatostatin-14: (SS-14), specific activity 2000 Ci/mmol from Amersham.
2. Unlabeled SS-14 (Sigma): make 1 m*M* stock in water, freeze in aliquots.
3. Acid wash buffer: 10 m*M* MES, pH 5.0 (2-[N-morpholino]ethane sulfonic acid); 120 m*M* NaCl; 0.9 m*M* $CaCl_2$; 0.5 m*M* $MgCl_2$.

3. Methods

3.1. Antagonist Binding to Intact Cells: [^{3}H]-N-methylscopolamine Binding to Muscarinic Receptors in NG108-15 Neuroblastoma Cells

1. Seed NG108-15 cells on polylysine-coated 24-well multiwell plates at 10^5 cells/well in DMEM containing 10% fetal bovine serum and glutamine. Incubate for between 2 and 4 d until confluent (*see* **Note 1**).
2. Remove from incubator and wash with 2 × 2 mL PBS-Ca,Mg to remove serum (*see* **Note 2**).
3. Remove PBS-Ca,Mg and add 0.5-mL [^{3}H]-N-methylscopolamine with or without unlabeled ligand, as shown diagrammatically in **Fig. 2** (*see* **Note 3**). Leave some wells with buffer only for use in counting cells.
4. Incubate overnight at 4°C to reach equilibrium.

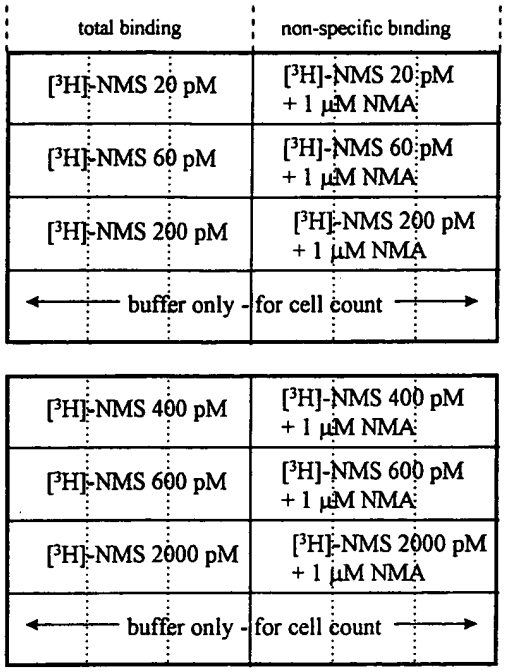

Fig. 2. Suggested multiwell plate layout for saturation analysis of 3H-N-methylscopolamine binding to intact cells.

5. Rinse each well rapidly with 2 × 1 mL PBS-Ca,Mg to remove unbound radioligand. Leave dry.
6. Add 0.25 mL of 0.5% Triton-X-100 to wells with radioactivity. Leave for at least 1 h to solubilize.
7. Add 0.25 mL PBS-EDTA (1 m*M*) to the wells containing cells for the cell count and leave for 10 min. Dislodge the cells by taking them up and down in a pipet tip and count in either a hemocytometer or Coulter counter (*see* **Note 4**).
8. Transfer solubilized radioactivity from wells to scintillation vials. Rinse with 0.25 mL water. Add 4 mL scintillant, mix well. Transfer to scintillation counter.
9. Data analysis is identical to that for saturation analysis in membrane binding assays (*see* Chapter 9).

3.2. Somatostatin Agonist Binding and Internalization in Intact Cells

1. Seed cells (CHO cells expressing transfected receptors at 10^4 cells/well or Neuro 2A cells expressing somatostatin receptor endogenously at 10^5 cells/well) on 24-well multiwell plates (*see* **Note 1**). Incubate CHO cells overnight. Incubate Neuro2A cells for 2–3 d until confluent.

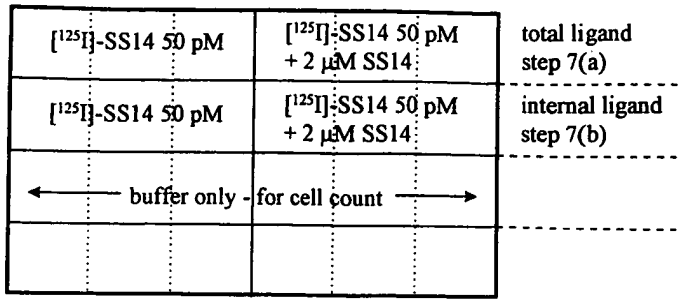

Fig. 3. Suggested multiwell plate layout for measuring total and internalized [^{125}I]-somatostatin 14.

2. Wash twice with PBS-Ca,Mg or DMEM/HEPES to remove serum (*see* **Note 2**).
3. Remove and replace with 0.2 mL PBS-Ca,Mg or DMEM/HEPES (*see* **Note 5**) at 37°C.
4. Place in a waterbath at 37°C, 10 min.
5. Add 0.05 mL of 1 n*M* [^{125}I]-SS14 to the wells and incubate for 5–60 min (*see* **Note 6**). Some wells should also include excess unlabeled SS14 (1 μ*M*) to define nonspecific internalization, as shown diagrammatically in **Fig. 3**. Leave some wells with buffer only for use in counting cells.
6. Terminate the incubation by removing the incubation mixture and washing very rapidly twice with 1 mL cold incubation buffer.
7. At this point, there are two choices (*see* **Fig. 3**):
   a. to measure total ligand (i.e., surface + internal), leave the cells to dry, and go on to **step 8** or
   b. to measure internalized ligand, incubate with 2 mL ice-cold acid wash buffer for 10 min, then remove and leave the cells to dry (*see* **Note 7**).
8. Solubilize the cells in 1% Triton-X-100 (v/v in water) for at least 1 h.
9. Transfer to scintillation vials and count in a gamma counter. No scintillant is required.
10. Perform a cell count as described in **Subheading 3.1., step 7**.

4. Notes

1. Use 24-well multiwell plates here because they support sufficient cells to give a good enough signal. For cells with very low receptor density, it might be necessary to use 12-well or even 6-well plates. It is best to avoid 96-well plates, as often there are not enough cells to give a good signal, and it is more difficult to wash the wells without dislodging the cells. NG108 cells and other neuronal cells (e.g., SH-SY5Y) do not stick down particularly well and therefore require some special treatment. First, choose the right brand of 24-well plate: We have used Nunc and Costar with some success. Other brands work less well. Some cells

adhere better after pretreating the plate with polylysine (add 0.5 mL 50 µg/mL poly-L-lysine in PBS, leave for at least 1 h or overnight, remove before adding cells). Above all, be very gentle when adding and removing buffer.

2. To wash, tilt the plate and remove the medium with a 1-mL pipet tip connected to a vacuum line. For neuronal cell lines, add the buffer very gently down the side of the well using a Gilson pipet with the end of the plastic tip cut off. Other cells are less fussy: Chinese Hamster Ovary cells (CHOs) are very strongly adherent and will tolerate washing with a repeating pipet, although it is still best not to direct the liquid directly at the cells. It is possible to use a 24-well plate washer from Semat Technical (St. Albans, Herts, U.K.) which is just a custom-modified Brandel Cell Harvester. The metal tubes from the head of a Cell Harvester are used to add and remove buffer. The hole in the delivery metal tube is at the side rather than the end of the tube so that the jet of liquid is aimed at the wall of the well rather than directly at the cells. The spacing of the metal tubes is adjusted for a 24-well plate to wash only six wells at a time. The flow rate of the delivery of buffer needs to be adjustable and quite slow to avoid dislodging the cells. There is no need for the filter block. The waste is collected in the usual manner for a cell harvester. It is important that all buffers contain calcium, as even CHO cells will detach after repeated washing without calcium present. Some authors report the use of glucose (1–4g/L) and/or bovine serum albumin (BSA, 0.2%) or horse serum in the incubation buffer for internalization studies. I have not found it to make a difference. Indeed, with somatostatin, there is some binding of radioligand to BSA, which becomes particularly relevant at the very low concentrations of radioligand that are often used.
3. The volume of [^{3}H]-NMS should be increased if using cells with high levels of receptor density in order to avoid ligand depletion (*see* Chapter 9). With transfected CHO cells, we seed the cells at lower densities (10^4 cells/well) to avoid this, since transfected cells often contain approx 10^6 receptors/cell, which may lead to ligand depletion, at least at lower concentrations of ligand, if not all.
4. It is likely that the washing procedures will cause some loss of cells. Therefore, it is important to count the number of cells in wells that have been through all of the same washing procedures as the ones that have been used for radioactivity. For NG108-15 cells, there are usually approx 10^5 cells/well at the end of the experiment.
5. For peptide ligands, it is often necessary to use peptidase inhibitors to prevent degradation of the peptide during the experiment. We have found that at very low cell densities, degradation of somatostatin is insignificant. However, at high cell densities, which are required when using cells expressing the receptor endogenously, peptide degradation can be significant. Use of peptidase inhibitors or analogs that are resistant to degradation is therefore desirable.
6. When using [^{125}I]-radioligands, relevant safety precautions should be taken. Once the radiolabel is present, all manipulations should be performed behind lead acetate screens. The water bath should also be screened. Hold the vacuum line with a clamp to increase the distance from the radioactivity. Note that > 90% of the radioactivity is removed with the incubation buffer at the end of the incuba-

tion. Therefore, shielding the waste container from the working area decreases exposure significantly. The radioactivity can be added to the cells with a repeating pipet to decrease exposure time. The working area should be monitored regularly and local safety procedures should be followed for all procedures involving radioactivity, including storage of isotopes and disposal of waste.

7. The choice of acid wash buffer requires careful consideration. The dissociation kinetics of the radioligand in the presence of GTP and physiological salt solution should be checked at a variety of pHs at the temperature to be used in the internalization experiment. We have used a buffer at pH 5.0 because this does allow measurement of ligand recycling afterward. Lower pH and high salt can reduce cell viability, although this is only important if using the cells after the acid wash. Many authors use 0.2*M* acetic acid, 0.5*M* NaCl, pH 2.5 ***(11)***. It is important to keep the temperature of the acid wash below 16°C to prevent further trafficking of receptor or ligand either in or out of the cell. Another aspect of the acid wash procedure that can be used to advantage is that it can dramatically decrease levels of nonspecific binding. It is partly for this reason that data for internalized ligand often have much smaller replicate error than surface binding has.

References

1. Birnbaumer, L., Abramowitz, J., and Brown, A. M. (1990) Receptor-effector coupling by G-proteins. *Biochim. Biophys. Acta* **1031,** 163–224.
2. Rasenick, M. M., Watanabe, M., Lazarevic, M. B., Hatta, S., and Hamm, H. E. (1994) Synthetic peptides as probes for G protein function. *J. Biol. Chem.* **269,** 21,519–21,525.
3. Koenig, J. A. and Edwardson, J. M. (1997) Endocytosis and recycling of G protein-coupled receptors. *Trends Pharmacol. Sci.,* **18,** 276–287.
4. Garland, A. M., Grady, E. F., Payan, D. G., Vigna, S. R., and Burnett, N. W. (1994) Agonist-induced internalization of the substance P (NK1) receptor expressed in epithelial cells. *Biochem. J.* **303,** 177–186.
5. Koenig, J. A., Edwardson, J. M., and Humphrey, P. P. A. (1997) Somatostatin receptors in Neuro2A neuroblastoma cells: ligand internalization. *Br. J. Pharmacol.* **120,** 52–59.
6. Yabaluri, N. and Medzihradsky, F. (1995) Reversible modulation of opioid receptor binding in intact neural cells by endogenous guanosine triphosphate. *Mol. Pharmacol.* **48,** 690–695.
7. Freitag, C., Svendsen, A. B., Feldthus, N., Lossl, K., and Sheikh, S. P. (1995) Coupling of the human Y2 receptor for neuropeptide Y and peptide YY to guanine nucleotide inhibitory proteins in permeabilized SMS-KAN cells. *J. Neurochem.* **64,** 643–650.
8. Koenig, J. A. and Edwardson, J. M. (1994) Kinetic analysis of the trafficking of muscarinic receptors between the plasma membrane and intracellular compartments. *J. Biol. Chem.* **269,** 17,179–17,182.
9. Fisher, S. K. (1988) Recognition of muscarinic cholinergic receptors in human SK-N-SH neuroblastoma cells by quaternary and tertiary ligands is dependent

upon temperature, cell integrity and the presence of agonists. *Mol. Pharmacol.* **33,** 414–422.

10. Wu-wong, J. R., Chiou, W. J., Magnuson, S. R., and Opgenorth, T. J. (1995) Endothelin receptor in human astrocytoma U373MG cells: binding, dissociation, receptor internalization. *J. Pharmacol. Exp. Ther.* **274,** 499–507.
11. Sorkin, A., Krolenko, S., Kudrjavtceva, N., Lazebnik, J., Teslenko, L., Soderquist, A. M., and Nikolsky, N. (1991) Recycling of epidermal growth factor-receptor complexes in A431 cells: identification of dual pathways. *J. Cell. Biol.* **112,** 55–63.
12. von Zastrow, M. and Kobilka, B. K. (1994) Antagonist-dependent and -independent steps in the mechanism of adrenergic receptor internalization. *J. Biol. Chem.* **269,** 18,448–18,452.
13. Pippig, S., Andexinger, S., and Lohse, M. J. (1995) Sequestration and recycling of β_2-adrenergic receptors permit receptor resensitization. *Mol. Pharmacol.* **47,** 666–676.

13a. Szekeres, P. G., Koenig, J. A., and Edwardson, J. M. (1998) Involvement of receptor cycling and receptor reserve in resensitization of muscarinic receptors in SH-SYRY human neuroblastoma cells. *J. Neurochem.* (in press).

14. Hertel, C., Coulter, S. J., and Perkines, J. P. (1985) A comparison of catecholamine-induced internalization of β-adrenergic receptors and receptor-mediated endocytosis of epidermal growth factor in human astrocytoma cells: inhibition by phenylarsine oxide. *J. Biol. Chem.* **260,** 12,547–12,553.
15. Heuser, J. E. and Anderson, R. G. W. (1989) Hypertonic media inhibit receptor-mediated endocytosis by blocking clathrin-coated pit formation. *J. Cell. Biol.* **108,** 389–400.
16. Moore, R. H., Sadnovnikoff, N., Hoffenberg, S., Liu, S., Woodford, P., Angelides, K., Trial, J., Cardsrud, N. D. V., Dickey, B. F., and Knoll, B. J. (1995) Ligand-stimulated β_2-adrenergic receptor internalization via the constitutive endocytic pathway into rab5-containing endosomes. *J. Cell. Biol.* **108,** 2983–2991.
17. Roettger, B. F., Rentsch, R. U., Pinon, D., Holicky, E., Hadac, E., Larkin, J. M., and Miller, L. J. (1995) Dual pathways of internalization of the cholecystokinin receptor. *J. Cell. Biol.* **128,** 1029–1041.
18. Lauffenburger, D. A. and Lindermann, J. J. (1993) *Receptors: Models for Binding, Trafficking and Signalling*. Oxford University Press, Oxford, U.K.

7

Autoradiography of Peptide Receptors

John Wharton and David A. Walsh

1. Introduction

An important step in understanding receptor function is determining the tissues and cells in which they are expressed. Classical physiological, biochemical, and membrane binding studies, however, usually provide inadequate spatial resolution to determine the anatomical and cellular localisation of specific receptors, particularly where there is a multiplicity of receptor subtypes. Therefore, alternative methods have been developed to provide the required anatomical and cellular resolution, the most widely used of which is in vitro receptor autoradiography. The methods are relatively simple and versatile and are applicable to the analysis of secondary messenger systems, ion channels, and enzymes (*see* Chapter 11) as well as receptors and may be used in combination with complementary techniques such as immunohistochemistry and *in situ* hybridization *(1)*. The widespread use of receptor autoradiography reflects the utility of the technique and the advantages it offers over membrane binding studies, in particular the capacity both to localize and quantify ligand binding within heterogeneous tissues without compromising either ligand binding or histological preservation. It is possible to detect and analyze regional differences in the distribution of receptor subtypes within a single tissue sample and thereby derive information that would be difficult, if not impossible, to obtain with other methods.

The essential steps in the autoradiographic detection of receptors comprise

1. Mounting unfixed cryostat tissue sections on slides.
2. Preincubating sections in buffer.
3. Incubating in buffer containing radiolabeled ligand.
4. Washing and drying sections.

From: *Methods in Molecular Biology, Vol. 106: Receptor Binding Techniques*
Edited by: Mary Keen © Humana Press Inc., Totowa, NJ

5. Generating macro- and/or microautoradiographic images of ligand binding sites. Numerous factors may influence the conditions adopted in each step of the procedure, and these have been reviewed previously *(1)*.

In this chapter, we discuss the autoradiographic localisation of natriuretic peptide and angiotensin II (ANG II) receptors, using ^{125}Iodinated ligands. The protocols described can be adapted to the detection of other ligand binding sites using other radioisotopes (*see* Chapter 11). Autoradiography of these peptide receptors illustrates issues of multiple receptor subtypes with differing distributions and pharmacology, the effects of G-protein coupling on ligand binding, interspecies differences in distribution and specificity, the availability of a variety of agonist and antagonist, peptide and nonpeptide ligands, and the localization of binding sites as an aid to the elucidation of their function.

The natriuretic peptide family has an important role in maintaining cardiovascular homeostasis and includes atrial natriuretic peptide (ANP), brain natriuretic peptide (BNP), C-type natriuretic peptide (CNP) and urodilatin *(2,3)*. The biological effects of these peptides are mediated by two classes of receptor, one of which comprises a monomeric transmembrane protein possessing an integral intracellular guanylyl cyclase domain and an extracellular domain that fulfils rigorous structural requirements for ligand binding and activity *(4,5)*. Two subtypes of this receptor class have been identified, so-called A and B natriuretic peptide receptors (NPR_A and NPR_B), which exhibit different rank orders of potency for natriuretic peptide-enhanced cyclic GMP production *(6,7)*. The other high-affinity receptor class (NPR_C) is a dimeric protein, composed of two disulphide-linked subunits, which lacks a guanylyl cyclase domain *(8)*. It is has been thought that this receptor subtype has a clearance role *(9)*. However, it also mediates functional responses and appears to be linked to other second-messenger systems *(10,11)*. NPR_C receptors are much less rigorous than NPR_A and NPR_B receptors in their structural requirements for ligand binding, and in addition to the endogenous natriuretic peptides, they display a high affinity for D-amino acid substitutions and ring-deleted analogs of ANP1-28 such as des[Gln^{18}, Ser^{19}, Gly^{20}, Leu^{21}, Gly^{22}]-rANP4-23 (C-ANP4-23) *(12)*. This analog has been used in autoradiographic studies as a selective ligand to distinguish NPR_C receptors in organs such as the kidney and heart, the NPR_C receptor subtype predominating in renal glomeruli and cardiac endocardium, respectively *(13–17)*. In contrast, the investigation of guanylyl cyclase-linked NPR_A and NPR_B receptors has been hampered by the lack of suitable antagonists. Although peptide analogs have been synthesized that exhibit selectivity for the guanylyl cyclase-linked receptor subtypes *(18)*, the best characterized receptor antagonist to date is a novel microbial polysaccharide, HS-142-1. This nonpeptide antagonist selectively binds to guanylyl cyclase-linked natriuretic

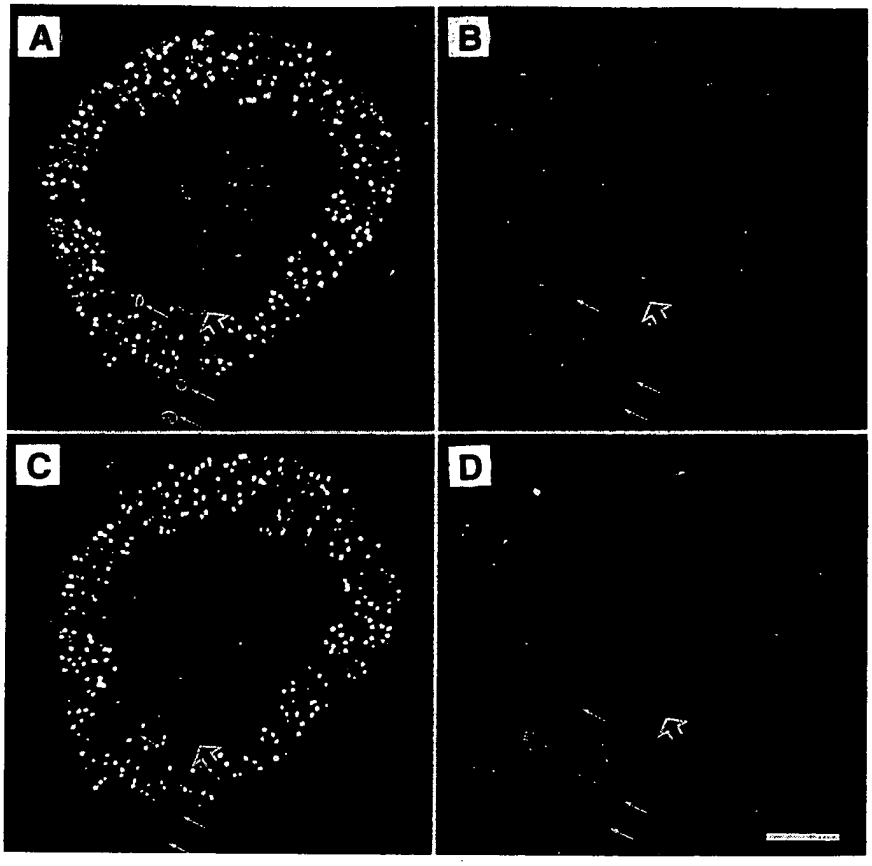

Fig. 1. Autoradiographic localization of [^{125}I]-rat ANP 1-28 binding in rat kidney. Serial sections incubated with 250 pM [^{125}I]-rat ANP 1-28 in the absence (**A**) or presence of either 10^{-6} M rat ANP 1-28 (**B**), 1 mg ml^{-1} HS-142-1 (**C**) or 1 mg ml^{-1} HS-142-1 and 10^{-6} M C-ANP4-23 (**D**). HS-142-1 and C-ANP4-23 are selective ligands for guanylyl cyclase-linked (NPR_A and NPR_B) and nonguanylyl cyclase-linked (NPR_C) natriuretic peptide receptors. The receptors exhibit a heterogeneous distribution pattern in glomeruli, inner medulla, vasa recta bundles, renal arteries (arrows) and smooth muscle in the renal papilla (open arrow). Reversal prints of film autoradiograms. Bar = 2mm.

peptide receptors and, unlike other ligands, it exhibits no apparent affinity for nonguanylyl cyclase-linked NPR_C receptors ***(19,20)***. Although HS-142-1 does not distinguish between NPR_A and NPR_B receptors, it may used in combination with the NPR_C receptor-selective ligand C-ANP4-23 to distinguish guanylyl and nonguanylyl cyclase-linked natriuretic receptors (***[16]***; **Fig. 1**).

A useful adjunct to the autoradiographic analysis of peptide receptors is the

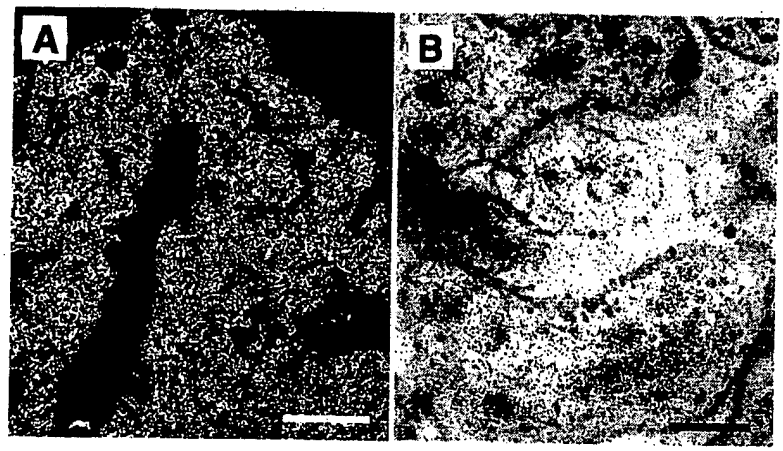

Fig. 2. Macro- and microautoradiographic localization of [^{125}I]-(S^1,I^8)ANG II binding in human placenta. Reversal film print of a film autoradiogram showing the distribution of AT_1 receptors in a section of placenta (**A**). Photomicrograph of a microautoradiogram, obtained using emulsion-coated cover-slip method, showing localisation of AT_1 receptors to microvessels in placental villi (**B**). Sections incubated with 250 pM [^{125}I]-(S^1,I^8)ANG II in the presence of 10^{-6} M PD123319, a selective nonpeptide AT_2 receptor antagonist. Bars = 2mm (a) and 50 μM (b).

increasing availability of antisera to receptor subtypes, and these may be used, together with radiolabeled ligands, to examine the cellular localization of receptor protein expression. For example, we have used a specific NPR_C receptor antibody, as well as receptor-selective ligands and in vitro autoradiography, to localize and measure NPR_C receptor expression in the rat heart, demonstrating that volume-induced ventricular hypertrophy is associated with downregulation of the NPR_C receptor in the endocardium *(17)*.

The actions of angiotensin II (ANG II) are mediated by specific membrane-bound receptors, of which two main subtypes have been identified, AT_1 and AT_2 receptors, by their pharmacological and molecular characteristics *(21)*. Both are members of the seven-transmembrane-domain superfamily of receptors and have a similar affinity for ANG II and the peptide antagonist (Sar^1,Ile^8)ANG II but may be distinguished by their distinct affinity for other peptide analogs and nonpeptide compounds. AT_1 receptors display a high affinity for nonpeptide antagonists such as losartan *(22,23)* and eprosartan *(24)*, whereas AT_2 receptors have high affinity for the nonpeptide antagonist PD 123319 *(25)* and peptide analogs such as CGP 42112A *(26)* and [p-amino-Phe^6]ANG II *(27)*. The two receptors may also be identified on the basis of their distinct sensitivity to the disulphide reducing agent dithiothreitol (DTT),

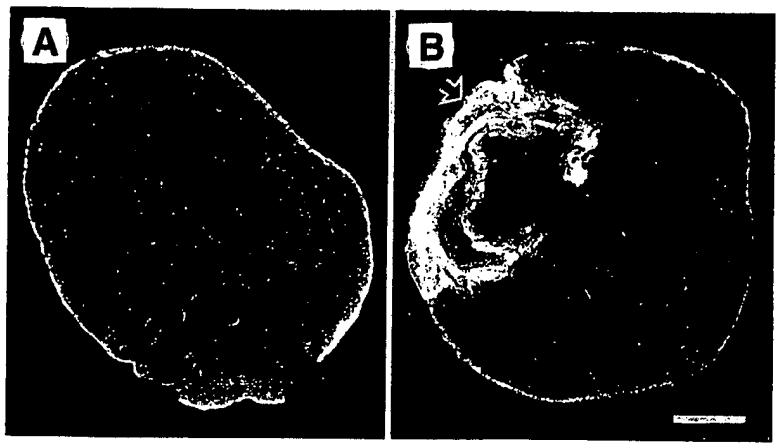

Fig. 3. Reversal prints of film autoradiograms showing [^{125}I]-(S^1,I^8)ANG II binding to rat ventricular myocardium 7 days after either sham operation (**A**) or myocardial infarction induced by left coronary artery ligation (**B**). Binding is increased (arrow) in the infarcted region of the left ventricle (LV) and corresponds to an increase in AT_1 receptor density associated with fibroblast infiltration and collagen deposition. Bar = 2mm.

binding to AT_1 receptors being inhibited by DTT, whereas that to AT_2 receptors is unaffected or enhanced in the presence of DTT *(22,28)*. Agonist binding to the two receptors also exhibits a differential sensitivity to guanine nucleotides *(25)*. These criteria have been employed to distinguish AT_1 and AT_2 receptors in autoradiographic studies of human tissues, including the kidney *(29,30)*, synovium *(31)*, and placenta (*[32]*; **Fig. 2**), and we have also used them to examine the changes in ANG II receptors in experimental models of myocardial infarction (*[33]*; **Fig. 3**) and angiogenesis *(34)*.

The functional importance of the cardiac AT_2 receptor subtype has yet to be established, but it has been shown to mediate a number of ANG II-induced responses in the cardiovascular system *(35–40)*, and autoradiographic observations indicate that the AT_2 receptor is selectively associated with regions of fibrosis in the human heart *(41)*. Other studies have also demonstrated developmental changes in the distribution of ANG II receptor subtypes in the mammalian cardiovascular system *(42,43)*.

In addition to a marked heterogeneity in the localization of AT_1 and AT_2 receptors, there are also important species differences in their distribution pattern. For example, most studies indicate that AT_1 sites represent the majority of cardiac ANG II receptors in experimental mammals whereas the AT_2 subtype predominates in membrane preparations of the human heart *(44–46)*.

Furthermore, there are important interspecies differences in the specificity of ANG II receptors for synthetic antagonists *(47)*. Interspecies heterogeneity appears to be a general feature of many peptide systems, raising difficulties in the extrapolation of data from animal models to man *(48)*. Receptor autoradiography provides one method by which such differences may be elucidated.

2. Materials

1. Thermostatically controlled laboratory space suitable for work with radioactive substances. Binding and ligand degradation are temperature-sensitive, and most peptide binding experiments are performed at 20–22°C.
2. Tissue-TEK™ O.C.T. mounting compound and cork discs (e.g., Histological Equipment, Ltd.).
3. Iso-Pentane (2-methylbutane) (e.g., BDH 10631), liquid nitrogen, thermos flask, and a pyrex or metal beaker.
4. Heat sealer and polythene layflat tubing (e.g., A1 Packagings, Ltd., London, U.K.).
5. Glass microscope slides (e.g., low iron BDH Premium 406/0184/04) and cover slips (e.g., BDH 406/0188/42).
6. Vectabond™ reagent (Vector Laboratories SP-1800) and acetone.
7. Cryostat, preferably motorized, capable of cutting frozen sections of reproducible thickness, usually 10 or 20 µm (e.g., Bright Instrument Co., Ltd.).
8. Buffers and protease inhibitors (**Table 1**).
9. Radiolabeled ligands (e.g., Amersham Life Sciences and NEN™ Life Science Products). Reconstitute according to manufacturers recommendations, aliquot (e.g., 100–400 µL) at appropriate concentration (e.g., 5 n*M*) and store at –20°C or lower.
10. Unlabeled peptides, peptide fragments/analogs and nonpeptide antagonists. Aliquot at appropriate concentration (e.g., 2×10^{-3} to 2×10^{-5} *M*) and store at –20°C or lower.
11. Protease-free bovine serum albumin, fraction V powder (e.g., Sigma A 3294).
12. Metal slide racks (24 capacity) and dishes (400–500 mL capacity).
13. Humidified incubation chambers. Moistened filter paper is laid between a pair of pipets, or under a suitable rack, in plastic petri dishes (14 cm dia.) accommodating four microscope slides. Alternatively, use perspex trays (*see* Chapter 11) or immunostaining slide trays.
14. Hair dryer. High air flow and "cold" settings are essential.
15. Dark room with safelight (e.g., Kodak 6B or Ilford 902/904 filters).
16. Autoradiography film (e.g., Hyperfilm™-^{3}H, 24 × 30 cm, Amersham RPN 12).
17. Autoradiography cassettes with side-lever closure (e.g., Genetic Research Instrumentation Ltd., Dunmow, U.K.) rather than clip-closure designs.
18. Radioactive standards (e.g., Amersham [^{125}I] Microscales™ RPA 523).
19. Bouin's fluid: 250 mL of 40% (w/v) concentrated formaldehyde solution, 750 mL saturated picric acid, with addition of 1 mL acetic acid per 100 mL immediately prior to use of fixative.

Table 1
Procedures for Natriuretic and Angiotensin II Ligands

Ligand	[^{125}I]-ANP 1-28	[^{125}I]-(Sar^1,Ile^8)Angiotensin II
Specific activity TBq/mmol	74	81.4
Concentration	0.25 n*M*	0.25 n*M*
Preincubation & wash buffer	30 m*M* PBS (pH 7.4), 123 m*M* NaCl	10 m*M* PBS (pH 7.4), 150 m*M* NaCl, 10 m*M* $MgCl_2$
Incubation buffer; to preincubation buffer, add:–	0.5% BSA, 28 μ*M* bacitracin	0.5% BSA, 28 μ*M* bacitracin, 5m*M* EDTA
Preincubation time	1 × 15 min	2 × 5 min
Incubation time	90 min at 20°C	90 min at 20°C
Wash at 4°C	2 × 5 min	2 × 5 min
Fixation	Bouin's, 30–60 min at 20°C	(Dry paraformaldehyde vapor, 30 min at 90°C)
Microscopic localization	Emulsion dipping	*see* **Note 24**
Exposure: Film	2 d at 4°C, by immersion in Bouin's fluid	3–4 d at 4°C
Slide	4–6 d at 4°C	7–14 d at 4°C

ANP, atrial natriuretic peptide; PBS, phosphate buffered saline; BSA, protease free bovine serum albumin; EDTA, ethylenediaminetetraacetic acid.

20. Stainless steel vertical slide rack (e.g., Raymond A Lamb U.K. E/89 and E/89.03)
21. Wire loop (2–3 cm dia.) made from nickel/chrome or platinum wire (~ 0.5 mm thick).
22. Nuclear emulsion (e.g., Amersham LM-1 RPN 40, or Ilford K5 diluted 1:1 in water) and dipping vessel (e.g., Amersham RPN 39).
23. Light-tight box suitable for autoradiography (e.g., Raymond A Lamb E/107 takes rack E/99).
24. Cyanoacrylate adhesive ("Superglue").
25. Developer (e.g., Kodak D19 #5027065), stop solution (0.1% acetic acid) and fixer (e.g., Champion Photochemistry, Brentwood, U.K., Amfix™ #80213, diluted 1 + 4 with tap water).
26. Histological staining solutions (e.g., hematoxylin and eosin).
27. 70% and absolute ethanol, xylene or Histoclear and dibutylphthalate polystyrene xylene (DPX) mounting medium.
28. Microscope equipped for transmitted light and dark-field illumination.
29. Image analysis system.

3. Methods

3.1. Preparation of Tissues and Sections (see Note 1)

1. Tissue samples are orientated in Tissue-Tek™ mounting compound, on labeled cork discs. Where possible, the tissue face should be parallel to the block and not be larger than about 2.25 cm^2 in area and 1.0 cm thick. Smaller pieces of tissue can be mounted together, and unstable samples may be supported with needles during freezing to facilitate accurate orientation. Very small samples (e.g., endoscopic or endomyocardial biopsies) can be placed in silver foil molds or embedded in liver prior to mounting on cork discs.
2. The samples are completely surrounded by Tissue-Tek™, immersed in a beaker of melting isopentane, and suspended in a thermos flask containing liquid nitrogen (*see* **Note 2**).
3. After immersion, the tissue block is inverted and left floating for several minutes to equilibrate with the freezing solution. Frozen tissues are transferred to labeled plastic bags or other suitable containers and stored either in liquid nitrogen or a freezer at −40°C to −70°C (*see* **Note 3**).
4. Glass microscope slides are pretreated with Vectabond™ to improve section adhesion (*see* **Note 4**). Rinse slides in a metal slide rack in acetone, then immerse in Vectabond reagent solution (7 mL in 350 mL acetone) for 5 min at room temperature, rinse in distilled water, and dry at 37°C.
5. Thin (e.g., 10 µm) sections of unfixed tissue are cut in a cryostat at −20°C to −30°C and thaw-mounted on slides prepared as above (*see* **Note 5**). Sections are air-dried with silica gel desiccant for 1 h at 4°C then used immediately, or stored at −20°C in sealed bags with silica gel (*see* **Note 6**).

3.2. Incubations

1. Batches of sections in slide racks are preincubated for 10 min in slide baths containing 400 mL preincubation buffer (i.e., buffer without either BSA or radiolabeled ligand) (*see* **Note 7** and **Table 1**).
2. Slides are removed from the preincubation buffer, gently tapped on absorbent paper, and excess buffer removed by wiping around the edge of each section. Wet absorbent paper is placed in the bottom of an incubation chamber and slides arranged horizontally (*see* **Note 8**).
3. Sections are covered with a measured volume (e.g., 100 µL) of incubation buffer containing either radiolabeled ligand alone (total binding), radiolabeled ligand together with an excess of unlabeled ligand (nonspecific binding) or radiolabeled ligand and unlabeled receptor-selective compounds to identify receptor subtypes. Sections are incubated for an appropriate time and temperature (*see* **Note 9** and **Table 1**).
4. Incubations are terminated by tapping the slide on absorbent paper, then rinsing twice by immersing batches of slides in an excess (e.g., 400 mL) of cold buffer.
5. Sections are briefly dipped in ice-cold distilled water and immediately dried under a stream of cold air, using a high-speed, nonheated hair drier (*see* **Note 10**).

3.3. Preparation of Film Autoradiograms

1. Slides are arranged with the sections facing upwards in an autoradiography cassette, together with [^{125}I]-radiolabeled standards (*see* **Note 11**). Unused spaces should be filled with clean glass slides. Attach an index sheet to the front of the cassette, showing the location of sections, the ligand(s) used, and date of exposure.
2. Under safelight conditions, radiosensitive film with the emulsion surface down is carefully apposed to the sections, and the cassette is closed (*see* **Note 12**). Expose for an appropriate time, either at 4°C or –20°C, away from vibrations and other movement (*see* **Note 13**).
3. Bring the cassette to room temperature before opening under safelight conditions. Carefully remove film and develop in Kodak D19 at 20°C for 3–4 min, stop in 0.1% (v/v) acetic acid, fix in Amfix (diluted 1 + 4 in tapwater) for 10 min, wash under running cold tapwater for 20 min, and rinse briefly in distilled water before hanging in a drying cabinet. (*see* **Notes 14–16**).

3.4. Quantification of Film Autoradiograms (see Notes 17,18)

1. The autoradiographic film is illuminated from behind by using a light box with stable electricity supply, and the image captured via a black and white video camera, with conversion from an analog-to-digital image. The energy level (gray level) of each discrete point or unit of the image (pixel) is digitally represented in a binary 8-bit system giving 256 (2^8) discrete gray levels, ranging from 0 (black) to 255 (white). To minimize the contribution of stray light, all measurements must be made under constant low lighting. Blank and opaque areas of film are used to correct for variations in light transmission or illumination of the optical system and a shading correction procedure employed.
2. A standard curve is constructed, using images of at least six radioactive standards. Each is selected using the cursor (*see* **Notes 19** and **20**).
3. Regions of interest in those autoradiographic images that were derived from radiolabeled tissue sections are identified by microscopic comparison with adjacent stained sections. Structures are delineated either by using the cursor or by thresholding according to optical density (*see* **Note 21**).
4. The integrated gray level values in these regions are related to the amount of ligand bound by transforming the data using the standard calibration curve derived for each film (*see* **Notes 22–23**).

3.5. Preparation of Microautoradiograms

The optimum method for producing microautoradiograms is dependent on the receptor being investigated and ligand used (*see* **Note 24** and Chapter 11).

1. Immerse radiolabeled sections in Bouin's fluid for 30–60 min at room temperature.
2. Thoroughly wash sections in water, and dry under a stream of cold air.
3. Warm LM-1 emulsion to 42°C in a water bath under safelight conditions (*see* **Note 25**).

4. Carefully pour emulsion into a warm dipping vessel at 42°C and leave to stand in the water bath. Use spare slides to test that the emulsion is free of bubbles and ready to use.
5. Dip the glass microscope slide vertically into the emulsion and immediately withdraw, gently scraping one side against the vial to remove excess emulsion. Place vertically on a drying rack, resting against the scraped side, and leave to dry in the dark for at least 1 h.
6. When dry, the emulsion-coated slides are transferred to plastic slide boxes containing silica gel, sealed with autoclave tape, labeled and exposed at 4°C (*see* **Note 26**).
7. Warm to room temperature, and open the slide box under safelight conditions. Place slides in a slide rack, and immerse in Kodak D19 developer for 3 min at 20°C, ensuring that developer gains access to the emulsion by vertical agitation. Stop in 0.1% acetic acid, fix in Amfix diluted 1+4 in tapwater for 6 min, and rinse for 20 min in running cold water.
8. Counterstain tissue sections (e.g., with hematoxylin and eosin), dehydrate through graded alcohols (once in 70% ethanol, twice in absolute ethanol), transfer to an organic medium (e.g., twice in xylene or Histoclear), and mount in DPX (*see* **Notes 27** and **28**).

3.6. Immunofluorescence Staining

The anatomical localization of binding sites is often further aided by immunostaining adjacent sections, using antisera to specific cell markers (*see* **Note 29**). Antisera to receptors, as well as other ligand-binding sites, are also available for immunohistochemical studies.

1. Cryostat sections, either radiolabeled or adjacent to those used for radiolabeling, are fixed by immersion of slides for 10 min in either cold acetone (–20°C) or buffered formal-saline (4% formaldehyde in phosphate buffered saline (PBS), pH 7.4).
2. Rinse slides in PBS (2 × 5 min), immerse in Pontamine Sky Blue counterstain solution (0.15 g Pontamine Sky Blue (BDH 34138 2A9) and 1.5 ml dimethyl sulphoxide in 30 ml PBS) for 30 min at room temperature, and rinse again in PBS (*see* **Note 30**).
3. Individual slides are taken out of the PBS, excess buffer removed by wiping around sections with absorbent paper and placed horizontal in an incubation tray containing wet absorbent paper.
4. Sections are covered with primary antiserum (diluted in PBS containing 0.1% BSA and 0.01% sodium azide), using a Pasteur or Eppendorf pipet, and incubated overnight at 4°C (*see* **Note 31**).
5. Terminate incubations by tapping the slide on absorbent paper, and rinse twice (2 × 5 min) by immersing batches of slides in PBS.
6. Repeat **step 3** and apply an appropriate optimally diluted fluorescent-labeled secondary antiserum for 1 h at room temperature.

7. Repeat step 6 and mount in PBS-glycerol (1:1) or use commercially available mountant with antifade agent (e.g., Vectashield™, Vector Laboratories H-1000) (*see* **Note 32**).

4. Notes

1. Tissue samples should be obtained in the best possible condition, keeping delays to a minimum. However, many receptors appear to be reasonably stable postmortem, and we have obtained comparable results using human tissues obtained at surgery and postmortem (less than 24 h after death).
2. Tissues (e.g., the lung) may be infused or inflated with Tissue-Tek (diluted 1:1 with phosphate-buffered saline) prior to freezing. Ideally, all air spaces in the tissue should be filled with mounting medium.
3. Tissues stored in liquid nitrogen have been kept for a number of years without detectable loss in peptide-binding capacity, but repeated warming to cryostat temperatures may have a detrimental effect.
4. Several methods for improving adherence of tissue sections to glass microscope slides have been described, including pretreatment with a 1–4% solution of 3-aminopropyltriethoxysilane (Sigma A3648) and coating slides with either poly-L-lysine (> 300,000 Sigma P1524) or chrome-alum gelatin. Pretreated slides are also commercially available (e.g., BDH Polysine 406/0178/00 and Superfrost plus 406/0179/00). Vectabond pretreatment is effective for most purposes, although some ligands may give high nonspecific binding to the surface of pretreated slides and require an alternative method to improve adherence. Vectabond treated slides may be kept for several months at room temperature prior to use.
5. Tissue sections should be cut serially, orientated in an identical manner on numbered slides, and be the same thickness and mounted on the same type of microscope slide as the radioactive standards. Multiple sections may be placed on the same slide, providing there is adequate space between them (*see* **Note 8**). If the sections are to be used for microautoradiography, they should not be placed near either end of the slide.
6. All sections should be treated similarly within each individual experiment. For example, when an experiment requires more sections than can be cut in a single session, all sections should be frozen before use. Keeping sections for prolonged periods at room temperature (>2 h) and repeated freezing and thawing should be avoided, as this may be detrimental both to ligand binding and tissue morphology.
7. Tissue sections are preincubated to encourage elution of endogenous ligand and nontissue bound enzymes capable of degrading ligand. Preincubation also permits tissue rehydration and equilibration with buffer. Optimum conditions are determined empirically by examining subsequent specific binding. Preincubation conditions may also be modified to investigate prior occupancy of binding sites by endogenous ligand. For example, washing sections in 300 m*M* NaCl (pH 4–5) for 30 min at 20°C removes bound [^{125}I]-ANP1-28 ligand while retaining both tissue morphology and ligand-binding capacity. In the case of G protein-coupled receptors, tissue sections may be preincubated in buffer containing GTP

to promote the dissociation of endogenous ligand. Controls should be included in such "desaturation" experiments to determine the proportion of binding sites that return to their high-affinity state, since desaturation often can *reduce,* rather than increase, specific binding.

8. In quantitative experiments, it is essential that incubation volumes are identical for each section, so that dilution by preincubation buffer and concentration by evaporation are constant (and minimized). Large incubation volumes reduce the likelihood that partitioning of ligand into the solid phase or enzymatic degradation of ligand will lead to ligand depletion during the experiment. However, volumes above 100 µL are less easily retained by surface tension, resulting in the buffer pools coalescing and running off the tissue sections. Mounting tissue sections at least 1 cm away from adjacent sections or the frosted end of the slide, wiping incubation buffer from around and between sections using absorbent paper, demarcating sections with a hydrophobic pen (e.g., DAKO Ltd., S2002), and horizontal positioning of slides may each help to localize buffer. However, be aware that some ligands bind to hydrophobic surfaces with high capacity. Sections must not be allowed to dry between preincubation and incubation steps, as this may be detrimental to the integrity of tissue morphology and ligand binding. Large runs are best loaded in batches, ensuring that incubation times remain constant between batches.
9. Incubation buffers, incubation conditions, and washing conditions are determined empirically to optimize binding (i.e., maximize the ratio between total and nonspecific binding). Duration of incubation is determined by the time to reach equilibrium binding at the stated ligand concentration and temperature. Low ligand concentrations, high molecular weight ligands, and low temperatures require longer incubations.
10. Rapid drying, at low temperature, minimizes diffusion of ligand from binding sites and thereby improves the resolution of autoradiographic images.
11. 24 × 30 cm film cassettes accommodate up to 33 microscope slides. Each film should be exposed with a series of radiolabeled standards, since slight differences in development times and temperatures can substantially affect optical densities. Standards should also have the same absorbance characteristics as the experimental tissue; therefore, it should ideally be made from a paste of that tissue. In practice, individual tissues contain heterogeneous structures, and we use commercially available radiolabeled polymer standards. These typically have the absorbance characteristics of brain paste. We have routinely used 10 µm thick cryostat sections and ^{125}I-labeled standards. However, radioactive-standard polymer blocks can be difficult to cut and 20 µm thick precut standards (e.g., Amersham [^{125}I] Microscales™ RPA 523) may be used together with 20 µm thick cryostat sections. Precut Microscale strips should be mounted on the same type of slide as the cryostat sections using superglue. ^{125}I has a half life of 60 days, and [^{125}I]-labeled standards must be regularly replaced. [^{14}C]-labeled standards have been used for [^{125}I]-labeled ligands. In our experience, although plots of optical density or gray level against specific activity for [^{125}I]- and [^{14}C]-

labeled standards give parallel curves, use of [^{14}C]-labeled standards results in underestimation of binding density (by a factor of 4.3 using [^{3}H]-Hyperfilm with a 1–3 day exposure).

12. Autoradiographic films which are not coated to protect the emulsion may give crisper images than do coated films. Uncoated films must be handled at the edges and care taken to avoid touching the emulsion layer (e.g., peel off the protective envelope, rather than sliding the film out, and develop the film manually with emulsion surface uppermost to avoid scratches). To avoid obtaining blurred images, it is essential that the film is closely apposed to the labeled sections and that nothing is interposed between film and slides (e.g., pieces silica gel or glass) (*see also* **Note 15**, below). To ensure correct orientation of Hyperfilm-^{3}H in the cassette, check that the only rounded corner of the film is in the top right hand corner of the cassette.
13. Exposure times are determined by the density of ligand binding, specific activity of the ligand, and the radioisotope that is used (*see* also Chapter 11). Low temperature exposure is used to preserve tissue integrity. Exposure at 4°C is usually adequate but –20°C may be required for exposures longer than 1–2 wk. Exposure should be sufficient to produce optical densities over the region of interest which are near the middle of the standard curve (*see* **Note 19**). If there is a wide range of binding densities within a tissue or between sections, multiple exposures of different durations may be required. It is essential that images are not saturated, as this would lead to underestimation of binding densities. When this affects the top of a binding inhibition curve, it will also lead to an overestimation of the 50% inhibitory concentration and an underestimation of the affinity of the inhibiting ligand.
14. Five liters of developer is prepared by dissolving D19 powder in water according to the manufacturers instructions and may be stored in 1 L aliquots in the dark, and reused several times until discolored.
15. Blurred images on film autoradiograms can be troublesome. They may result from a number of factors and limit both localization and quantification of binding sites, particularly on small structures. Ensure that no solid particles such as silica gel or detached tissue were interposed between slides and film, that slides were packed next to each other with no overlapping, that all slides were of the same thickness, that all space in the cassette was filled with "blank" slides, and that the film was not trapped in the edge of the cassette. Repeat the exposure. If images are still blurred, it may be that slides were dried too slowly or at too high a temperature, that the tissue section was too thick, or that morphology has not been well preserved. Low resolution may a feature of underexposed images (low contrast between positive and background binding), or overexposed images (film saturated over regions with positive binding and excessive silver grain deposition in adjacent regions from oblique emissions). Finally, some apparently blurred images accurately reflect the distribution of binding sites; for example, if binding is to inflammatory cells that are diffusely distributed in or around tissue structures. Compare the autoradiogram with microscopic preparations.

16. Film autoradiograms may be photographed for reproduction or cut up and placed in an enlarger to produce reversal or pseudodark-field black and white photographs, using high contrast (grade 5) paper. For comparisons to be valid, all prints must be made using identical exposure and development conditions. Prints of high quality can be obtained with this method, but it may be time consuming to reproduce a full range of autoradiographic images, showing total as well as nonspecific binding. Alternatively, an image analysis system may be used to reproduce macroautoradiograms, as well as undertake quantitative studies. This approach offers several advantages, including the ability to obtain pseudocolor and edited images by using software such as Adobe Photoshop™. Several images can be combined, producing composite prints for publication. Electronic images can be used to generate 35 mm transparencies (e.g., Lasergraphics LFR Mark II) and combined with other elements (photographic and graphic images, text, animations, and video clips), using computer programs such as Microsoft Power Point™.
17. Quantitative autoradiographic techniques are required to characterize those ligand-binding sites that have been localized, demonstrating that the binding is specific, time and temperature dependent, saturable, and reversible. Although it is possible achieve this at the microscopic level by grain counting, most investigators use film autoradiograms and computer-assisted image processing to obtain quantitative data. To quantify film autoradiograms, tissue sections must be coexposed with calibrated radioactive standards in order to permit the estimation of molar quantities of ligand bound to the tissue sections.
18. A variety of suitable image processing systems are available, the essential components being an illumination box, video camera, computer, image processing board (frame grabber), and video monitor. The processing board serves several functions, including analog-to-digital conversion of the image, temporary storage of the captured image, and digital-to-analog conversion to display the image. Both conventional video tube and solid-state charge-coupled device (CCD) cameras may be suitable, providing there is a linear relationship between the light input intensity and the output of the camera (i.e., the camera has a Gamma of 1.0). The camera should also have a manually selectable black level and gain.
19. The relationship between gray levels or optical density and tissue radioactivity is not linear. Optical density does not increase as rapidly as tissue radioactivity. The linearity of the response is greater with shorter duration exposures, but these may result in autoradiograms that are too faint. Hyperfilm approaches saturation at an optical density value of 1.0, and the lower limit of optical density detection is about 0.01. Therefore, it is important that all measurements are made within this range near the middle of the standard curve and that any standards giving values at the upper and lower end of the range are not used.
20. A number of possible mathematical transformations have been used to transform image gray levels or optical density values as a linear function of the ligand concentration in tissue sections. Except for very low and very high levels of activity,

a linear relationship exists between the natural log plots of optical density versus radioactivity and if the linear 0–255 scale of gray values is plotted as a function of the logarithm of ligand concentration.

21. Only structures with detectable binding can be visualized on film autoradiograms, although the location of other structures may sometimes be inferred from their spatial relationship to visible adjacent structures. Delineation of structures according to their optical densities on film autoradiograms introduces a potential bias that tends to increase measured optical densities. When delineating structures by thresholding, it is important that the regions that are thresholded are comparable between tissue sections. Aim to include a similar area of thresholded structure per unit area of tissue section, rather than fixing thresholds at specified optical densities.
22. Binding data can be expressed as moles of ligand bound per unit area of tissue section (e.g., amol/mm or fmol/mm) or related to the protein content of the tissue (e.g., fmol/mg protein), using a densitometric method and the dye Coomasie Blue G-250 to stain tissue sections and protein standards.
23. Phosphor screen imagers are increasingly being used as an alternative to film autoradiography, as they provide sensitive and reusable screens, have a high dynamic range, and produce images in less time than conventional autoradiography. On the other hand, this expensive technology also suffers from some of the same disadvantages as film autoradiography; the apposition between the image and stained section is lost during processing and the lifespan of cassettes is relatively short. The spatial resolution of binding sites is also limited and has not yet surpassed that of conventional film-based autoradiography.
24. High anatomical resolution of receptor localization is achieved using microautoradiographic techniques. We have found that chemical fixation of ligands to binding sites by immersion in Bouin's fluid prior to dipping in emulsion is generally applicable for most [^{125}I]-labeled peptides, including the natriuretic peptides. Regional differences in ligand-binding densities are maintained when compared with film autoradiograms and tissue morphology preserved for microscopic examination. However, in comparison to other peptide receptors, we have found that [^{125}I]-(Sar^{1}, Ile^{8}) angiotensin II binding to ANG II receptors is more readily dissociated when labelled sections are immersed in fixative and emulsion. Adequate fixation can be achieved by exposure to dry paraformaldehyde vapor for 30 min at 90°C. Be sure to wear protective clothing, use an appropriate sealed container, do not allow tissue sections to come in contact with the paraformaldehyde powder, and transfer to a fume cupboard and allow to cool to room temperature before opening. Paraformaldehyde vapor has the disadvantage of damaging tissue morphology and reducing reactivity to hematoxylin. Alternative approaches for localizing ligands that cannot easily be fixed to tissue sections are described in Chapter 11.
25. Providing LM-1 emulsion is stored in the dark at 4°C, away from radioactive sources; it may be used several times. Alternatively, under safelight conditions,

warm Ilford K5 emulsion to 42°C in a waterbath, dilute 1:1 with warm tap water, make single-use aliquots (approximately 10 mL each), and store in a light-tight container at 4°C, away from radioactive sources.

26. Exposure times for microautoradiographic preparations are usually two to three times longer than those required for film autoradiograms and need to be determined empirically to obtain the optimum results for each ligand and tissue. It is often helpful to have a series of identically labeled preparations that may be developed at different times.
27. When the DPX mountant is dry, emulsion-coated slides need to be thoroughly cleaned prior to microscopic examination and photography. Dried emulsion may be removed using household bleach, water, and tissues.
28. Microautoradiographic preparations may be examined using either bright-field, dark-field, or epi-illumniation. Bright-field illumination enables the distribution of silver grains in the emulsion to be related directly to the underlying tissue structure. It can be difficult to focus on both the stained tissue and silver grains simultaneously, and it is preferable to focus on the overlying silver grains for photography and, if necessary, include additional photomicrographs to show tissue structure. Dark-field or epi-illumination is useful when the density of specific silver grains and background labelling is relatively low. Photomicrographs should be taken using suitable film for epi-illuminated, microautoradiographic, fluorescent preparations (e.g., Fugichrome Provia 400 or Kodak TRI-X 400), and for sections viewed with transmitted light (e.g., Kodak Ektachrome 64 or T-MAX 100).
29. Indirect immunfluorescence staining is relatively simple and is well suited for combined autoradiographic and immunohistochemical studies, however; other methods offer greater sensitivity (e.g., peroxidase-antiperoxidase and avidin-biotin) and may be used in conjunction with procedures that intensify the diaminobenzidine reaction product (e.g., Nickel-glucose oxidase).
30. Immunostaining may be enhanced by immersing fixed sections in PBS containing 0.2% Triton-X100 for 30 min prior to counterstaining.
31. Optimum antibody dilutions have to be established empirically and may vary according to the type of tissue and method of fixation used, as well as the immunostaining technique used.
32. It can be helpful to counterstain cell nuclei (e.g., Hoechst 33342) prior to mounting sections or use mountants which incorporate a nuclear stain (e.g., Vectashield with 4',6-diamidino-2-phenylindole (DAPI) or propidium iodide, Vector Laboratories, H-1200/1300).

References

1. Wharton, J., Walsh, D. A., Rutherford, R. A. D., Knock, G. A., and Polak, J. M. (1993). *In vitro* autoradiographic localisation and characterization of binding sites, in *Receptor Autoradiography: Principles and Practice* (Wharton, J. and Polak, J. M., eds.) Oxford University Press, Oxford, pp. 79–105.
2. Wilkins, M. R., Nunez, D. J., and Wharton, J. (1993) The natriuretic peptide family: turning hormones into drugs. *J. Endocrinol.* **137,** 347–359.

3. Anand-Srivastava, M. B. and Trachte, J. E. (1993) Atrial natriuretic factor receptors and signal transduction mechanisms. *Pharmacol. Rev.* **45,** 455–497.
4. De Léan, A., Thibault, G., Seidah, N. G., Lazure, C., Gutkowska, J., Chrétien, M., Genest, J., and Cantin, M. (1985) Structure-activity relationships of atrial natriuretic factor (ANF) III. Correlation of receptor affinity with relative potency on aldosterone production in zona glomerulosa cells. *Biochem. Biophys. Res. Commun.* **132,** 360–367.
5. Chinkers, M. Garbers, D. L., Chang, M., Lowe, D. G., Chin, H., Goeddel, D. V., and Schulz, S. (1989) A membrane form of guanylate cyclase is an atrial natriuretic peptide receptor. *Nature (London).* **338,** 78–83.
6. Bennett, B. D., Bennett, G. L., Vitangcol, R. V., Jewett, J. R., Burnier, J., Henzel, W., and Lowe, D. G. (1991) Extracellular domain IgG fusion proteins for three human natriuretic peptide receptors. Hormone pharmacology and application to solid phase screening of synthetic peptide antisera. *J. Biol. Chem.* **266,** 23,060–23,067.
7. Suga, S., Nakao, K., Hosoda, K., Mukoyama, M., Ogawa, Y., Shirakami, G., Arai, H., Saito, Y., Kambayashi, Y., Inouye, K., and Imura, H. (1992) Receptor selectivity of natriuretic peptide family, atrial natriuretic peptide, brain natriuretic peptide, and C-type natriuretic peptide. *Endocrinol.* **130,** 229–239.
8. Porter, J. G., Arfsten, A., Fuller, F., Miller, J. A., Gregory, L. C., and Lewicki, J. A. (1990) Isolation and functional expression of the human atrial natriuretic peptide clearance receptor cDNA. *Biochem. Biophys. Res. Commun.* **171,** 796–803.
9. Maack, T., Suzuki, M., Almeida, F. A., Nussenzveig, D., Scarborough, R. M., McEnroe, G. A., and Lewicki, J. A. (1987) Physiological role of silent receptors of atrial natriuretic factor. *Science.* **238,** 675–678.
10. Prins, B. A., Weber, M. J., Hu, R. M., Pedram, A., Daniels, M., and Levin, E. R. (1996) Atrial natriuretic peptide inhibits mitogen-activated protein kinase through the clearance receptor. Potential role in the inhibition of astrocyte proliferation. *J. Biol. Chem.* **271,** 14,156–14,162.
11. Anand-Srivastava, M. B., Sehl, P. D., and Lowe, D. G. (1996) Cytoplasmic domain of natriuretic peptide receptor-C inhibits adenylyl cyclase. Involvement of a pertussis toxin-senstive G protein. *J. Biol. Chem.* **271,** 19,324–19,329.
12. Scarborough, R. M., McEnroe, G. A., Arfsten, A., Kang, L-L., Schwartz, K., and Lewicki, J. A. (1988) D-amino acid-substituted atrial natriuretic peptide analogs reveal novel receptor recognition requirements. *J. Biol. Chem.* **263,** 16,818–16,822.
13. Brown, J., Salas, A. A., Singleton, A., Polak, J. M., and Dollery, C. T. (1990) Autoradiographic localization of atrial natriuretic peptide receptor subtypes in rat kidney. *Am. J. Physiol.* **259,** F26–F39.
14. Rutherford, R. A. D., Wharton, J., Needleman, P., and Polak, J. M. (1991) Autoradiographic discrimination of brain and atrial natriuretic peptide binding sites in rat kidney. *J. Biol. Chem.* **266,** 5819–5826.
15. Rutherford, R. A. D., Wharton, J., Gordon, L., Moscoso, G., Yacoub, M. H., and Polak, J. M. (1992) Endocardial localization of natriuretic peptide binding sites in human fetal and adult heart. *Eur. J. Pharmacol.* **212,** 1–7.

16. Rutherford, R. A. D., Matsuda, Y, Wilkins, M. R., Polak, J. M., and Wharton, J. (1994) Identification of renal natriuretic peptide receptor subpopulations by use of the nonpeptide antagonist, HS-142-1. *Br. J. Pharmacol.* **113,** 931–939.
17. Brown, L. A., Rutherford, R. A. D., Nunez, D. J. R., Wharton, J., Lowe, D. G., and Wilkins, M. R. (1997) Downregulation of natriuretic peptide C-receptor protein in the hypertrophied ventricle of the aortovenocaval fistula rat. *Cardiovasc. Res.* **36,** 363–371.
18. Mimeault, M., Fournier, A., Féthiere, J., and De Léan, A. (1993) Development of natriuretic peptide analogs selective for the atrial natriuretic factor-R_{1A} receptor subtype. *Mol. Pharmacol.* **43,** 775–782.
19. Morishita, Y., Sano, T., Kase, H., Yamada, K., Inagami, T., and Matsuda, Y. (1992) HS-142-1, a novel nonpeptide atrial natriuretic peptide (ANP) antagonist, blocks ANP-induced renal responses through a specific interaction with guanylyl cyclase-linked receptors. *Eur. J. Pharmacol.* **225,** 203–207.
20. Tanaka, T., Ichimura, M., Nakajo, S., Snajdar, R. M., Morishita, Y., Sano, T., Yamada, K., Inagami, T., and Matsuda, Y. (1992) HS-142-1, a novel non-peptide antagonist for atrial natriuretic peptide receptor, selectively inhibits particulate guanylyl cyclase and lowers cyclic GMP in LLC-PK1 cells. *Biosci. Biotech. Biochem.* **56,** 1041–1045.
21. Timmermans, P. B. M. W. M., Wong, P. C., Chiu, A. T., Herblin, W. F., Benfield, P., Carini, D. J., Lee, R. J., Wexler, R. R., Saye, J. A. M. E., and Smith, T. D. (1993) Angiotensin II receptors and angiotensin II receptor antagonists. *Pharmacol. Rev.* **45,** 205–251.
22. Whitebread, S., Mele, M., Kamber, B., and DeGasparo, M. (1989) Preliminary biochemical characterization of two angiotensin II receptor subtypes. *Biochem. Biophys. Res. Comm.* **163,** 284–291.
23. Chiu, A. T., McCall, D. E., Price, W. A., Wong, P. C., Carini, D. J., Duncia, J. V., Johnson, A. L., Wexler, R. R., Yoo, S. E., and Timmermans, P. B. M. W. M. (1990) Nonpeptide angiotensin II receptor antagonists. VII. Cellular and biochemical pharmacology of DuP 753, an orally active antihypertensive agent. *J Pharmacol. Exp. Ther.* **252,** 711–718.
24. Weinstock, J, Keeman, R. M., Samanen, J., Hempel, J., Finkelstein, J. A., Franz, R. G., Gaitanpooulos, D. E., Girard, G. R., Gleason, J. G., Hill, D. T., Morgan, T. M., Peisoff, C. E., Aiyar, N., Brooks, T. M., Fredrickson, T. A., Ohlstein, E. H., Ruffolo, R. R., Stack, E. J., Sulpizio, A. C., Weidley, E. F., and Edwards, R. M. (1991) 1-(Carboxybenzyl)-imidazole-5-arcylic acids: Potent and selective angiotensin II receptor antagonists. *J Med. Chem.* **34,** 1514–1517.
25. Dudley, D. T., Panek, R. L., Major, T. C., Lu, G. H., Bruns, R. F., Klinkefus, B. A., Hodges, J. C., and Weishaar, R. E. (1990) Subclasses of angiotensin II binding sites and their functional significance. *Mol. Pharmacol.* **38,** 370–377.
26. Whitebread, S., Taylor, V., Bottari, S. P., Kamber, B., and DeGasparo, M. (1991) Radio-iodinated CGP 42112A: a novel high affinity and highly selective ligand

for the characterization of angiotensin AT_2 receptors. *Biochem. Biophys. Res. Commun.* **181,** 1365–1371.

27. Speth, R. C. and Kim, K. H. (1990) Discrimination of two angiotensin II receptor subtypes with a selective agonist analogue of angiotensin II, p-aminophenylalanine^6 angiotensin II. *Biochem. Biophys. Res. Commun.* **169,** 997–1006.
28. Chiu, A. T., McCall, D. E., Nguyen, T. T., Carini, D. J., Duncia, J. V., Herblin, W. F., Uyeda, T., Wong, P. C., Wexler, R. R., Johnson, A. L., and Timmermans, P. B. M. W. M. (1989) Discrimination of angiotensin II receptor subtypes by dithiothreitol. *Eur. J Pharmacol.* **170,** 117–118.
29. Sechi, L. A., Grady, E. F., Griffin, C. A., Kalinyak, J. E., and Schamblelan, M. (1992) Distribution of angiotensin receptor subtypes in rat and human kidney. *Am. J. Physiol.* **262,** F236–F240.
30. Gröne, H-J., Simon, M., and Fuchs, E. (1992) Autoradiographic characterization of angiotensin receptor subtypes in fetal and adult human kidney. *Am. J. Physiol.* **262,** F326–F331.
31. Walsh, D. A., Suzuki, T., Knock, G. A., Blake, D. R., Polak, J. M., and Wharton, J. (1994) AT_1 receptor characteristics of angiotensin analogue binding in human synovium. *Br. J. Pharmacol.* **112,** 435–442.
32. Knock, G. A., Sullivan, M. H. F., McCarthy, A., Elder, M. G., Polak, J. M, and Wharton, J. (1994) Angiotensin II (AT_1) vascular binding sites in human placentae from normal-term, preeclamptic and growth retarded pregnancies. *J. Pharmacol. Exp. Ther.* **271,** 1007–1015.
33. Lefroy, D. C., Wharton, J., Knock, G. A., Suzuki, T., Crake, T., Morgan, K., Polak, J. M., and Poole-Wilson, P. A. (1996) Regional changes in angiotensin II receptor density after experimental myocardial infarction. *J. Mol. Cell. Cardiol.* **28,** 429–440.
34. Walsh, D. A., Hu, D. E., Wharton, J., Catravas, J. D., Blake, D. R., and Fan T. P. F. (1997) Sequential development of angiotensin receptors and angiotensin I converting enzyme during angiogenesis in the rat subcutaneous sponge granuloma. *Br. J. Pharmacol.* **120,** 1302–1311.
35. Brilla, C. G., Zhou, G., Matsubara, L., and Weber, K. T. (1994) Collagen metabolism in cultured rat cardiac fibroblasts: response to angiotensin II and aldosterone. *J. Mol. Cell. Cardiol.* **26,** 809–820.
36. Lokuta, A. J., Cooper, C., Gaa, S. T., Wang, H. E., and Rogers, T. B. (1994) Angiotesin II stimulates the release of phospholipid-derived second messengers through multiple receptor subtypes in heart cells. *J. Biol. Chem.* **269,** 4832–4838.
37. Stoll, M., Steckelings, M., Paul, M., Bottari, S. P., Metzger, R., and Unger, T. (1995) The angiotensin AT2-receptor mediates inhibition of cell proliferation in coronary endothelial cells. *J. Clin. Invest.* **95,** 651–657.
38. Nakajima, M., Hutchinson, H. G., Fujinaga, M., Hayashida, W., Morishita, R., Zhang, L., Horiuchi, M., Pratt, R. E., and Dzau, V. J. (1995) The angiotensin II type 2 (AT_2) receptor antagonizes the growth effects of the AT_1 receptor:

gain-of-function study using gene transfer. *Proc. Natl. Acad. Sci. USA* **92,** 10,663–10,667.

39. Levy, B. I., Benessiano, J., Henrion, D., Caputa, L., Heymes, C., Duriez, M., Poitevlin, P., and Samuel, L. (1996) Chronic blockade of AT2-subtype receptors prevents the effect of angiotensin II on rat vascular structure. *J. Clin. Invest.* **98,** 418–425.
40. Booz, G. W. and Baker, K. M. (1996) Role of type 1 and type 2 angiotensin receptors in angiotensin II-induced cardiomyocyte hypertrophy. *Hypertension* **28,** 635–640.
41. Brink, M., Erne, P., De Gasparo, M., Rogg, H., Schmid A., Stulz, P., and Bullock, G. (1996) Localization of the angiotensin II receptor sutypes in the human atrium. *J. Mol. Cell. Cardiol.* **28,** 1789–1799.
42. Grady, E. F., Sechi, L. A., Griffin, C. A., Schamblelan, M., and Kalinyak, J. E. (1991) Expression of AT_2 receptors in the developing rat fetus. *J. Clin. Invest.* **88,** 921–933.
43. Viswanathan, M., Tsutsumi, K., Correa, F. M. A., and Saavedra, J. M. (1991) Changes in expression of angiotensin receptor subtypes in the rat aorta during development. *Biochem. Biophys. Res. Commun.* **179,** 1361–1367.
44. Nozawa, Y., Haruno, A., Oda, N., Yamasaki, Y., Matsuura, M., Yamada, S., Inabe, K., Kimura, R., Suzuki, H., and Hoshino, T. (1994) Angiotensin II receptor subtypes in bovine and human ventricular myocardium. *J. Pharmacol. Exp. Ther.* **270,** 566–571.
45. Regitz-Zagrosek, V., Friedel, N., Heymann, A., Bauer, P., Neu, M., Rolfs, A., Steffen, C., Hildebrandt, A., Hetzer, R., and Fleck, E. (1995) Regulation, chamber localization, and subtype distribution of angiotensin II receptors in human hearts. *Circulation* **91,** 1461–1471.
46. Rogg, H., De Gasparo, M., Graedel, E., Stulz, P., Burkart, F., Eberhard, M., and Erne, P. (1996) Angiotensin II-receptor subtypes in the human atria and evidence for alterations in patients with cardiac dysfunction. *Eur. Heart J.* **17,** 1112–1120.
47. Nishimura, H., Walker, O., Patton, C., Madison, A., Chiu, A., and Keiser, J. (1994) Novel angiotensin receptor subtypes in fowl. *Am. J. Physiol.* **267,** R1174–1181.
48. Walsh, D. A., Wharton, J., Blake, D. R., and Polak, J. M. (1993) Species and tissue specificity of vasoactive regulatory peptides. *Int. J. Tissue Cell. Reactions* **15,** 109–124.

8

Measurement of Brain Gaba-Benzodiazepine Receptor Levels In Vivo Using Emission Tomography

Anne Lingford-Hughes and Andrea Malizia

1. Introduction

Knowledge about the neurobiology of the brain is fundamental to our understanding of neuropsychiatric disorders. There are a number of different approaches that have been successfully used to investigate brain function in neuropsychiatric disorders and to inform development of treatment strategies. These have involved animal models, human postmortem studies, measures of neurotransmitters and their metabolite levels in blood, cerebrospinal fluid (CSF), or urine, and neuroendocrine or physiological challenges. All these have severe limitations, as they are surrogate measures. Animal models of human brain function and pathology are inevitably limited by phylogenetic differences. There are inherent problems in using post-mortem tissue, such as antemortem medical complications and tissue instability after death. It is also hard to disentangle whether any changes seen are primary or secondary to the disease or to the treatment received. Although the other three approaches are in vivo and overcome some of these difficulties, it can be problematic to interpret the results with regard to a single neurotransmitter system or to changes in a discrete neuroanatomical location.

The development of techniques, such as positron emission tomography (PET) and single photon emission tomography (SPET) allow us to explore neurobiology and neuropharmacology in the functioning brain. Consequently, significant advances in our knowledge of dysfunctional activity associated with neuropsychiatric disorders have been made. PET and SPET can be used to define cerebral activity, receptor distribution, the neurochemistry of psychoactive drugs, and, possibly, functional neurochemistry in vivo. Furthermore, the

From: *Methods in Molecular Biology, Vol. 106: Receptor Binding Techniques*
Edited by: Mary Keen © Humana Press Inc., Totowa, NJ

dynamic nature of PET and SPET can be exploited to assess the effects of physiological or pharmacological challenges during the scanning procedure. For instance, anxiety can be induced during the scanning procedure, and its effects at a receptor can be visualized by assessing the displacement of the radioactive tracer from its receptor. Similarly, the activity of a drug at a particular receptor can be evaluated by administering the drug during the scanning procedure.

The clinical use of these techniques is as yet in its infancy; however, it is likely that PET and SPET will become be increasingly used in drug development and in clinical psychopharmacology. For instance, these techniques have been used to quantify levels of the receptor in a number of neuropsychiatric disorders such as epilepsy, Huntington's disease, Friedrich's ataxia, Alzheimer's disease, panic disorder, alcoholism and also to assess the degree of occupancy of central benzodiazepine receptors by lorazepam, clonazepam, midazolam, and zolpidem (*see* **ref.** *1* for review).

1.1. Basic Principles of PET and SPET

Both PET and SPET involve giving a radioactively labeled ligand that results in the emission of gamma radiation. Cameras placed around the head detect these emissions.

In PET, the radioactive nuclei that label the molecule of interest emit positrons (positively charged particles which have the same mass as electrons) that annihilate when they collide with an electron in the surrounding matter thus emitting two 511 KeV photons at 180 degrees to each other. The electronics of a PET camera are arranged so as to detect these photons that are absorbed at the same time by spatially opposite crystals, thus determining the line of response (LOR) of the disintegration. This arrangement has considerable advantage in terms of sensitivity as all the events within the detection solid angle are utilized. PET cameras are made by contiguous rings of detectors. These were originally separated by lead septa so that any single detector would only "see" detectors from its own or adjacent rings. More recently, the septa have been removed so that the information is acquired on coincidences from the whole volume. This has further increased the sensitivity of PET *(2)* but for fully quantitative images, it requires a correction for scattered events which can be obtained by measurement *(3)* or calculated theoretically (*see* **ref.** *4* for review).

Commonly used positron emitting nuclei are ^{15}O (half life ($t_{1/2}$) 2 minutes), ^{11}C ($t_{1/2}$ 20 min) and ^{18}F ($t_{1/2}$ 109 min). The ability to label carbon is of particular importance and is one of the main advantages of PET as, in principle, it allows labeling of most molecules of interest. However the short half-life of ^{15}O and ^{11}C mean that radioligand production facilities and scanning equip-

ment have to be in close physical proximity, thus limiting the general availability of PET and increasing its cost.

In SPET, the radioactive isotopes used are ^{123}I-iodine and ^{99}-technetium (^{99m}Tc) which emit only a single photon (cf PET). Currently ^{123}I-iodination is used to label neuroreceptor ligands. The longer half-life of iodine ($t_{1/2}$ about 13 h) and of ^{99m}Tc ($t_{1/2}$ about 6 h) means that an onsite generator is not required with many ligands being commercially produced. These isotopes are of lower energy than those used in PET; hence, scatter and absorption is more of a problem. As with PET, the detector is a crystal that on contact with a photon releases light that is converted into an electric signal. In order to help calculate the location of the emission and reduce detection of widely scattered photons, collimators are placed in front of the detectors. These are lead cylinders that prevent any photons at stray angles from being detected. Attenuation, correction, or estimation of the effect of tissue absorption is calculated mathematically. Thus, compared to PET, the sensitivity (the percentage of emitted photons detected) and resolution (ability to spatially resolve two anatomically distinct regions) are lower in SPET. Further attenuation correction cannot be measured in SPET and has to be calculated. However, technological advances in acquisition and analysis of images means that SPET resolution is no longer necessarily inferior to PET. Moreover, the lower cost of SPET and its wider availability can make it a more attractive option than PET.

1.2. Receptor Theory and Quantification of Receptor Levels

Traditionally, receptors are characterized by performing binding experiments either in a test tube or with autoradiography. Receptor theory, which is based on the law of mass action of receptor occupancy, is applied to interpret the data. This states that unbound ligand reversibly binds to its receptor at a rate dependent on the concentration of the ligand and receptor. The rate of their dissociation is thus proportional to the concentration of bound ligand and receptor and, at equilibrium, the rates of association and dissociation are equal. Nonspecific binding can then be determined as the nonsaturable part of the binding curve or as the amount of radioactivity in the presence of an excess of cold ligand. Furthermore, the preparation that often involves considerable washing eliminates the potential complication of endogenous ligands binding to the receptor under study.

However, in vivo imaging techniques are different in two major respects: In vivo imaging is performed with tracer amounts of radioligand, and the tomographic signal is total radioactivity present.

1. In vivo Imaging is performed with tracer amounts of radioligand. For successful evaluation, the techniques are dependent on the administration of tracer amounts

of radiolabel. This means that the total amount of ligand administered will have very low receptor occupancy. Thus, in in vivo binding experiments, the relative affinity of the radioligand, with respect to exogenous or endogenous competing ligands, does not significantly effect the tomographic signal. On the other hand, quality control of the amount of cold ligand coinjected at the time of radioligand administration is essential. In other words, it is important to check that a high specific activity has been injected. Although there is no universal agreement on how much cold ligand is allowable, most laboratories would agree that it is best to administer an amount that produces less than 1% occupancy. Given the limited sensitivity of the techniques, it is, however, likely that up to 3–5% occupancy may be acceptable.

2. The tomographic signal is the total radioactivity present in a volume of tissue. The signal recovered from tomography represents the sum of all the radioactivity within a voxel (typically up to 1 cm^3 in size): thus, it is the sum of activity in the blood (parent compound and metabolite, protein bound, platelet, and white cell bound, within all cells as well as in plasma), in blood vessel walls (receptors, nonspecific binding), in the glia and neurons (specific and nonspecific binding) and in the interstitial fluids and synapses (the so-called free compartment). In order to make sense of the signal in terms of specific binding, a reference input function has to be picked, and assumptions are made about the relationship between the reference input and the signal from the tissue of interest. Two main methods are employed to generate a reference signal: first, the use of counts from a brain area assumed to have no specific binding but the same amount of signal from all other components; second, the use of a metabolite and blood cells corrected plasma input function that is related to the tissue-binding parameters of interest by a mathematical model. Thus, depending on the ligand, it is possible to model the kinetics of a radiolabeled neuroreceptor ligand to account for factors including blood flow, blood concentration of parent compound and ligand in extravascular, nonspecific receptor compartments. Both methods described above have advantages and drawbacks; however, since assumptions have to be made for the analysis to be valid, it is essential that the in vivo pharmacokinetic characteristics of radioligands used neuroimaging experiments should be thoroughly worked out before starting clinical experiments. This has been achieved for the PET benzodiazepine-$GABA_A$ ligand [^{11}C]flumazenil *(5–8)* and for the SPECT equivalent [^{123}I]iomazenil *(9–11)*.

Obviously, there are many factors that make radioligands unsuitable for in vivo studies such as the radioligand binding to multiple receptor sites, radiolabeled metabolites of the radioligand interfering with binding pharmacological effects at low injected doses, release of endogenous transmitters, different times to reach equilibrium in regions of interest with low and high numbers of receptors. Many of these issues, however, can be overcome through optimization of the pharmacology and biochemistry of the radiolabeled ligand. For instance, polar metabolites that do not cross the blood-brain barrier, rapid clearance from

blood, rapid association rate and high specificity and selectivity are all desirable attributes of a radioligand (for review *see* **ref. *12***). In addition, it is always important to check that the scanning and analysis protocols selected to generate binding maps have been shown to be independent of the influence of blood flow (delivery and washout).

An additional problem is generated by nonspecific binding. With in vitro binding studies, nonspecific binding capacity can be determined by using excess of competing cold ligand. Although this is, in theory, applicable to in vivo imaging, routinely performing this in practice is problematic. This is because the extra dose of radiation required, and the scanning time generally required by such studies results in less tolerable experimental conditions to subjects. Such studies to assess the nonspecific binding component are usually performed as part of validating a new ligand when an estimate of population nonspecific binding is achieved. Because of this problem development of a new in vivo ligand is aimed to produce one with very low nonspecific binding to minimize its contribution to the image acquired. A widely used method of estimating the level of vascular signal, plus nonspecific binding is to measure the amount of ligand uptake in an area known to be devoid of receptors, described as a reference region. With regard to the $GABA_A$-benzodiazepine receptor, identifying such a region is problematic, as the $GABA_A$ receptor is widely distributed, and no true reference area exists ***(6,13)***. However, both these compounds have low nonspecific binding (about 1% of specific for [^{123}I]iomazenil and about 10% for [^{11}C]flumazenil) and these figures can be entered in calculations ***(5)***.

Since at least two scans are required to measure both the apparent receptor density (Bmax) and the affinity (Kd) of radioligand at the receptor, scanning protocols that require one scan only can only produce maps of Binding Potential (BP = Bmax/Kd) or of Volume of Distribution (V_D; ratio of tissue concentration of ligand to plasma concentration that is proportional to binding potential). Since alterations in the affinity (Kd) are rarely thought to underlie neuropsychiatric disorders, any difference in BP or V_D can be interpreted as owing to changes in the apparent concentration of receptors (Bmax[apparent]).

1.3. Subject Selection

Depending on the protocol, general exclusion criteria should include major medical illness, including diabetes, blood dyscrasias, previous reaction to iodine and/or cardiovascular abnormalities. Ethical permission will need to be obtained from local committees and a radiation safety board. Although local committees will vary, in vivo imaging studies in women of child-bearing age will need further justification.

2. PET

2.1. Ligand Preparation

PET imaging of benzodiazepine-$GABA_A$ receptors can be achieved by using [^{11}C]flumazenil. Flumazenil is the prototype benzodiazepine receptor antagonist, and it has been used in PET studies to assess benzodiazepine site density and affinity in man and monkeys. Synthesis of [^{11}C]flumazenil presents no particular difficulties *(14)*, and our laboratory routinely produces up to 3400 MBq per synthesis with a specific activity of up to 45,000 MBq/μmol. Up to 10 μg of flumazenil are injected at the beginning of this scan.

2.2. Scanning Procedure

The subject is prepared in a room adjacent to the scanner where, after completing the necessary interviews, questionnaires and examination, a venflon (20 or 22G) is inserted under local anesthesia in the radial artery at the wrist, preferably in the nondominant arm, about one hour before the beginning of the scan. Another venflon is placed in the contralateral antecubital vein. Both lines are then kept patent by regular injections of small volumes of saline.

The volunteer moves to the scanning room where, using external head anatomy (external auditory meatus and inferior orbital notch), lines corresponding to the pitch of the brain's anterior commissure-posterior commissure (AC-PC) plane are traced on his forehead. The subject is then positioned on the scanner bed, his head is placed in a holder that minimizes movement and edged into the scanner outlet. The scanner gantry is then tilted so that the detector rings are parallel to the AC-PC plane. Our head scanner (CTI-Siemens 953B) has a maximum field of view in the z direction of 112 mm, so that the whole brain cannot be imaged for many volunteers. Thus an a priori decision has to be made on whether the scan should include the motor-sensory cortex or the bottom part of the temporal lobes, pons, and cerebellum. For most of our [^{11}C]flumazenil scans, we are interested in data from the cerebellum and temporal cortex; therefore, the upper part of the brain is excluded.

Once the patient is in position within the scanner a short (two minutes) transmission scan is performed using rotating Germanium rods. This establishes the rough positioning of the head within the scanner; if the position needs to be adjusted, the bed is slid in or out of the scanner to achieve optimal placement. A long transmission scan is then performed (10 min), which allows a measured attenuation correction to be carried out. This corrects for the absorption of emitted radiation by the head tissues; if it was not performed, structures such as the basal ganglia, which are at the center of the object, would appear faint, as a higher proportion of the photons emitted from the middle are absorbed by surrounding tissue and skull. The radial artery canula is then connected to a

long piece of tubing that passes over a Bismuth Germanate (BGO) counter for the "on line" continuous recording of radioactivity in the blood throughout the scan. The arterial blood is drawn by a pump at 5 mL/min initially and then at 2ml/min from 10 min after the beginning until the end of the scan.

While the patient is prepared in the scanner, [^{11}C]flumazenil is produced in the chemistry synthesis laboratory using ^{11}C labelled methyliodide from the cyclotron. The radioligand is then checked by the Quality Control (QC) laboratory for content and purity; this verifies that the correct substance has been produced and that there are no contaminants. [^{11}C]Flumazenil is then brought to the scanning room in a glass vial in a lead container, and an aliquot is taken for injection. The radiographer who is in the scanning room calculates the volume that needs to be injected to deliver the right amount of radioactivity and measures it in a counter positioned at the corner of the scanning room.

We usually administer 200–340 MBq of radioactivity, which corresponds to 1.8–2.5 mSv of absorbed radiation (equivalent to 8–12 mo background radiation in the U.K.). [^{11}C]Flumazenil is injected in the ante-cubital vein as a bolus, 30 s after the beginning of the scan to allow a "background" frame. All the tubing and "dead" space connected to the antecubital vein is rapidly flushed with 20 ml of saline to avoid any radioactive material being left in it. The syringe that has been used for injecting the radioligand and the vial are sent back to the QC labs to verify the dose injected and the specific activity at the time of injection. All the laboratories in the building have Rugby clocks in order to able to synchronize recordings and to be able to back calculate radioactivity emission.

Patients are asked to lie in the scanner with their eyes open and to keep as still as possible. We find it useful to position some support under the volunteer's knees to make lying down for a prolonged period more comfortable. In addition, since the scanning rooms are air conditioned to maintain an optimum environment for the crystal detectors, it is important to make sure that the subject is adequately covered with blankets. Particular attention is devoted to the position and temperature of the wrist with the arterial line; it should be kept warm and as immobile as possible. Patient's head position is checked for movement at the end of single frames. In addition, the head is kept in position for the first three minutes frame, as this has a high number of counts, good anatomical resolution, and can therefore be used as a standard space to realign subsequent frames to. The scanning information is recorded in a number of discrete frames.

The typical protocol we use consists of one background frame (30 s), three 1 min frames, nineteen 3 min frames, and 15 min frames after that for a total of 90 or 105 min, depending on the type of study. Arterial counts are collected throughout the scan, and 5 mL aliquots are drawn at 2.5, 10.5, 20.5, 35.5, 50.5,

and 65.5 min for the well counter calibration of the count data and at 3,4,5,6,10,20,35 and 60 min the measurement of the concentration of [^{11}C]flumazenil and its metabolites. At the beginning and end of any discrete arterial blood sample, a foot switch is pressed to record the exact timing of the withdrawal. Because the scanner is operated with the lead septa retracted (increasing sensitivity), measurements have to be taken correct for radiation scatter. This is done by collecting counts from two energy windows during the scan. At the end of the scan, the patient is kept in the scanner until all the scanning information has been downloaded to disk.

2.3. Data Analysis

2.3.1. Generation of Parametric Maps of Radioligand Binding and Delivery

The study data are collected in sinograms that record a map of the coincident counts detected by each pair of detectors along a LOR. This data is then reconstructed to produce spatial maps of radioactivity within the object, in this case the head. There are a number of techniques that can be used for this tomographic reconstruction; we use filtered backprojection with a Hanning filter that affords a good compromise between computational time expense and resolution. At the same stage, measured corrections are applied for attenuation and scatter.

At the end of this process, the data are in a tomographic format for each separate frame. In our laboratory, this is in CTI format and is then transferred to Analyze format for ease of image viewing and analysis. This data represents the sum of blood and tissue radioactivity information in a particular volume (known as voxel) of the object over a particular time frame. For our scans, the whole volume is made up of $128 \times 128 \times 31$ voxels and is measured over 26–27 time periods during the scan. Hence, for each voxel, a time activity curve can be generated that represents the response of the radioactive signal in that particular space over the time of the scan. However, this assumes that no movement has occurred in the head position during the scan. Since the whole procedure takes 2.5 h, this is very unlikely; therefore, at this stage of the analysis, we routinely use realignment algorithms that readjust the spatial location of the images acquired at different times using the first three minutes' frame as the standard. These algorithms use a least squares optimization method. [^{11}C]flumazenil is a particularly good ligand for this process, as it has widespread cortical distribution; this means that as the radioligand maps change from being dominated by delivery to being dominated by binding, there is no substantial difference in signal intensity over the whole cortex, thus avoiding errors owing to change in ligand distribution (changes in distribution occur in

the basal ganglia, thalami, and cerebellum but have little weighting in this process because of the number and distribution of cortical voxels).

Once the images have been realigned, the signal from each voxel has to be expressed as a calculated binding or delivery parameter. In order to separate the signal from the various compartments in which the radioligand is present, a reference input function is needed. For [^{11}C]flumazenil, we use an arterial plasma input function. Other laboratories have used the pons or the white matter *(6,13)*. We regard both of these as unsatisfactory, with the present techniques, as the pons is small, difficult to define, and has significant benzodiazepine-$GABA_A$ binding whereas the white matter signal is contaminated by spillover from adjacent cortical and subcortical structures (known as the partial volume effect). The arterial plasma input function is generated by the continuous arterial blood counts obtained during the scan that are calibrated using information from the discrete samples measured in the well counter.

Cross calibration with the scanner counts is ensured by separately scanning radioactive "phantoms" before or after the patient scan. "Phantoms" are sources of radioactivity that have known amounts of activity in them and that can therefore be used to determine the absolute values that correspond to a particular number of scanner counts. In addition, the whole blood counts are converted to plasma counts and corrected for the presence of radioactive metabolites over the course of the scan. [^{11}C]flumazenil metabolites (whether labeled or not) are polar and do not cross the blood brain barrier; this is an important fact, as otherwise, the calculation of binding parameters can be seriously jeopardized in the absence of a "good" brain reference area that would only represent blood, free tissue, and nonspecific binding radioactivity.

Once these corrections have been applied, the modified plasma information is used as an "input" function to determine the pharmacokinetic parameters of interest from each individual voxel's time activity curve. We prefer to use the technique of Spectral Analysis that generates parametric maps of radioligand distribution in the brain *(15*; **Fig. 1***)*. These correspond to the regional volume of distribution of [^{11}C]flumazenil. Volume of distribution in this case is defined as the ratio, at equilibrium, of the amount of radioligand present in tissue over the amount present in plasma. It is a measure that is proportional to B_{max}/K_d but that also incorporates nonspecific binding, which, for [^{11}C]flumazenil, represents about 10% of the signal. The advantage of spectral analysis is that it produces good fits to the data without being constrained by a priori compartmental models. Ligand delivery maps can also be obtained. These are related to "K1 maps" that represent regional blood flow, extraction and capillary permeability. The V_D and delivery maps from different individuals are then ready for use in comparisons between groups of subjects.

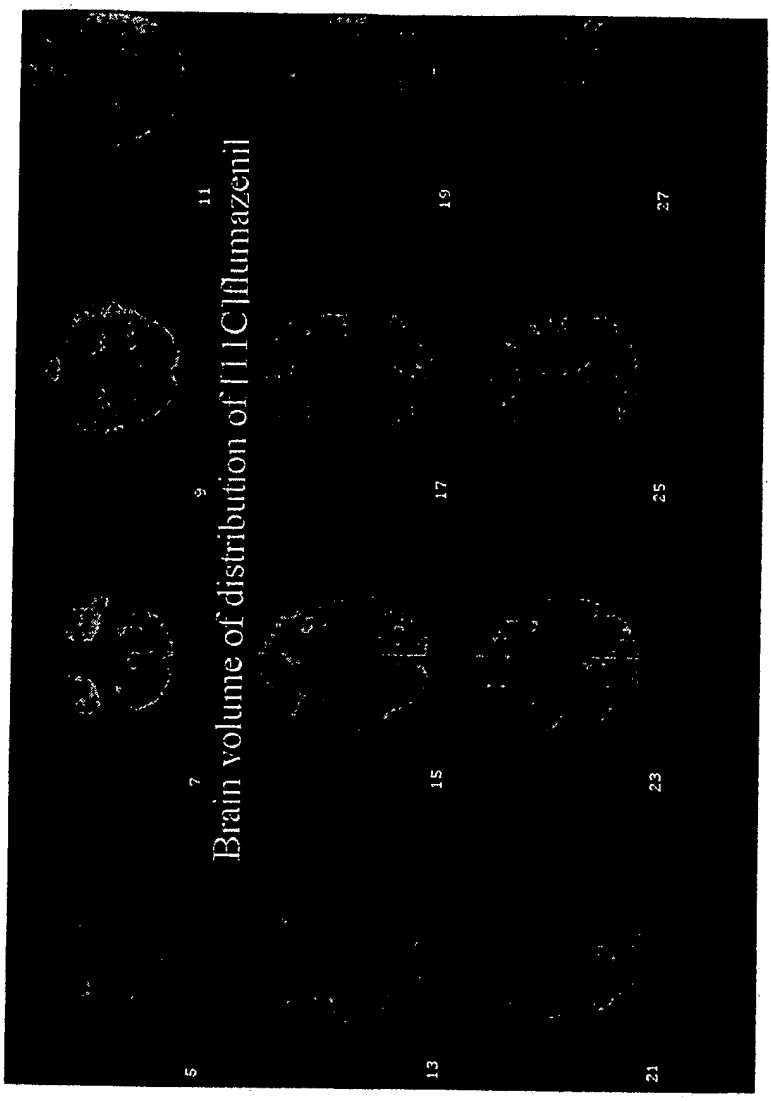

Fig. 1. The brain volume of distribution of [^{11}C] flumazenil.

2.3.2. Comparisons Between Subjects

In order to compare information from different subjects, PET investigators have to make sure that data from the same anatomical regions are related. We favor using spatial normalization methods from statistical parametric mapping (SPM) which translate the data from all the individuals into an idealized inter-

nationally recognized, standard stereotactic space. This is achieved by a number of linear and nonlinear translations that match the images from an individual to a standard template and result in all the data being in the same stereotactic space. This is a well validated technique that has allowed the realization of PET as a tool to investigate metabolic and regional blood flow activation. It has also been successfully used, for example, in the characterization of cortical heterotopia using either [^{11}C]flumazenil V_D images or structural MRI *(16)*, thus confirming that the warping necessary to place the objects in standardized space does not alter the essential anatomical structure of the image.

Once the images have been thus transformed, we utilize two analysis methods. The first places a library of rectangular regions of interest (ROIs) over the image and the voxels within the rectangles are used to determine the values corresponding to particular regions; this method matches previous ROIs techniques but has the advantage that the ROIs are not placed manually thus removing possible investigator bias. However, we consider it to be suboptimal, as it only utilizes part of the information collected and unnecessarily smoothes the data by averaging over a number of voxels. The second method is a voxel-based analysis which utilizes the whole data set without further averaging and is achieved by using the statistical facilities of SPM. For either methods, absolute data can be used if accurate calibration has been possible; alternatively the global intersubject variability can be removed by "normalizing" each scan to a population mean. Relative methods have the advantage of being more sensitive in the detection of regional differences between groups. There are different ways of achieving "normalization," we prefer to use proportional scaling, as the assumptions underlying other models may not be met by radioligand studies.

2.4. Comments

There are a variety of problems that can interfere with the successful collection of PET scan data once the preparation has started. These are failure to cannulate the radial artery, failure to maintain a patent viable outflow from the cannula, failure to synthesise [^{11}C]flumazenil, production of inadequate amounts of the radioligand, presence of impurities which make administration inadvisable, computer "crashes," electrical and electronic failures in any of the equipment used, excessive delay in the patient, and scanner preparation leading to too low radioligand-specific activity, excessive volunteer anxiety in the scanner leading to a premature departure, and failure of the computer in writing the information to a hard disk. All these have occurred in our experiments.

A particular problem that is worth emphasizing separately is the need for scanner calibration with "phantoms." Under optimal conditions, this is a very

stable measure and can be performed infrequently (weekly or monthly). However, if temperature control is not adequate in the scanning room the characteristics of the BGO detectors in the camera alter and the recorded phantom calibration factor can vary by as much as ± 20%. This is of no importance for relative analyses, as it is only a scaling problem, but it is essential if absolute quantification is sought. We would therefore advise experimenters who require absolute measures to check the stability of the scanner with every scan. It is equally important to regularly calibrate the well counter.

3. SPET

3.1. Ligand Preparation

To label the benzodiazepine receptor in SPET, the iodinated analog of the receptor antagonist, flumazenil (Ro 15-1788), Ro 16 -0154 (ethyl 7-iodo-5,6-dihydro-5-methyl-6-ox-o-4H-imidazol[1,5-a][1,4]-benzodiazepine-3-carboxylate) is used. This compound, iomazenil, is available commercially from Mallinckrodt Medical, B. V., Petter, Holland. Compared to the ^{11}C form of flumazenil used in PET, [^{123}I] iomazenil has 10-fold higher affinity (K_D = 0.66nM at 37°C) at the benzodiazepine receptor *(17)*.

Validating iomazenil's pharmacology has involved a detailed autoradiographic and displacement study. In monkeys, a comparison between in vivo SPET images and ex vivo and in vitro autoradiographs demonstrated that the distribution of iomazenil in the SPET images and autoradiographs was equivalent to the known distribution of benzodiazepine receptors from previous in vitro studies *(18)*. In vivo displacement studies have also been performed with five different benzodiazepine ligands, diazepam, alprazolam, clonazepam, Ro 16 0154, and Ro 15 1788. The in vivo displacing potency of these drugs highly correlated with their affinities determined by in vitro homogenate binding *(19)*.

In man, whole-body scintographic studies estimated an average effective dose equivalent of 5mSv for the recommended dosage of 150 MBq [^{123}I]iomazenil *(20)*. This level of radiation exposure is within dose limits deemed acceptable *(21,22)*. To prevent significant thyroid uptake of ^{123}I-iodine, potassium iodate tablets (80 mg, twice a day) are taken for two days prior to the scan, on the scanning day and for two days after the SPET scan. [^{123}I]iomazenil is excreted largely unchanged in urine; therefore, subjects are advised to drink plenty of water after the scan and should be reminded about taking the remaining iodate tablets.

3.2. Scanning Procedure.

The following is a description of the so-called "bolus injection" technique and using a brain dedicated multidetector rotating gamma camera (e.g., GE

Neurocam). Although protocols have been used involving infusion of [^{123}I]iomazenil *(9)*, these are less acceptable to patient comfort and involve lengthier scanning and more radioactivity. The actual scanning protocol will depend on the camera available and hence only the principles of the following protocol, rather than the exact details will be applicable to other systems. Since scanning procedures are rarely less than a few hours, cameras that allow either subjects to be easily and exactly repositioned, or acquire 3D data-sets which can be coregistered later, are of immense benefit.

The subject is asked to arrive at least 15 min prior to the start of the scanning procedure. Most study protocols require filling out questionnaires, which can be done in this period. For the intravenous injection, a venflon is placed in an antecubital vein. The method described in detail here does not involve blood sampling, but if it was required for kinetic modelling, a venflon is placed in the other antecubital vein. Subjects rarely find the SPET scanner intimidating, since it is not claustrophobic, and they can see out at all times. When quantifying neuroreceptor levels, it is acceptable to allow the subjects to listen to music of their choice throughout the scan.

After being positioned comfortably in the scanner, the [^{123}I]iomazenil is injected intravenously in a bolus over about 5 s. A three-way tap then allows the syringe containing the [^{123}I]iomazenil to be flushed with 20 mL of saline. In our protocol using the GE-Neurocam and [^{123}I]iomazenil, after at least one minute the first acquisition is commenced; in the GE-Neurocam, the lack of counts in the brain in the first minute would result in artefacts in the reconstruction process. Each whole brain acquisition lasts approximately 12 min. Exact timing of each acquisition is not crucial, but should be noted, and a consecutive series of whole brain images is acquired up to a minimum of 3 h. Our protocol involves eight consecutive 12 min scans (128 projections of 15 s each) followed by half an hour break, then a final acquisition of 36 min (128 projections of 40 s each). The entire scanning procedure therefore takes about 3 h. A major advantage of using this camera is that the subject is able to move every 12 min, since there are no difficulties in repositioning. Being able to move every 12 min and the longer break at two hours helps with subject compliance.

The first few images acquired postinjection of [^{123}I]iomazenil are dominated by blood flow. The level of [^{123}I]iomazenil in the blood after 60 min is very low; thus, images obtained after this time reflect brain uptake. For iomazenil, nonspecific binding is regarded as negligible (~ 1%) and can be ignored when quantifying the level of benzodiazepine receptors. Thus, all radioactive emissions from the brain is taken to reflect iomazenil specifically bound to the benzodiazepine receptor. Generally, psuedoequilibrium for most cortical regions is obtained three hours post injection of [^{123}I]iomazenil.

3.3. Image Analysis

3.3.1. Generation of Parametric Maps or Radioligand Binding

To assess the levels of GABA-benzodiazepine receptors, we favor using the image of [^{123}I]iomazenil uptake at 180 min post-injection, which has been shown to be a good approximation of the volume of distribution (V_D) of GABA-benzodiazepine receptors in the brain *(10,23, see* **Fig. 2***)*. When using this image, the first step in performing intergroup comparison is to identify either a reference or a normalization region. A reference region is one that is devoid of receptors and represents nonspecific binding. If no reference region is available, a region for normalization of the image has to be used in order to permit interscan comparison. A normalization region ideally should be one which is not affected by the condition under study. This may be problematic, if all regions in the brain are hypothesized to be involved in the neuropsychiatric condition under study. We have used the mean counts in either white matter or the cerebellum for this purpose. The cerebellum was used when no difference was apparent between the two groups under study *(24)*. In another study, the white matter was used, since there was no region that had not been affected by the condition under investigation.

3.3.2. Comparisons Between Subject Groups

There are a number of software packages available to coregister the images, including those from SPM. However, we have used a count-based difference algorithm involving only affine, i.e., linear, transformations and no warping. Similarly to PET, a standard template can then be applied to assess regional levels of GABA-benzodiazepine receptors. Alternatively to compare the levels of GABA-benzodiazepine receptors between groups, voxel-based analysis can be performed. We currently use an inhouse software package based on SPM. This compares the mean image of each group, voxel by voxel, and produces a map of voxels that are significantly different between the groups. To assess the significance of differences between the two groups of subjects, unpaired t-tests are performed at every voxel, and the size and peak magnitude of clusters of significant voxels are then assessed to correct for multiple comparisons ($p < 0.05$). This allows more subtle and regionally specific differences in the level of GABA-benzodiazepine receptor between groups to be identified. In addition, as explained, there is no investigator bias.

3.4. Comments

We have considered other ways of calculating the level of GABA-benzodiazepine receptor using [^{123}I]iomazenil and SPET in effort to make it

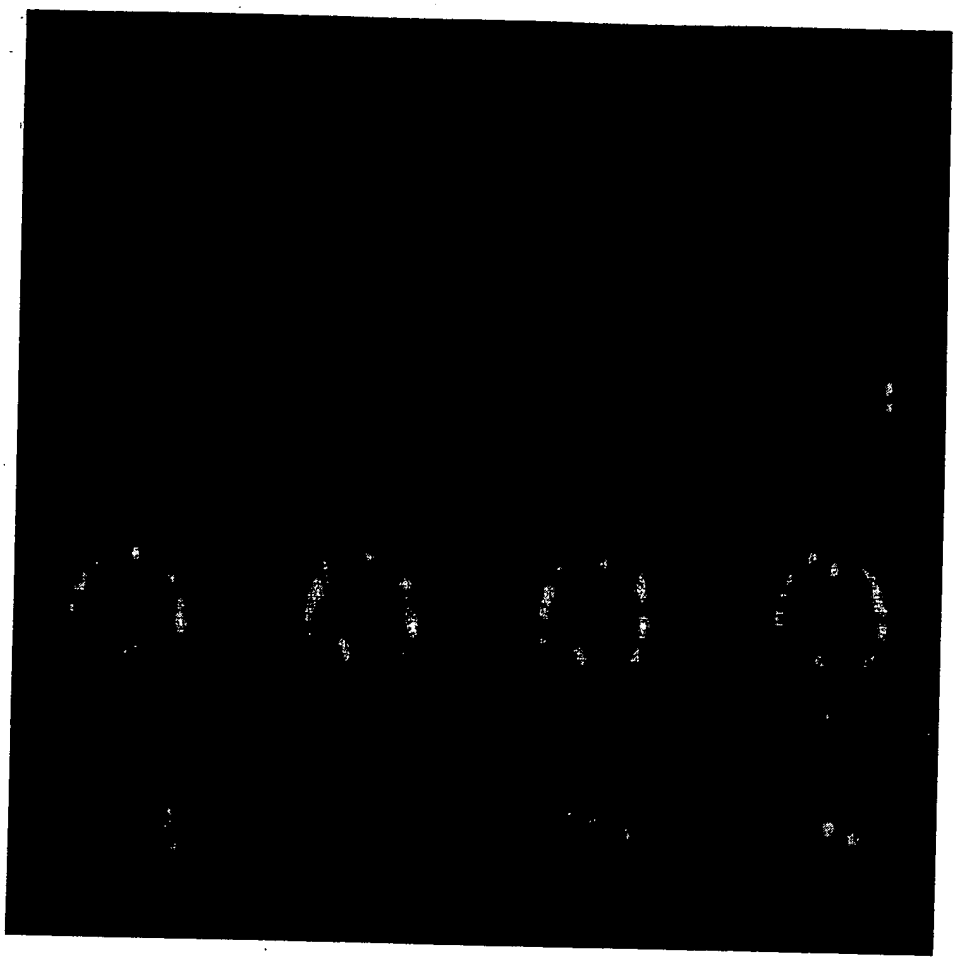

Fig. 2. A ^{123}I-iomazenil SPET image taken at 180 minutes showing uptake within the cerebral cortex and cerebellum. Courtesy of Institute of Nuclear Medicine.

more quantitative. Advantages of using the three-hour image are that a subject need only tolerate a relatively short time in the camera and that blood sampling is not required. Originally, we sampled so-called "arterialized" venous blood (a heated blanket is placed on the arm to enhance blood flow, such that venous blood is more arterial in content) from the forearm at 30 s, 1, 2, 3, 4, 5, 10, 15, 20, 30, 45, 60, 90, 120 and 180 min post [^{123}I]iomazenil injection. Unfortunately, we found difficulties in accurately modeling the first few minutes postinjection when the level of radioactivity in the blood is changing the most rapidly. An alternative is to normalizing a single late venous sample (around

20 min) to a published standard arterial curve. However, we have shown that although both these methods provide a reasonable approximation to the true plasma curve, the systematic errors introduced by this procedure precludes quantitative comparisons of benzodiazepine receptors in groups of subjects where only subtle changes are expected. It has been shown that for accurate kinetic modeling, arterial blood sampling is required frequently, at least every 5 s initially. Obviously, this is not practical without special equipment.

It is noteworthy to remember that the resolution of SPET is around 10 mm; hence, small regions will never be identified by this procedure and inevitably cortical regions can only be deemed as right/left, superior/inferior etc.

4. Conclusions

In vivo neuroimaging is the only technique available to investigate the neurochemistry and psychopharmacology of neuropsychiatric disorders and their treatments. Considerable investment has to be made in this area in order to produce useful radioligands and to validate the analytical methodology with each new radiotracer. Both [^{11}C]flumazenil and [^{123}I]iomazenil have been well characterized in the last decade. They both are useful radioligands in delineating the GABA-benzodiazepine receptor in vivo in man. It is imperative that their potential is now realized to the fullest in investigating the human brain.

Acknowledgements

ALH and ALM are Wellcome Training Fellows.

References

1. Malizia, A. L. and Richardson, M. (1995) Benzodiazepine receptors and positron emission tomography: ten years of experience. A new beginning? *J. Psychopharmacology* **9,** 355–368.
2. Spinks, T., Jones, T., Bailey, D., et al. (1992) Physical performance of a positron tomograph for brain imaging with retractable septa. *Phys. Med. Biol.* **37,** 1637–1655.
3. Grootoonk, S., Sinks, D., Sachin, D., Spuyrou, N., and Jones, T. (1996) Correction for scatter in 3D brain PET using the dual energy method. *Phys. Med. Biol.* **41,** 2757–2774.
4. Msaki, P., Bentourkia, M., and Lecomte, R. (1996) Scatter degradation and correction models for high resolution PET. *J. Nucl. Med.* **37,** 2047–2049.
5. Lassen, N., Bartenstein, P., Lammertsma, A., et al. (1995) Benzodiazepine receptor quantification in vivo in humans using [11C]flumazenil and PET: application of the steady state principle. *J. Cereb. Blood Flow Metab.* **15,** 152–165.
6. Abadie, P., Baron, J. C., Bisserbe, J., et al. (1992) Central benzodiazepine receptors in human brain : estimation of regional Bmax and Kd values with positron emission tomography. *Eur. J. Pharm.* **213,** 115–120.

7. Price, J., Mayberg, H., Dannals, R., and et al. (1993) Measurement of benzodiazepine receptor number and affinity in humans using tracer kinetic modelling positron emission tomography and [11C] flumazenil. *J. Cereb. Blood Flow Metab.* **13,** 656–657.
8. Malizia, A., Gunn, R., Wilson, S., et al. (1996) Benzodiazepine site pharmacokinetic/pharmacodynamic quantification in man: direct measurement of drug occupancy and effects in the human brain in vivo. *Neuropharmacology* **35,** 1483–1491.
9. Laruelle, M., Abi-Dargham, A., Al-Tikriti, M., et al. (1994) SPECT quantification of [123I]iomazenil binding to benzodiazepine receptors in nonhuman primates : II Equilibrium analysis of constant infusion experiments and correlation with in vitro parameters. *J. Cereb. Blood Flow Metab.* **14,** 453–465.
10. Onishi, Y., Yonekura, Y., Tanaka, F., et al. (1996) Delayed image of iodine-123 iomazenil as a relative map of benzodiazepine receptor binding : the optimal scan time. *Eur. J. Nuc. Med.* **23,** 1491–1497.
11. Videbaek, C., Freiberg, L., Holm, S., et al. (1993) Benzodiazepine receptor equilibrium constants for flumazenil and midazolam determined in humans with single photon emission tomography tracer [123I] iomazenil. *Eur. J. Pharm.* **249,** 43–51.
12. Pike, V. (1993) Positron emitting ligands for studies of *in vivo* probes from human psychopharmacology. *J Psychopharmacology* **7,** 139–158.
13. Litton, J. E., Hall, H., and Pauli, S. (1994) Saturation analysis in PET - analysis of errors due to imperfect reference regions. *J. Cereb. Blood Flow Metab.* **14,** 358–361.
14. Maziere, M., Hantraye, P., Prenant, C., Sastre, J., and Comar, D. (1984) Synthesis of an ethyl 8 fluoro 5,6 dihydro-5-[11C]methyl-6-oxo-4H imidazol[1,5a][1,4] benzodiazepine-3-carboxylate (Ro 15-1788-11C). A specific radioligand for the in vivo study of central benzodiazepine receptors using Positron Emission Tomography. *Int. J. Appl. Radiat. Isot.* **35,** 973–976.
15. Cunningham, V. and Jones, T. (1993) Spectral analysis of dynamic PET studies. *J. Cereb. Blood Flow Metab.* **13,** 15–23.
16. Richardson, M., Friston, K., Sisodiya, S., et al. Cortical grey matter and benzodiazepine receptors in malformations of cortical development: a voxel-based comparison of structural and functional imaging data. Brain 1997; in press.
17. Johnson, E., Woods, S., Zoghbi, S., McBride, B., Baldwin, R., and Innis, R. (1990) Receptor binding characterization of the benzodiazepine radioligand 123I Ro16-0154 : potential probe for SPET imaging. *Life Sciences* **47,** 1535–1546.
18. Sybirska, E., Al-Tikriti, M., Zoghbi, S., Baldwin, R., Johnson, E., and Innis, R. (1992) SPECT imaging of the benzodiazepine receptor : Autoradiographic receptor density and radioligand distribution. *Synapse* **12,** 119–128.
19. Innis, R., Al-Tikriti, M., Zoghbi, S., et al. (1991) SPECT imaging of the benzodiazepine receptor : feasibility of in vivo potency measurements from stepwise displacement curves. *J. Nuc. Med.* **32,** 1754–1761.
20. Verhoeff, N., Erbas, B., Kapucu, O., Busemann Sokole, E., Blok, H., and van Royen, E. (1993) Quantification of central benzodiazepine receptor binding potential in the brain with 123I-iomazenil SPECT : technical and interobserver variability. *Nuc. Med. Commun.* **14,** 634–643.

21. World Health Organization (WHO) (1977) Report of a WHO expert committee. Use of ionising radiations and radionuclides on human beings for medical research, training and non-medical purposes. Technical report series 611, Geneva, WHO.
22. International Commission on Radiological Protection (1996) Recommendations of the International Commission on Radiological Protection, 1990, ICRP Publication 62. Oxford, UK: Pergamon.
23. Acton, P., Lingford-Hughes, A., Pilowsky, L., and Ell, P. (1997) Comparison of relative and absolute quantification of benzodiazepine receptors using iodine-123-iomazenil and SPET. *Nuc. Med. Commun.*, submitted.
24. Lingford-Hughes, A., Acton, P., Gaconivic, S., and Suckling, J. (1997) Reduced levels of the GABA-benzodiazepine receptor in the absence of grey matter atrophy in alcohol dependency. *Br. J. Psychiatry*, submitted.

III

General Considerations

9

Analysis of Binding Data

Edward C. Hulme

1. Introduction

1.1. Basic Concepts

A receptor is an allosteric macromolecule (usually associated with a particular cell type) that binds a specific chemical substance (usually secreted by another cell) and in the process undergoes a defined conformational change that triggers a series of biochemical and physiological events within the target cell.

By definition, all receptors must be capable of existing in a minimum of two states, an inactive ground state (R) and an active state (R*) that transduces a signal. The distribution of the receptor population between the two states is altered, or alternative states induced, by the binding of specific ligands. The simplest representation of this process is the two-state equilibrium model of receptor binding (**Fig. 1**). This is the minimum mechanism necessary to relate receptor binding to pharmacology.

In the context of this model, an agonist is defined as a ligand whose binding favors the activated state of the receptor. There may also be inverse agonists, whose binding favors the ground state of the receptor. A pure antagonist is a ligand that performs a balancing act, binding with equal affinity to both ground and activated conformations of the receptor, without affecting the equilibrium between them.

In addition to these two basic conditions, the receptor may be able to exist in additional states. There can be more than one active form, or there may be inactive desensitized states, which manifest distinct conformations, or are distinguished by specific secondary modifications such as phosphorylation. Ideally, receptor binding studies are done under conditions such that the binding of the ligand does not irreversibly alter the receptor, and the ligand is stable

From: *Methods in Molecular Biology, Vol. 106: Receptor Binding Techniques*
Edited by: Mary Keen © Humana Press Inc., Totowa, NJ

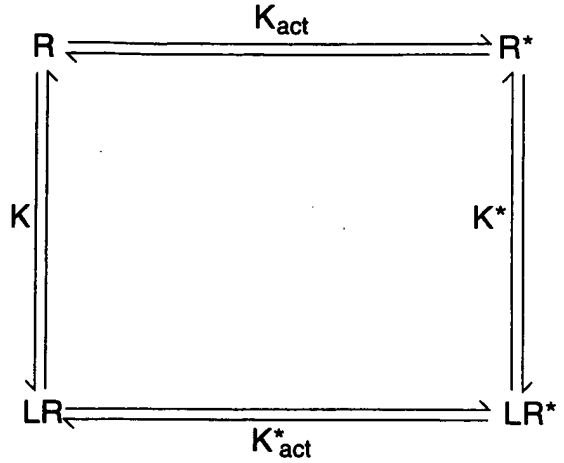

Fig. 1. A simple two-state model of receptor activation. R represents the ground state and R* the activated state of the receptor.

under the conditions of the assay. This allows binding equilibrium between receptor and ligand to be attained. In principle, fulfillment of this condition permits the mechanism of interaction between different ligands at the receptor to be probed and facilitates the extraction of quantitative binding constants and cooperativity factors. These parameters can be used to try to understand the pharmacology and biochemistry of receptor activation.

In this chapter, I have first outlined the basic theory of receptor-ligand interactions, as applied to the major classes of cell surface receptors. Following this, guidelines are given for the derivation of equations describing binding processes in a form appropriate for the analysis of experimental data, for the actual acquisition of the data itself, and for the process of identifying and interpreting a model that fits the experimental data. Some comments are given on several of the more popular commercial packages available for the analysis of binding experiments. Finally, the more useful equations that may be applied to the analysis of binding data are listed. Several of these equations go beyond what is available in commercial packages. Finally, I describe the major forms of artifact that affect binding experiments, with advice for avoiding them.

1.2. The Receptor Binding Assay

The basic protocol of binding assays is, in principle, straightforward *(1)*:

1. Make a preparation containing the receptor.
2. Select a suitable labeled ligand.

3. Incubate the receptor preparation with a chosen concentration of the labeled ligand for a defined time at a defined temperature.
4. Measure the bound and/(sometimes) or free ligand concentration.
5. Repeat steps 3 and 4 with the addition of unlabeled ligands or modulating agents, as defined by the aims of the experiment.
6. Analyze the data to extract quantitative estimates of rate constants, affinity constants, or cooperativities.
7. Relate the estimates of the binding parameters to pharmacologically-determined values describing receptor activation or blockade and analyze them for mechanistic information.

Step 4 usually involves a rapid physical separation of bound from free ligand, such as membrane filtration. However, advances in technology mean that this is not always necessary. For instance, the receptor preparation may take the form of the overexpressed receptor protein immobilized on a Biacore surface plasmon resonance chip or on scintillation proximity beads, which generate a signal from ligand binding without the need for a mechanical separation.

1.3. The Molecular Nature of Receptor-Ligand Interactions

1.3.1. Monomeric Receptor—One-Ligand Interaction

In the simplest case, the receptor can be assumed to exist in one predominant state (say the inactive ground state) and the ligand to bind without displacing the equilibrium between the ground and activated states. In terms of **Fig. 1**, we write K_{act}, $K^*_{act} \div 0$. The binding of the labeled ligand to the receptor can then be described as a simple bimolecular association reaction

$$R + L \underset{k_{21}}{\overset{k_{12}}{=}} RL \tag{1}$$

k_{12} is the association rate constant (on-rate) of the labeled ligand. The rate of formation of receptor-ligand complex is

$$k_{12}[R][L] \tag{2}$$

k_{21} is the dissociation rate constant of the receptor-ligand complex. The rate of breakdown of this complex is given by

$$k_{21}[RL] \tag{3}$$

At equilibrium, the net rate of formation of receptor ligand complex

$$d[RL]/dt = k_{12}[R][L]\text{-}k_{21}[RL] \tag{4}$$

is zero, so that

$$k_{12}[R][L] = k_{21}[RL] \tag{5}$$

$$[RL]/([R][L]) = k_{12}/k_{21} \quad (6)$$

k_{12}/k_{21} is referred to as the *affinity constant* of the binding reaction, K. An alternative is to define the *dissociation constant*, K_D, which is k_{21}/k_{12} , or 1/K. In this chapter, binding equations are given in terms of the K value, which has the merit that its value increases as the affinity of the ligand increases. The dissociation constant has the seductive property that it is the value of the free ligand concentration that produces 50% occupancy of the binding sites. The units of K are M^{-1}, while those of K_D are M. Although the choice between them is somewhat a matter of personal preference, it is the opinion of this author that binding equations are less cumbersome and easier to formulate in terms of affinity constants than dissociation constants, and this is the convention used throughout this chapter.

Both receptor and ligand are distributed among different forms and are subject to conservation equations

$$[R] + [RL] = [R_T] \quad (7)$$

$$[L] + [RL] = [L_T] \quad (8)$$

where the subscript T represents the total concentration of the receptor or ligand. In the simplest case, $[L_T]$ is much greater than $[R_T]$, so that the free ligand concentration is not reduced (depleted) by formation of the receptor-ligand complex. In this case, the differential **Eq. 4** is readily solved to give

$$[RL] = ([RL_0] - [RL_{eq}])e^{-(k_{12}[L] + k_{21})t} + [RL_{eq}] \quad (9)$$

where RL_0 is the initial concentration of receptor-ligand complex (commonly zero in a simple association experiment), and RL_{eq} is the concentration of receptor-ligand complex at equilibrium. This equation implies that the concentration of RL changes monoexponentially from its initial value to its final value with an apparent rate constant $k_{12}[L] + k_{21}$ which depends both on the intrinsic rate constants of the association and dissociation reactions and on the concentration of ligand. If the effective concentration of ligand is suddenly reduced to zero, either by dilution or by the addition of a large excess of a second, unlabeled ligand that competes for the same binding site, the receptor ligand complex dissociates monoexponentially with a rate constant that is purely determined by the off-rate

$$[RL] = [RL_0]e^{-k_{21}t} \quad (10)$$

Eqs. 9 and **10** can be used to determine the association and dissociation rate constants of labeled ligands.

The equilibrium level of binding is given by

$$[RL] = ([R_T]K[L])/(1 + K[L]) \quad (11)$$

which can also be written

$$[RL] = ([R_T][L])/(K_D + [L]) \quad (12)$$

Eqs. 12 and **13** are forms of the simple Langmuir isotherm. They predict a hyperbolic saturable dependence of the concentration of the receptor-ligand complex on the free ligand concentration.

Eqs. 9–12 represent the simplest possible descriptions of a receptor binding interaction. Real systems will almost always behave in a more complex way. Even the two-state system shown in **Fig. 1** is capable of generating a tri-exponential ligand association time course. However, few investigators are likely to have the means to investigate complex kinetic behavior in detail, and they are referred to the classic descriptions of enzyme kinetics *(1)*. In contrast, the behavior of the scheme shown in **Fig. 1** remains simple at equilibrium, but the effective affinity constant is now a composite of the three constants describing the underlying equilibria in the system. Thus

$$K_{app} = (K + K_{act}.K^*)/(1 + K_{act}) \quad (13)$$

The equilibrium binding properties of the two-state model, and their implications for receptor pharmacology, have been extensively discussed by Samama et al. *(2)*.

1.3.2. Monomeric Receptor—Two-Ligand Interaction

1.3.2.1. The Ternary Complex Model

The obvious extension of the one receptor–one ligand scenario is the interaction of two ligands with a single receptor, where generally one ligand is a labeled probe and the other an unlabeled competitor or modulator. In the most general case, both ligands can bind simultaneously to the receptor to form a ternary complex (**Fig. 2**). In fact, the ternary complex model provides a suitable basis for describing many of the situations that one encounters in practice, both at the level of receptor–ligand interactions and at the level of receptor–effector and receptor–effector–intracellular ligand interactions. Several equations derived from the ternary complex model are presented and discussed in **Subheading 2.9.**

A defining feature of the ternary complex model is that the binding constant of one ligand depends on the concentration of the other, thus the apparent affinity constant for the ligand L shows the following dependence on the concentration of the second ligand, A:

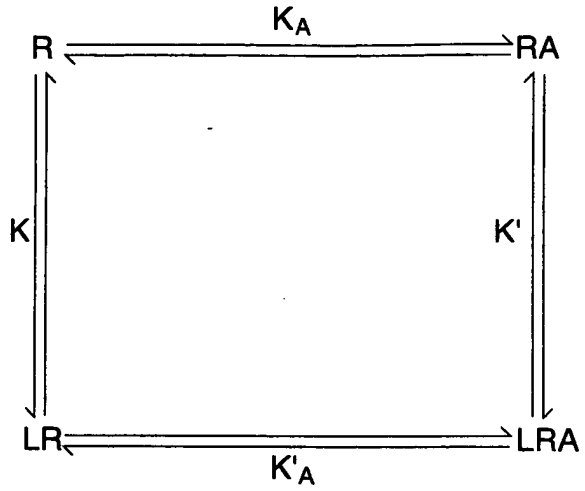

Fig. 2. Ternary complex model of the interaction of two ligands at a single receptor. The second ligand may either be a low-molecular-weight compound or an effector macromolecule, such as a G protein.

$$K_{app} = K(1 + K'_A[A])/(1 + K_A[A]) \quad (14)$$

Provided that both of the interacting ligands are present in large excess over the total concentration of receptor, their equilibrium-binding curves continue to follow simple hyperbolic saturation functions. As the concentration of one of the ligands increases from zero to a receptor-saturating value, so the affinity constant for the other changes from an initial value K to a final limiting value given by $K' = K.K'_A/K_A$. It is possible to encounter *positive cooperativity* ($K'/K = K'_A/K_A = \alpha < 1$) or *negative cooperativity* ($K'/K = K'_A/K_A = \alpha < 1$) where α is the cooperativity factor. Positive cooperativity is mechanistically very important in the superfamily of G protein-coupled receptors and underlies the essential step in activation, in which the binding of an agonist to a receptor increases its affinity for the guanine nucleotide-free form of the cognate G protein. Negative and positive cooperativity between drug-binding sites on receptors is also a quite frequent and pharmacologically important phenomenon *(3,4)*.

Ligand binding that conforms to the simple hyperbolic Langmuir isotherm ceases to operate when the free concentration of one or the other of the ligands is significantly reduced as a result of its binding to the receptor. For instance, this may happen in the case of a G protein-coupled receptor, when the effective concentrations of receptor and G protein are nearly equivalent. It should be noted that interactions of the latter kind, between large molecules that are con-

fined to two dimensions by their membrane-association, are not well understood either in theory or in practice. Depletion can also evoke receptor-binding artifacts. These arise when the product of the receptor concentration and the affinity constant becomes comparable to the ligand concentration.

1.3.2.2. Competitive Interactions

The competitive interaction between two ligands represents one of the most common situations encountered in receptor pharmacology. It can be understood as an extreme case of the ternary complex model, in which the binding of one ligand totally excludes the binding of the other, so that no ternary complex is formed. In **Eq. 14** $K'_A = K' = 0$ so

$$K_{app} = K/(1 + K_A[A]) \tag{15}$$

This is the situation when the binding sites for two ligands overlap substantially, so that they occupy the same space in the binding site, the so-called *volume exclusion effect*. A major distinction between competition and negative cooperativity is that in the case of competition, an increase in the concentration of the competing ligand reduces the affinity constant for the other ligand (say the tracer ligand) without limit. In practice, however, the difference between competition and extreme negative cooperativity may be impossible to detect by means of equilibrium-binding experiments alone.

1.3.2.3. Kinetics

The presence of a second ligand complicates the kinetic behavior of a ligand-receptor interaction. Even the simplest case, that of a competitive interaction, leads to complex kinetic behavior, which can be counterintuitive in its effects. The main point is that the presence of a competitor ligand will often introduce a slow phase into the binding of a tracer ligand, frequently to the point where the approach to equilibrium becomes limited by the dissociation rate constant of the tracer. In the performance of binding experiments, it is necessary to remember that the time course of tracer binding in the absence of a competing ligand is not a good guide to the binding in the presence of the competing ligand. In general, the rate of approach to equilibrium is dominated by the kinetics of the slowest reaction step. As a rule of thumb, where simple competition is believed to operate, the binding reaction should be incubated for five times the half-time of the slowest step in the reaction mechanism. However, a competing ligand will not affect the time-course of a dissociation reaction.

In the case of allosteric interactions, the effects on tracer kinetics can be even more profound. This is because in the limit the tracer binds to or dissociates from the complex of the receptor with the second ligand. *A priori*, it is impossible to predict the effect that this will have. Both acceleration and decel-

eration of the tracer kinetics are possible. Often, the slowing will be extreme. The allosteric ligand may "plug" access to the binding site so that the tracer can neither enter nor leave without prior dissociation of the allosteric partner. Thus, a test for allosterism is to vary the concentration of the putative cooperative ligand and measure its effect on a relatively simple parameter, such as the dissociation rate constant of the tracer.

1.3.3. Multiple Binding Sites

More often than not, radioligand binding data cannot be accommodated by single-site models. There are two distinct classes of explanation for this. The first is that there exist separate receptor populations; for instance, receptor subtypes with different primary sequences, distinct secondary modifications, or even stable conformational isoforms of a single sequence. This situation is relatively easy to deal with analytically, merely requiring summation of the functions describing single-site models.

The second is that a uniform class of receptors acquires effective heterogeneity by interaction with other molecules. Such interactions can be highly specific, as in the case of receptor-G protein complex formation, or more nebulous, as when molecules occur in a series of different microenvironments; for instance, membranes with different phospholipid compositions. Heterogeneity is most readily sensed by ligands that induce large conformational changes in the receptor, as is commonly the case with agonists of high efficacy.

Some aspects of receptor heterogeneity can be accommodated by the ternary complex model of binding. This is the case, for instance, with the simpler receptor-G protein interaction models, which do not envisage the dissociation of the G protein into its component α and $\beta\gamma$ subunits. A few of the simpler versions of these models are discussed in the methods section of this chapter. While the full interaction of agonist, receptor, G protein, and guanine nucleotide has been extensively simulated ***(5)***, the calculations are too complex to handle within the context of commercially available fitting programs, and the equations contain parameters that cannot be determined without the ability to manipulate the relative concentrations of G protein subunits.

1.3.4. Receptor Oligomers

If the receptor is intrinsically oligomeric and is composed of multiple subunits, several of which have ligand binding sites, models of greater complexity that incorporate cooperativity between binding sites need to be considered. Such cooperativity may be either positive or negative. Discussion of these issues reaches back to the pioneering work of Monod, Wyman, and Changeux and Koshland, and has been extensively reviewed by Wells ***(6)***. In no class of receptors can the issues of cooperativity be ignored.

1.3.4.1. Ligand-Gated Ion Channels

Ligand-gated channels are intrinsically oligomeric. Binding of a minimum of two ligand molecules is usually necessary to open the channel. Ligand binding shows positive cooperativity, with a Hill coefficient of up to 2. The kinetics of ligand binding are also complex. The equilibrium and kinetic properties of some such systems have been extensively investigated using fluorescent agonist analogs *(7)*.

1.3.4.2. Receptor Tyrosine Kinases and Cytokine Receptors

Ligand-induced dimerization is integral to the activation mechanism of these receptors. This involves transphosphorylation of one component of the receptor dimer by the other, followed by the recruitment of intracellular components *(8)*. The quantitative analysis of these more complex enzymatic processes is beyond the scope of this chapter.

1.3.4.3. G-Protein-Coupled Receptors

The activation mechanisms involve induction of a ternary (or actually, quaternary, agonist-Receptor-G$\alpha\beta\gamma$ complex), which can be regarded as the active form *(5,9)*. There is also the possibility that the receptors themselves may, under some circumstances, exist as oligomers *(10–12)*, which may or may not have functional significance for the kinetics of agonist binding *(13)*. Specific receptor sequences may mediate oligomerization *(14)*, although the evidence for this is still controversial.

In general, therefore, receptor oligmerization must be regarded as more the rule than the exception, and there is a necessity to consider the use of more complex models of binding. The problem lies in designing experiments that can exploit such models *(6)*.

1.4. Outline of Data Analysis Methods

Any binding method will produce a signal Y (the dependent variable) as a function of ligand concentration(s), $L_{i,k}$, which constitute the independent variable(s) controlled by the experimenter. Y may be, for instance, the disintegrations per minute (dpm) output of scintillation counter, as a function of radioligand concentration in a binding assay. A primary requirement is to ensure that binding experiments are done in such a way as to ensure, as far as possible, the absence of systematic errors or artifacts in the data.

The aim of data analysis is to determine the most appropriate function $F(p_j;L_{i,k})$, where p_j are parameters to be determined, which fits the signal in such a way that the distribution of the data points around the fitted curve is statistically random. The scientific requirement is to identify a function that reflects the underlying molecular events and whose parameters therefore have

a meaning at the mechanistic level. This is not an elementary matter and may not always be possible, owing to our ignorance of the molecular nature and constitution of the system. If so, an empirical function, such as the Hill equation (**Subheading 2.9.4.**), may have to be be used.

Mathematically, the values of the parameters p_j, which yield the best description of the data, are determined by minimizing χ^2, the weighted residual sum of squares of the differences between the calculated value S, and the measured value Y. If there is only a single variable ligand, the quantity to be minimized is

$$\chi^2 = \Sigma w_i[Y_i - F(p_j, L_i)]^2$$

Here, Y_i is the measured value of the signal for the i^{th} ligand concentration, and w_i is a weighting factor, to be determined either empirically or theoretically. This expression is easily generalized to take account of more than one variable ligand.

2. Methods

2.1. Formulating Models of Binding Processes

2.1.1. The Golden Rule

Formulate the model to fit the experimental data *as measured.*

This means that the model should use as input the *measured* values of the dependent variable(s) (e.g., dpm, optical density, and so forth) and the *untransformed values* of the independent variables (e.g., dpm, molar concentration). The assumption behind least-squares fitting is that there is no error whatever in the independent variable. Obviously, this is not completely true. However, any transformation of the independent variable only compounds any error.

2.1.2. Express the Parameters in an Appropriate Form

Monte Carlo simulations have shown that errors in binding constants are log-normally distributed. Thermodynamically, this reflects the fact that, in a binding reaction, one is measuring a free energy of binding, which is proportionate to the log of the affinity constant. Therefore, models should be formulated in such a way that binding constants and concentrations are expressed in a logarithmic form. This stipulation does not apply to rate constants.

2.1.3. Acquire Enough Data to Define the Parameters Accurately

This may mean using an extended range of concentrations or may require the exploitation of more than one independent variable to uncover otherwise hidden properties of the system (*see* **Subheading 3.4.1.**). It is also advisable to

replicate data points sufficiently (we use triplicate or quadruplicate measurements) to obtain reasonable estimates of the standard errors associated with each of the measurements for use as weighting factors in curve fitting.

2.1.4. Empirical or Mechanistic Model?

When the data fit a simple model, e.g., a monoexponential association or dissociation curve or a simple one-site binding curve, there is no problem in making a choice. This is often the situation when the ligand is an antagonist, which may bind without inducing a major conformational rearrangement of the receptor. However, many ligands, particularly agonists whose binding induces a conformational change that leads to the activation or recruitment of effector mechanisms, manifest complex binding properties. Often, the investigator is faced with difficulties in deciding how to analyze the binding curve to extract parameters that are meaningful and not misleading.

In complex situations, it can make sense to hedge one's bets by trying to apply both an empirical model, such as the Hill equation (or logistic equation), which provides parameters that essentially allow the recreation of the binding data, and a mechanistic model such as a multisite, or ternary complex model. One has to be acutely aware of the limitations of the models to avoid overinterpretation of the results. In most studies, it actually pays to try to go beyond binding studies to functional data. The combination offers much more insight into receptor mechanisms than either class of data alone. In specialized cases, binding methodology can be adapted to provide functional data, as in the case of agonist-stimulated GTPγS binding to G-proteins *(15,16)*.

The investigator should never lose sight of the truism that an adequate fit of a model to a data set is merely permissive, in the sense that it shows the underlying mechanism to be one possible description of the process underlying the observations. It does not prove the mechanism to be the only one possible, although it may be the minimum mechanism that can describe the data, and thus provide a working model of the process.

2.1.5. Analysis vs Display

The aim of modeling binding data is

1. To test the adequacy of particular models as descriptions of a data set and to eliminate inadequate ones.
2. In the testing process, to derive statistically valid parameter estimates, which can provide a basis for the evaluation of proposed mechanisms or for comparisons of data sets derived under different experimental conditions.

This is the analytical task. There is also the task of displaying the results of the analysis, and this is often done by means of linear transformations of the

data. These do not, in general, provide an adequate basis for the analysis itself, but can be valuable in pointing out deviations from models or in taking in results at a glance.

2.2. The Algebraic Formulation of Mechanistic Models of Equilibrium Processes

2.2.1. Principles

The algorithm for derivation of an algebraic model for a binding process is the following:

1. Write down the equilibrium equations describing the formation of each intermediate in the mechanism.
2. Back-substitute in each equation in such a way that the concentration of all intermediates are expressed in terms of one central intermediate, which may be the intermediate to be determined, or the free receptor concentration, and the independent variables.
3. Substitute the expressions for the concentrations of the intermediates in the conservation equation(s) for the various components of the system, e.g., receptor, G protein, and ligand. Nonspecific binding processes should be included at this point.
4. Solve the resulting equation(s) for the concentrations of the central intermediate(s). This may be done explicitly or numerically.
5. Calculate the measured quantities from those of the central intermediate, taking into account other processes such as nonspecific binding and the presence of background signal.
6. Reformulate the resultant expression so that the variables, and the parameters to be determined by fitting, are expressed in a statistically valid way.

2.2.2. Example

This process is best illustrated by an example. Suppose that we have a simple ligand binding process

$$R + L = RL; \text{ affinity constant K}$$

accompanied by a nonspecific binding process

$$\text{NSB} = \text{N}[L]$$

expressing $[LR]$ in terms of $[R]$ and $[L]$

$$[RL] = \text{K}[R][L].$$

The conservation equation for ligand is

$$[L_T] = [L] + [RL] + \text{N}[L].$$

The conservation equation for receptor is

$$[R_T] = [R] + [RL].$$

Expressing R in terms of RL gives

$$[R] = [RL]/(\mathrm{K}[L]).$$

Expressing L in terms of RL gives

$$[L] = ([L_T]\text{-}[RL])/(1+\mathrm{N}).$$

Substituting into the conservation equation for receptor gives

$$[R_T] = [RL] + [RL](1+\mathrm{N})/(\mathrm{K}([L_T]\text{-}[RL])).$$

Expanding this gives

$$[RL]^2 - [RL]([R_T] + [L_T] + (1+\mathrm{N})/\mathrm{K}) + [R_T][L_T] = 0.$$

This quadratic equation is then solved to yield $[RL]$ in terms of the independent variable $[L_T]$, and the parameters $[R_T]$, K, and N. To simplify, we write

$$T1 = ([R_T] + [L_T] + (1+\mathrm{N})/\mathrm{K})$$

$$T2 = [R_T][L_T].$$

Then

$$[RL] = (T1 - \mathrm{SQRT}(T1^2 - 4T2))/2.$$

Note that it is necessary to choose the correct root of the equation.

The further development of this expression into a form suitable for fitting experimental data involves first adding the term for nonspecific binding:

$$\mathrm{NSB} = \mathrm{N}[L] = \mathrm{N}([L_T] - [RL])/(1+\mathrm{N})$$

$$[B_{\mathrm{TOT}}] = [RL] + \mathrm{NSB}$$

and then converting total binding, B_{TOT}, into the actual measured value. It is necessary to give some thought to the units involved at this point. For instance, the above equations contain quadratic terms in receptor and ligand concentrations. If these are expressed in absolute molar terms, the products can become very small numbers, which causes problems for the fitting algorithm. It makes sense to try to arrange the calculations so that the numbers involved remain within a few orders of magnitude of 1; for instance, concentrations can be expressed in nanomolar form, and affinity constants can be expressed as nM^{-1} instead of M^{-1} if the receptor concentration in the assay is in the nM range, and the K_d is in the nM range. In this case, in a radioligand binding experiment, we may write

$$F = 2220*\text{SPACT}*[B_{TOT}]$$

where SPACT is the specific activity of the radioligand (in Ci/mmol) and 2220 is the conversion factor from nanocuries (nCi) to dpm.

Finally, we express the K value in logarithmic form

$$K = 10^{PK}$$

where, in the context of these equations, and throughout this chapter, capital "P" is used as a shorthand for $\log_{10}$ (not $-\log_{10}$). Thus, the parameters to be determined by the fitting program are, finally, PK [in units of log $(nM)^{-1}$, so that an affinity constant of 10^9, K_d 10^{-9}, comes out as 0.0), R_T (in units of n*M*), and N, the coefficient of nonspecific binding, which is a dimensionless number dependent on the properties of the assay.

A further development of this model is to add a second ligand, A. This could, for instance, be an unlabeled competing ligand used to define nonspecific binding. The simplest assumption is that there is a large excess of competitor over receptor, so that receptor-specific binding does not significantly reduce (deplete) the free concentration of A. The effect of this is to reduce the value of K in the above equations, so that

$$K_{app} = K/(1+ K_A[A])$$

where K_A is the affinity constant of the competing ligand. K_{app} is the apparent affinity constant for the tracer ligand in the presence of the competitor. The factor 1 + K[*A*] is called the Cheng-Prusoff shift *(17)*.

This apparent affinity constant can be substituted in the above equations, so that B_{TOT} is now a function of two independent variables, [*L*] and [*A*]. In this form, the model can be used for the analysis of competitive interactions, provided that the binding of the competing ligand does not result in its depletion. It also lends itself to the analysis of saturation-binding curves, in which the binding of a series of increasing concentrations of the tracer ligand is measured in the absence and the presence of a receptor-saturating concentration of a competing ligand. Its advantage is that it allows both the specific and nonspecific binding components to be analyzed simultaneously, thus enhancing the accuracy of determination of the nonspecific binding coefficient, the overall accuracy of the affinity constant, and the total concentration of receptor sites.

This model is included in the list given in SigmaPlot format in **Subheading 2.9.** Most of these models are derived from the general mechanism for allosteric interaction of two ligands at a receptor. Each model is accompanied by a set of notes on its use. Also included are some models that can be used for the semiempirical analysis of receptor functional responses. More advanced topics, particularly the formulation and solution of mechanistic schemes for com-

plex receptor models involving the existence of oligomeric structures have been comprehensively reviewed and described by Wells *(6)*.

2.3. Data Acquisition and Weighting

2.3.1. Calculation of Weighting Factors

All measurements are associated with an error, which will arise partly from instrumental properties (e.g., counting error) and partly from experimental variations (e.g., pipeting errors, variations in the amounts of membranes harvested, and so on). The existence of errors means that some data points will be more accurately determined than others. To extract statistically unbiased parameter estimates by fitting a given data set to a given model, the natures and magnitudes of these errors must be taken into account.

In binding experiments, errors are generally proportional to the magnitude of the signal (proportional error), although, if the signal is small in relation to the background, and the data acquisition instrument is a scintillation counter, the error may become proportional to the square root of the signal (Poissonian error). It is possible to develop a theoretical or empirical error function for a given experiment. More generally, however, measurements are replicated, providing an estimate of the standard error of the mean of each data point used in fitting. The assumption is that data points have a normal error distribution. Thus, for n replicates Y_i of a given observation

$$\text{mean} = \Sigma Y_i/\text{n}$$

$$\text{standard deviation (S.D.)} = \sqrt{[(\Sigma(Y_i - \text{mean})^2/(n - 1)]}$$

$$\text{standard error of mean (S.E.M.)} = (\text{S.D.}/\sqrt{n}).$$

In order to make this calculation at all realistic, the observations need to be replicated at least three times.

In the minimization of sum of squares of the residuals, the function minimized is

$$\chi^2 = \Sigma w_i[Y_i - F(p_j,L_i)]^2$$

where w_i is the weight associated with the i^{th} observation. The weight is usually taken to be proportional to $1/\text{SEM}^2$ for that observation, provided that the SEM is not out of line (either abnormally high or low) with that of surrounding observations. To smooth out variations in the SEMs of individual data points, it is possible to fit the individual values to an appropriate function of Y_i, e.g, a polynomial, or a theoretical weighting function, and then to use the smoothed values to weight the data points. In general, this is not necessary. However, it should be emphasized that the assumption that the weights of all data points

are identical (simple weighting), therefore, that all data points contribute equally to the analysis is incorrect in principle for binding experiments, and that although this may not necessarily have much effect on the the parameter values themselves, it will often affect one's estimate of the reliability of the parameter estimates.

2.3.2. Outliers

Every now and again, an experimental mistake (usually a gross pipeting error) will lead to a point that is obviously wrong and whose error falls well outside the normal error distribution that data points are assumed to follow. One way to handle this situation is simply to leave out the point altogether. Another more objective approach is to employ "robust" weighting ***(18)***. This is actually incorporated into some statistically numerate fitting packages, such as GraFit ***(19)***. If Z_i is the residual between the fitted curve and the observation, weighted by multiplication with the weighting value in use for that point, the value $u_i = Z_i/(6\Sigma\text{abs}(Z_i)/N)$ is calculated and an additional bisquare weight applied, which is the following.

$$b_i = (1-u_i^2)^2 \text{ if } \text{abs}(u_i) \leq 1$$

$$b_i = 0 \text{ if } \text{abs}(u_i) > 1$$

2.3.3. Is It Better to Replicate Observations Or to Use More Data Points?

It depends on the accuracy of the observations. In principle, the mean values of the observed variable at a number of discrete points on a binding curve can be determined to any desired degree of precision by sufficient repetition. This may allow one to reject an oversimplified model with a decisiveness that would be impossible even with an infinite number of single observations, however closely spaced, because of their intrinsic variability. On the other hand, by definition, determination of a function at a series of discrete points does not provide information about what goes on between them, although requirements of continuity provide constraints. In practice, some compromise is necessary. Publication-quality data call for estimates of the variance of points to be provided, and this requires a minimum of duplicate, and preferably triplicate or quadruplicate, determination of data points. On a typical 48-place Brandel filter, 5 log units of ligand concentration can be spanned in 0.5 log unit intervals with quadruplicate measurements, which is usually good enough. However, discrimination between more complex models may require a higher density of data points, or the simultaneous analysis of multiple data sets, or both. For the most thorough and comprehensive discussion of these issues, the reader is referred to Wells ***(6)***.

2.4. How Does One Perform the Fit?

The aim is to choose a model that determines a function $F(p_j,L_i)$ in which the parameters p_j are determined by a fitting algorithm, usually provided within the context of a commercially available fitting package, in such a way that the distribution of the data points around the fitted curve is statistically random. Mathematically, the values of the parameter p_j that yield the best description of the data obtainable within the constraints of the model are determined by minimizing χ^2, the weighted sum of the squares of the differences between the calculated value and the measured value of the signal.

The model is formulated following the guidelines given above and inserted into the fitting package. It is the user's responsibility to provide, or to provide the means, of estimating (although recent updates of fitting routines may be able to do this automatically), initial parameter estimates, as well as to stipulate the most appropriate method of weighting the data. The parameter estimates are then refined iteratively, by an algorithm that implements a least-squares algorithm, usually the Marquardt-Levenberg method, which is a blend of the method of steepest-descents with the Gauss-Newton method *(6)*. The user should also have control over parameter ranges (e.g., parameters can be constrained to be positive) or over features of the implementation of the minimization routine, such as the step length or number of iterations to be performed. The user can usually specify the convergence criteria to be applied; for instance, the maximum relative change in parameter magnitude per iteration, which indicates that the calculation can be terminated. It is desirable to be able to perform simultaneous analysis of multiple data sets and to have the facility to hold parameters in common between them, if necessary.

2.5. Does the Model Fit the Data?

Visual inspection is quite a good way to assess how good the fit is. It is very valuable to produce a plot of the residuals between the data points and the fitted curve as a function of the independent variable. A systematic deviation between the fitted curve and the model will show up in the form of grouped positive and negative residuals. The fitted curve will also commonly miss at both extremities. On the other hand, if the fit is acceptable, the residuals should be randomly distributed about the fitted curve. Any good-fitting program should allow a residual plot to be constructed without effort.

Residual correlation can be put on a more quantitative basis by means of a runs test *(6)* or by the calculation of the correlation coefficient between each successive weighted residual and its neighbor. Thus, the residuals are written as two arrays (z_1, z_2, z_3 . . . z_{n-1}) and (z_2, z_3, z_4 . . . z_n), and the correlation coefficient, r, between them calculated. Correlated residuals will lead to a posi-

tive value of r, whose significance can be calculated by the computation of Fisher's t-statistic

$$tF = r([n-3]/[1-r^2])^{1/2}$$

where n is the number of data points included. This value can be looked up in standard statistical tables.

Inspecting residuals gives a qualitative impression of the goodness of fit. However, one is often attempting to choose between two models that both more or less fit the data. If they are characterized by different numbers of undetermined parameters (as, say, in a one-site as opposed to a two-site model), one may calculate the F-statistic

$$F = ([\chi_1^2 - \chi_2^2]/[df1 - df2])/(\chi_2^2/df2)$$

where *df1* and *df2* are the number of degrees of freedom of the two fits, namely the number of data point minus the number of parameters determined by the fit. It is usually the case that using a model with a larger number of unset parameters will give an improved fit to the data set, and calculation of the F-statistic provides an objective test of whether the inclusion of extra parameters is justified by the improvement in the fit.

These statistical techniques can also be applied to the analysis of multiple data sets in which certain parameters are held common, whereas others are allowed to vary. This is possible within the environment provided by packages such as SigmaPlot and GraFit. These more complex procedures are beyond the scope of this chapter. Further discussion is to be found in Wells ***(6)***, and in the GraFit manual ***(19)***.

2.6. Example

The use of these tests is best illustrated by a worked example. **Figure 3** shows experimental data representing a competition experiment with a ligand that binds to two separate classes of binding sites with apparent affinities of $10^6 M^{-1}$ and $10^4\ M^{-1}$. The two classes of binding sites are present in equal amounts. The total binding is 1000 dpm and the nonspecific binding 50 dpm. There is a total of five parameters.

The data are typical of that obtained in a simple competition experiment. There are 15 data points acquired in the presence of the competitor. Also included are background and nonspecific binding measurements. In order to accurately determine the extremities of the binding curve, it is often possible to include these values in the fit, giving the total binding measurement a notional competitor concentration two orders of magnitude less than the lowest actual competitor concentration used (provided that it caused no inhibition) and giving the nonspecific binding measurement a competitor concentration two

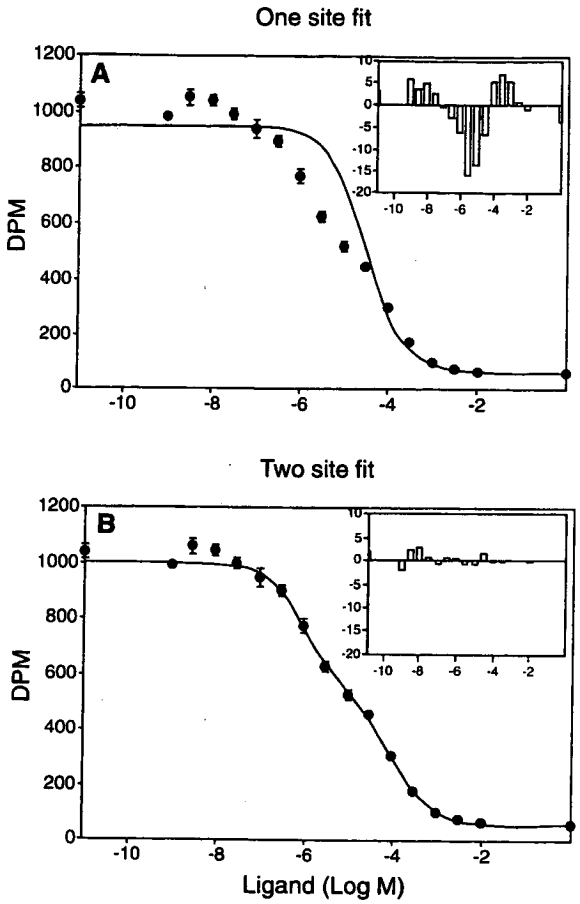

Fig. 3. Fits of (**a**) one-site and (**b**) two-site models of binding to a competition curve. The insets show plots of the residuals of the fits against the log of the ligand concentration.

orders of magnitude higher than the highest actual concentration used, assuming that the latter gave full inhibition of binding. This can only be done when the mechanism of inhibition is competitive.

Figure 3A shows the results of fitting an inappropriate model, in this case a one-site model of binding (**Subheading 2.9.5.**). It is clear from visual inspection that the fitted curve is a poor description of the data. This is obvious from the plot of the weighted residuals, which shows how, in a typical fashion, the fitted curve undershoots the total binding, crosses the experimental data, and overshoots the nonspecific binding, although by a smaller amount, because of the lower standard error of the data. The deviation is confirmed by calculation

of the nearest neighbor residual correlation coefficient (**Subheading 2.9.10.**), which gives a t value of 3.47 (14 degrees of freedom), which is significant at $p < 0.01$. In contrast, fitting a two-site competition model (**Subheading 2.9.5.**) gives the curve shown in **Fig. 3B**. It is immediately obvious that the fit is better. This is confirmed by the plot of weighted residuals which are, first, smaller, and second, uncorrelated ($t = -0.27$, $p > 0.5$). In this case, calculation of the F-statistic is almost superfluous, but application of the transform given in **Subheading 2.9.11.** gives a value of 185 (2,12 degrees of freedom), which simply confirms the obvious, that in this case the two-site model is a much better fit than the one-site model. In most cases, the differences are less clear.

2.7. What is the Significance of Parameters Determined by Fitting?

Fitting routines always produce estimates of the standard errors of the fitted parameters. These are calculated from a matrix (the covariance matrix) that arises during the minimization process and are an indication of the range over which a given parameter can be varied without significantly affecting the residual sum of squares *(6)*. However, they cannot be taken as statistically independent measures of parameter standard errors, unless the parameters are totally uncorrelated, in the sense that one parameter can be varied without affecting the estimates of the others. This is almost never the case. Fitting routines also commonly provide an estimate of the dependence of parameter estimates on other parameter estimates, which is a measure of parameter correlation. What this means is that a change in one parameter can be, in part, compensated for by a change in other parameters. For instance, in the fit presented in **Fig. 3B**, the fraction of high-affinity binding sites and the two affinity constants all have quite high correlations (0.88, 0.57, 0.86). Values very close to 1.0 indicate two parameters are almost completely correlated and that the model may usefully be simplified; for instance, by defining a single parameter that is the product of the two parameters in question, and rewriting the model equation to take that into account. An example is given in **Subheading 2.9.7.** where the parameter KT is the product of three individual components.

It is sound advice, as in any experimental situation, to regard estimates of fitted parameters from a given experiment as single numbers and to repeat the *entire* experiment the requisite number of times (e.g., three times) necessary to calculate estimates of the means and standard errors of each parameter. It must be emphasized that such calculations should be performed on parameters that are expressed in forms known to be normally distributed (e.g., affinities should be expressed in a logarithmic form and concentrations of sites in a linear form).

2.8. Fitting Packages

2.8.1. SigmaPlot 3.0 and 4.0 for Windows

Supplied by SPSS Inc. (Chicago, IL; Erkrath, Germany: www.spss.com). It requires at least a 486, 66 MHz processor with at least 16 MB of RAM and 20 MB of hard disk space minimally running Windows 3.1 with WIN32s version 1.30C, or Windows 95. An alternative is Windows NT 3.51 or 4.0 with 24 MB RAM and 20 MB hard disk space.

SigmaPlot is essentially a graphics package with an add-on curve-fitting facility based on the Marquardt-Levenberg algorithm, which is robust and efficient. It allows the user to insert equations formulated in the SigmaPlot transform language. The equations can contain up to 25 undetermined parameters and up to 10 independent variables. This is enough for most situations encountered in curve fitting. By careful formulation of the equations, it is possible to perform multiple curve fits and so fit several data sets simultaneously. However, it is not immediately obvious how one does this (*see* **Subheading 2.9.9.1.**).

The user usually has to provide initial estimates of the unknown parameters. A facility is available for "automatic" initial estimation for equations that can be linearized. The user has control over the progress of the iterations, can limit changes in the step length, and can control the convergence criteria. A useful feature is that the models used in fitting can just as easily be used for simulation.

The program provides estimates of parameter errors and parameter correlation. Annoyingly, it is not possible to incorporate the full results (e.g., parameters and standard errors) into the worksheet using standard cut and paste commands with the mouse; keyboard strokes also have to be used.

A defect in SigmaPlot is that the equation definition language is not sufficiently flexible to formulate models that employ iteration to find numerical solutions to the binding equations themselves, at least in the context of the fitting routine. This limits the equations that can be used to those that can be solved analytically, which excludes the more complex equations involving multiple ligand depletion, and anything more than the simplest versions of the ternary complex model of receptor-G protein interaction. In this respect, despite their apparent sophistication, packages such as SigmaPlot are actually less flexible than the Fortran programs of 30 years ago.

SigmaPlot makes it easy to transform the results of curve-fits into display formats. However, the user has to write the equations and so has to master the transform language.

SigmaPlot graphics are flexible. However, the graphics package feels quite cumbersome to use and has annoying features that have to be learned. Three-

dimensional plots are possible. The output is of publication quality. SigmaPlot 4.0 also incorporates a report editor.

SigmaPlot is a good enough program to make the user who invests sufficient effort in it to stay committed. It could still be made much less cumbersome and more flexible.

2.8.2. GraFit

Supplied by Erithacus Software (Staines, U.K.). Requires 486 processor with Windows 3.1, at least 1 MB of memory and 5 MB of hard disk space.

This program was written by an enzymologist, and it incorporates most of the features that one might look for in a program for binding data analysis. The latest versions include a GOTO statement in the equation definition language, which makes iterative programming a possibility. Up to 30 unset parameters can be used. The user can adjust the convergence criteria for the fit. Automatic estimation of initial parameter values is possible. The creation of a residual plot is made easy. Linear transformations of the data and fit for display purposes are also simple. There are a number of useful basic equations. The analysis of multiple data sets is catered for, with parameter-sharing options available. The F-test for goodness-of-fit is provided. However, there is no indication of parameter correlations. The manual is informative and educational. The graphics package is not as flexible as that of SigmaPlot but is still of publication quality. This package may well be the best buy for its combination of user-friendliness, intelligent design, and excellent manual.

2.8.3. GraphPad Prism

Supplied by GraphPad Software Inc (San Diego, CA: www.graphpad.com). Requires Windows 3.1 or higher. A Mac version is available.

This package was written by a kineticist and is aimed at pharmacologists. Its design and implementation show acute awareness of the difficulties that can affect binding studies. There are built-in equations for the analysis of the main categories of binding experiments, and statistical tests for goodness of fit allow the program to assess which of two models provides a better fit to a given data set. User-designed equations can be entered in a multiline format. Residual plots are easily constructed. A depletion-corrected version of the saturation binding experiment is provided. It is possible to omit outlying factors from the analysis. The data handling and graphics facilities are intelligently designed; for instance, means and standard errors are calculated automatically. All stages of the analysis process, from data input through the analysis to derive binding parameters to the generation of graphs and page layouts, are "linked and live," in the sense that a change to the data worksheet feeds through to all of the other linked processes, without the need for repeating the analysis or plotting proce-

dures. This is a very powerful feature. The downside is that models incorporating more than one independent variable are not catered for. The graphics quality is high, and the program is designed for the production of finished reports. It is user-friendly, incorporating tips and hints, with many useful features. The manual is also very good and informative. This package is a good buy for those concerned with the routine analysis of binding data; for instance, from high-throughput screening.

2.8.4. KELL

Supplied by Biosoft (Cambridge, U.K.: www.biosoft.com). Requires Windows 3.1 or higher.

KELL stands for KINETIC, EBDA, LIGAND, and LOWRY. The KINETIC module calculates association and dissociation rate constants from time courses. EBDA and LIGAND are for analyzing direct saturation and competition assays, using multiple sites models. These are supposed to be "exact" and so depletion-corrected. LIGAND is based on the program orginally written by Munson and Rodbard *(20)*. It incorporates the F-test and the runs test for goodness-of-fit. The disadvantage of these programs is that they are limited to predefined equations.

2.8.5. Spreadsheets

In principle, the fitting of binding equations can also be performed within spreadsheets such as EXCEL *(21)*. However, these lack the facilities associated with designer programs, such as GraFit, and represent a "halfway house" between these and the construction of a fitting package using routines from a mathematical subroutine library. They may have advantages of promoting the automation of routine data analysis and report generation.

2.8.6. Others

There are, of course, many other sources of fitting programs. Internet addresses for some of them are summarized in **Table 1**.

2.9. Equations for Data analysis

2.9.1. Introduction

All of the model equations given here are written in SigmaPlot 3.0 transform language, which is similar to BASIC. Note that any text appearing to the right of a semicolon is regarded as a comment. In some of the models, this facility is used to provide alternative methods of processing the equations to suit different experimental situations. The "iterations = 0" option is used for simulation of the equations with the parameters retaining their starting values. In some cases, these equations are presented with typical sets of initial esti-

Table 1
Internet Addresses for Graph Plotting and Data Analysis*

Product	URL
SigmaPlot	www.spss.com
Prism	www.graphpad.com
KELL	www.biosoft.com
Tecplot	www.amtec.com
Plotit	www.plotit.com
Axum	www.adeptscience.co.uk
UNISTAT	www.adeptscience.co.uk
EasyPlot	www.cherwell.com
pro Fit (for Mac)	www.cherwell.com
StatView	www.cherwell.com
MLAB	www.civilized.com
Scientist	www.micromath.com
DeltaGraph	www.deltapoint.com
Fig P	www.biosoft.com
Origin	www.microcal.com
SlideWrite Plus	www.slidewrite.com
Stanford Graphics	www.vni.com
Visual Data Analysis Tools	www.fortner.com
PSI Plot	www.polysoftware.com

*Most sites provide free demos.

mates, which need to be changed as appropriate. Note that in these equations the prefix P is used to indicate a logarithm to the base 10.

2.9.2. Radioligand Kinetics in the Presence of a Competitor

[Parameters]

k12 = 1E7; on-rate for radioligand
k21 = 1E-3; off-rate for radioligand
k13 = 1E7; on-rate for competing ligand
k31 = 1E3; off-rate for competing ligand
R0 = 1E-10; molar concentration of free binding sites
BGD = 1E-12; nonspecific background, as molar concentration

[Variables]

Y = col(1); total dpm bound, in this calculation
t = col(2); time, in seconds
w = 1(col(3)^2); calculate weight from SEM of measurements

[Equations]

SPACT = 85; specific activity of tracer
;R0 = 1E-10; can be fixed, or treated as an unset parameter
RL0 = 0; initial concentration of receptor-tracer complex
RA0 = 0; initial concentration of receptor-competitor complex
L = 3.5E-10; molar concentration of radioligand
A = 1E-4; molar concentration of competitor
k12L = k12*L
k13A = k13*A
KL = k12L/k21; calculate effective affinity constant of tracer
KA = k13A/k31; calculate effective affinity constant of competitor
RT =R0+RL0+RA0; conservation equation for competitor
RLE = KL*RT/(KL+KA+1); equilibrium concn. of receptor-tracer complex
c1 = k12L+k21+k13A+k31; set up equations
c2 = k21*k13A+k31*k12L+k31*k21
AA = (-c1+sqrt([c1*c1-4*c2]))/2; determine exponents
BB = (-c1-sqrt(c1*c1-4*c2))/2
DRL0 = k12L*R0-k21*RL0; calculate initial rate of binding
PA = (DRL0+BB*([RLE-RL0]))/(AA-BB); amplitudes of components
PB = (AA*([RL0-RLE])-DRL0)/(AA-BB)
RL = PA*exp(AA*t)+PB*exp(BB*t) + RLE; calculate solution
F = SPACT*2220*(RL+BGD)*1E9; the result is assumed to be in dpm
Fit F to Y with weight w

[Constraints]

[Options]

;iterations = 0

2.9.2.1. General Comments

This is the general model for binding of a tracer ligand to a receptor in the presence of an arbitrary concentration of a competing ligand. It is useful both for simulation and fitting of the results of kinetic experiments. Its only drawback is that it does not make allowance for the depletion of either of the two ligands. Its use should therefore be restricted to situations where ligand depletion is less than 10%. It should be noted that even when the population of binding sites is simple and homogeneous, the presence of a competing ligand will generally induce a biexponential association time-course, and that one of the two components will have a half-time that is determined by the slowest step in the kinetic system, commonly the dissociation rate of the tracer ligand. It is essential to realize this in the planning of binding experiments and to choose an incubation time that is sufficient to allow equilibrium to be achieved. *This should be at least five times the half-time of the slowest step.*

If the competing ligand is absent, the equations reduce to the simple monoexponential forms given in **Eqs. 9** and **10** of the introduction. These are readily linearized for display purposes, either by plotting

$$-\log_e(1-RL/RL_{eq}) \text{ vs } t \qquad \text{(association time-course)}$$

or by plotting

$$-\log_e RL \text{ vs } t \qquad \text{(dissociation time-course)}$$

If there are multiple populations of binding sites, the association or dissociation curves can be fitted to sums of exponential functions. These may incorporate both time-independent and time-dependent components of nonspecific binding. Such functions are provided within most commercially-available fitting programs, such as SigmaPlot or GraFit.

Tracer ligand dissociation can be induced by physical dilution (so that the tracer concentration falls to, say, 100-fold below its K_d), or, more practically, by the addition of a large excess of an unlabeled competing ligand; for instance, a concentration in excess of $100 \times K_d(1 + K^*[L^*])$, where K_d refers to the competitor, K* is the affinity constant of the tracer, and L^* its concentration. The aim is that the unlabeled competitor, which should *not* be the unlabeled tracer, unless displacement of nonspecific binding is known not to be a problem, will simply prevent rebinding of any tracer that dissociates.

2.9.2.2. Allosteric Modulation of the Dissociation Rate Constant

An important case occurs when the tracer ligand and an added allosteric agent bind to form a ternary complex. In this case, tracer dissociation occurs, in part, from the complex of the receptor with the unlabeled ligand. In the simplest case, the allosteric agent retains rapid kinetics in the presence of the tracer ligand and remains in equilibrium throughout the dissociation process. In the terms defined in **Fig. 2** of the introduction,

$$RL = RL_0\exp\{(-k_{21} + k'_{21}K'_A[A])/(1 + K'_A[A])\}.$$

Here, k_{21} is the dissociation rate constant of the tracer ligand from the free receptor, and k'_{21} the corresponding value for the complex of the allosteric ligand with the receptor. This value may be either larger or smaller than k_{21}.

RL_0 is the concentration of receptor-tracer complex at time zero. The significance of this equation is that it can be used to estimate a value for K'_A, the affinity of the allosteric agent for the receptor-tracer complex. It should be noted that it is still, in general, necessary to add a receptor-saturating concentration of a ligand that competes directly with the tracer, to ensure the absence of tracer rebinding.

2.9.3. One-Site Model of Radioligand Binding in the Presence of a Competing or Allosteric Ligand, Expressed in Terms of Total Radioligand Concentration

[Parameters]

PKL = 0.5; log10 affinity constant of tracer, expressed as nM^{-1}
PKA = -3; log10 affinity constant competitor, nM^{-1}
;PK1A = -5; $\log_{10}$ affinity constant, ternary complex formation
RT = 0.0026; total concn. of receptor binding sites, in nM
N = 0.0009; proportionality coefficient for nonspecific binding
BGD = 15; counter background

[Variables]

LTDPM = col(1); total tracer ligand concn., nM
A = col(2); concn. of competing or allosteric ligand, nM
DPMTOT = col(3); mean total bound dpm
W = 1/col(4)^2; calculate weight from SEMs of observations

[Equations]

SPACT = 85; specific activity of tracer ligand, Ci/mmole
;PKA = 1.0; fixed high value of PKA for definition of tracer NS
KL = 10^PKL
KA = 10^PKA
;K1A = 10^PK1A
LT = (LTDPM-BGD)/(2220*SPACT); calculate total ligand concn
KAPP = KL/(1 + KA*A); competitive interaction
;KAPP = KL*(1 + K1A*A)/(1 + KA*A); allosteric interaction
T1 = LT + RT + (1 + N)/KAPP; set up and solve equations
T2 = RT*LT
ROOT = SQRT(T1*T1 - 4*T2)
RL = (T1 - ROOT)/2; calculate concn. of receptor-ligand complex
L = (LT - RL)/(1 + N); calculate concn. of free ligand
BTOT = RL + N*L; calculate total binding
F = 2220*SPACT*BTOT + BGD; convert to DPM and add background
FIT F TO DPMTOT WITH WEIGHT W

[Constraints]

RT > 0
NS > 1E-5
BGD > 0

[Options]

stepsize = 1

• 2.9.3.1. General Comments

A common situation is that there is an element of depletion of the tracer ligand (which necessarily has high affinity for the receptor), but not of the competing ligand. As a rough guide, if $K[R_T] > 0.1$, the depletion of the tracer ligand will exceeed 10%. This set of equations is suitable for analyzing tracer binding under such conditions, provided that the the tracer is chemically and radiochemically pure. Formats include inhibition experiments or direct tracer saturation experiments. The latter requires the addition to the worksheet of data measured in the presence of a receptor-saturating concentration of the competing ligand and specification of the affinity constant of the ligand used to determine nonspecific binding. The total and nonspecific binding components are then fitted simultaneously. This is statistically preferable to an initial subtraction of nonspecific from total binding.

Provided that there is no significant (<10%) depletion, specific binding can be calculated for display purposes from the experimental data and the fitted points, with the aid of the transform presented in the **Subheading 2.9.3.2.**

The equations are readily adapted to fit allosteric interactions as well as strict competition. Note the expression of parameters in n*M* terms. This avoids the occurrence of very small numbers generated by the quadratic form of the equations.

2.9.3.2. Display and Plotting of Results of Saturation Binding Analysis, Assuming <10% Radioligand Depletion

```
I = ##; number of column containing tracer ligand concentrations
N = $$; number of observations, assumed equal for total and NS
RT = %%; fitted total receptor conc., fmol/ml
BGD = ££; background of scintillation counter
SPACT = &&; specific activity of tracer, Ci/mmol
LTMOL = (col(I,1,N)-BGD)*1e-9/(2220*SPACT); concn. of tracer ligand
LTLOG = log(LTMOL); log for display purposes
SPEC = col((I+2),1,N)-col((I+2),(N+1),(2*N)); calculate spec. binding
SPECMOL = SPEC*1000/(2220*SPACT); convert to fmol/ml
SPECFIT = col((I+4),1,N)-col((I+4),(N+1),(2*N))
FITMOL = SPECFIT*1000/(2220*SPACT); fmol/ml
SE = sqrt(col((I+3),1,N)^2+col((I+3),(N+1),(2*N))^2); SE of spec
SEMOL = SE*1000/(2220*SPACT)
col(I+10) = LTMOL
col(I+11) = LTLOG
col(I+12) = SPECMOL
col(I+13) = SEMOL
col(I+14) = FITMOL
```

col(I+15) = SPECMOL*100/RT; convert to occupancy by division by RT
col(I+16) = SEMOL*100/RT
col(I+17) = FITMOL*100/RT

2.9.3.3. Use of Transform

This transform assumes that the data are set out in adjacent worksheet columns, in the order total ligand, competing ligand, bound ligand, and SEM, and that in each column the values for total binding precede the values for nonspecific binding. There are options for plotting total binding, specific binding, or occupancy of the binding sites as a function of the ligand concentration or of the logarithm of the ligand concentration. The semilogarithmic occupancy-concentration plot is particularly useful for display purposes, because it allows the representation of binding curves with different affinity constants as a series of parallel, symmetrical, sigmoid curves whose position on the log concentration axis depends only on the affinity constant describing the curve. It also gives a clear visual indication of whether near-saturation of the binding sites has been achieved; 90% saturation requires a ligand concentration which is 10-fold higher than the K_d value, and this should be taken as a minimum requirement.

The standard method of linearizing saturation binding data for display purposes is by means of a *Scatchard plot,* in which the ratio of specifically bound to free ligand is plotted against the concentration of bound ligand (B/F vs B). In the simplest case, this yields a straight line whose slope is $-K$ (or $-1/K_d$), and whose intercept on the x-axis is the total concentration of binding sites. Deviations from linearity imply cooperativity. Plots that are convex upward, or even pass through a maximum, may indicate positive cooperativity, whereas plots that are concave upward may indicate negative cooperativity or heterogeneity of the binding sites. Alternatively, either situation can arise from the occurrence of binding artifacts ***(6)***. It should be noted that *fitting a straight line to a Scatchard plot does not give statistically acceptable estimates of binding parameters.* The error distribution is complex because of the transformation of the data. Also, the measured binding contributes to both the y and x coordinates of the points. Thus the experimental error is not confined to the y-axis, violating the basic assumption of least-squares fitting.

2.9.3.4. Binding Curves That Deviate from the Simple One-Site Model

If the fitted curves deviate significantly from the data points, then it is necessary to consider more complex models. These may be models in which the ligand binds to multiple independent classes of sites or cooperative models, in which negative or positive cooperativity occurs within an oligomeric structure.

There is little hope of being able to analyze these more complex situations under conditions of ligand depletion, which should thus be avoided. In the case of two independent classes of binding sites, the equation for bound ligand takes the form

$$BTOT = RT1*K1*L/(1+K1*L) + RT2*K2*L/(1+K2*L) + N*L$$

while in the case of homotropic cooperativity, the corresponding equation is

$$BTOT = RT*(K1*L+2*K2*L^2)/(1+ K1*L+K2*L^2) + N*L$$

The use of cooperative models of ligand binding has been extensively discussed by Wells *(6)*.

2.9.4. Analysis of Competition Curves by Means of the Hill Equation

[Parameters]

BSPEC = 1000
BNS = 100
PK = 6.0; $\log_{10}$ K (apparent affinity constant)
NH = 0.8; Hill coefficient (slope factor)

[Variables]

PA = col(1); $\log_{10}$ competing ligand concn
Y = col(2); bound dpm
W = 1/col(3)^2; column 3 contains the SEMs

[Equations]

K = 10^PK
A = 10^PA
F = BSPEC/(1+(K*A)^NH) +BNS
fit F to Y with weight W

[Constraints]

NH < 0.3

[Options]

2.9.4.1. General Comments

The Hill equation embodies the standard method of deriving empirical parameters, which can be used to describe a competition curve that deviates from the simple Langmuir isotherm, namely the log of the apparent affinity constant, K, and the Hill coefficient or slope factor, n_H. The use of these parameters is noncontroversial and provides a useful first-pass analysis of binding data, particularly when the molecular nature of the binding process is unknown. However, it should be realized that the apparent affinity constant derived from the Hill equation is not a true bimolecular binding constant.

Values of n_H that are less than 1.0 can indicate negative cooperativity between linked binding sites or receptor heterogeneity, either attributable to the existence of discrete receptor subpopulations or to the interaction of a homogenous population of receptors with other components, such as GTP binding proteins. Alternatively, they may arise from certain binding artifacts. Values of n_H greater than 1 may indicate the occurrence of positively cooperative interactions between successive molecules of the competing ligand or may reflect binding artifacts (*see* **Subheading 3.**).

2.9.5. Multisite Competition Model—No Depletion of Radioligand or Competing Ligand

```
[Parameters]
  BSPEC1 = 1000; specific binding for the three components
  BSPEC2 = 1000
  BSPEC3 = 1000
  BNS = 50; nonspecific binding
  PK1 = 6.0; log affinity constants for the three components
  PK2 = 4.0
  PK3 = 3.0

[Variables]
  PA = col(1)
  Y = col(2)
  W = 1/col(3)^2

[Equations]
  A = 10^PA
  K1 = 10^PK1
  K2 = 10^PK2
  K3 = 10^PK3
 F = BNS + BSPEC1/(1 + K1*A) + BSPEC2/(1+K2*A) + BSPEC3/(1+K3*A)
 FIT F TO Y WITH WEIGHT W
```

2.9.5.1. General Comments

These equations are readily adapted to one, two, or three-site analyses by "commenting out" one or more of the sites. No prior assumptions are made about the affinity of the tracer ligand for the various subpopulations. The K values obtained are therefore apparent values, and require to be corrected for the tracer ligand occupancy once the appropriate Cheng–Prusoff correction factors can be calculated. The use of these equations is rapid and convenient in situations in which ligand depletion is less than 10%.

2.9.6. Two-Site Competition Model of Binding, with Allowance for Depletion of the Radioligand, and Resulting Changes in Nonspecific Binding

[Parameters]

R1T = 0.004; concentration of site 1, expressed as nM
R2T = 0.01; concentration of site 2, expressed as nM
PKA1 = -0.5; log affinity of competitor, sites 1, as nM^{-1}
PKA2 = -1.5; log affinity of competitor, sites 2, as nM^{-1}
N = 0.003; coefficient of nonspecific binding
BGD = 15; counter background

[Variables]

PA = col(1); log concentration of competing ligand, nM
DPM = col(2)
W = 1/col(3)^2

[Equations]

SPACT = 48; radioligand specific activity
LT = 0.03906; total radioligand concentration, nM
PK1 = 1.8; radioligand affinity for site 1, log nM^{-1}
PK2 = 1.8; radioligand affinity for site 2, log nM^{-1}
K1 = 10^PK1; affinity of radioligand for site 1
K2 = 10^PK2; affinity of radioligand for site 2
KA1 = 10^PKA1; affinity of competitor for site 1
KA2 = 10^PKA2; affinity of competitor for site 2
A = 10^PA
T1 = 1+KA1*A
T2 = 1+KA2*A
T3 = K1*LT/(1 + N)
T4 = K2*LT/(1 + N)
T5 = K1*R1T/(1 + N)
T6 = K2*R2T/(1 + N)
T7 = T1+T3
T8 = T2+T4
a0 = T3*T4
a1 = -(T3*T8 + T4*T7 + T5*T4 + T3*T6)/3
a2 = (T7*T8 + T5*T8 + T5*T4 + T6*T7 + T3*T6)/3
a3 = -(T5*T8 + T6*T7)
HH = a0*a2 - a1*a1
GG = a0*a0*a3 - 3*a0*a1*a2+2*a1*a1*a1
DISC = GG*GG + 4*HH*HH*HH
RCOMP = SQRT(GG*GG/4 - DISC/4)
THETA = ACOS(GG/(2.0*RCOMP))
CUBR = SQRT(-HH)

ROOT1= -2*CUBR*COS(THETA/3); the solution is the root of a cubic
DELTA = (ROOT1 - a1)/a0
RL = LT*DELTA
L = (LT-RL)/(1 + N); concn. of free ligand
BOUND = RL + N*L; total binding
F = BOUND*SPACT*2220 + BGD; conversion to dpm
Fit F to DPM with weight W

[Constraints]

[Options]

2.9.6.1. General Comments

This set of equations can be used to analyze two-site competition curves when radioligand depletion exceeds 10%, provided that the radioligand is chemically and radiochemically pure and of known specific activity. Ideally, a set of competition curves should be performed at a series of different radioligand concentrations that span (from 0.1 to 10x) its K_d. Analysis of such a data set will provide the log K values for the radioligand and competitor at both classes of binding sites and is a stringent test of the adequacy of the competitive binding model. The potential for rebinding radioligand displaced from one set of sites to the other, unoccupied sites leads to a cubic equation, which is solved using complex algebra. Because of the potential for generating very small numbers, affinity constants, and concentrations have been expressed in nanomolar units. They can be rescaled as appropriate. The complexity of these equations illustrates why depletion should be avoided.

2.9.7. Ternary Complex Model of Ligand Competition, Normalized by Division by Total Concentration of Receptor Sites

[Parameters]
PK = 5.0; affinity of competitor for free receptor, log M
PKT = 6.0; apparent high affinity binding constant, log M
GTrt = 0.5; ratio of total G protein to total receptor
BSPEC = 1000; specific tracer binding
BNS = 50; nonspecific binding

[Variables]
PA = col(1); competitor concentration, log M
Y = col(2)
W = 1/col(3)^2

[Equations]
PKGRT = -4; log(KG*RT) is a measure of precoupling
;GTrt = 0.382; fix this ratio if necessary

```
A = 10^PA
K = 10^PK
KT = 10^PKT
KGRT = 10^PKGRT
T1 = 1 + K*A
T2 = KGRT+KT*A
TEMP1 = T1*T2
TEMP2 = (GTrt - 1)*T2 + T1
F1 = - TEMP2 + SQRT(TEMP2*TEMP2 + 4*TEMP1)
Rrt = F1/(2.0*TEMP1); ratio of free R to total R
RGrt = Rrt*GTrt*KGRT/(1 + Rrt*T2); ratio of RG complex to total R
F = (Rrt + RGrt)*BSPEC + BNS; both R and RG are assumed to bind
Fit F to Y with weight W
```

[Constraints]

[Options]

```
;iterations = 0
```

2.9.7.1. General Comments

This is the ternary complex version of the two-site model, in which a single receptor binds to a single G protein, governed by an affinity constant KG. The agonist has different affinities for the free receptor (K) and the receptor-G protein complex (K1). Such a model leads to the appearance of multiple binding sites, provided that the effective concentration of receptor is equal to or greater than the effective concentration of G protein. The key parameters in describing the behavior of this system are K, the affinity of the agonist for the free receptor, Gt/Rt, the ratio of G protein to receptor, KT, a composite parameter corresponding to the product KG*K1*RT, governing the induction of the high affinity ternary complex, and KG*RT, which governs the degree of precoupling of the receptor to the G protein *(22)*. Thus K and KT are the equivalents of low (K) and high (KH) affinity agonist binding constants derived from a two-site analysis. Numerically, the values obtained are very similar for the two methods of analysis. However, there is a key mechanistic difference, which is that KT is *not* a bimolecular binding constant, but reflects a trimolecular process in which both the agonist and the G protein participate. Unlike KH, KT depends on the level of expression of the receptor.

In this formulation, the binding of the agonist reduces the availability of free receptor and the RG complex, both of which are assumed to be labeled by the radiotracer with equal affinities. The apparent afinity constants K and KT have to be corrected for the Cheng–Prusoff shift. If the RG complex is not labeled

by the radiotracer, the contribution from RG can be edited out. This model can be extended to cover the case of one receptor interacting with two populations of G proteins, although the algebra becomes more complex, once again involving a cubic equation. The solution to this problem is available on request.

2.9.8. Analysis of Dose-Response Curves Using the Logistic Equation

[Parameters]
PK = 7.0; log K = - Log(EC_{50})
NH = 1.0; Slope factor
RMAX = 1000; maximum stimulated response
BASAL = 400; basal signal

[Variables]
PA = col(1)
Y = col(2)
W = 1/col(3)^2

[Equations]
A = 10^PA
K = 10^PK
KXN = (K*A)^NH
F = KXN*RMAX/(1 + KXN) + BASAL
FIT F TO Y WITH WEIGHT W

[Constraints]

[Options]

2.9.8.1. General Comments

In certain instances, binding assays can be used to assess receptor function; for instance, by agonist stimulation of the binding of a radiolabeled guanine nucleotide to a coupled G protein ***(15)***. In this case (as is usually the case in functional assays in whole cells), the signal is an increasing function of the agonist concentration. An empirical analysis of such a dose-response curve can be performed with a four-parameter logistic function (essentially the same as a Hill plot), which will provide an apparent affinity K (–log EC_{50}), a slope factor (NH), as well as estimates of the basal and maximum stimulated responses. The above equation can be combined with the Schild equation for the analysis of agonist dose-response curves in the presence of increasing concentrations of an antagonist. This allows a semi-empirical analysis of the competition between agonists and antagonists to be carried out in a compact and convenient experimental design ***(16)***.

2.9.9. Ternary Complex Direct Agonist Binding Model, Normalized by Division by Total G Protein Concentration

```
[Parameters]
  PK = 4.0; Affinity of agonist for free receptor, log M
  PKG1GT = 1; log(KG1*GT). KG1 is the affinity of G for AR complex
  RTgt = 10; Total receptor/total G protein
  RMAX = 1000
  BASAL = 50

[Variables]
  PA = col(1)
  Y = col(2)
  W = 1/col(3)^2

[Equations]
  PKGGT = -1; Log (KG*GT). KG is the affinity of G for free R
  ;RTgt = 10; fix this if necessary
  ;PK = ##; specify this value if necessary
  K = 10^PK
  KG1GT = 10^PKG1GT
  KGGT = 10^PKGGT
  A = 10^PA
  T2 = 1+KGGT/(K*KG1GT*A)
  TEMP2 = RTgt/T2+1/T2+(1+1/(K*A))/(KG1GT*T2^2)
  TEMP1 = RTgt/(T2^2)
  ARGgt = (TEMP2-SQRT(TEMP2*TEMP2-4*TEMP1))/2.0
  RGgt = ARGgt*(T2-1)
  F = (ARGgt+RGgt)*RMAX + BASAL
  fit F to Y with weight W

[Constraints]

[Options]
  ;iterations = 0
```

2.9.9.1. General Comments

This model calculates the ratio of the sum of the agonist-induced and precoupled receptor-G protein complexes to the concentration of G protein. Assuming that these have equal catalytic activities, this can be taken as a measure of the receptor-induced response. The parameters characterizing this model are K, the affinity of the agonist for the free receptor, RT/GT, the concentration ratio of receptor to accessible G protein, KG*GT, which is a measure of precoupling in the absence of agonist, and KG1*GT, which can be taken as a measure of agonist efficacy. One way to use this model is to employ

an estimate of K taken from a binding study and then to use the equations to calculate KG1*GT, subject to an assumption about the value of the ratio RT/GT *(23)*. The latter may be estimated from the extent to which the agonist dose-response curve can be right-shifted by reduction of the concentration of functional receptors before the maximum response is depressed. The agonist-independent activity attributable to precoupling of receptor and G protein can be assessed by measuring the ability of an antagonist to depress the basal response in the absence of agonist. It is often possible to assume that there is essentially no precoupling between receptor and G protein (KG = 0; T2 = 1 in the above equations). By using a set of columns containing "switch" variables consisting of blocks of 1's or zeros to multiply the column containing the primary data, and thus pick out different individual data sets, it is possible to analyse simultaneously a set of dose-response curves acquired after different extents of receptor expression (or blockade). This allows the estimation of the global values of K and KG1*GT, as well as the values of RT/GT appropriate to each data set.

2.9.10. Calculation of Nearest-Neighbor Correlation Coefficient, and Fishers t-statistic.

```
n = ££; insert the number of weighted residuals
i = ##; the data start in column i
stdev1 = stddev(col(i)); col i contains residuals 1,2,3..n - 1
stdev2 = stddev(col(i + 1)); col i + 1 contains residuals 2,3,4...n
me1 = mean(col(i))
me2 = mean(col(i + 1))
col(i + 2) = (col(i) - me1)*(col(i + 1) - me2)
cov = mean(col(i + 2))
correl = cov/(stdev1*stdev2); calculate the correlation coefficient¬
put correl into col(i + 3,1); Calculate NNRC
t = correl*sqrt((n - 3)/(1 - correl*correl)); Fisher's t-statistic
put t into col(i + 3,3); t has n - 3 degrees of freedom
```

2.9.10.1. General Comments

This transform calculates the value of the nearest-neighbor correlation coefficient of the residuals and the value of Fishers t-statistic, which can be tested for significance at n-3 degrees of freedom, where n is the number of data points included in the calculation. A value of $p < 0.05$ indicates that the model probably deviates significantly from the fitted data. The residuals used in the calculation are the weighted residuals derived from the fit.

2.9.11. F-Test for Significance of Improvement of Fit

```
i = ##; column i contains the weighted residuals from fit 1
j = $$; column j contains the weighted residuals from fit 2
```

```
df1 = ££; degrees of freedom fit 1
df2 = ??; degrees of freedom, fit 2
col(i + 1) = col(i)*col(i)
ss1 = total(col(i + 1)); residual sum of squares, fit 1
col(j + 1) = col(j)*col(j)
ss2 = total(col(j + 1)); residual sum of squares, fit 2
F = (ss1 - ss2)*df2/((df1 - df2)*ss2); calculate F
put F into col(j + 2)
```

2.9.11.1. General Comments

This is a test of the hypothesis that using a model of increased complexity provides a significant improvement in the quality of the fit. The value of F can be looked up in standard tables, using degrees of freedom corresponding to $df1$-$df2$, $df2$. A value of $p > 0.05$ indicates that the more complex model is not supported by the data.

3. Notes

3.1. Avoiding Problems in Binding Studies

A large number of potential problems afflict receptor binding studies. They fall under five major headings: inadequate experimental design, inadequate analysis, procedural problems, ligand impurity or instability, and problems associated with the receptor preparation. The more obvious problems are readily avoided by carrying out a series of ranging experiments to determine the best assay conditions. Others are more insidious. A full discussion of binding problems is given by Hulme and Birdsall *(1)*. The survey given here concentrates mostly on the problems that are fully within the control of the experimenter.

3.2. Inadequate Experimental Design

3.2.1. Failure to Achieve Equilibrium

In setting up a new binding assay, it is essential to perform measurements of tracer ligand association and dissociation early on. These should be done at both subsaturating and near receptor-saturating concentrations of the ligand and in the absence and presence of the competitors or modulators of interest.

The incubation time necessary to allow a ligand association or dissociation reaction to achieve 97% of its final equilibrium value under all conditions is five times the half-time of the slowest dissociation process in the system. Thus, while the tracer ligand alone may equilibrate rapidly under the conditions of the experiment, this cannot be assumed to remain the case in the presence of competitors, or modulators. If the interaction between the tracer and the addi-

tional ligand is strictly competitive, the minimum incubation time used in equilibrium binding experiments should be at least five times the dissociation half-time of the slower of the two ligands. Normally, this will be the tracer, which will necessarily have high affinity for the receptor. Thus, it is essential to estimate the dissociation rate constant of the tracer ligand. Ideally, this should be done by pre-equilbrating the receptor with several concentrations of tracer ligand, spanning its K_d (0.1-10 × K_d), and then initiating dissociation by addition of a strict competitor at a concentration sufficient to saturate the receptor in the presence of the tracer. This can be computed as $100 \times Kd(1+[L^*]/K_d^*)$, where K_d refers to the competitor and K_d^* to the tracer. Experiments of this kind, carried out at a range of different concentrations of competing or modulating ligands, may also give an indication of whether their interaction with the tracer has an allosteric component.

Having defined a minimum incubation time, experiments should be performed that extend this by two- or threefold in order to check its adequacy, particularly in the presence of concentrations of competitors or modulators that have a substantial effect on binding.

Failure to attain equilibrium in a binding experiment can distort both saturation binding and competition measurements, leading to errors in the estimation of binding constants (both over- and underestimation of affinity are possible, depending on the kinetics of tracer and competitor), in the concentrations of binding sites, and to spurious apparent positive cooperativity. Further details are given by Hulme and Birdsall *(1)*.

Other factors can also be responsible for failure to achieve a steady-state in binding experiments. These can include receptor instability, which leads to binding that peaks and then diminishes with time, or receptor occlusion (often a result of the presence of sealed membrane vesicles), which can lead to upward "creep," after the initial phase of the binding reaction is complete. These phenomena are considered further in **Subheading 3.6.**

3.2.2. Ligand Depletion

Ligand depletion (normally more of a potential problem in the case of the tracer) occurs when a significant fraction of the ligand becomes receptor-bound. Some assay methods, for instance, equilibrium dialysis and equilibrium gel-filtration, rely on this phenomenon to produce a signal. Under more routine assay conditions, for instance, in membrane filtration assays, undetected ligand depletion can seriously distort the analysis of ligand saturation and competition assays.

To avoid distortion of binding assays, the aim should be to hold ligand depletion to less than 10%. The important factors to consider are the affinities

of the ligand(s) and the total concentrations of ligands and receptor binding sites.

Depletion problems are most acute at low levels of receptor saturation. Depletion of a subsaturating concentration of a single ligand, say the tracer in the absence of competitors, will exceed 10% if $K[R_t] > 0.1$. Thus, when working at ligand concentrations below the K_d, it is desirable to keep the concentration of receptor binding sites below $0.1 \times K_d$. Here K_d refers to the ligand of highest affinity, normally the tracer. This concentration may, however, be too low to generate an adequate signal in the binding assay.

There are two options. One is to increase the total volume of the assay, so that a greater number of binding sites are harvested. This may not always be practical. The other is to use a higher ligand concentration. Working at a higher degree of receptor saturation both increases the signal and diminishes depletion (for instance, at $10 \times K_d$, depletion is approximately 10% of its value below the K_d). However, the ratio of specific:nonspecific binding is also decreased, and ligand inhibition curves are subject to larger corrections for tracer occupancy. Thus, one has to be certain of the mechanism of interaction in order to apply appropriate corrections. It is sound advice to perform inhibition experiments at different degrees of receptor saturation in order to attempt to ascertain or confirm mechanisms, at least in key instances.

Depletion artifacts can have serious consequences for competition curves *(24,25)*. In the case of a simple competitive interaction, it produces a right-shift equivalent to $D/(1\text{-}D)$, where D is the fractional depletion of the tracer in the absence of competitor *(1)*, which is additive with the Cheng–Prusoff shift. In the case of multisite competition curves, the effect of depletion is to cause underestimation of the relative fraction of the high affinity sites *(1)*. This is because the low-affinity binding sites buffer the tracer displaced from the high-affinity sites. Working under depletion conditions introduces additional nonlinearities into the binding interactions and should be avoided. While depletion of up to 30% may be correctable under ideal circumstances using the equations given above, for instance, when the tracer ligand is chemically and radiochemically pure, and its binding characteristics have been properly defined, it may be assumed that depletion in excess of 50% will invalidate the experiment. A knowledgeable referee can be expected to question data which are obtained under such conditions. A particularly insidious hazard may be "unseen" depletion, caused by partitioning of a hydrophobic ligand into membranes, which then washes out during the wash phase of a filtration assay, and so remains undetected. If this is suspected, centrifugation of the assay mixture and sampling of the supernatant without washing may be diagnostic.

3.3. Procedural Inadequacies

3.3.1. Separation Problems

Many of the routine methods for the performance of ligand binding assays such as rapid filtration, or centrifugation, are reliant on the physical separation of receptor-bound from free ligand, followed by measurement of one or both components. Such separations may either be incomplete, or subject to losses. Other methods, such as the scintillation proximity assay, surface plasmon resonance, and fluorescence assays are not subject to these particular hazards, but present problems of their own *(26)*.

3.3.2. Incomplete Recovery and Losses of Bound Ligand

These may be caused by physical losses or by dissociation of bound ligand during the washing procedure. Avoidance of such problems requires optimization of the assay, for instance, by choosing an appropriate filter to retain the particles under investigation, and by choosing conditions that retard dissociation during washing, for instance, by precooling the filters, by using ice-cold buffer washes, by varying the ionic conditions, or by the addition to the wash buffer of allosteric modulators that slow dissociation. Dissociation during washing should be assessed by varying the number of washes or the total wash time. The adequacy of recovery can also be checked by ultracentrifugation of the assay mix at 100,000*g* for 1 h, followed by counting of the membrane pellet. Losses of radioligand during washing procedures should ideally be held to less than 10%. As a rough guide, for simple bimolecular association process with association rate constants of approx 10^7 $M^{-1}s^{-1}$ at 30°C (they may be slower, but are unlikely to be much faster), the time taken for dissociation of 10% of the radioligand can be calculated as $10^{-8} \times K$ where K is the affinity constant. For instance, a receptor-ligand complex with a dissociation constant of 10^{-8} will lose 10% of its bound radioactivity in 1 s. Cooling of the filter and wash buffer may still extend this time sufficiently to make a filtration assay a feasible procedure, but, this is close to the lower limit of affinity for this procedure. Other assay methods, which do not disturb the equilibrium, may be more appropriate.

3.3.3. Nonspecific Binding of Ligands to Components of the Assay System

Ligands may bind to assay tubes or pipet tips. This can cause depletion artifacts. Appropriate pretreatment of tubes (e.g., by siliconization), or additions to assay buffers (e.g., of carrier proteins or peptides) may help to prevent such

occurrences. Ligands may also bind nonspecfically to filters, sometimes in a displaceable manner. This can simulate the appearence of a low-affinity, high-capacity class of binding sites. A common maneuver is to presoak glass fiber filters with 0.1% polyethylene imine in deionized water (60 min is enough) before placing them in the filtration apparatus and prewashing with cold buffer. This minimizes the nonspecific binding of cationic ligands and may help to retain small membrane fragments through interaction with sialic acid moieties. Of course, it should not be used if the ligand is anionic (e.g., GTPγS)! Carrying out the pretreatment at 4°C minimizes effects on the physical structure of the filters.

3.3.4. Improper Definition of Nonspecific Binding

It is essential to estimate nonspecific binding accurately. This is best done by the inclusion in the assays of a high-affinity, receptor-specific ligand, preferably having a chemical structure as different as the pharmacology allows from that of the tracer, at a concentration that is sufficient to inhibit more than 99% of the receptor-specific binding of the tracer, namely $100 \times K_d[L](1 + [L^*]/K_d^*)$. Preferably, several ligands belonging to distinct structural classes should yield convergent estimates of nonspecific binding. In general, it cannot be regarded as safe practice to use a standard (e.g., 100-fold) excess of the unlabeled version of the tracer ligand to define specific binding, since nonreceptor binding may also be inhibited. Inclusion of part of the nonspecific binding within the apparently specific component can lead to the identification of a spurious class of receptor sites. The accurate estimation of nonspecific binding is also essential in the identification of negatively cooperative mechanisms of ligand interaction, in which inhibition of tracer binding may plateau at a level close to, but not exactly equal to, 100%. The difference may be very small but may still indicate an entirely different binding mode from that employed by the tracer ligand *(27)*.

3.4. Analytical Errors

3.4.1. Use of an Inappropriate Model of Binding

This is a very difficult area. Occam's Razor is the essential tool. The simplest model compatible with the data is the one to use. If that turns out to be a single-site competition or allosteric interaction model, then at least the affinity constants derived should represent bimolecular binding constants. In more complex case, particularly in the case of "flat" agonist binding curves, one is initially advised to use an empirical model, such as the Hill equation. More complex models should be based on what is known about the molecular mecha-

nism of the system, and the parameters derived from them should not be overinterpreted.

A particular problem is the detection of a low-affinity population of binding sites, which has a similar abundance to the high-affinity population readily detectable by direct tracer binding *(28)*. It is normally not possible to extend the direct tracer saturation curve over a range sufficient to detect such a population, which is anyway likely to be obscured by the decreasing specific:nonspecific ratio. In unlabeled vs labeled tracer competition curves, the apparent affinity for the high-affinity population moves closer and closer to that of the low-affinity population as the tracer concentration is increased, because of the Cheng–Prusoff shift. The only advice that can be given is to perform unlabeled vs labeled ligand competition experiments at a series of tracer concentrations and to look for any correlation of the calculated K value of the competitor and the tracer concentration. If such a correlation exists, the complexity of the binding model may need to be increased.

3.5. Ligand Problems

A variety of binding artifacts can arise from uncertainties associated with the ligands used in them, particularly the tracer ligand. The main flavors are ligand impurity, incorrect specific activity, and ligand instability and losses, which may be intrinsic or engendered by interaction with the receptor preparation; for instance, by enzymic degradation.

Artifacts of this nature may not be easy to detect. The main advice that can be offered is first to always follow the manufacturer's instructions in the handling of ligands. Let radiochemicals warm to room temperature before opening them, to avoid the condensation of water vapor. Chemical and radiochemical purity can be checked, if necessary, by TLC or HPLC procedures, usually provided by the manufacturer with the ligand data sheet. The purity of a ligand can also be checked by measuring its "bindability," that is, the fraction capable of being receptor-bound. Provided that the affinity of the receptor-ligand interaction is sufficiently high, this is done by titrating a fixed concentration of the ligand with increasing concentrations of receptor. Of course, nonspecific binding has to be taken into account in this process. Details are given by Hulme and Birdsall *(1)*. A particular point to be aware of is that many radioligands are sold as pure enantiomers, and that these can gradually racemize over the course of time, reducing the bindability. Impurities become a particularly serious problem in situtations under which there is radioligand depletion, which will only apply to the bindable component, and will distort the estimation of free ligand concentration, which is implicit even in the equations given in this chapter.

Measurements of bindability do not address the question of specific activity. This can be checked by comparing estimates of ligand affinity from direct tracer saturation binding curves with those from cold vs hot inhibition curves, provided that the affinity of the ligand has not been altered by the labeling process *(29)*. The two estimates should then agree within experimental error. If more than one tracer ligand is available, binding capacity estimates using the different ligands can be compared and should be in reasonable agreement. Ligand metabolism can be retarded by the use of specific enzyme inhibitors *(1)*. Detailed guidelines on this depend on the nature of the ligand and the system in which it is being employed. Degradation of the ligand under the conditions of the assay is easy to detect by TLC or HPLC methods or by measuring the ability of an aliquot of ligand that has been incubated with the receptor preparation and then separated to bind to a subsequent batch of receptor.

3.6. Receptor Preparation

Artifacts attributable to the nature of the receptor preparation itself include receptor instability, the occlusion of binding sites, and contamination with endogenous ligands/modulators, which may interfere with binding.

Receptor instability can become a severe problem during the long incubations that are necessary to achieve equilibrium with high-affinity ligands and should be suspected if specific binding peaks and then diminishes over time. A check for instability is to incubate an aliquot of the receptor preparation in the absence of ligands and then check its binding activity as a function of time. The main source of receptor instability is proteolysis, and proteolytic inhibitors appropriate to the receptor preparation under investigation should be tried. The Calbiochem and Boehringer catalogues are good sources of advice on this issue, providing inhibitor cocktails for different sources. More details are given in *(1)*.

The occlusion of binding sites is a frequent phenomenon in membrane preparations and arises from the generation of inside-out vesicles. The phenomenon can sometimes be diagnosed if a greater concentration of receptor sites is detected using a nonpolar ligand, which can penetrate closed vesicles, rather than a polar ligand, which is excluded. If such phenomena are detected, it may be possible to permeabilize vesicles with agents such as saponin (0.01–0.1%), although it should be realized that permeabilizing agents are surface-active and may perturb features of receptor-effector coupling in unanticipated ways.

A somewhat related problem is the presence in tissue preparations of transmitters or other substances that may bind to the receptors and obscure features of their binding behavior. A particularly good example is that of the A_1 adenosine receptor, in which endogenous vesicular adenosine leaks out, and partially occupies the high-affinity G protein-coupled sites, leading to the

appearence of GTP-sensitive antagonist binding. This problem is ameliorated by the addition of a specific enzyme, adenosine deaminase, which metabolizes the transmitter in combination with a permeabilizing agent *(30)*.

References

1. Hulme, E. C. and Birdsall, N. J. M. (1992) Strategy and tactics in receptor-binding studies, in *Receptor-Ligand Interactions, A Practical Approach* (Hulme, E. C., ed.) IRL, Oxford, U.K., pp. 63–176.
2. Samama, P., Cotecchia, S., Costa, T., and Lefkowitz, R. J. (1993) A mutation-induced activated state of the β_2-adrenergic receptor: Extending the ternary complex model. *J. Biol. Chem.* **268,** 4625–4636.
3. Lazareno, S. and Birdsall, N. J. M. (1995) Detection, quantitation and verification of allosteric interactions of agents with labelled and unlabelled ligands at G protein-coupled receptors: Interactions of strychnine and acetylcholine at muscarinic receptors. *Mol. Pharmacol.* **48,** 362–378.
4. Birdsall, N. J. M., Farries, T., Gharagozloo, P., Kobayashi, S., Kuonen, D., Lazareno, S., et al. (1997) Selective allosteric enhancement of the binding and actions of acetylcholine at muscarinic receptor subtypes. *Life Sci.* **60,** 1047–1052.
5. Onaran, H. O., Costa, T., and Rodbard, D. (1992) $\beta\gamma$ subunits of guanine nucleotide binding proteins and regulation of spontaneous receptor activity: Thermodynamic model for the interaction between receptors and guanine nucleotide-binding protein subunits. *Mol. Pharmacol.* **43,** 245–256.
6. Wells, J. W. W. (1992) Analysis and interpretation of binding at equilibrium, in *Receptor-Ligand Interactions, A Practical Approach* (Hulme, E. C., ed.) IRL, Oxford, U.K.
7. Prinz, H. and Maelicke, A. (1992) Ligand binding to the membrane-bound acetylcholine receptor from Torpedo marmorata: a complete mathematical analysis. *Biochem.* **31,** 6728–6738.
8. Lemmon, M. A. and Schlessinger, J. (1994) Regulation of signal transduction and signal diversity by receptor oligomerization. *Trends Biochem. Sci.* **19,** 459–463.
9. Costa, T., Ogino, Y., Munson, P. J., Onaran, H. O., and Rodbard, D. (1992) Drug efficacy at guanine nucleotide-binding regulatory protein-linked receptors: thermodynamic interpretation of negative antagonism and of receptor activity in the absence of ligand. *Mol. Pharmacol.* **41,** 549–560.
10. Wreggett, K. A. and Wells, J. W. (1995) Cooperativity manifest in the binding properties of purified cardiac muscarinic receptors. *J. Biol. Chem.* **270,** 22,488–22,499.
11. Neubig, R. R. (1994) Membrane organisation in G protein mechanisms. *FASEB J.* **8,** 939–946.
12. Hebert, T. E., Moffet, S., Morello, J. P., Loisel, T. P., Bichet, D. G., Barrett, C., and Bouvier, M. (1996) A peptide derived from a β2-adrenergic receptor transmembrane domain inhibits both receptor dimerization and activation. *J. Biol. Chem.* **271,** 16,384–16,392.

13. Hirschberg, B. T. and Schimerlik, M. I. (1994) A kinetic model for oxotremorine M binding to recombinant porcine m2 muscarinic receptors expressed in Chinese hamster ovary cells. *J. Biol. Chem.* **269,** 26,127–26,135.
14. Maggio, R., Barbier, P., Fornai, F., and Corsini, G. U. (1996) Functional role of the third cytoplasmic loop in muscarinic receptor dimerization. *J. Biol. Chem.* **271,** 31,055–31,060.
15. Lazareno, S., Farries, T., and Birdsall, N. J. M. (1993) Pharmacological characterisation of guanine nucleotide exchange reactions in membranes from CHO cells stably transfected with human muscarinic receptors M1-M4. *Life Sci.* **52,** 449–456.
16. Lazareno, S. and Birdsall, N. J. M. (1993) Pharmacological characterization of acetylcholine-stimulated [^{35}S]GTPγS binding mediated by human muscarinic m1-m4 receptors: antagonist studies. *Br. J. Pharmacol.* **109,** 1120–1127.
17. Cheng, Y. C. and Prusoff, W. H. (1973) Relationship between the inhibition constant (K_I) and the concentration of inhibitor which causes 50 per cent inhibition (I_{50}) of an enzymatic reaction. *Biochem. Pharmacol.* **22,** 3099–3108.
18. Mosteller, F. and Tukey, J. W. (1977) *Data Analysis and Regression*, Addison-Wesley, Reading, MA.
19. Leatherbarrow, R. J. (1992) GraFit Version 3.0, Erithacus Software Ltd., Staines, U.K.
20. Munson, P. J. and Rodbard, D. (1980) LIGAND: a versatile computerised approach for characterization of ligand-binding systems. *Anal. Biochem.* **107,** 220–239.
21. Bowen, W. P. and Jerman, J. C. (1995) Nonlinear regression using spreadsheets. *Trends Pharmacol. Sci.* **16,** 413–417.
22. Page, K. M., Curtis, C. A. M., Jones, P. G., and Hulme, E. C. (1995) The functional role of the binding site aspartate in muscarinic acetylcholine receptors, probed by site-directed mutagenesis. *Eur. J. Mol. Pharmacol.* **289,** 429–437.
23. Lu, Z.-L., Curtis, C. A., Jones, P. G., Pavia, J., and Hulme, E. C. (1996) The role of the aspartate-arginine-tyrosine triad in the m1 muscarinic receptor: mutations of aspartate 122 and tyrosine 124 decrease receptor expression but do not abolish signalling. *Mol. Pharmacol.* **51,** 234–241.
24. Wells, J. W., Birdsall, N. J. M., Burgen, A. S. V., and Hulme, E. C. (1980) Competitive binding studies with multiple sites: effects arising from depletion of the free radioligand. *Biochim. Biophys. Acta* **632,** 464–469.
25. Goldstein, A. and Barrett, R. W. (1987) Ligand dissociation constants from competition binding assays—errors associated with ligand depletion. *Mol. Pharmacol.* **31,** 603–609.
26. Schuck, P. and Minton, A. P. (1996) Kinetic analysis of biosensor data: elementary tests for self-consistency. *Trends Biochem. Sci.* **21,** 458–460.
27. Birdsall, N. J. M., Burgen, A. S. V., Hulme, E. C., Stockton, J. M., and Zigmond, M. J. (1983) The effect of McN-A-343 on muscarinic receptors in the cerebral cortex and heart. *Br. J. Pharmacol.* **78,** 257–259.

28. Swillens, S., Waelbroeck, M., and Champeil, P. (1995) Does a radiolabelled ligand bind to a homogeneous population of non-interacting receptor sites? *Trends Pharmacol. Sci.* **16,** 151–155.
29. Segel, I. H. (1994) The effects of labeled and unlabeled impurities on the analysis of equilibrium binding and initial velocity data by means of Scatchard plots. *J. Theoret. Biol.* **171,** 267–280.
30. Cohen, F. R., Lazareno, S., and Birdsall, N. J. M. (1996) The affinity of adenosine for the high- and low-affinity states of the human adenosine A1 receptor. *Eur. J. Pharmacol.* **309,** 111–114.

10

Definition of Receptors in Radioligand-Binding Experiments

Mary Keen

1. Introduction

The fundamental purpose of radioligand-binding experiments is to study the binding of drugs to receptors. Thus, a key question to be addressed is whether or not the binding site detected in the experiment really corresponds to the receptor of interest. However, the identification of binding sites as receptors is by no means a simple problem and is one that has dogged binding studies from their inception. The essence of the problem is this: the definition of a receptor is functional—drugs bind to receptors and produce a response. However, no response is measured in binding experiments.

2. Specific Binding

The everyday definition of receptor binding used in radioligand-binding experiments is that of "specific binding," i.e., that proportion of the binding of the radioligand that can be inhibited or displaced by an unlabeled compound known to bind to the receptor of interest. It is necessary to determine specific binding in all radioligand-binding experiments, because even the best radioligands do not bind solely to the receptor of interest; some binding will occur as a result of a nonspecific association of radioligand with the lipid membrane, the filter, the assay tube, and so forth. However, the observation that binding is displaceable is not sufficient to conclude that compounds bind to a receptor, let alone to the particular receptor of interest.

Displaceable binding suggests that the ligand is binding to a finite number of sites in a reversible fashion (*see* **Note 1**). This is characteristic of ligands binding to receptors but is, of course, not limited to receptor sites. Exactly the

From: *Methods in Molecular Biology, Vol. 106: Receptor Binding Techniques*
Edited by: Mary Keen © Humana Press Inc., Totowa, NJ

same characteristics would be expected if the drug were binding to an enzyme or uptake site, for instance; indeed, this can be exploited to study these types of molecules using the binding assay technique (*see* Chapters 11–13, for example). However, there are also many instances of displaceable binding of radioligands to filters, tubes, cell culture plates *(1)*, and so forth so the existence of "specific binding" is not necessarily indicative of a biological system, let alone a receptor.

What is the best ligand to use to define nonspecific binding? The use of a ligand that is structurally dissimilar to the radioligand should minimize the risk of the two ligands binding to the same enzymes or uptake sites, and so on, but in some cases, only one ligand (e.g., the natural agonist) or a few structural analogs, are available. Cost may also be a factor, as relatively high concentrations of the competing ligand are required to suppress binding of the radioligand to all of the receptors.

3. Does Specific Binding Correspond to Receptor Binding?

Various criteria can be employed in an attempt to determine whether the specific binding detected in a binding experiment really represents binding to a receptor.

3.1. Binding Characteristics

Clearly, the binding ought to fulfill the usual criteria expected of receptors; binding should be saturable and reversible (which is implicit in the definition of specific binding), stereoselective, and of high affinity. However, all of these characteristics can also apply perfectly well to binding to other sites, such as enzymes.

Simple receptor theory suggests that receptor binding will exhibit "mass action" kinetics, whereby the binding of the ligand to the receptor (R) is governed by the concentration of the ligand ([*L*]), its association and dissociation rate constants (k_{+1} and k_{-1}, respectively), and the total number of receptors ([R_T]) as follows:

$$L + R \underset{k_{-1}}{\overset{k_{+1}}{\rightleftharpoons}} LR$$

at equilibrium,

$$\frac{[L][R]}{[LR]} = \frac{k_{-1}}{k_{+1}} = K_D \text{ and } [LR] = [R_T]\frac{[L]}{[L] + K_D}$$

While these assumptions about the nature of the ligand-receptor interaction seem eminently reasonable, their slavish application to the results of binding

experiments can, under certain circumstances, present something of a problem. Equilibrium binding curves indicative of a single population of sites are reassuring, but they may represent binding solely to a nonreceptor site, or the affinity of the receptor and a nonreceptor site may be sufficiently similar to give the appearance of a single population of sites. Moreover, there are many instances of genuine receptors where more complex binding curves are apparent, e.g., receptors that exhibit positive or negative cooperativity *(2)* or where the binding assay distinguishes receptor subtypes etc. *(3)* The measurement of binding kinetics can present even more problems. Whereas a ligand binding to a single population of noninteracting sites *ought* to exhibit monoexponential on and off rates, many commonly do not; this may reflect slow isomerization of the ligand-receptor complex to a higher affinity conformation *(4)*, but it does not necessarily indicate binding to multiple sites and/or nonreceptor sites.

3.2. Tissue Distribution

Another sensible assumption would seem to be that the tissue distribution of binding sites should reflect the known distribution of the receptor of interest. There are, however, some genuine reasons why this might not always appear to be the case. It is not always possible to detect receptors on a particular tissue using binding, because of low receptor density and/or high levels of nonspecific binding; sadly, there is no direct relationship between receptor density and the magnitude or importance of a functional response. Conversely, binding studies have frequently revealed high densities of receptors on cells where their existence was not previously suspected; examples include many neurotransmitter receptors in the brain and dihydropyridine receptors in skeletal muscle *(5)*. However, if binding occurs in the absence of any tissue, it is unlikely to represent a receptor!

3.3. Pharmacology

Examination of the binding characteristics of a ligand and the distribution of binding sites may thus give some indication of whether the site represents a receptor. Nevertheless, the best way to determine whether or not a binding site represents a particular receptor is to correlate the activity of drugs in the binding assay with their activity in a functional assay. The definition of a receptor in a binding assay should always be considered a provisional assumption; even for well-established assays, the discovery of a drug whose activity appears different in functional and binding assays must always question the validity of the binding assay. However, there are some legitimate reasons for differences between functional and binding assays, and these will be considered in context (*see* **Subheading 3.3.2.**).

If the specific binding of a radioligand actually represents binding to the receptor of interest, all ligands known to bind to that receptor should give the same estimate of nonspecific binding; that is, they should displace all of the radioligand that binds to the receptor and only that which binds to the receptor. Conversely, drugs that do not act at the receptor should not displace binding. This is an extremely important test and is probably the observation most likely to alert the experimenter to cases of nonreceptor binding. Therefore, it is good practice to include a "standard" estimate of nonspecific binding in all assays to allow direct comparison of how much binding is displaced by different ligands. It is still necessary to use common sense, however, particularly with regard to concentrations. Many ligands will start to displace nonspecific binding at high enough concentrations—in the definition of nonspecific binding, more is not necessarily better (*see* **Note 2**). Furthermore, all drugs lose selectivity at high enough concentrations and may well start to displace receptor binding, even if they would not normally be expected to interact with that site.

There are some genuine instances of ligands that do interact at the same receptor but do not displace 100% of the specific binding. This situation arises if the ligands bind at distinct sites on the receptor, interacting allosterically, such that both ligands can bind simultaneously. For example, gallamine inhibits the binding of [^{3}H]-N-methylscopolamine to muscarinic acetylcholine receptors in this way *(6)*. Indeed, binding is probably the best method for investigating allosteric interactions at receptors—it yields "clean," "tight" data, the kinetics of ligand binding can be really determined, and the binding step can be studied more or less in isolation.

A more rigorous test is that the affinities of the ligands that interact with a binding site should correspond with the affinities of these ligands obtained in functional studies. Obtaining this correlation can be somewhat problematic, however. Although it is fairly straightforward to obtain affinities from binding experiments, this may not be the case for functional studies.

3.3.1. Determining Antagonist Affinities

It is much easier to determine the affinity of an antagonist than it is to determine the affinity of an agonist, but even so, it is by no means always uncomplicated. Under the right conditions, antagonist affinities can be obtained from functional studies with great rigor by using the Schild technique *(7)*. These affinity estimates should then be directly comparable with affinities obtained from binding assays, and any discrepancies must question the validity of the binding assay. As an example, there is an excellent correlation between functional and binding affinities for approx 40 muscarinic antagonists, suggesting

that in this case at least, the binding site really does represent a *bona fide* receptor *(8)*.

However, it is not always easy to obtain reliable estimates of affinity from functional assays. The Schild method works very well in "classical" isolated tissue systems (e.g., the guinea pig ileum), in which it is possible to achieve equilibrium: the concentration of the antagonist at the receptor can be estimated with some confidence, and multiple concentration vs response curves can readily be obtained. However, it is virtually impossible to achieve these conditions in behavioral experiments, for example, and can be extremely difficult using electrophysiological techniques. Furthermore, the affinity of antagonists measured in binding assays may be dependent on the conditions of the assay (temperature, ion composition of buffer, and so on.). In order to allow any comparison, it may be important to keep the conditions in the binding assay as similar as possible to those of the functional assay.

3.3.2. Determining Agonist Affinities

This is much more problematic than determining antagonist affinities. The behavior of agonists in binding assays tends to be more dependent on the precise assay conditions than that of antagonists, consequently it is even more important to try and use similar conditions to those of the functional assay within the dictates of maintaining receptor stability. Agonists also commonly recognize multiple affinity states or exhibit cooperative interactions. This presumably reflects their ability to activate the receptor, but it complicates a direct comparison between functional and binding assays.

The biggest problem, however, is that functional assays cannot give direct estimates of agonist affinity. The response to an agonist depends both on the occupancy of the receptor by the agonist (which, of course, depends on agonist affinity) and on the efficacy of the agonist-receptor complex. Consequently, a potent agonist may produce responses at low concentrations, because it has high affinity for the receptor. However, it is equally possible that it may have a rather low affinity, but be highly efficacious, producing effects at very low receptor occupancy. Techniques exist for obtaining estimates of affinity from concentration vs response curves, but these methods are not uncomplicated and may depend on invalid assumptions *(9)*. Hence, obtaining a low affinity for a potent agonist need not necessarily be a reason for discarding a binding assay.

It is also possible for agonists at certain receptors to have a higher affinity in the binding assay than their potency in functional studies would suggest. This situation is particularly common for agonists binding to receptors with integral

ion channels, such as the nicotinic acetylcholine receptor *(10)*. The discrepancy between functional and binding affinity presumably occurs because the binding assay approaches equilibrium. For many of the ion channel type receptors, equilibrium seems to be an inactivated state, in which a receptor has very high affinity for agonist but cannot open to initiate a response. Functional studies necessarily detect a nonequilibrium, intermediate state in which agonists bind to closed channels with a somewhat lower affinity and induce them to open.

A commonly used strategy to avoid the need to determine precise affinity values is to compare the order of potency of various drugs in functional and binding assays. The potency of antagonists depends only on their affinity, so antagonists should exhibit the same order of potency in functional and binding assays, if both assays are detecting the same receptor. However, as previously outlined, the potency of an agonist in a functional assay depends both on its affinity and on its efficacy, and thus there is no *a priori* reason why agonist orders of potency need be identical in the two assays (*see* **Note 3**).

4. Displaceable, Nonreceptor Binding

In situations where a radioligand does bind in a displaceable fashion to nonreceptor sites, it might be possible to circumvent the problem by using a different radioligand or by removing the nonreceptor site by, for example, purifying a plasma membrane preparation, silanizing assay tubes, or by including saturating concentrations of substances that will suppress the "unwanted" component of binding. This last approach works best when the unwanted binding represents binding of a rather nonselective radioligand to another receptor site (*[11]* and Chapter 3). Where none of these strategies is applicable, the magnitude of the problem depends on how easy it is to distinguish nonreceptor binding from binding to the receptor of interest.

The stable prostacyclin analog, [^{3}H]-iloprost, is widely used as a radioligand for the IP prostanoid receptor, producing half-maximal occupancy at concentrations of about 10 n*M*. However, at concentrations above 50 n*M*, a substantial component of the displaceable binding of [^{3}H]-iloprost is to a low-affinity, high-capacity, nonreceptor site, which probably corresponds to the low-affinity prostanoid site reported in other studies *(12)*. It is possible to minimize the impact of this nonreceptor binding by careful experimental design; e.g., by avoiding the use of saturation experiments to characterize iloprost binding, instead using self-competition experiments in which a low (< 10 n*M*) concentration of [^{3}H]-iloprost is used to selectively label the receptor sites, and the ability of unlabeled iloprost to inhibit this binding is investigated. Failure to recognize the existence of this nonreceptor site can lead to an underestimation

of the affinity of iloprost for the IP receptor and a substantial overestimation of the number of IP receptor sites.

The nonreceptor site labeled by the adenosine receptor agonist [^{3}H]-N-ethylcarboxamidoadenosine ([^{3}H]-NECA) presents rather more of a problem. The NG108-15 cell expresses adenosine A_2 receptors, and [^{3}H]-NECA labels a high density of displaceable binding sites in NG108-15 cell membranes. There is a good correlation between the affinities of five adenosine A_2 receptor ligands (three antagonists and two agonists) in binding and functional assays, which initially suggested that the [^{3}H]-NECA binding site represented the A_2 receptor. However, other known A_2 receptor agonists do not displace [^{3}H]-NECA binding at all ***(13)***, emphasizing the importance of investigating as wide a range of ligands as possible when attempting to identify receptor sites. The affinity of this nonreceptor site is very similar to that expected for the A_2 receptor, so it is not possible to alter the concentration of [^{3}H]-NECA to selectively label the receptor. It *is* possible to suppress the nonreceptor binding with ATP or its nonhydrolyzable analog AppNHp, which are not expected to bind to the A_2 receptor at the concentrations used. However, no displaceable binding of [^{3}H]-NECA can be detected in NG108-15 cells in the presence of ATP, suggesting that the A_2 receptor density is too low to be distinguished from the noise in this system.

5. The Nature of the Nonreceptor Sites

The nature of these irritating nonreceptor sites is obviously many and varied. Some of them may be enzymes or uptake sites; the [^{3}H]-NECA site may well be a heat shock protein, as many of these proteins bind adenosine, adenine nucleotides, and their analogs ***(14)***. The existence of displaceable binding sites on the binding assay "hardware" (tubes, filters, and so on) is perhaps surprising, but they are not at all uncommon ***(1)***; furthermore, there is a (tongue-in-cheek) report of specific saturable binding of pepperoni to pizza ***(15)***! Under the right (or, rather, wrong) circumstances, a very nonspecific interaction of ligand with a filter can look like binding to a very low-affinity, high-capacity site ***(16)***. However, sometimes these nonreceptor binding sites turn out to be real functional receptors after all.

There are many examples of cases where binding studies have revealed previously unrecognized subtypes of receptors. Subtypes may be suspected, if there is a difference between functional and binding affinities obtained from different tissues or if the selective ligand exhibits biphasic or shallow binding curves, suggesting the existence of subtypes within a particular tissue ***(3,8)***. Indeed, binding studies are much more sensitive than functional studies for distinguishing receptor subtypes within a tissue or cell. There are also several

instances of a functional role being ascribed to sites that have been widely considered to be binding "artifacts," such as the imidazoline sites (*[17]* and Chapter 3) and the AT_2 angiotensin receptor *(18)*.

Identification of these sites as receptors is still absolutely dependent on showing that they are functional—i.e., that the interaction of drugs with these sites produces a response. This functional response can be extremely hard to characterize, especially in brain, necessitating the use of behavioral, electrophysiological, or biochemical second-messenger assays. The problem is compounded as there may be no clues as to the type of response that the novel receptor is likely to produce.

6. Conclusion

The failure to distinguish receptor from nonreceptor binding has produced confusing results and has given the whole field of radioligand binding something of a bad name. However, it is important not to throw the baby out with the bath water. A marked expansion in the use of binding assays took place in the late 1970s and early 1980s, at a time when there was considerable resistance to the "unnecessary" proliferation of receptor subtypes; an article on the problem of nonreceptor binding written in this period includes a plea for a return to the concept of the "unitary" opiate receptor *(19)*. However, it is now clear from cloning studies that there are more receptor subtypes than were dreamed of by even the most slapdash "grinder and binder."

The ease and precision of the binding technique mean that it is capable of detecting differences between receptor subtypes, and of finding new receptors, in situations that would be very difficult if using functional assays. By using a few common-sense rules, most of the potential pitfalls of the technique can be avoided. Be critical, sensible, and open-minded, and, above all, remember that you can never be absolutely sure that a binding site is really a receptor.

7. Notes

1. It is possible to determine the specific binding of an irreversible radioligand by determining to what extent binding can be suppressed by coincubation or preincubation of the receptor preparation with an unlabeled ligand. However, bear in mind that if the binding is allowed to reach equilibrium, the irreversible ligand will always "win," and no suppressible binding will be detectable.
2. If inhibition of radioligand binding by an unlabeled ligand plateaus at the level of nonspecific binding determined by other ligands, but then starts to inhibit nonspecific binding at higher concentrations, it is sensible to use concentrations on the plateau to define nonspecific binding.
3. Exactly the same arguments apply when comparing orders of potency in two functional assays, e.g., from different tissues.

References

1. Fowler, C. J., Martinsson, T., and Brannstrom, G. (1993) Specific binding of [^{3}H]-[Sar9, Met(02)11]-substance P to tissue culture plates is found when substance P is used to define nonspecific binding. *Meth. Findings Exp. Clin. Pharmacol.* **15,** 337–343.
2. Bufton, K. E., Steward, L. J., Barber, P. C., and Barnes, N. M. (1993) Distribution and characterisation of the [^{3}H]-granisetron-labelled $5HT_3$ receptor in the human forebrain. *Neuropharmacol.* **32,** 1325–1331.
3. Hammer, R., Berrie, C. P., Birdsall, N. J. M., Burgen, A. S. V., and Hulme, E. C. (1980) Pirenzepine distinguishes between subtypes of muscarinic receptor. *Nature* **283,** 90–92.
4. Kloog, Y., Egozi, Y., and Sokolovsky, M. (1979) Characterization of muscarinic acetylcholine receptors from mouse brain: evidence for regional heterogeneity and isomerization. *Mol. Pharmacol.* **15,** 545–558.
5. Flockerzi, V., Oeken, H. J., Hofmann, F., Pelzer, D., Cavalie, A., and Trautwein, W. (1986) Purified dihydropyridine-binding site from skeletal muscle T-tubules is a functional calcium channel. *Nature* **323,** 66–68.
6. Stockton, J. M., Birdsall, N. J. M., Burgen, A. S. V., and Hulme, E. C. (1983) Modification of the binding properties of muscarinic receptors by gallamine. *Mol. Pharmacol.* **23,** 551–557.
7. Arunlakshana, O. and Schild, H. O. (1959) Some quantitative uses of drug antagonists. *Br. J. Pharmacol. Chemother.* **14,** 48–58.
8. Birdsall, N. J. M. (1984) The relation of receptor binding studies to receptor function. *Eur. J. Respir. Dis.* **135 (Suppl),** 107–113.
9. Keen, M. (1991) Testing models of agonism for G protein coupled receptors. *Trends Pharmacol. Sci.* **12,** 371–374.
10. Colquhoun, D. and Rang, H. P. (1976) Effects of inhibitors on the binding of iodinated α-bungarotoxin to acetylcholine receptors in rat muscle. *Mol. Pharmacol.* **12,** 519–535.
11. Stowe, R. L. and Barnes, N. M. (1996) Further pharmacological characterisation of [^{3}H]-5-CT binding in rat brain tissues. *Br. J. Pharmacol.* **119,** 366P.
12. Keen, M., Kelly, E. P., and MacDermot, J. (1991) Guanine nucleotide sensitivity of [^{3}H]-iloprost binding to prostacyclin receptors. *Eur. J. Pharmacol.* **207,** 111–117.
13. Keen, M., Kelly, E. P., Nobbs, P., and MacDermot, J. (1989) A selctive binding site for [^{3}H]-NECA that is not an adenosine A_2 receptor. *Biochem. Pharmacol.* **38,** 3827–3833.
14. Hatayama, T., Yasda, K., and Nishiyama, E. (1994) Characterization of high molecular mass heat shock proteins and 42°C specific heat shock proteins in murine cells. *Biochem. Biophys. Res. Commun.* **204,** 357–365.
15. Guth, P. S. (1982) The structurally specific, stereospecific saturable binding of pepperoni to pizza. *Trends Pharmacol. Sci.* **3,** 467–467.
16. Hulme, E. C. (ed.) (1992) *Receptor-Ligand Interactions. A Practical Approach.* IRL, Oxford University Press, Oxford, U.K.

17. Carpene, C., Collon, P., Remaury, A., Cordi, A., Hudson, A., Nutt, D., et al. (1995) Inhibition of amine oxidase activity by derivatives that recognize imidazoline I_2. *J. Pharmacol. Exp. Ther.* **272,** 681–688.
18. Regitzzagrosek, V., Neuss, M., Holzmeister, J., Warneck, C., and Fleck, E. (1996) Molecular biology of angiotensin receptors and their role in human cardiovascular disease. *J. Mol. Med.* **74,** 233–251.
19. Laduron, P. (1983) More binding, more fancy. *Trends Pharmacol Sci.* **4,** 333–335.

IV

The Use of Binding to Study Nonreceptor Sites

11

Autoradiography of Enzymes, Second Messenger Systems, and Ion Channels

David A. Walsh and John Wharton

1. Introduction

Autoradiographic detection of ligand binding to tissue sections has been used to localize, quantify, and characterize a diverse range of sites. Enzymes have been studied using selective inhibitors, ion channels using naturally occurring toxins, and second messenger systems using inositol polyphosphates. Ligand binding complements immunohistochemistry and *in situ* hybridization by permitting pharmacological characterization and quantification of active sites. Localization, affinity, and specificity of binding sites for ligands can be correlated with functional studies performed with the same pharmacological agent. Bioactive ligands are often identified before their targets have been fully characterized, and radiolabeled ligands may become available before molecular and immunological reagents have been developed. A pharmacologically active agent may be synthesized before the endogenous ligand for its binding site has been identified, and autoradiographic methods may help elucidate the site of action of such agents.

However, ligand binding studies are not without their difficulties. Binding depends on the accessibility of functional protein and may be affected by a wide variety of buffer conditions, the presence of endogenous ligand, or shedding of binding sites from the tissue surface. Therefore, ligand binding densities do not necessarily reflect expression or total concentration of binding protein, but they are only a snapshot of what is available under the experimental conditions tested. A particular difficulty with many enzymes and inositol polyphosphate receptors is their often low affinity for available ligands, resulting in elution of specific binding during wash procedures. Furthermore,

From: *Methods in Molecular Biology, Vol. 106: Receptor Binding Techniques*
Edited by: Mary Keen © Humana Press Inc., Totowa, NJ

nonpeptide ligands such as enzyme inhibitors often cannot be covalently linked to their binding site, making microscopic localization difficult. Fortunately, maximal binding capacities (B_{max}) are typically several orders of magnitude greater than for peptide receptors, and limitations on the sensitivity of autoradiography can often be overcome by increasing the ligand concentration.

In this chapter, we discuss the autoradiographic detection of enzymes, ion channels, and second messenger systems, illustrated by angiotensin converting enzyme (ACE), nitric oxide synthase (NO), vanilloid "receptors," guanosine triphosphate (GTP) binding proteins (G proteins), and inositol polyphosphate receptors. Specific protocols described for these sites are intended to illustrate approaches that may be used to develop binding protocols for other systems.

In Chapter 7, we dealt primarily with peptide ligands that can be radiolabeled to high specific activity with ^{125}Iodine. Not all ligands can be chemically labeled with ^{125}Iodine. Furthermore, radioiodination has the potential disadvantage of structurally modifying the ligand, thereby changing its binding characteristics compared with the nonlabeled ligand. Replacement of ^{2}H with ^{3}H retains the structure and chemical characteristics of the nonlabeled ligand. Autoradiographic images of [^{3}H]-labeled ligands typically have higher resolution than [^{125}I]- or [^{35}S]-labeled ligands, but they require exposures over periods of weeks or months, rather than days. Ligands containing sulphur groups may be labeled with ^{35}S and require exposures of only hours.

ACE is a dipeptidyl peptidase that converts angiotensin I to the potent vasoconstrictor octapeptide angiotensin II, and which also catalyses the inactivation of bradykinin and the sensory neuropeptide substance P *(1)*. Each molecule of endothelial ACE has two zinc-containing catalytic sites, although these may not have identical activities *(2)*. ACE has been extensively investigated by quantitative autoradiography of radiolabeled inhibitor binding. [^{3}H]-labeled captopril was used in early experiments to study the localization of ACE *(3)*. Mendelson described the use of a radioiodinated tyrosyl derivative of the ACE inhibitor lisinopril, [^{125}I]351A, which has the advantage of higher specific activity *(4)*. [^{125}I]351A binds to either active site of ACE, its binding is inhibited by other competitive ACE inhibitors, by ACE substrates such as angiotensin I, bradykinin, and substance P, and by chelators of the active site zinc atom *(4–6)*. Binding density correlates with enzyme activity, as determined using synthetic substrates in tissue homogenates *(4,5)*. [^{125}I]351A binds to ACE with nanomolar affinity, but cannot be covalently linked using conventional fixatives. Therefore, emulsion-dipping is not possible but microscopic localization can be achieved by matching film autoradiograms with histochemically stained sections. Antibodies to human and rat ACE are widely available, and the distribution of immunoreactivity closely parallels that of [^{125}I]351A binding *(7)*.

[^{125}I]351A binding permits quantification of the amount of ACE localized to specific tissue structures. Immunohistochemistry is most useful in confirming the cellular localization of ACE. Increased [^{125}I]351A binding may represent upregulated ACE expression, or an increase in the number of cells bearing ACE. A combination of techniques is most appropriate for interpreting such data. [^{125}I]351A binding has been used to demonstrate changes in the amount of tissue bound ACE during treatment with ACE inhibitors, during pathological processes such atherosclerosis and during angiogenesis and tissue repair ***(7–10)***.

Nitric oxide (NO) is a free radical with many biological functions, including endothelium-dependent vasodilation and macrophage-dependent cytotoxicity ***(11)***. NO is generated from L-arginine by a family of enzymes known as nitric oxide synthases (NOS). Endothelial and neuronal NOS are constitutively expressed, whereas activated macrophages and some other cell types can express an inducible NOS. Constitutive NOS have high affinities for L-arginine and are mainly calcium-dependent, whereas inducible NOS has lower affinity, higher capacity, and generally lacks calcium dependence. Likewise, constitutive NOS generate relatively small amounts of NO in response to specific stimuli, for example, substance P or acetyl choline, whereas inducible NOS can persistently generate large amounts of NO. Binding of the NOS inhibitor N^G-[2,3,4,5-^{3}H]nitro-L-arginine ([^{3}H]-L-NOARG) provides a quantitative measure of *in situ* NOS activity, but is not entirely specific for any particular isoform ***(12,13)***. The distribution of [^{3}H]-L-NOARG binding to vascular endothelium and in the central nervous system and its high affinity suggest binding is predominantly to constitutive, rather than inducible NOS ***(14,15)***. This view has been supported by comparison with NOS localization by *in situ* hybridization ***(16)***. The recent development of inhibitors with greater selectivity for NOS isoforms has provided valuable tools for the further characterization of NOS-like binding sites ***(15)***. Autoradiographic studies have demonstrated that NOS can be up- or downregulated in vein grafts and during preeclampsia ***(14,17)***.

A variety of toxins and pharmacological agents have been identified that bind specifically and often with very high affinity to membrane ion channels through which they mediate their biological effects. Resiniferatoxin binds with high affinity to vanilloid receptors ***(18)***. Resiniferatoxin or capsaicin, the pungent component of red chili pepper, activate vanilloid receptors on fine unmyelinated sensory nerves, causing them to release neuropeptides including substance P and calcitonin gene-related peptide ***(19)***. Sustained stimulation is neurotoxic for sensory nerves. [^{3}H]resiniferatoxin binding can be used to localise and quantify this class of sensory nerve in the central nervous system

(20,21). The biological role, endogenous ligand, and molecular structure of [^{3}H]resiniferatoxin binding sites remain to be fully elucidated (*see* **Note Added in Proofs**). Therefore, radioligand binding is one of the few available methods for studying these sites *(21)*. [^{3}H]resiniferatoxin is lipophilic and special protocols have been developed to minimize nonspecific binding. Autoradiography with [^{3}H] resiniferatoxin has been used to demonstrate changes in vanilloid receptor densities in dorsal root ganglia *(22)*.

The nonhydrolyzable GTP analogues [^{3}H]-5'guanylylimidodiphosphate ([^{3}H]GppNHp) and [^{35}S]-guanosine 5'-*O*-(3-thiotriphosphate) ([^{35}S]GTPγS) have been used in autoradiographic studies of G proteins in tissues (**Figs. 1** and **2**) *(23–25)*. However, GTP binds with similar affinities to heterogeneous proteins, including the small GTP-binding proteins such as the *ras* gene product, and the α-subunits of heterotrimeric G proteins which mediate signal transduction by the seven transmembrane family of cell surface receptors *(26,27)*. Identification of the particular G proteins responsible for altered [^{35}S]GTPγS binding is best performed by using specific antisera on membrane preparations following gel electrophoresis, or by Northern blotting and *in situ* hybridization. Some indication of the specificity of [^{35}S]GTPγS binding can be obtained by demonstrating coupling to receptors. Agonists enhance [^{35}S]GTPγS binding to receptor-coupled G proteins by increasing their affinity for GTP and its analogues, and by decreasing their affinity and thereby encouraging dissociation of guanosine diphosphate (GDP) (*[28]* and Chapter 13). For example, angiotensin II increases [^{35}S]GTPγS binding to AT_1 receptor-coupled G proteins *(29)*. However, only a small proportion of total [^{35}S]GTPγS binding sites in a tissue will represent a given Gα species coupled to a particular receptor subtype (**Fig. 2**). Demonstration of agonist enhancement requires conditions under which [^{35}S]GTPγS binding to noncoupled G proteins will be low, typically achieved by chelating divalent cations with EDTA, and by coincubation with an excess of nonradiolabeled GDP. Opioid enhancement of [^{35}S]GTPγS binding has recently been demonstrated autoradiographically in rat brain sections *(25)*. Other approaches to investigating receptor-G protein coupling in tissue structures include the inhibition of agonist binding by GTP and its analogs, and by specific antisera that block the interaction of G protein and receptor *(30,31)*. Autoradiography with guanosine nucleotide analogs has been used to study decreased densities of G proteins following cerebral ischaemia, and opioid receptor activated G proteins in rat brain *(24,25)*.

Inositol polyphosphates are important second messengers, the best characterized being inositol 1,4,5 trisphosphate (IP_3), which mediates cellular actions of agonists of a broad range of G protein-coupled receptors, including adrenaline, bradykinin, substance P, and angiotensin II *(32)*. IP_3 is generated together with diacyl glycerol by the action of phospholipase C on membrane-derived

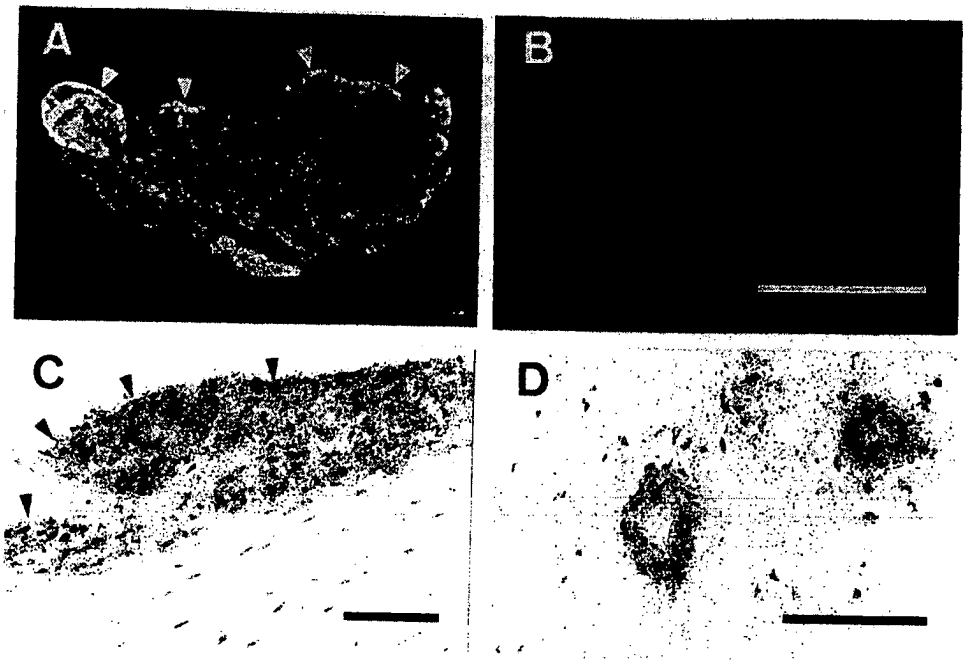

Fig. 1. Localization of [^{35}S]GTPγS binding to human synovium. (**A**) Binding of 0.1 nM [^{35}S]GTPγS to the lining region (arrowheads) and annular binding to blood vessels (arrows), with less dense binding to intervening stroma in synovium from a patient with rheumatoid arthritis. (**B**) Nonspecific binding to a section consecutive to that shown in (A) in the presence of an excess (1 μ*M*) unlabeled GTPγS. (**C**) Dense specific binding indicated by silver grains overlying lining cells in synovium from a patient with osteoarthritis with less dense binding to underlying stroma. Arrowheads indicate synovial surface. (**D**) Specific binding to blood vessels in synovium from a patient with osteoarthritis. The autoradiographic method permits the simultaneous localization and characterization of binding to different structures within a tissue. The density of [^{35}S]GTPγS binding sites was greater on lining cells (B_{max} 47 (95% CI, 22 to 101) fmol mm^{-2}) and blood vessels (B_{max} 39 (95% CI, 29 to 52) fmol mm^{-2}) than on stroma (B_{max} 10 (95% CI, 2 to 43) fmol mm^{-2}, $P < 0.05$), but did not differ significantly between synovia from patients with rheumatoid arthritis (n = 6), osteoarthritis (n = 8) and chondromalacia patellae (n = 7). **A** & **B**: Reversal prints of film autoradiograms. Bar = 3 mm. **C** & **D**: Emulsion dipped preparations. Bar = 100 μ*M*.

phosphatidyl choline. IP_3 binds intracellular proteins (IP_3 receptors) stimulating an increase in intracellular calcium concentrations. IP_3 can itself be catalytically converted to other inositol polyphosphates, for example by phosphorylation to inositol 1,3,4,5 tetrakisphosphate (IP_4) which may, in turn, serve other second messenger functions through interaction with specific bind-

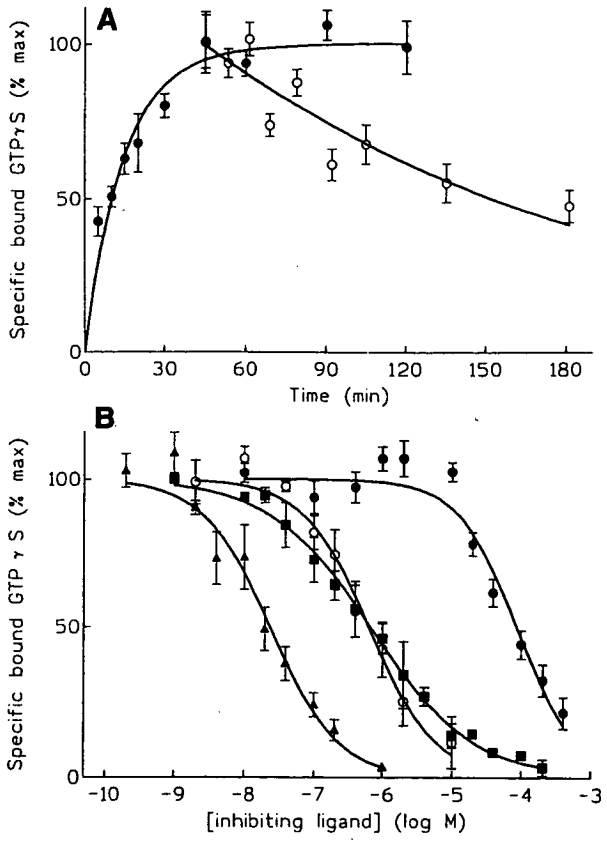

Fig. 2. Characteristics of [^{35}S]GTPγS binding to human synovium. (A) Association (●) and dissociation ($oc) of 1 n*M* [^{35}S]GTPγS binding to synovial blood vessels at 22°C. Dissociation was initiated after 45 min incubation with 1 n*M* [^{35}S]GTPγS by transfer of sections to an excess of buffer without [^{35}S]GTPγS. The optimal incubation time for subsequent equilibrium binding studies was determined by these experiments to be 45 min. It is undetermined whether dissociation of [^{35}S]GTPγS indicates dissociation from its binding protein or loss of G protein from the section. (B) Inhibition of specific [^{35}S]GTPγS binding to synovial blood vessels by unlabeled GTPγS (▲), the non-hydrolysable GTP analog Gpp(NH)p (■), GTP (○) and guanosine diphosphate (GDP) (●). Typical of binding to enzymes, non-hydrolysable ligands often have higher affinity than hydrolyzable ligands, and substrates (GTP) have higher affinity than products (GDP). The shallow slope for inhibition by Gpp(NH)p (n_{Hill} = -0.6 [95% CI, −0.4 to −0.8]) may reflect heterogeneity of binding sites. The K_i value for GTP (1.1 (95% CI, 0.2 to 5.2) μ*M*) may be underestimated due to hydrolysis of GTP by its binding protein during incubation. Specific binding was also inhibited by EDTA by 78% (95% CI, 53% to 90%) consistent with magnesium-dependent binding to G proteins. Note that B_{max} values for [^{35}S]GTPγS are approximately 1000-fold greater than for typical

ing sites. Binding sites for [^{3}H]-labeled inositol polyphosphates can be localized, quantified, and characterized autoradiographically, and, at least some of these, are likely to be identical to the receptors that mediate their biological actions ***(33,34)***. Inositol polyphosphate binding sites, however, have diverse characteristics, and their biological roles have not all been elucidated. In particular, the synthetic inositol polyphosphate inositol 1,2,6 trisphosphate (α-trinositol), which is believed not to occur in vivo, bound selectively and specifically with high affinity to sites in vascular and nonvascular smooth muscle in both humans and rats ***(34)***. These sites shared some characteristics with [^{3}H]$IP_4$4 binding sites, namely low pH optimum and independence on divalent cations but displayed different distributions and specificities for related inositol polyphosphates to [^{3}H]$IP_4$4 binding sites in the same tissues. The biological role for these sites remain to be determined, although mediation of the vasodilator effects of α-trinositol has been proposed. The nature of any endogenous ligand for the α-trinositol binding site also remains to be determined. Experience with nonpeptide ligands for peptide receptors indicates that synthetic ligands may show little structural resemblance to their endogenous counterparts. Autoradiography has been used to investigate changes in inositol polyphosphate binding sites following cerebral ischaemia, and to help characterise the sites of action of inositol polyphosphate analogues ***(34,35)***.

Autoradiography therefore may be useful for the localization and quantification of well-characterized sites such as ACE, providing information that is complementary to that obtained by immunohistochemistry and in situ hybridization. In addition, it provides a valuable tool for studying ligands with known biological activity whose sites of action are not known, either anatomically or molecularly. Pharmacological characterization permits more direct correlation with functional data than is often possible in immunohistochemical and molecular studies.

The same materials and procedures described for peptide receptor autoradiography (see Chapter 7) are also applicable to the analysis of binding sites in general. Some duplication in the details provided is therefore inevitable. However, in this chapter, we have focused on the adaptation of protocols for examination of second messenger systems, ion channels, and enzymes.

Fig 2. (*see previous page*) G protein-coupled receptors on blood vessels, such as NK_1 receptors for substance P and AT_1 receptors for angiotensin II. These agonists did not significantly affect [^{35}S]GTPγS association or dissociation rates, equilibrium binding or inhibition by GDP in these experiments.

2. Materials

1. Thermostatically controlled laboratory space suitable for work with radioactive substances at 4°C to 37°C.
2. Tissue-TEK™ O.C.T. mounting compound and cork discs (e.g., Histological Equipment, Ltd.).
3. Isopentane, liquid nitrogen, thermos flask, and a pyrex or metal beaker.
4. Heat sealer and polythene layflat tubing (e.g., A1 Packagings Ltd., London, U.K.).
5. Glass microscope slides (e.g., low iron BDH Premium 406/0184/04) and coverslips (e.g. BDH 406/0188/42).
6. Vectabond™ reagent (Vector Laboratories SP-1800) and acetone.
7. Cryostat, preferably motorized, capable of cutting frozen sections of reproducible thickness, usually 10 or 20 µm (e.g., Bright Instrument, Co. Ltd.)
8. Radiolabeled ligands (e.g., Amersham International, Little Chalfont, UK, & DuPont, NEN™ Life Science Products, Hounslow, UK). Reconstitute according to manufacturers recommendations, aliquot at appropriate concentration, and store at –20°C or lower.
9. Unlabeled ligands, aliquotted at appropriate concentrations and stored at –20°C or lower.
10. Buffers and enzyme inhibitors (*see* **Table 1**).
11. Protease-free bovine serum albumin, fraction V powder (e.g., Sigma A 3294).
12. Metal slide racks (24 capacity) and dishes (400–500 mL capacity).
13. Humidified incubation chambers. Perspex trays (25 × 25 cm) with lids are ideal. Four rods (e.g., plastic pipets) are attached with adhesive inside the base in parallel pairs 4 cm apart to support microscope slides. Moistened absorbent paper is laid between the two pairs of rods.
14. Hair dryer. High air flow and "cold" settings are essential.
15. Dark room with safelight (e.g., Kodak 6B or Ilford 902/904 filters).
16. Autoradiography film (e.g., Hyperfilm™-^{3}H, 24 × 30 cm, Amersham RPN 12).
17. Autoradiography cassettes with side lever closure (e.g., Genetic Research Instrumentation Ltd., Dunmow, U.K.) rather than clip-closure designs.
18. Radioactive standards (e.g., Amersham [^{125}I] Microscales™ RPA 523, [^{14}C]-labeled standards from American Radiolabelled Chemicals, St. Louis, MO).
19. Nuclear emulsion (e.g., Ilford K5 diluted 1:1 in water, or Amersham LM-1 RPN 40). Dipping vessel (e.g., Amersham RPN 39). Light-tight box (e.g. Raymond Lamb E/107 takes rack E/99).
20. Wire loop (2–3 cm dia.) made from nickel/chrome or platinum wire (~ 0.5 mm thick).
21. Cyanoacrylate adhesive ("Superglue").
22. Developer (e.g., Kodak D19 #5027065) and fixer (e.g., Champion Photochemistry, Brentwood, U.K., Amfix™ #80213, diluted 1 + 4 with tap water).
23. Histological staining solutions (e.g., hematoxylin and eosin).
24. 70% and absolute ethanol, xylene or Histoclear and dibutylphthalate polystyrene xylene (DPX) mounting medium.

25. Microscope equipped for transmitted light, dark-field, and epi-illumination.
26. Image analysis system.

3. Methods

Methodological details are based on those developed for peptide receptors (Chapter 7). What follows is a summary of the protocol with notes which relate specifically to non-peptide ligands.

3.1. Preparation of Sections

1. Unfixed tissues are mounted to cork blocks, frozen in melting isopentane and stored at −70°C.
2. Glass microscope slides are pretreated to improve section adhesion, for example with Vectabond™ reagent (Vector Laboratories, Peterborough, U.K.) (*see* **Note 1**).
3. Thin (10 µm) sections of unfixed tissue are cut in a cryostat at −20°C to −30°C and thaw mounted on prepared slides. Sections are air dried with silica gel desiccant for 1 h at 4°C then used immediately, or stored at −20°C in sealed bags with silica gel.

3.2. Incubations

1. Preincubate sections in slide racks in baths containing 400 mL preincubation buffer (buffer A, **Table 1**).
2. Remove individual slides from the preincubation buffer, gently tap on absorbent paper, remove excess buffer by blotting around the edge of the section, and place horizontally in an incubation chamber.
3. Load sections with a measured volume of incubation buffer containing radiolabeled ligand alone, or together with unlabeled ligand, and incubate for the appropriate time at the stated temperature (**Table 1**, *see* **Note 2**).
4. Terminate incubations by tapping the slide on absorbent paper to remove ligand, then rinse twice by immersion in a slide rack in an excess buffer A, for the stated times at 4°C (**Table 1**, *see* **Note 3**).
5. Dip sections into ice-cold distilled water, then immediately dry under a stream of cold air, using a nonheated hair drier.

3.3. Preparation of Film Autoradiograms

1. Arrange slides with the sections facing upwards in an autoradiography cassette, together with appropriate radiolabeled standards (*see* **Note 4**).
2. Under safelight conditions, appose uncoated radiosensitive film, emulsion-down, to the sections and close the cassette. Seal the cassette in a polythene bag containing dry silica gel (*see* **Note 5**).
3. Expose for an appropriate time (**Table 1**) at 4°C or −20°C away from vibrations and other movement (*see* **Note 6**).
4. Bring the cassette to room temperature before removing it from the bag, and open under safelight conditions. Develop in Kodak D19 at 15 to 20°C for 3 min, stop

Table 1
Procedures for Specific Ligands

Ligand	[^{125}I]351A	[^{3}H]-L-NOARG	[^{3}H]resiniferatoxin	[^{35}S]GTPγS	[^{3}H]IP_4
Specific activity (TBq $mmol^{-1}$)	74	1.9	3.2	44	0.9
Concentration	0.03 n*M*	100 n*M*	2 n*M*	0.1 or 1 n*M*	5 n*M*
Buffer A	10 m*M* PBS	50 m*M* Tris-HCl	10 m*M* HEPES	50 m*M* Tris-HCl	50 m*M* Na acetate
			2 m*M* $MgCl_2$	25 m*M* $MgCl_2$	
			320m*M* sucrose	1 m*M* EGTA	1 m*M* EGTA
			0.75 m*M* $CaCl_2$	2 m*M* DTT	
			5.8 m*M* NaCl		
			5 m*M* KCl		
	pH 7.4	pH 7.3	pH 7.4	pH 7.9	pH 5.0
Buffer B (A+)	0.2% BSA	10 μ*M* $CaCl_2$	0.1% BSA	—	—
Preincubation	2 × 5 min	1 × 15 min	2 × 5 min	2 × 5 min	2 × 10 min
Incubation	3 h at 22°C	30 min at 20°C	60 min at 37°C	30 min at 22°C	90 min at 4°C
Rinse at 4°C	2 × 5 min	2 × 5 min	2 × 5 min	2 × 5 min	2 × 2.5 min
			20 m*M* TrisHCl, 0.1% BSA, 0.1% α_1 acid glycoprotein		
Fixation	—	—	—	30 min Bouin's solution	—
Microscopic localisation	IHC	Cover slip	Cover slip	Dip	Cover slip
Exposure; film	4 d at 4°C	6 wk at 4°C	4 wk at −20°C	2 to 6 h at 4°C	3 wk at −20°C
slide	—	8 wk at 4°C	8 wk at −20°C	1 week at 4°C	3 mon at −20°C

Abbreviations: BSA; enzyme free bovine serum albumin, DTT; dithiothreitol, EGTA; ethylene glycol-bis N,N,N′,N′-tetraacetic acid, [^{35}S]GTPγS; [^{35}S]-guanosine 5′-*O*-(3-thiotriphosphate), HEPES; *N*-2-hydroxyethylpiperazine-*N*′-2-ethanesulphonic acid, IHC; antibodies available for immunohistochemistry, IP_4; inositol 1,3,4,5 tetrakisphosphate, L-NOARG; N^G-[2,3,4,5-^{3}H]nitro-L-arginine, PBS; phosphate buffered saline.

in tapwater, fix in Amfix (diluted 1 + 4 in tapwater) for 5 min, then rinse in running cold tap water for 20 min, before hanging to dry.

3.4. Quantification of Film Autoradiograms

1. Illuminate the autoradiographic film from behind using a stabilized light box in a darkened room, and capture and convert the image to a digital image via a video camera. Blank and opaque areas of film are used to correct for variations in light transmission or illumination of the optical system and employ a shading correction procedure.
2. Construct a standard curve, selecting images of at least six radioactive standards using the cursor.
3. Identify and delineate specific regions of interest on the autoradiographic images of radiolabeled tissue sections either by using the cursor or by thresholding according to optical density.
4. The integrated gray level values in these regions are transformed using the standard calibration curve derived for each film, thereby giving the amount of ligand bound.

3.5. Preparation of Microautoradiograms (See Notes 7 and 8)

1. Warm an aliquot of diluted Ilford K5 emulsion and the dipping vial to 42°C. Pour emulsion into the vial.
2. Dip a 22 mm × 64 mm glass cover slip vertically into the emulsion and immediately withdraw, gently scraping one side against the vial to remove excess emulsion. Place vertically on a drying rack, resting against the scraped side, and leave to dry in the dark for 1 h.
3. Put cyanoacrylate adhesive at one end of the unscraped side of the cover slip and appose to the face of the microscope slide bearing the tissue section to which ligand has been bound. The cover slip should be glued to the frosted part of the slide such that the face that is apposed to the tissue section can later be levered up. Place in an autoradiography cassette, filling space with "blank" slides. Overlay with card, and close the cassette, so that cover slip and section are apposed under pressure.
4. Place in a sealed plastic bag with silica gel, and expose for the required time at –20°C.
5. Warm to room temperature then open the cassette under safelight conditions. Apply one paper clip across cover slip and slide at the end that is attached by adhesive, to prevent the cover slip detaching from the slide. Apply another paper clip across the opposite end of the slide, inserting its tongue under the cover slip, thereby levering the cover slip away from the tissue section.
6. Place in a slide rack and immerse in Kodak D19 developer for 3 min at 20°C, ensuring that developer gains access to the emulsion by vertical agitation. Stop in tap water, fix in Amfix diluted 1 + 4 in tapwater, rinse for 20 min in running water, then counterstain, for example with hematoxylin and eosin.

8. Dehydrate through graded alcohols (once in 70% ethanol:30% distilled water, then twice in absolute ethanol), then transfer to an organic medium (e.g., twice in xylene or Histoclear). Drop dibutylphthalate polystyrene xylene (DPX) between the coverslip and tissue section then remove the paper clips. Before the DPX is completely dry, place the slides between paper and cards in an autoradiography cassette and close under pressure in order to minimize the distance between emulsion and section.

4. Notes

1. We have found Vectabond pretreatment effective for most purposes, although some ligands, such as [^{3}H]-α-trinositol, give high non-specific binding to the surface of pretreated slides and, in such cases, untreated slides are preferred.
2. Although 37°C may be considered "physiological," both ligand and binding site may be more stable at lower temperatures, particularly if the tissue contains (unknown) enzymes capable of their degradation. Failure to reach a stable equilibrium binding was observed as an 'n' shaped association curved with many peptide ligands 37°C, and with IP_4 at 20°C. Evaporation is also more of a problem at higher temperatures. Incubations at 4°C should be performed with precooled sections and buffers. Ligand is loaded in a cold room.
3. Nonspecific binding, being of lower affinity, dissociates more rapidly than does specific binding during washing. Where specific binding is of very high affinity (K_d < 0.1 n*M*), prolonged washes at room temperature may increase the ratio between specific and nonspecific binding by facilitating dissociation of ligand from low affinity, nonspecific sites, at the same time retaining binding to specific sites. With many enzymes and inositol polyphosphate receptors, affinity for radiolabelled ligands may be much lower than this (K_d > 10 n*M*). Under these circumstances, important dissociation of ligand from specific binding sites may occur during even short wash periods. Washes should then be performed in ice-cold buffer for short periods (e.g., 2 × 1 min) determined empirically to maximize specific binding.
4. Radiolabeled standards should be of the same thickness as experimental sections, particularly when using radioisotopes with highly penetrating emissions. 10 μ*M* represents an infinite thickness to emissions from ^{3}H, but not from ^{125}I. [^{3}H]-, [^{125}I]- or [^{14}C]-labeled polymer standards can be used for [3H]-, [^{125}I]- or [^{35}S]-labeled ligands, respectively.
5. Uncoated autoradiography films are essential for [^{3}H]-labeled ligands, whose emissions will be absorbed by protective coatings.
6. Exposure times depend on the radioisotope, specific activity, and the density of binding. [^{35}S]-labeled ligands typically require short exposure times (e.g., hours) whereas [^{3}H]-labeled ligands typically require weeks or months.
7. Chemical fixation of ligands to binding sites and subsequent dipping in radiosensitive emulsion is described in Chapter 7. Most nonpeptide ligands, however, cannot easily be linked covalently to binding sites. One approach is to use ligands

with reactive moieties which can crosslink to the tissue, as in photoaffinity labeling. Such procedures have been described in autoradiographic studies, although reduced affinity compared with the parent compound has proved a problem in our hands. Use of emulsion-coated cover slips is described here. With these, the emulsion tends not to be as closely apposed to the section as in dipped preparations, and resolution is correspondingly inferior. With care and high activity ligands, however, localization to structures of approximately 50 μM diameter can be achieved. An alternative method, using a wire loop to apply the emulsion to the tissue section, is described in **Note 8**. To our knowledge, "stripping film," that is, prepared emulsion film that can be floated onto the surface of sections at low temperature, is no longer commercially available.

8. As an alternative to using emulsion-coated cover slips, a layer of emulsion may be applied to unfixed radiolabeled sections using a wire loop. LM-1 emulsion is warmed to 42°C under safelight conditions, then removed from the water bath and allowed to "semi-gel" at room temperature. A wire loop is dipped into the emulsion and applied to the section when the emulsion in the loop appears uniform and stable as viewed under the safelight. If the emulsion is uneven or appears to flow in the loop, it has not gelled sufficiently. Holding the loop above and parallel to the slide, a gentle tap or blow of air may be required to aid the transfer of the gel onto the tissue section.

Note Added in Proofs

A vanilloid receptor has recently been cloned from rodent dorsal root ganglia and found to be a thermosensitive, non-selective cation channel *(36)*.

References

1. Kenny, A. J., Stephenson, S. L., and Turner, A. J. (1987) Cell surface peptidases, in *Mammalian Ectoenzymes*. (Kenny, A. J. and Turner, A. J., eds.), Elsevier, Amsterdam, pp. 169–210.
2. Wei, L., Clauser, E., Alhenc-Gelas, F., and Corvol, P. (1992) The two homologous domains of human angiotensin I-converting enzyme interact differently with competitive inhibitors. *J. Biol. Chem.* **267,** 13,398–13,405.
3. Strittmatter, S. M. and Snyder, S. H. (1984) Angiotensin-converting enzyme in the male rat reproductive system: autoradiographic visualization with [3H]captopril. *Endocrinology* **115,** 2332–2341.
4. Mendelsohn, F. A. O. (1984) Localization of angiotensin converting enzyme in rat forebrain and other tissues by in vitro autoradiography using ^{125}I-labelled MK351A. *Clin. Exp. Pharmacol. Physiol.* **11,** 431–436.
5. Correa, F. M. A., Guilhaume, S. S., and Saavedra, J. M. (1991) Comparative quantification of rat brain and pituitary angiotensin-converting enzyme with autoradiographic and enzymatic methods. *Brain Res.* **545,** 215–222.

6. Sun, Y., Diaz-Arias, A. A., and Weber, K. T. (1994) Angiotensin-converting enzyme, bradykinin, and angiotensin II receptor binding in rat skin, tendon, and heart valves: an in vitro, quantitative autoradiographic study. *J. Lab. Clin. Med.* **123,** 372–377.
7. Sun, Y., Cleutjens, J. P., Diaz-Arias, A. A., and Weber, K. T. (1994) Cardiac angiotensin converting enzyme and myocardial fibrosis in the rat. *Cardiovasc. Res.* **28,** 1423–1432.
8. Zambetis-Bellesis, M., Dusting, G. J., Mendelsohn, F. A., and Richardson, K. (1991) Autoradiographic localization of angiotensin-converting enzyme and angiotensin II binding sites in early atheroma-like lesions in rabbit arteries. *Clin. Exp. Pharmacol. Physiol.* **18,** 337–340.
9. Sun, Y. and Weber, K. T. (1996) Angiotensin-converting enzyme and wound healing in diverse tissues of the rat. *J. Lab. Clin. Med.* **127,** 94–101.
10. Walsh, D. A., Hu, D. E., Wharton, J., Catravas, J. D., Blake, D. R., and Fan T. P. F. (1997) Sequential development of angiotensin receptors and angiotensin I converting enzyme during angiogenesis in the rat subcutaneous sponge granuloma. *Br. J. Pharmacol.* **120,** 1302–1311.
11. Moncada, S., Palmer, R. M., and Higgs, E. A. (1991) Nitric oxide: physiology, pathophysiology, and pharmacology. *Pharmacol. Rev.* **43,** 109–142.
12. Michel, A. D., Phul, R. K., Stewart, T. L., and Humphrey P. P. (1993) Characterization of the binding of [3H]-L-NG-nitro-arginine in rat brain. *Br. J. Pharmacol.* **109,** 287,288.
13. Kidd, E. J., Michel, A. D., and Humphrey, P. P. (1995) Autoradiographic distribution of [3H]L-NG-nitro-arginine binding in rat brain. *Neuropharmacology* **34,** 63–73.
14. Rutherford, R. A., McCarthy, A., Sullivan, M. H., Elder, M. G., Polak, J. M., and Wharton, J. (1995) Nitric oxide synthase in human placenta and umbilical cord from normal, intrauterine growth-retarded and pre-eclamptic pregnancies. *Br. J. Pharmacol.* **116,** 3099–3109.
15. Hara, H., Waeber, C., Huang, P. L., Fujii, M., Fishman, M. C., and Moskowitz, M. A. (1996) Brain distribution of nitric oxide synthase in neuronal or endothelial nitric oxide synthase mutant mice using [^{3}H]L-NG-nitro-arginine autoradiography. *Neuroscience* **75,** 881–890.
16. Burazin, T. C. and Gundlach, A. L. (1995) Localization of NO synthase in rat brain by [^{3}H]L-NG-nitro-arginine autoradiography. *Neuroreport* **6,** 1842–1844.
17. Jeremy, J. Y., Dashwood, M. R., Timm, M., Izzat, M. B., Mehta, D., Bryan, A. J., and Angelini, G. D. (1997) Nitric oxide synthase and adenylyl and guanylyl cyclase activity in porcine interposition vein grafts. *Ann. Thoracic Surg.* **63,** 470–476.
18. Szallasi, A. and Blumberg, P. M. (1990) Specific binding of resiniferatoxin, an ultrapotent capsaicin analog, by dorsal root ganglion membranes. *Brain Res.* **524,** 106–111.
19. Holzer, P. (1991) Capsaicin: cellular targets, mechanisms of action, and selectivity for thin sensory neurons. *Pharmacol. Rev.* **43,** 143–201.

20. Winter, J., Walpole, C. S., Bevan, S., and James, I. F. (1993) Characterization of resiniferatoxin binding sites on sensory neurons: coregulation of resiniferatoxin binding and capsaicin sensitivity in adult rat dorsal root ganglia. *Neuroscience* **57,** 747–757.
21. Szallasi, A., Blumberg, P. M., Nilsson, S., Hokfelt, T., Lundberg, J. M. (1994) Visualization by [^{3}H]resiniferatoxin autoradiography of capsaicin-sensitive neurons in the rat, pig and man. *Eur. J. Pharmacol.* **264,** 217–221.
22. Szallasi, A., Nilsson, S., Farkas-Szallasi, T., Blumberg, P. M., Hokfelt, T., and Lundberg, J. M. (1995) Vanilloid (capsaicin) receptors in the rat: distribution in the brain, regional differences in the spinal cord, axonal transport to the periphery, and depletion by systemic vanilloid treatment. *Brain Res.* **703,** 175–183.
23. Gehlert, D. R. and Wamsley, J. K. (1986) In vitro autoradiographic localization of guanine nucleotide binding sites in sections of rat brain labeled with [3H]guanylyl-5'-imidodiphosphate. *Eur. J. Pharmacol.* **129,** 169–174.
24. Aoki, H., Onodera, H., Yamasaki, Y., Yae, T., Jian, Z., and Kogure, K. (1992) The role of GTP binding proteins in ischemic brain damage: autoradiographic and histopathological study. *Brain Res.* **570,** 144–148.
25. Sim, L. J., Selley, D. E., and Childers, S. R. (1995) In vitro autoradiography of receptor-activated G proteins in rat brain by agonist-stimulated guanylyl 5'-[gamma-[^{35}S]thio]-triphosphate binding. *Proc. Natl. Acad. Sci. U.S.A.* **92,** 7242–7246.
26. Fields, T. A. and Casey, P. J. (1997) Signalling functions and biochemical properties of pertussis toxin-resistant G-proteins. *Biochem. J.* **321,** 561–571.
27. Denhardt, D. T. (1996) Signal-transducing protein phosphorylation cascades mediated by Ras/Rho proteins in the mammalian cell: the potential for multiplex signalling. *Biochem. J.* **318,** 729–747.
28. Brandt, D. R. and Ross, E. M. (1985) GTPase activity of the stimulatory GTP-binding regulatory protein of adenylate cyclase, Gs. Accumulation and turnover of enzyme-nucleotide intermediates. *J. Biol. Chem.* **260,** 266–272.
29. Bottari, S. P., Taylor, V., King, I. N., Bogdal, Y., Whitebread, S., and de Gasparo, M. (1991) Angiotensin II AT_2 receptors do not interact with guanine nucleotide binding proteins. *Eur. J. Pharmacol.* **207,** 157–163.
30. Georgoussi, Z., Carr, C., and Milligan, G. (1993) Direct measurements of in situ interactions of rat brain opioid receptors with the guanine nucleotide-binding protein G_o. *Mol. Pharmacol.* **44,** 62–69.
31. Walsh, D. A., Suzuki, T., Knock, G. A., Blake, D. R., Polak, J. M., and Wharton, J. (1994) $AT_1$1 receptor characteristics of angiotensin analog binding in human synovium. *Br. J. Pharmacol.* **112,** 435–442.
32. Joseph, S. K. (1996) The inositol triphosphate receptor family. *Cell. Signal.* **8,** 1–7.
33. Worley, P. F., Baraban, J. M., Colvin, J. S., and Snyder, S. H. (1987) Inositol trisphosphate receptor localization in brain: variable stoichiometry with protein kinase C. *Nature* **325,** 159–161.

34. Walsh, D. A., Mapp, P. I., Polak, J. M., and Blake, D. R. (1995) Autoradiographic localisation and characterisation of [^{3}H]α-trinositol (1S-*myo*-inositol-1,2, 6-trisphosphate) binding sites in human and mammalian tissues. *J. Pharmacol. Exp. Therapeut.* **273,** 461–469.
35. Nagata, E., Tanaka, K., Gomi, S., Mihara, B., Shirai, T., Nogawa, S., Nozaki, H., Mikoshiba, K., and Fukuuchi, Y. (1994) Alteration of inositol 1,4,5-trisphosphate receptor after six-hour hemispheric ischemia in the gerbil brain. *Neuroscience* **61,** 983–990.
36. Caterina, M. J., Schumacher, M. A., Tominaga, M., Rosen, T. A., Levine, J. D., and Julius, D. (1997) The capsaicin receptor: a heat-activated ion channel in the pain pathway. *Nature* **389,** 816–824.

12

Whole Human Brain Autoradiography of Serotonin Re-Uptake Inhibitors

Michelle Qume and Jacqueline K. Miller

1. Introduction

Most of the autoradiography performed in human brain involves cutting sections from blocks of tissue or single hemispheres containing relevant areas. The resultant images are restricted to the particular region being studied and do not allow an overview of the plane in which the region is situated; hence, it is not always possible to make a direct comparison of binding in regions from different areas of the brain in the same image. Whole brain sections allow symmetrical measurements to be made from both hemispheres, and the visual image obtained may be compared with images obtained from Positron Emission Tomography (PET) scanning. The effects of unilateral lesion on receptors in the adjacent hemisphere may be determined, and the distribution of receptor sites affected by disease states can be mapped across the width of the brain to see if there is an asymmetrical pattern of receptor modification or loss.

The successful use of selective serotonin re-uptake inhibitors (SSRIs) such as paroxetine, imipramine, and fluoxetine has shown that the serotonin transporter plays a major role in defining the etiology and treatment of depression. By investigating the drugs that act at the serotonin re-uptake site, it may be possible to gain a further understanding of serotonin and its role in affective disorders.

There are two distinct mechanisms for serotonin uptake in neuronal tissues. The transporter present on vesicle membranes is characterized by its sensitivity to reserpine and tetrabenazine and the fact that vesicular uptake is unaffected by neurotoxic lesions of serotonergic neurones *(1,2)*. The second transport mechanism is found on neuronal membranes and is distinguished by

From: *Methods in Molecular Biology, Vol. 106: Receptor Binding Techniques*
Edited by: Mary Keen © Humana Press Inc., Totowa, NJ

its sensitivity to cocaine, imipramine, and the SSRIs, and the inhibition of binding of these drugs following lesions of the 5-HT terminal *(1,3)*. In this chapter, reference to the serotonin transporter will be limited to the second transport site.

The high affinity uptake of serotonin into astrocytes has been demonstrated in primary cultures and *in situ (4–6)*. Reports indicate that the serotonin uptake sites in glial and neuronal tissues do not show identical pharmacological or distribution profiles *(7)*, suggesting that these two serotonin transporters may not be related. However, it would be prudent to bear in mind glial binding capacity when performing radioligand binding experiments with serotonin reuptake inhibitors in brain tissue.

1.1. Human Tissue

Animal models of disease states have traditionally been used to investigate neuropathological changes under controlled circumstances, enabling viable statistical analysis to be performed. Early experiments using human brain tissue were hampered by a lack of sufficient sample sizes and uncertainty of the effect of variables such as age at death, *post mortem* delay, gender, and drug history. As technology has developed, and systematic collection of matched brain samples has increased, as well as the establishment of rapid autopsy programs *(8)*, extensive information regarding basic biochemical and neuroanatomical patterns in the human brain has been gathered. As a result of these developments, rapid progress has been made in the field of human neuropharmacology, and the use of human *post mortem* brain tissue is now a fundamental part of research into disease states of the human brain.

Availability of human brain samples can still be a problem, samples in both control and disease states may be obtained from brain banks around the country. With the help of clinicians, actual whole brains may be obtained following *post mortem*, as well as biopsy samples following surgical procedures, although the availability of adequate controls for surgical biopsies is very limited. It is important that neuropathological histological analysis is performed on the tissues to confirm the presence of the disease state under investigation (or not, in the case of control tissue), and to exclude the possibility of the presence of "unwanted" disorders. Tissue and patient history should also be screened to exclude the possibility of infectious disorders such as prion disorders, hepatitis, and AIDS, for investigator safety.

Following removal of the brain, it is usually sliced sagitally into its two hemispheres, with one hemisphere fixed for neuropathological examination and other procedures requiring fixation, whereas the other hemisphere is frozen (sectioned or not as the case may be). This is not suitable for whole brain

autoradiography; consequently, the tissue may be sliced coronally (2–4 cm), with sections divided into fixing and frozen groups as required, or else only a relevant portion of the brain removed and fixed.

Post mortem brains are very often from patients who died from disease states, normally at the end point of the disease. Following disease courses is therefore very difficult, with cause and effect questions being raised, *in vivo* imaging techniques such as PET should help to address these questions. Severity of the disease states is an important factor, and choosing tissues from patients with very severe disorders may bias results.

Obtaining adequate tissue, especially control tissue, is often a difficult procedure; as a result, details such as age, gender, agonal state, drug history, *post mortem* delay, storage length, and treatment of the brain including fast/slow freezing, use of cryoprotectants, and sectioning before freezing should be obtained and samples matched where possible, although compromises must often be made. Multiple regression analysis of details (e.g., as in **ref. *9***) may be used to determine effects (if any) of these variables on biochemical assays if the sample groups are large enough. It is possible to simulate *post mortem* conditions of body cooling and cold storage by using rat heads slowly cooled to room temperature, then stored at 4°C for varying amounts of time ***(10)***. The brains may then be used for radioligand binding (or other assay), allowing identification of possible changes in biological activity associated with *post mortem* delay.

This chapter explains a technique for preparing human whole brain (both hemispheres) autoradiography sections as well as autoradiography of serotonin re-uptake sites using [^{3}H]-paroxetine and [^{3}H]-imipramine. Cutting quality sections from whole human brain requires practice, pig brain obtained from an abattoir is useful preventing wastage of scarce human tissue. For optimization of radioligand binding assays, small samples of human tissue may be used, as these are more readily available. Both assays for the determination of paroxetine and imipramine binding sites are modified from that of Cortes et al. ***(11)***. 5 n*M* [^{3}H]-Paroxetine and 10 n*M* [^{3}H]-imipramine are used with the inclusion of 20 μ*M* citalopram or 100 μ*M* desipramine, respectively, to assess nonspecific binding (which may be 40–80% of total). Example autoradiograms obtained with this method are shown in **Fig. 1** with typical specific binding data detailed in **Table 1**.

2. Materials

1. Whole human brain.
2. Knife suitable for slicing brain or commercially available meat slicer.
3. White backing card.

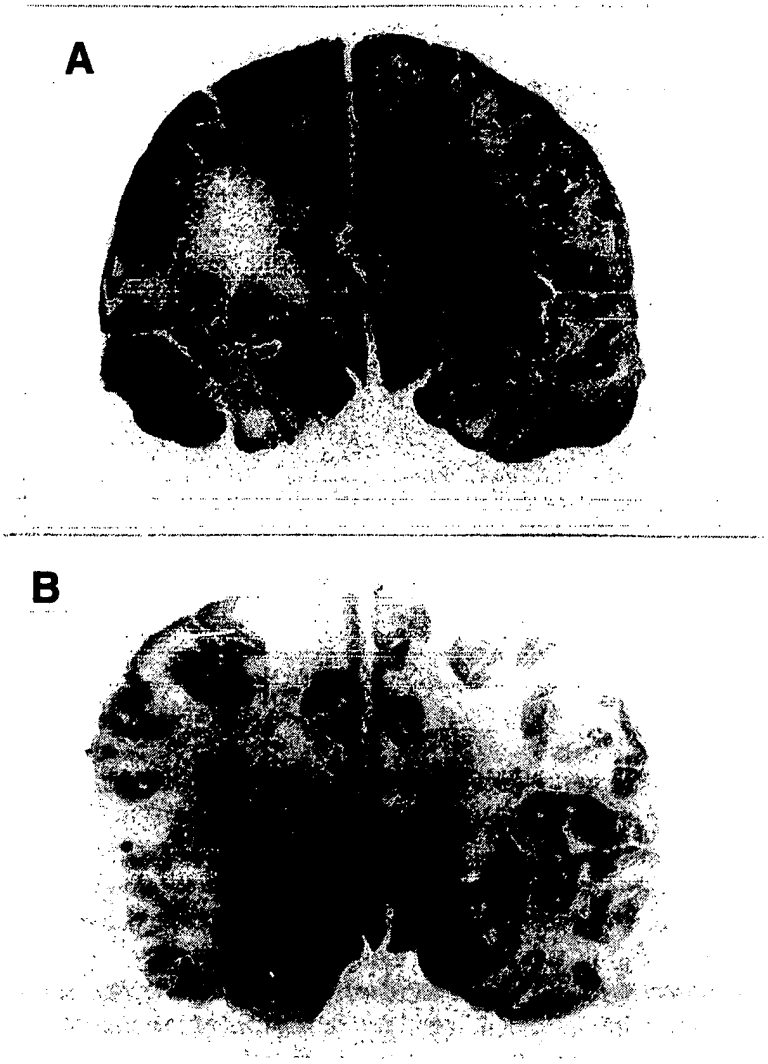

Fig. 1. Typical autoradiograms showing the total distribution of: (**A**) 5 n*M* [^{3}H]-paroxetine and (**B**) 10 n*M* [^{3}H]-imipramine binding sites in thalamic and hypothalamic regions of whole human coronal brain sections.

4. Airtight plastic bags that are large enough to store tissue slices.
5. Carboxymethylcellulose (CMC): 2% (Sigma-Aldrich Company Ltd., Poole, Dorset, U.K.) in distilled water, cooled to 4°C (*see* **Note 1**.)
6. Wooden frame suitable for embedding brain slices, with an aluminium base plate. **Fig. 2** shows a frame made "inhouse" for this purpose (*see* **Note 2**).

Table 1
Typical Values of Specific [^{3}H]-paroxetine (5 n*M*) and [^{3}H]-imipramine (10 n*M*) Binding to 5-HT Re-Uptake Sites in Human Whole Brain Sections

Region	[^{3}H]-Paroxetine	[^{3}H]-Imipramine
Cerebral aqueduct	153 ± 32	62 ± 6
Superior central raphe	430 ± 79	127 ± 14
Basal pons	40 ± 10	5 ± 2
Superior cerebellar peduncle	16 ± 6	5 ± 2
Hypothalamus	108 ± 11	53 ± 7
Midline thalamic nuclei	152 ± 34	56 ± 10
Anterior thalamic nuclei	34 ± 9	36 ± 9
Lateral thalamic nuclei	22 ± 8	42 ± 12
Dorsomedial thalamic nuclei	50 ± 15	41 ± 10
Caudate nuclear body	48 ± 18	58 ± 11
Globus pallidus	33 ± 4	32 ± 6
Putamen	40 ± 13	34 ± 6
Amygdala	72 ± 19	27 ± 6

Data was produced using a Quantimet 970 image analyser and is expressed as mean ± s.e.m, n = 3.

7. Vacuum grease.
8. Membrane: Hybond N$^+$, positively charged nylon membrane (Amersham International P.L.C., Little Chalfont, Buckinghamshire, U.K.) or Electran (BDH, Merck Ltd., Lutterworth, Leicestershire, U.K.), cut to size: 15 × 13cm (*see* **Notes 2** and **3**).
9. Cryostat suitable for sectioning whole human brain: e.g., LKB PMV 2500-modified for cutting human tissue.
10. Plastic holder/spatula to smooth the membrane over the tissue block (*see* **Notes 2** and **4**).
11. Adhesive tape: e.g., Sellotape.
12. Perspex "window" frames to attach membrane backed sections, capable of fitting into the 5 L wash chamber (item 20). The overall dimensions of the "inhouse" produced frames are 23 × 20 cm (0.5 cm thick perspex) and with the window of 17.5 × 15 cm.
13. Incubation buffer: 50 mM Tris HCl, 120 mM NaCl, 5 mM KCl, pH 7.4. (Sigma-Aldrich Company Ltd., Poole, Dorset, U.K. or BDH, Merck Ltd., Lutterworth, Leicestershire, U.K.). Buffer is required at 4°C for [^{3}H]-imipramine incubation and washing (*see* **Note 5**).
14. [^{3}H]-Paroxetine: 5 nM (NEN Life Science, Harlow, U.K.) (*see* **Notes 6** and **7**).
15. Citalopram: 20 µM (available on application from H. Lundbeck, Copenhagen, Denmark), to assess nonspecific binding for [^{3}H]-paroxetine binding (*see* **Note 6**).

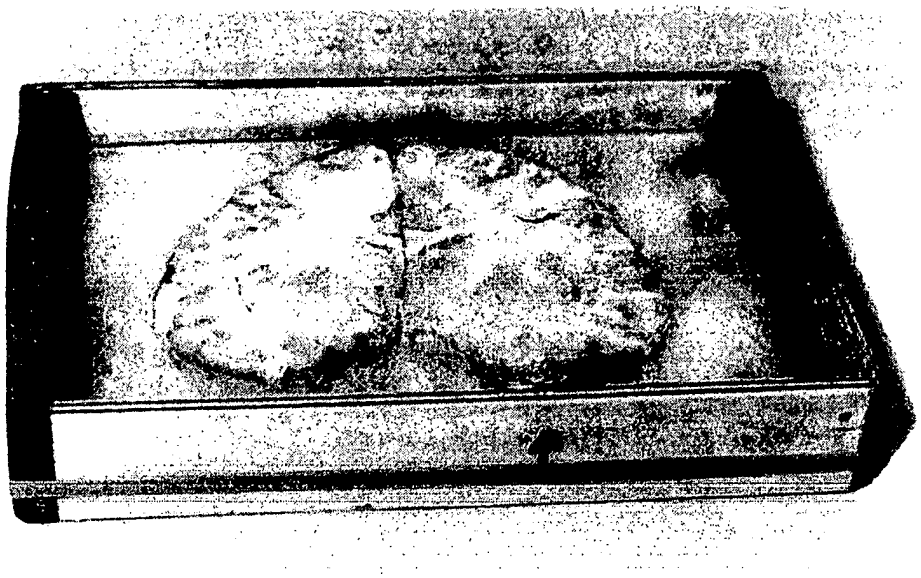

Fig. 2. Each whole brain slice is embedded in a 2% carboxymethylcellulose solution and frozen to a solid block in a wooden frame with an aluminium base plate. The frame was made up of 2 "L" shaped pieces, allowing easy removal of the slice.

16. [^{3}H]-Imipramine: 10 n*M* (NEN Life Science, Harlow, U.K.) (*see* **Note 6** and **7**).
17. Desipramine: 100 µ*M* (Sigma-Aldrich Company Ltd., Poole, Dorset, U.K.), to assess nonspecific binding for [^{3}H]-imipramine binding (*see* **Note 6**).
18. Scintillation fluid: e.g. Optiphase Safe (FSA Laboratory Supplies, Leicestershire, U.K.).
19. Scintillation counter: e.g. Tri Carb 1500TR (Canberra Packard, Pangbourne, Buckinghamshire, U.K.).
20. Perspex 5 L wash chamber (produced "inhouse") allowing 6–8 perspex frames (item 12) to slide in and be held in a vertical position, similar to normal slide racks and washing chamber, but on a larger scale.
21. Glass plates (20 cm × 20 cm).
22. Short tipped Pasteur pipet.
23. Vacuum pump.
24. Cool air hairdryer.
25. Freeze drier (*e.g.* Edwards Micro Modulyo, Edwards High Vacuum International, Crawley, West Sussex, U.K.).
26. SprayMount: (3M United Kingdom PLC, 3M House, Bracknell, Berks, U.K.).
27. Dark room with appropriate safe-light conditions (*see* **Note 8**).

28. Hyperfilm-[^{3}H] (Amersham International P.L.C., Little Chalfont, Buckinghamshire, U.K.).
29. [^{3}H]-Microscales (Amersham International P.L.C., Little Chalfont, Buckinghamshire, U.K.).
30. X-ray cassettes (Genetic Research Instrumentation Ltd, Essex. U.K.).
31. Film wash baths (4 are required): *e.g.*, BDH, Merck Ltd., Lutterworth, Leicestershire, U.K.
32. Kodak D-19 developer: 1 in 4 dilution, with distilled water, 2.5 L should be sufficient (Kodak-Pathe, Paris, France) (*see* **Note 9**).
33. Kodak Unifix fixative: 1 in 4 dilution, with distilled water, 2.5 L should be sufficient (Kodak-Pathe, Paris, France) (*see* **Note 9**).
34. Densitometric image analysis system: e.g., MicroComputer Imaging Device (MCID), Imaging Research, Inc., Ontario, Canada.

3. Methods

In order to reduce ice crystal formation, all handling procedures should be carried out as swiftly as possible (*see* **Note 10**).

3.1. Cutting Whole Brain Coronal Sections

3.1.1. Collection and Storage of Tissue

Whole human brains are obtained post mortem. Histological analysis should be performed on some of the tissue to confirm neurological disease status (e.g., Alzheimer's disease, prion disease or control). To avoid the risk of infection from diseases such as hepatitis B and HIV, brains from patients with a history of drug abuse, hemophilia, or homosexuality may be excluded.

Following *post mortem*, remove the whole brain and either freeze to –80°C directly (*see* **Note 12**), or else slice into 1–3 cm coronal sections using a brain knife (*see* **Note 13**), place on card, to help prevent distortion (*see* **Note 12**), and then place in individual, labelled airtight plastic bags and freeze at –80°C. Whole brains that were previously frozen may later be brought up to a temperature of –20°C and cut into 1–3 cm coronal sections using a commercially available meat slicer (*see* **Note 13**). Store these sections at –80°C in individual labeled airtight plastic bags.

3.1.2. Embedding Brain Slices

1. Remove slice from the freezer and place in the wooden frame (**Fig. 2**; *see* **Note 14**).
2. Embed the section by pouring over the chilled CMC.
3. Store overnight at –20°C and then remove slice from frame. If the embedded slice is to be stored prior to sectioning they may be kept, in sealed bags, at –80°C (*see* **Note 15**.)

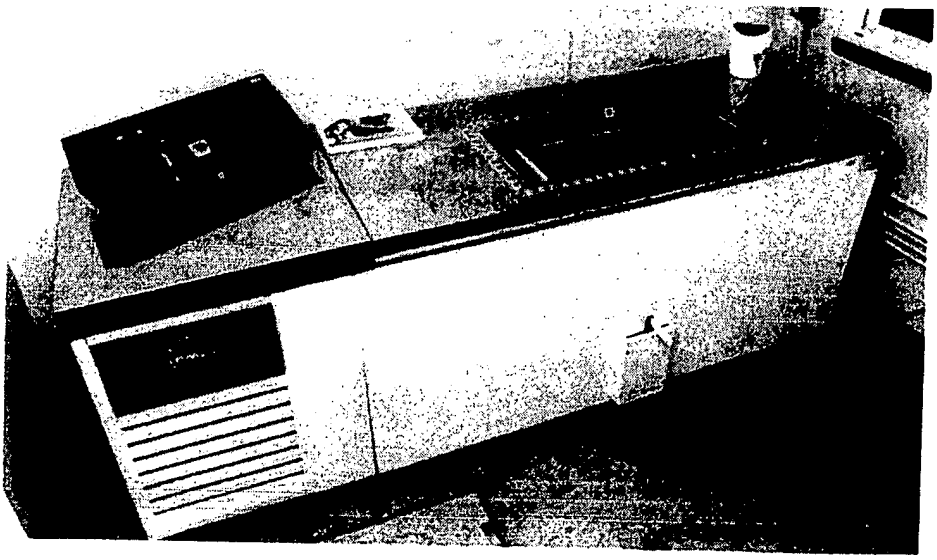

Fig. 3. An LKB PMV 2500 whole body cryostat modified for human tissue use.

3.1.3. Sectioning of Tissue

1. Section the brain using a LKB PMV 2500 whole body cryostat (**Fig. 3**). Cut 40 μ*M* thick sections; a knife angle of 20° and a temperature of −16°C was used in these experiments (*see* **Note 16**).
2. Stick embedded tissues to the stage using semi-liquid 2% CMC (4°C) as an adhesive (**Fig. 4**).
3. Leave the block to equilibrate to −16°C in the cryostat for 2–3 hours.
4. Shave the tissue block down to expose the areas of interest by cutting relatively thick sections (90–150 μ*M*).
5. Place a piece of the positively charged membrane over the tissue block.
6. Smooth the membrane over the tissue with the plastic spatula, then while cutting the section, gently press the spatula against the membrane at the knife edge. The tissue should adhere to the membrane as the section is being cut (*see* **Note 17, Fig. 5**).
7. The membrane may be carefully labeled with a pencil below the area of the section (*see* **Note 18**).
8. Thaw mount the section onto the membrane for 5 min, (*see* **Note 19**) and secure to perspex frames with adhesive tape.
9. Store these sections in labelled airtight bags at −20°C for subsequent binding.

3.2. Autoradiographic Distribution of SSRIs

3.2.1. Autoradiographic Distribution of [^{3}H]-Paroxetine

Binding is normally carried out in triplicate with serial sections alternated between binding conditions (i.e. total, nonspecific and test compounds, if using).

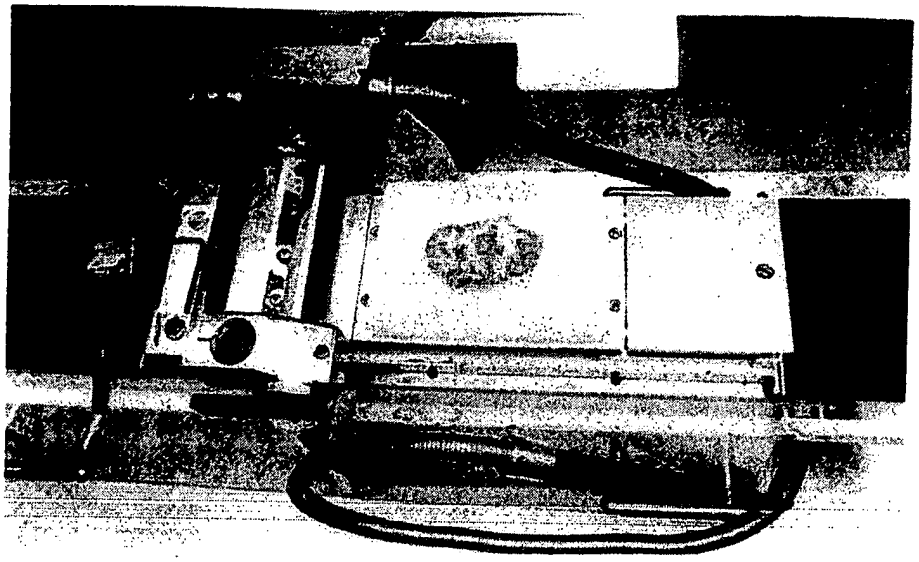

Fig. 4. The frozen block of CMC embedded tissue is secured to an aluminium stage and screwed down onto the moveable platform of the cryostat.

1. Remove sections from freezer and equilibrate to room temperature for 1 h.
2. Preincubate in buffer for 15 min in 5 L perspex wash chambers.
3. Allow sections to dry at room temperature, remove from perspex frames, leaving the adhesive tape on the frame, and place onto glass plates, sections facing upwards.
4. Pour 10–15 mL (depending on area to be covered) of [^{3}H]-paroxetine in incubation buffer over the section drop by drop to form a pool of incubation medium (*see* **Note 20**). Nonspecific binding may be determined by the inclusion of 20 μM citalopram.
5. Incubate at room temperature for 2 h (*see* **Note 21**).
6. Aspirate the radioligand buffer from around the section with a Pasteur pipet attached to a vacuum pump, taking care not to scratch the section.
7. Rinse the sections for a few seconds in buffer.
8. Reattach the sections to the adhesive tape on the perspex frames by stapling (they will not adhere when wet).
9. Wash off excess radioligand by placing the sections in the 5 L wash chambers containing fresh incubation buffer for 2 × 60 min, at room temperature.
10. Remove excess buffer and salts by dipping the sections in distilled water for 4 s.
11. Dry the sections under a stream of cool air using a hairdryer.
12. Complete the drying process by placing the sections in a freeze drier for 1 h.
13. When thoroughly dry, remove the sections from the frames.
14. Glue to white backing card with SprayMount, label the card.

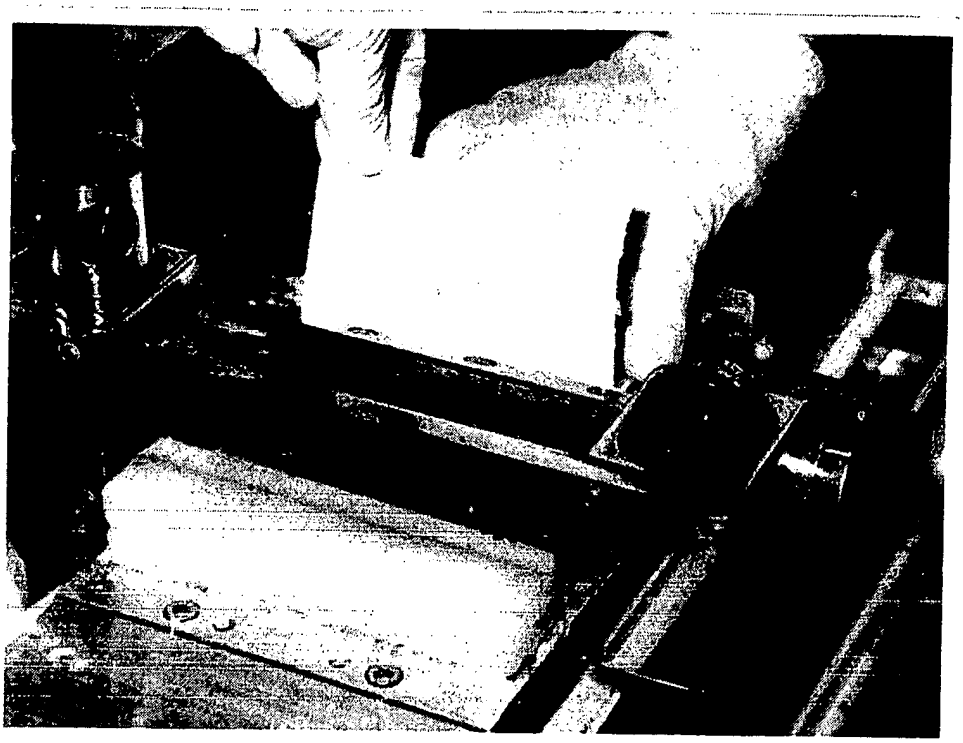

Fig. 5. As the 40 μ*M* section is cut, it adheres to the membrane and is pulled up and away from the knife edge. A plastic spatula is pressed against the knife edge to ensure uniform adhesion to the membrane.

15. Carefully place the section, tissue side up, in a light proof X-ray cassette and place a calibrated [^{3}H]-microscale on the card (*see* **Note 22**).
16. In a dark room under safe-light conditions, carefully apply the sections to Hyperfilm-[^{3}H] with emulsion side towards the film (*see* **Note 23**). Close and label the cassette.
17. Store at room temperature (*see* **Note 24**) for 4 wk (*see* **Note 25**).

3.2.2. Autoradiographic Distribution of [^{3}H]-Imipramine

The procedure is essentially the same as that for [^{3}H]-Paroxetine (**Subheading 3.2.1.**), although the following steps are altered:

Step 4. 10 nM [^{3}H]-Imipramine in incubation buffer (4°C is used for the radioligand incubation, non-specific binding may be determined by the inclusion of 100 μ*M* desipramine.
Step 5. Incubate at 4°C for 1 h incubation (*see* **Note 26**).
Step 8. Washing is carried out in the 5 L wash chambers for 10 and then 20 min using chilled incubation buffer (*see* **Note 27**).

Step 16. Owing to the higher specific activity of the radioligand batch used, 2 wk apposition was sufficient (*see* **Note 25**).

3.3. Development and Fixation of Autoradiograms

1. Prepare 4 film wash baths in order from left to right (*see* **Note 28**):
   a. Developer.
   b. Running tap water (*see* **Note 29**).
   c. Fixative.
   d. Running tap water (*see* **Note 29**).

This procedure is carried out in a dark room under safe-light conditions, with the film *carefully* handled (*see* **Note 23**).

2. Remove the film carefully from the cassettes.
3. Place film, apposed side up (to minimize scratching) in developer (bath 1) and agitate/rock gently for 60–90 seconds.
4. Carefully remove film to bath 2 and wash film for 1 min under running tap water.
5. Place film into bath 3 (fixative) for 3 min, agitating/rocking gently.
6. Wash in bath 4 for 25 min under running tap water (*see* **Notes 29** and **30**).
7. Air dry overnight.

3.4. Analysis

The optical density of the photographic images generated on film may be measured using an image analyzing system. Using the calibration curve obtained from the [^{3}H]-microscales, the optical density can be converted to nCi/mg tissue, allowing the expression of the binding as fmol/mg tissue. Specific binding is defined as the difference between total and nonspecific binding.

4. Notes

1. CMC is an embedding matrix providing structural support during sectioning. The solution may be prepared upto 1 wk prior to use and stored in the fridge.
2. These items may be pre-cooled by placing in a fridge/cryostat prior to use, helping to prevent warming of the tissue.
3. A number of adhesive tapes may be used to hold sections while they are being cut. There are three main types of adhesives used: synthetic, rubber- and resin-types, and silicone-treated adhesives. Results of experiments indicated that different ligands bind with differing affinity to tape, with [^{3}H]-paroxetine binding highly. Membranes (with a lower binding affinity for the radioligands used) were therefore subsequently used for determination of binding. It is much easier to cut good quality sections onto tape than membranes; therefore, this should not be ruled out as an option in experiments with other radioligands. Unfortunately, the use of support structures to enable sectioning of tissue does tend to increase non-specific binding, but it is necessary for the production of suitable sections.
4. Although a plastic spatula was used for these experiments, a "print" roller may be employed instead.

5. Buffer may be made up the day before use; this is especially recommended with the large volumes (20 L) involved and the 4°C buffer required for [^{3}H]-imipramine binding.
6. Drug solutions are made up in incubation buffer on the day of assay.
7. The amount of radioactivity in the incubation medium may be estimated by aliquoting a known amount of the medium into a scintillation vial, vortexing with scintillation cocktail, and counting on a scintillation counter.
8. Instructions supplied with the film should indicate what safe-lighting conditions are suitable.
9. This may be made up in advance and stored at room temperature in a cupboard in the darkroom.
10. Safety is a very important factor when working with both radiochemicals and human tissues. Protective clothing, eye protection, and gloves should all be worn. Precautions should be taken to minimize contamination (both of workers and equipment), including adequate labeling. Disinfection of all surfaces and equipment is required, as is careful disposal of contaminated waste.
11. The most obvious artefact found with human whole brain autoradiography is the formation of ice crystals within the tissue. The larger the volume of tissue being frozen (e.g., whole brains), the more slowly the heat dissipates out from the centre of the block. This results in ice-crystal formation that can distort the microstructure by physically breaking up the tissue. When the tissue is brought up to room temperature, the ice crystals melt and evaporate, leaving cracks. These cracks in the tissue mean that the backing material is exposed to the radioligand during incubation; subsequently, they show up when the film is developed. Since the amount of exposure to the film through these cracks is not constant, any quantitative image analysis may lead to inaccurate results.

    Ideally, the brain should remain at –80°C during all handling procedures until it is brought up to –20°C for sectioning; however, this is not possible. If the brain is frozen whole, it has to be brought up to –20°C to cut it into 1–3 cm slabs that are then stored at –80°C until required. When each slab is embedded, the outer surface of the tissue comes into contact with semi-liquid embedding medium (CMC) chilled to 4°C. This is then stored at –20°C overnight before sectioning. During these procedures, it is impossible to avoid ice crystal formation. Quirion et al. *(12)* suggested that slicing the brain into 1 cm slabs immediately after autopsy and rapidly freezing them in isopentane at –40°C would reduce ice crystal formation. Rosene et al. *(13)* carried out an extensive study on the effect of ice crystal freezing artefacts and the use of cryoprotectants. To produce optimum freezing conditions, they submerged the brain in a cryoprotectant solution of 20% glycerol and 2% dimethylsulphoxide (DMSO) for a minimum of 4 d at –4°C before freezing the tissue. Two percent DMSO was employed to improve the infiltration rate of the glycerol. The use of this solution improves the quality of the sections by reducing ice crystal formation and also prevent tissue damage from brittle cracking. However, the use of cryoprotectants is dependent on the

tissue being fixed *post mortem*, and the use of fixative may alter the binding of radioligands.

12. It is important that the brain remains in its original shape during freezing and is not squashed.
13. When the whole brain is being cut into slices, it is important to cut them as symmetrically as possible.
14. A thin layer of vacuum grease may be used to coat the inside of the frame to facilitate easy removal of the slice.
15. Slices should be brought up to a temperature of −20°C prior to sectioning. Remove from the −80°C freezer and place in a −20°C freezer overnight.
16. The use of a sharp machine-honed knife is essential for preventing undue tissue damage during the sectioning process. Knives should be changed regularly to reduce both the possibility of tissue cracks and variability in section thickness.
17. The amount of pressure placed on the membrane over the tissue section is crucial to the integrity of the section being cut. Too much pressure leads to a better-cut section, but it tends to compact the tissue, resulting in a section far smaller than the original block size. Without enough pressure, the section does not hold to the membrane; it falls off as it is being handled.
18. Care should be taken during all procedures that the section can be identified, as well as pencil marking, the use of sticky labels on the perspex frames and glass plates will aid this.
19. To reduce ice-crystal formation, attempts have been made to use sections that had not been thaw-mounted onto the membranes; however, these could not withstand the incubation and washing procedures.
20. A border of vacuum grease drawn around each section will prevent spreading of incubation buffer.
21. Rolled-up tissue paper soaked in buffer around the glass plate and a perspex lid helps reduces evaporation.
22. The microscales are therefore at the same level as the section.
23. Film should be gently handled, so as not to scratch the emulsion; either hold at the edges or a corner *away* from that near the section.
24. It is best to store these cassettes in the dark (e.g., a drawer) to prevent light from entering.
25. The duration of exposure depends on the specific activity of the particular batch of radioligand used, those employed in this technique were [^{3}H]-paroxetine (15–21 Ci/mmol) and [^{3}H]-imipramine (53 Ci/mmol).
26. Use of a cold-room or cooling plate (4°C) is helpful, although incubating sections may be carefully placed in a refrigerator.
27. If necessary, this wash may be carried out in a cold-room, fridge, or else some incubation buffer may be frozen in ice cube trays and the resulting "ice" cubes placed in the wash chamber to prevent the temperature from rising, although for a maximum 20 min wash, this should not be a great problem.

28. It is very important that the various baths are laid out, so the worker can easily identify them under safe-light conditions.
29. The baths should be positioned so that the stream from the running tap does not fall directly onto the film and that the water flows *gently* over the film.
30. Normal lighting conditions may be resumed during this step.

Acknowledgments

The authors gratefully acknowledge Professor N. G. Bowery, in whose laboratory the experiments were performed; Dr Ian Tulloch for his help, and Andrew Billinton for his advice. We also wish to thank St. George's Hospital, London and Runwell Hospital, Essex for the provision of human tissue and SmithKline Beecham for their financial support.

References

1. Ross, S. B. (1982) The characteristics of serotonin uptake systems, in *Biology of Serotonergic Transmission* (Osborne, N. N. ed.), Wiley, London, pp. 159–195.
2. Slotkin, T. A., Seidler, F. J., Withmore, W. L., Lau, W. L., Salvaggio, M., and Kirksey, D. F. (1978) Uptake and specificities of ^{3}H-norepinephrine and ^{3}H-serotonin in preparation from whole brain and brain regions. *J. Neurochem.* **31,** 961–968.
3. Marcusson, J. O. and Ross, S. B. (1990) Binding of some antidepressants to the 5-hydroxytryptamine transporter in brain and platelets. *Psychopharmacol.* **102,** 145–155.
4. Katz, D. M. and Kimelberg, H. K. (1985) Kinetics and autoradiography of high affinity uptake of serotonin by primary astrocyte cultures. *J. Neurosci.* **5,** 1901–1908.
5. Kimelberg, H. K. (1986) Occurrence and functional significance of serotonin and catecholamine uptake by astrocytes. *Biochem. Pharmacol.* **33,** 2273–2281.
6. Anderson, E. J., McFarland, D., and Kimelberg, H. K. (1992) Serotonin uptake by astrocytes *in situ*. *Glia* **6,** 9–18.
7. Whitaker, P. M., Vint, C. K., and Morin, R. (1983) ^{3}H-Imipramine labels sites on brain astroglial cells not related to serotonin uptake. *J. Neurochem.* **41,** 1319–1323.
8. Procter, A., Doshi, B., Bowen, D., and Murphy, E. (1990) Rapid autopsy brains for biochemical research: Experiences in establishing a programme. *Int. J. Ger. Psych.* **5,** 287–294.
9. Procter, A. W., Francis, P. T., Holmes, C., Webster, M. T., Qume, M., Stratmann, G. C., Doshi, R., Mann, D. M. A., Harrison, P. J., Pearson, R. C. A., and Bowen, D. M. (1994) β-Amyloid precursor protein isoforms show correlations with neurones but not with glia of demented subjects. *Acta Neuropathol.* **88,** 545–552.
10. Procter, A. W., Stratmann, G. C., Francis, P. T., Lowe, S. L., Bertolucci, P. H. F., and Bowen, D. M. (1991) Characterisation of the glycine modulatory site of the N-Methyl-D-Aspartate receptor ionophore complex in human brain. *J. Neurochem.* **56,** 299–310.

11. Cortes, R., Soriano, E., Pazos, A., Probst, A., and Palacios, J. M. (1988) Autoradiography of antidepressant binding sites in the human brain: localization using ^{3}H-imipramine and ^{3}H-paroxetine. *Neuroscience* **27,** 473–496.
12. Quirion, R., Robitaille, Y., Martial, J., Chabot, J.-G., Lemoine, P., Pilapil, C., and Dalpe, M. (1987) Human brain receptor autoradiography using whole hemisphere sections. *Synapse* **1,** 446–454.
13. Rosene, D. L., Roy, N. J., and Davis, B. J. (1986) A cryoprotection method that facilitates cutting frozen sections of whole monkey brains for histological and histochemical processing without freezing artifact. *J. Histochem. Cryochem.* **34,** 1301–1315.

13

Measurement of Agonist-Stimulated [^{35}S]GTPγS Binding to Cell Membranes

Sebastian Lazareno

1. Introduction

This chapter describes a functional assay which measures the increase in guanine nucleotide exchange at G-proteins in cell membranes, resulting from agonist binding to G-protein-coupled receptors (GPCRs), by monitoring the binding of [^{35}S]GTPγS, a radiolabeled, hydrolysis-resistant analog of GTP (guanosine triphosphate), in the presence of unlabeled GDP (guanosine triphosphate).

The function of GPCR activation is to stimulate GTP/GDP exchange at G-proteins *(1)* (**Fig. 1**). In a cell, the guanine nucleotide exchange cycle is initiated by the binding of an agonist-occupied (or "activated") GPCR to a heterotrimeric G-protein in the cell membrane. This stimulates the dissociation of GDP from the α subunit of the G-protein, allowing endogenous GTP to bind in its place. In turn, this causes the dissociation of the receptor and the Gα-GTP and Gβγ subunits of the G-protein. The Gα-GTP and Gβγ subunits can each activate effectors such as adenylyl cyclase, phospholiase C, and ion channels *(1)*. The Gα-GTP is inactivated by an intrinsic GTPase activity, which hydrolyzes the GTP to GDP, and Gα-GDP in turn inactivates the Gβγ by binding to it. This results in an inactive GDP-containing heterotrimeric G-protein that is ready for the next activation cycle.

This process can be monitored in vitro by incubating cell membranes containing G-proteins and GPCRs with GDP and [^{35}S]GTPγS. Binding of [^{35}S]GTPγS, like GTP, stimulates dissociation of Gα-[^{35}S]GTPγS and Gβγ. However, unlike GTP, [^{35}S]GTPγS is relatively resistant to hydrolysis by the intrinsic GTPase of Gα. It dissociates slowly from Gα and therefore accumulates in the membranes. The effect of receptor activation on [^{35}S]GTPγS bind-

From: *Methods in Molecular Biology, Vol. 106: Receptor Binding Techniques*
Edited by: Mary Keen © Humana Press Inc., Totowa, NJ

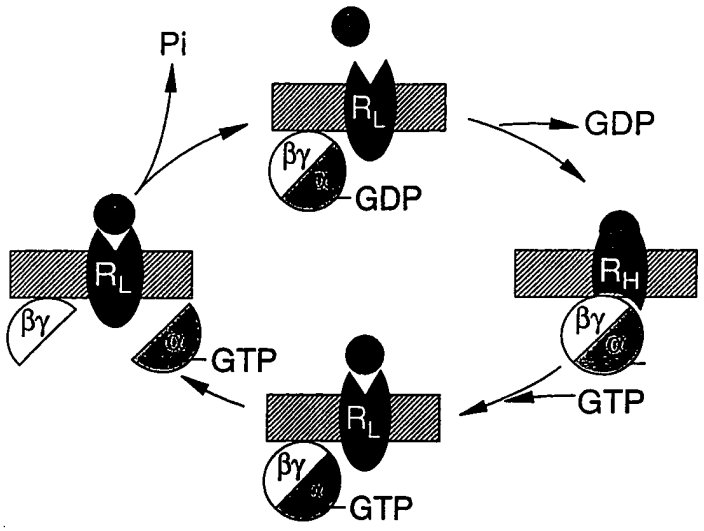

Fig. 1. Guanine nucleotide (GDP/GTP) exchange cycle at G-proteins (αβγ) stimulated by agonist (**A**) binding to receptor (high agonist affinity state, R_H, or low agonist affinity state, R_L).

ing in the presence of GDP is catalytic in that it increases the rate of [^{35}S]GTPγS binding rather than the equilibrium level of [^{35}S]GTPγS binding. Consequently, this is intrinsically a nonequilibrium binding assay (*see* **Note 1**).

The assay of agonist-stimulated [35S]GTPγS binding has a number of useful features:

1. It can use the same membrane preparations and assay conditions used in studies that measure radioligand binding to the GPCR, thus allowing a direct comparison of agonist action and agonist occupancy of the receptor.
2. It allows a measure of agonist action in systems where the subsequent effector mechanisms are unknown.
3. It allows a direct comparison of receptor activation with receptors that activate different G-protein-regulated effector systems.
4. It is convenient, easy, quick, and relatively accurate.

The method used to measure agonist-stimulated [^{35}S]GTPγS binding is a modification of methods described by Jakobs et al. *(2,3)*.

2. Materials

1. [^{35}S]GTPγS: (NEN;1000–1400 Ci/mmol) (*see* **Note 2**).
2. Cell membranes: Prepare these as indicated in **Subheading 3.1.**

3. Homogenizing buffer: 20 m*M* Hepes/Na Hepes, pH 7.4, 10 m*M* EDTA. Protease inhibitors and reducing agents may also be included if required *(4)*. It is convenient to prepare or purchase stock solutions of 500 m*M* EDTA, which is stored at room temperature, and 1*M* Hepes/Na Hepes, which is stored at 4°C. A mixture of equal volumes of 1*M* Hepes and 1*M* Na Hepes should have a pH of approx 7.5 when diluted to 20 m*M*.
4. Membrane storage buffer: 20 m*M* Hepes/Na Hepes, pH 7.4, 0.1 m*M* EDTA.
5. Assay buffer: 20 m*M* Hepes/Na Hepes, pH 7.4, 100 m*M* NaCl, 10 m*M* $MgCl_2$, 1 μ*M* GDP (*see* **Note 3**).
6. Washing buffer: 10 m*M* sodium phosphate buffer, pH 7.4. A mixture of Na_2HPO_4 and NaH_2PO_4, each at 10 m*M*, in the ratio 1.4:0.6 v/v, has a pH of approx 7.4.
7. Protein assay reagents: Most standard protein assays (e.g., Lowry or Bradford assays) are suitable.
8. Teflon spatula.
9. Polytron homogenizer or similar.
10. Refrigerated centrifuge and tubes suitable for centrifugation at 40,000*g*.
11. Cell harvester (e.g., Brandel) and Whatman GF/B filters (Semat, St. Albans Herts).

3. Methods

3.1. Preparation of Membranes

1. Wash the cells (e.g., CHO cells) twice with 10-mL ice-cold homogenization buffer and scrape them off the culture plate with a teflon spatula and 2 × 3 mL ice-cold homogenization buffer.
2. Homogenize the cells with 3–4 5-s bursts of a Polytron homogenizer (setting 6, with 30 s on ice between bursts).
3. Dilute the homogenate to 30 mL with ice-cold homogenization buffer, and centrifuge at 40,000*g* for 10 min at 4°C.
4. Discard the supernatant and rehomogenize the pellet in 30-mL ice-cold membrane storage buffer. Centrifuge at 40,000*g* for 10 min at 4°C.
5. Repeat **Step 4**.
6. Resuspend the pellet in approx 5-mL ice-cold membrane storage buffer.
7. Determine the protein content (*see* **Note 4**).
8. Dilute the membrane preparation to 2 mg/mL protein with ice-cold membrane storage buffer and store in 0.5-mL aliquots at –70°C.

3.2. Measurement of Agonist Effect

1. Thaw an aliquot of frozen membranes and dilute to a concentration of 20 μg protein/mL in ice-cold assay buffer containing 1-μ*M* GDP (*see* **Note 3**). Store on ice.
2. Prepare 5-mL polystyrene test tubes in triplicate (*see* **Note 5**) with 10 μL of each test agent made up to 100 times the final concentration required in the assay.
3. Thaw an aliquot of [^{35}S]GTPγS and dilute a portion to a concentration of about

10 n*M* in assay buffer; if the original [^{35}S]GTPγS has been stored at 10-fold dilution, dilute it a further 100-fold (*see* **Note 2**).
4. Add the diluted [^{35}S]GTPγS to the diluted membranes, 10-μL label for each milliliter of membranes and mix well. At 4°C, in the presence of GDP, binding of 0.1 n*M* [^{35}S]GTPγS is very slow.
5. Distribute 1 mL aliquots of membranes + GDP + [^{35}S]GTPγS to the prepared tubes.
6. Incubate the samples at 30°C for 30 min.
7. Filter the samples over wetted (with water) glass fiber filters (Watman GF/B), and wash twice with 3-ml ice-cold washing buffer (*see* **Notes 6–8**).
8. Distribute the filter disks to scintillation vials and add scintillation fluid (see **Note 9**).
9. Distribute 10-μL diluted [^{35}S]GTPγS (or 100-μL membranes + label) in duplicate to scintillation vials for measurement of added label.
10. Determine the radioactivity in each sample using scintillation spectroscopy (*see* **Note 9**).

3.3. Measurement of Antagonist Affinity

1. Potent antagonists often have slow dissociation kinetics, so expose the membranes to the agonist and antagonist for sufficient time, e.g., 30 min, for binding equilibrium of both ligands to be attained before addition of [^{35}S]GTPγS to the assay. For consideration of the experimental design, *see* **Note 10**.
2. Perform **steps 1–3** of **Subheading 3.2.**
3. Distribute 1-mL membranes + GDP to the prepared tubes.
4. Incubate the samples at 30°C for 30 min.
5. Add 10 μL [^{35}S]GTPγS to the samples.
6. Perform **steps 6–10** of **Subheading 3.2.**
7. Analysis of the data is discussed in **Note 11**.

3.4. Quantitation of Allosteric Modulator

Some GPCRs, such as the muscarinic and adenosine A1 receptors, contain a second site at which agents can bind, with the effect of modulating the affinity of a directly acting ligand, such as the endogenous agonist *(5)*.

1. Use an experimental design suitable for Schild analysis (*see* **Note 10**).
2. If the allosteric agent has rapid dissociation kinetics (i.e., a Kd > 10^{-7} *M*), then use the procedure of **Subheading 3.2.**, otherwise use the procedure of **Subheading 3.3.**
3. Analysis of the data is discussed in **Note 12**.

3.5. Simultaneous Measurement of Agonist Binding and [^{35}S]GTPγS Binding

The [^{35}S]GTPγS binding assay can be modified to allow simultaneous measurement of antagonist binding and functional effects on agonist-stimulated

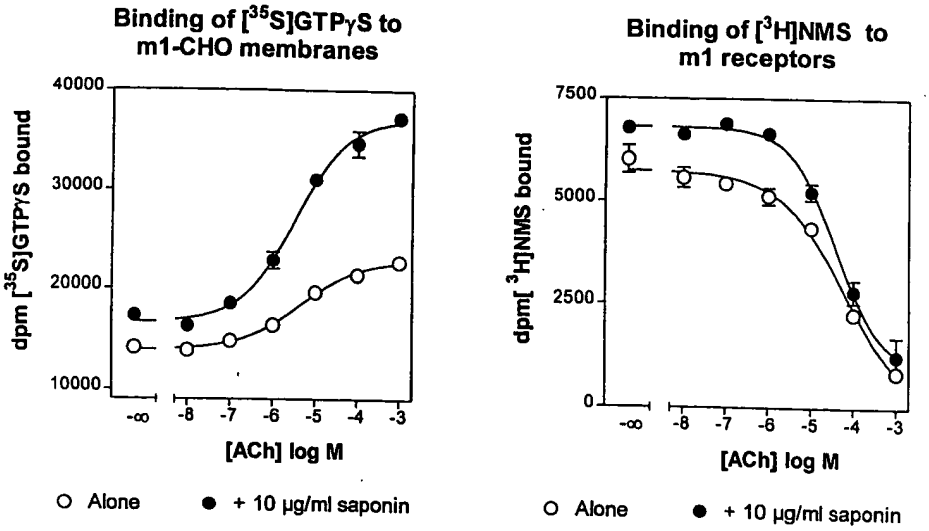

Fig. 2. Dual label experiment to measure simultaneously the effect of saponin on ACh stimulation of [^{35}S]GTPγS binding to G-proteins and inhibition of antagonist radioligand (^{3}H-NMS) binding to muscarinic m1 receptors stably expressed in CHO cells; 0.1-µ*M* GDP was present. The assay was conducted in duplicate.

[^{35}S]GTPγS binding *(6)*. An example of data from this type of assay is shown in **Fig. 2**.

1. Prepare tubes with 10-µL agonist and 1-mL membranes containing GDP.
2. Add 10 µL [^{3}H]antagonist radioligand, and incubate at 30°C until binding is at equilibrium.
3. Add 10-µL diluted [^{35}S]GTP*S* to each tube and continue the incubation for 30 min.
4. Filter over-wetted (with water) filters, and wash twice with 3-mL ice-cold washing buffer (*see* **Notes 6** and **8**).
5. Distribute the filter disks to scintillation vials, and add scintillation fluid (*see* **Note 13**).
6. Determine the radioactivity in each filter using the dual ^{3}H/^{35}S label program provided with the scintillation counter (*see* **Notes 13** and **14**).

3.6. Improving the Signal-to-Noise Ratio

If the signal-to-noise ratio is low, the following steps may help:

1. Optimize the assay as described in **Notes 3** and **6**. Check incubation time and temperature.
2. Purify the plasma membrane preparation with sucrose density gradient centrifugation *(7)*.

3. Include 10 μg/mL saponin in the assay (~1:1 saponin:membrane protein). We have found (**ref. *8*** and S. Lazareno, unpublished observations; *see* **Fig. 2**) that this increases the signal-to-noise ratio without perturbing the pharmacological characteristics of the preparation, though possible effects of saponin on the pharmacological parameters being studied should be assessed. Other authors have used alamethicin as a permeabilizing agent ***(9)***.
4. Stop the reaction by adding high concentrations of unlabeled GTPγS (e.g., 10 μ*M*) and competitive antagonist. Allow the label to dissociate for 45 min before filtration. This may yield a modest (10–30%) increase in the signal-to-noise ratio.

4. Notes

1. If the only effect of agonist activation is to increase the rate of GTPγS binding and not the equilibrium level, agonist-stimulated binding (i.e., the difference between [^{35}S]-GTPγS binding in the presence and absence of agonist), should increase over time, reach a maximum, and then decline to zero; agonist-stimulated binding would not exist under equilibrium conditions. However, it is possible that agonist-stimulated GTPγS binding can be seen at equilibrium, though the size of the stimulation would be less than under nonequilibrium conditions.

   In our hands, the binding of low concentrations of [^{35}S]-GTPγS in the presence of GDP to CHO cell membranes containing muscarinic receptors is very slow and has not reached equilibrium by 3 h (**Fig. 3**). Both sets of data in the figure are consistent with an effect of agonist on only the rate of binding, but since basal binding was almost linear with time, no firm conclusions can be drawn from such data about the situation at equilibrium. From an admittedly incomplete survey of the literature, there does not seem to be any study that has explicitly addressed the question of whether agonist-stimulated [^{35}S]-GTPγS binding can be seen at equilibrium. Many studies in the literature that report kinetic data have used relatively early time points, as we did, and are similarly inconclusive ***(18–27)***. In some studies, it is clear that binding in the absence and presence of agonist differed only at initial time points and was the same at equilibrium, as predicted by a purely catalytic mechanism ***(28–30)***. However, in some other studies [^{35}S]-GTPγS binding over time in the absence and presence of agonist would appear to reach different asymptotic levels, which has either been claimed as stimulated binding at equilibrium ***(31,32)*** or has not been commented on by the authors ***(33–36)***.

   A mechanistic interpretation of agonist-stimulated [^{35}S]-GTPγS binding at equilibrium is provided by the model of Onaran et al. ***(37)***, which is an extended version of the classic Ternary Complex model of De Lean et al. ***(38)***. The model contains a receptor, a G-protein α subunit, and a G-protein βγ subunit: the receptor has binding sites for a hormone and α; α has binding sites for a guanine nucleotide, receptor and βγ; and βγ binds only to α. The properties of the model are determined by the concentrations of the reactants, the various bimolecular affinity constants, and in particular by the cooperative interactions between

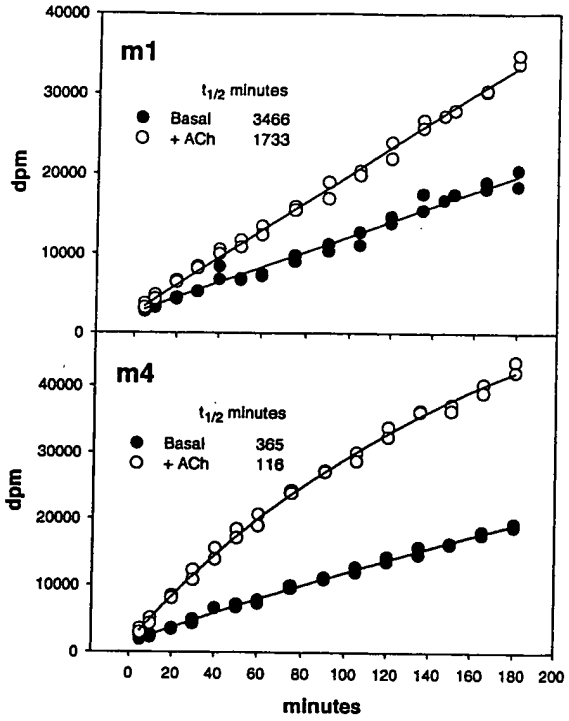

Fig. 3. Membranes from CHO cells containing m1 or m4 muscarinic receptors were incubated in a buffer containing 20 m*M* HEPES, 100 m*M* NaCl, 10 m*M* $MgCl_2$, pH 7.4, with 0.1 n*M* ^{35}S-GTPγS (260,000 dpm) and GDP (0.1 μ*M* for m1, 1 μ*M* for m4) in the absence and presence of 1-m*M* ACh at 30°C for the indicated times. The two curves for each receptor subtype were fitted to exponential functions with a common asymptote. The association half times at m1 receptors are not well defined—the data were equally well fitted with straight lines. The data points are from a single experiment conducted in duplicate.

ligands binding at different sites on the same molecule; for example, positive cooperation between an agonist and α subunit binding to the receptor accounts for agonist efficacy, negative cooperativity between a receptor and GDP binding to an α subunit accounts for agonist stimulation of GDP/GTPγS exchange at α, and positive cooperativity between βγ and GDP binding to an α subunit promotes the inactivation of both α and βγ subunits by mutual binding. Agonist-stimulated [^{35}S]-GTPγS binding at equilibrium could be explained if the receptor were positively cooperative with GTPγS for binding to α and if the concentrations of receptor and α were similar, so that a substantial fraction of α could be bound to the receptor at equilibrium. With cell membrane preparations, however, it is often observed that a single receptor can stimulate the binding of [^{35}S]-GTPγS to a number of G-proteins *(2,19,27,32,39)*, suggesting that the concentration of α

subunits is many times greater than the concentration of receptor, and only a small fraction of the α subunits could be bound to receptor at equilibrium. Nevertheless, if binding occurs in the presence of high concentrations of GDP, even with a 10-fold excess of α subunits over receptors, the model can be made to generate levels of agonist-stimulated GTPγS binding, which are substantial, relative to basal levels—absolute levels of stimulated binding must always be less than the receptor concentration. The existence and precise values of agonist-stimulated binding generated by the model depend critically on the values assigned to the elements of the model, and it is not known if any empirical instance of agonist-stimulated [^{35}S]-GTPγS binding at equilibrium can be explained by this model. A more elaborate model, in which receptors interact with dimers or oligomeric arrays of G-proteins, can also account for agonist-stimulated [^{35}S]-GTPγS binding at equilibrium *(32)*. Future models may need to account for other membrane components that can modulate [^{35}S]-GTPγS binding *(21)*.

Although observations of agonist-stimulated [^{35}S]-GTPγS binding at equilibrium may be consistent with a model of G-protein activation, there are other mechanisms that could generate these observations. In some studies using reconstituted preparations of purified G-proteins and/or receptors, the increased [^{35}S]-GTPγS binding seen at long time points in the presence of agonist was attributed to an increased stability of the G-protein when coupled to the receptor *(40)*. Another possible explanation relates to observations that [^{35}S]-GTPγS binding may be only partially reversible *(18,32,41)*, that is, a proportion of bound [^{35}S]-GTPγS dissociates very slowly, if at all. This suggests that [^{35}S]-GTPγS association kinetics may also have a very slow component that might be undetected in assays measuring the much faster component of association. A third possibility is that G-protein activation may alter the physical properties of the cell membrane: Abramson et al. *(42)* found that arachidonic acid and other *cis*-unsaturated fatty acids increased [^{35}S]-GTPγS binding that was claimed to be at equilibrium, and we have found that saponin increases [^{35}S]-GTPγS binding under nonequilibrium conditions and binding of the muscarinic radioligand [^{3}H]-NMS under equilibrium conditions (**Fig. 2**), though we have not studied its effect on [^{35}S]-GTPγS binding at equilibrium.

The question of whether agonist-stimulated [^{35}S]-GTPγS binding is an equilibrium or nonequilibrium phenomenon has practical consequences. In attempts to better characterize the effects of agonists on [^{35}S]-GTPγS binding to membrane preparations in the presence of GDP, a number of studies report the results of GTPγS saturation curves in the absence and presence of agonist (usually performed with inhibition curves using unlabeled GTPγS). Such studies in the presence of agonist usually show an increased affinity of GTPγS with no change in Bmax *(41)* or the conversion of a proportion of the binding sites to a higher affinity *(31)*. The interpretation of such experiments depends crucially on whether or not agonist-stimulated binding has reached equilibrium. If it has, the interpretation of the experiment in terms of changes in GTPγS Bmax and Kd may be valid,

though complex. However, if [^{35}S]-GTPγS binding in the absence and presence of agonist has not reached equilibrium, the results of such saturation studies do not have a simple mechanistic interpretation ***(43)***.

2. [^{35}S]GTPγS is currently supplied by NEN at a concentration of about 10^{-5}*M* in a buffer containing 10-m*M* tricine and 10-m*M* dithiothreitol, pH 7.6. It should be diluted at least 10-fold in this buffer and stored at −70°C in aliquots sufficient for two or three assays, in order to minimize radiochemical decomposition. According to the volumes and dilutions recommended in this chapter, this will result in a concentration of 1-μ*M* dithiothreitol in the assay.
3. The precise concentrations of NaCl and $MgCl_2$, and particularly of GDP required for the optimal signal-to-noise ratio (maximal agonist-stimulated binding/basal binding), should be determined for each receptor-G-protein preparation. For some receptors, for example, muscarinic m1 receptors expressed in CHO cells, agonists stimulate [^{35}S]GTPγS binding in the absence of GDP, and inclusion of up to 0.1-μ*M* GDP in the [^{35}S]GTPγS binding assay reduces basal binding without reducing stimulated binding. For other receptors, such as the muscarinic m2 receptor, GDP is absolutely required for agonist stimulation, and 1-μ*M* GDP was found to provide optimal results; 10-μ*M* GDP was required with the adenosine A1 receptor ***(8,10)***. In all cases, sufficient bound counts must be obtained for accurate measurement. However, no more than about 10% of added [^{35}S]GTPγS should be bound, so less m1 receptor membrane is used (5-μg protein/mL) than m2 receptor membrane (20 μg/mL). Note that GDP reduces agonist potency in the [^{35}S]GTPγS binding assay ***(6)***.
4. The concentrated membranes may be stored at −70°C and later thawed for protein determination, dilution, and refreezing without loss of stimulated [^{35}S]GTPγS binding activity.
5. As this is a binding assay, the variability between replicates is usually small, 2–5% of the mean counts; consequently, duplicate measures are often sufficient. On the other hand, the stimulation of binding by agonist above basal values may be less than twofold; as a result, triplicate or even quadruplicate determinations may be necessary.
6. We find cold water to be acceptable for washing the filters. The filter blank, measured in the absence of membranes, is usually less than 0.5% of added label. Occasionally, however, much larger filter blanks occur, for reasons not yet resolved. Large filter blanks may be reduced by washing in phosphate buffer. Nonspecific binding, measured in the presence of 10-μ*M* unlabeled GTPγS, is usually close to filter-blank levels.
7. As far as possible, experiments should be designed so that all the data contributing to an experimental question are obtained from a single filter (e.g., 24 or 48 samples), depending on the configuration of the cell harvester. If this is not possible, two or more filters should be used, each containing a single replicate of each experimental condition—in this way, the variability between filters because of small differences in washing procedure or incubation time is evenly distributed across all experimental conditions. In order to minimize possible position

effects of the cell harvester, the second replicates may be filtered in reverse order—this is easily achieved by reversing the order in which samples are filtered then reversing the filter before distributing the filter disks to scintillation vials.

8. Two types of contamination may occur if a cell harvester is used with both [^{3}H] ligands and [^{35}S]GTPγS.
   a. The tubing will be contaminated with ^{35}S, which will leach out and contaminate ^{3}H assays. We have observed contamination of over 1000 dpm per sample. The contamination is progressively reduced during one day as more ^{3}H assays are filtered but is higher at the start of the next day. We cope with the problem by routinely counting ^{3}H with a dual-label program.
   b. Serious filter blank problems occur with [^{35}S]GTPγS if the filter is exposed to even very small amounts (1 part in 10^7 w/v) of polyethyleneimine (PEI). In many radioligand binding assays, filters are soaked with 0.1% PEI to reduce the binding of charged radioligands. The filtration apparatus will become contaminated with PEI, and [^{35}S]GTPγS binding assays using the same apparatus will often have some spuriously high readings, especially with the first filter of the day. The solution is to filter washing buffer or water through two filters (or, much cheaper, paper towels) before filtering [^{35}S]GTPγS.
9. Filters that are dried before addition of scintillation fluid can be counted immediately. Counting of wet filters will provide a good indication of the result of the assay, but for accurate data, the prepared vials should be left overnight and then inverted and shaken repeatedly to ensure that the water in the filter has completely dissolved in the scintillation fluid.
10. The affinity of a competitive antagonist is estimated in functional studies by constructing agonist concentration-effect curves, both alone and in the presence of various fixed concentrations of antagonist, and analyzing the data with Schild analysis *(11)*. This design allows the detection of any changes in basal activity, the Emax or the shape of the agonist curve in the presence of antagonist. If it can be assumed that the antagonist does not alter Emax or agonist slope, it is simpler and more efficient to estimate antagonist affinity with this assay by using an inhibition curve design. In this case, a minimum of two concentration-effect curves are required: an agonist curve alone and an antagonist curve in the presence of a fixed agonist concentration. The effect of the antagonist on basal activity should also be measured, although this information may not contribute to the data analysis.
11. Although the data may be analyzed using linear transformations and even "by eye" interpolations from graphs *(12,13)*, ideally, the data should be analyzed using nonlinear regression analysis (the manual provided with the Prism program (GraphPad) contains an introduction to nonlinear regression and other useful topics: the relevant chapters are freely available on the World Wide Web at http://www.graphpad.com). Some programs (e.g., Prism, *see* **ref. *14***) can only handle one independent variable (e.g., drug concentration). Others (e.g., SigmaPlot [Jandel] and modern spreadsheets *[15]*) can handle two or more independent vari-

ables (e.g., agonist and antagonist concentrations). Equations containing one independent variable are marked (*), those containing two independent variables are marked (**). Schild plot designs can be analyzed in the traditional way *(11)* or by fitting the complete data set, together with agonist [*A*] and antagonist [*B*] concentrations, directly to the "integrated logistic-Schild equation" *(12,13,16)*

$$\text{Effect} = \frac{\text{Emax} - \text{basal}}{1 + \left\{\frac{[\text{EC50}]}{[A]} \cdot \left[\left(\frac{[B]}{Kb}\right)^{s} + 1\right]\right\}^{b}} + \text{basal} \qquad (1)\ (**)$$

to yield estimates of basal activity, Emax, agonist EC50, agonist slope factor *b*, antagonist dissociation constant Kb, and Schild slope *s*.

Inhibition curve designs can be analysed in three ways *(12,13)*.

1. Using a SigmaPlot-type program, fit the complete data set to **Eq. 1**.
2. Using a Prism-type program
   a. fit the agonist curve to a logistic function

$$\text{Effect} = \frac{\text{Emax} - \text{basal}}{1 + \left(\frac{[\text{EC50}]}{[A]}\right)^{b}} + \text{basal} \qquad (2)\ (*)$$

   b. fit the antagonist curve to **Eq. 1**, with [*A*] set to the fixed agonist concentration, and basal, Emax, EC50 and *b* set to the values obtained from the analysis of the agonist curve, to leave a single independent variable.
3. Using a Prism-type program
   a. fit both curves to logistic functions (**Eq. 2**).
   b. calculate Kb, the antagonist dissociation constant, by inserting the values of the fixed agonist concentration [*A*], the EC50, and slope *b* of the agonist fit and the IC50 from the antagonist fit, into the "functional Cheng–Prusoff equation" *(17)*.

$$\text{Kb} = \frac{[\text{IC50}]}{\left[2 + \left(\frac{[A]}{[\text{EC50}]}\right)^{b}\right]^{1/b} - 1} \qquad (3)$$

This analysis assumes that the antagonist Schild slope is 1.

12. If the agent does not affect basal activity, Emax, or the shape of the agonist curve, then the complete data set, together with the concentrations of agonist [*A*] and allosteric agent [*X*], can be fitted to the equation

$$\text{Effect} = \frac{\text{Emax} - \text{basal}}{1 + \left(\frac{[\text{EC50}]}{[A]} \cdot \frac{1 + [X] / \text{Kx}}{1 + \alpha.[X] / \text{Kx}}\right)^{b}} + \text{basal} \qquad (4)\ (**)$$

to yield estimates of the dissociation constant of the allosteric agent, Kx, and the cooperativity with the agonist, α *(5)*.

13. Filters that are dried before addition of scintillation fluid can be counted immediately. Otherwise, it is important that all of the water in the filter disk be dissolved in the scintillation fluid (*see* **Note 7**). ^{3}H is much more quenched by water than ^{35}S, and if the filter disk is wet, the dual label program will not function correctly, and the results will be qualitatively incorrect.
14. Ideally, one isotope should not give more than approx 30 times the counts given by the other isotope.

References

1. Neer, E. J. (1995) Heterotrimeric G proteins: organizers of transmembrane signals. *Cell* **80,** 249–257.
2. Hilf, G., Gierschik, P., and Jakobs, K. H. (1989) Muscarinic acetylcholine receptor-stimulated binding of guanosine 5'- O-(3-thiotriphosphate) to guanine-nucleotide-binding proteins in cardiac membranes. *Eur. J. Biochem.* **186,** 725–731.
3. Wieland, T. and Jakobs, K. H. (1994) Measurement of receptor-stimulated guanosine 5'-O-(gamma-thio)triphosphate binding by G proteins. *Methods Enzymol.* **237,** 3–13.
4. Sweeney, M. (1995) Measurement of the GTPase activity of signal-transducing G-proteins in neuronal membranes, in *Methods in Molecular Biology*, vol. 41 (Kendall, D. A. and Hill, S. J., eds.), Humana, Totowa, NJ, pp. 51–61.
5. Lazareno, S. and Birdsall, N. J. M. (1995) Detection, quantitation, and verification of allosteric interactions of agents with labeled and unlabeled ligands at G protein-coupled receptors: interactions of strychnine and acetylcholine at muscarinic receptors. *Mol. Pharmacol.* **48,** 362–378.
6. Lazareno, S., Farries, T., and Birdsall, N. J. M. (1993) Pharmacological characterization of guanine nucleotide exchange reactions in membranes from CHO cells stably transfected with human muscarinic receptors m1-m4. *Life Sci.* **52,** 449–456.
7. Hilf, G. and Jakobs, K. H. (1989) Activation of cardiac G-proteins by muscarinic acetylcholine receptors: regulation by Mg2+ and Na+ ions. *Eur. J. Pharmacol.* **172,** 155–163.
8. Cohen, F. R., Lazareno, S., and Birdsall, N. J. M. (1996) The effects of saponin on the binding and functional properties of the human adenosine A1 receptor. *Br. J. Pharmacol.* **117,** 1521–1529.
9. Hilf, G. and Jakobs, K. H. (1992) Agonist-independent inhibition of G protein activation by muscarinic acetylcholine receptor antagonists in cardiac membranes. *Eur. J. Pharmacol.* **225,** 245–252.
10. Lorenzen, A., Fuss, M., Vogt, H., and Schwabe, U. (1993) Measurement of guanine nucleotide-binding protein activation by A1 adenosine receptor agonists in bovine brain membranes: stimulation of guanosine-5'-O-(3-[35S]thio)triphosphate binding. *Mol. Pharmacol.* **44,** 115–123.
11. Kenakin, T. (1993) *Pharmacologic Analysis of Drug-Receptor Interaction*, Raven, New York.

12. Lazareno, S. and Birdsall, N. J. M. (1993) Estimation of competitive antagonist affinity from functional inhibition curves using the Gaddum, Schild and Cheng–Prusoff equations. *Br. J. Pharmacol.* **109,** 1110–1119.
13. Lazareno, S. and Birdsall, N. J. M. (1993) Estimation of antagonist Kb from inhibition curves in functional experiments: alternatives to the Cheng–Prusoff equation. *Trends Pharmacol. Sci.* **14,** 237–239.
14. Lazareno, S. (1994) Graphpad prism (Version 1.02): software review. *Trends Pharmacol. Sci.* **15,** 353,354.
15. Bowen, W. P. and Jerman, J. C. (1995) Nonlinear regression using spreadsheets. *Trends Pharmacol. Sci.* **16,** 413–417.
16. Waud, D. R. (1975) Analysis of dose-response curves, in *Methods in Pharmacology* (Daniel, E. E. and Paton, D. M., eds.) Plenum, New York, pp. 471–506.
17. Leff, P. and Dougall, I. G. (1993) Further concerns over Cheng–Prusoff analysis [see comments]. *Trends Pharmacol. Sci.* **14,** 110–112.
18. Berstein, G., Blank, J. L., Smrcka, A. V., Higashijima, T., Sternweis, P. C., Exton, J. H., and Ross, E. M. (1992) Reconstitution of agonist-stimulated phosphatidylinositol 4,5-bisphosphate hydrolysis using purified m1 muscarinic receptor, Gq/11, and phospholipase C-beta 1. *J. Biol. Chem.* **267,** 8081–8088.
19. Traynor, J. R. and Nahorski, S. R. (1995) Modulation by mu-opioid agonists of guanosine-5'-O-(3-[35S]thio)triphosphate binding to membranes from human neuroblastoma SH-SY5Y cells. *Mol. Pharmacol.* **47,** 848–854.
20. Kurose, H., Katada, T., Haga, T., Haga, K., Ichiyama, A., and Vi, M. (1986) Functional interaction of purified muscarinic receptors with purified inhibitory guanine nucleotide regulatory proteins reconstituted in phospholipid vesicles. *J. Biol. Chem.* **261,** 6423–6428.
21. Sato, M., Kataoka, R., Dingus, J., Wilcox, M., Hildebrandt, J. D., and Lanier, S. M. (1995) Factors determining specificity of signal transduction by G-protein-coupled receptors. Regulation of signal transfer from receptor to G-protein. *J. Biol. Chem.* **270,** 15,269–15,276.
22. Shiozaki, K. and Haga, T. (1992) Effects of magnesium ion on the interaction of atrial muscarinic acetylcholine receptors and GTP-binding regulatory proteins. *Biochemistry* **31,** 10,634–10,642.
23. Florio, V. A. and Sternweis, P. C. (1989) Mechanisms of muscarinic receptor action on G(o) in reconstituted phospholipid vesicles. *J. Biol. Chem.* **264,** 3909–3915.
24. Baker, S. P. and Potter, L. T. (1981) Altered states of cardiac beta adrenoreceptors. *Biochem. Pharmacol.* **30,** 3361–3364.
25. Kaldenberg-Stasch, S., Baden, M., Fesseler, B., Jakobs, K. H., and Wieland, T. (1994) Receptor-stimulated guanine-nucleotide-triphosphate binding to guanine-nucleotide-binding regulatory proteins. Nucleotide exchange and beta-subunit-mediated phosphotransfer reactions. *Eur. J. Biochem.* **221,** 25–33.
26. Richardson, R. M. and Hosey, M. M. (1992) Agonist-induced phosphorylation and desensitization of human m2 muscarinic cholinergic receptors in Sf9 insect cells. *J. Biol. Chem.* **267,** 22,249–22,255.

27. Liang, M. N. and Garrison, J. C. (1991) The epidermal growth factor receptor is coupled to a pertussis toxin-sensitive guanine nucleotide regulatory protein in rat hepatocytes. *J. Biol. Chem.* **266,** 13,342–13,349.
28. Munshi, R., Pang, I. H., Sternweis, P. C., and Linden, J. (1991) A1 adenosine receptors of bovine brain couple to guanine nucleotide-binding proteins Gi1, Gi2, and Go. *J. Biol. Chem.* **266,** 22,285–22,289.
29. Senogles, S. E., Spiegel, A. M., Padrell, E., Iyengar, R., and Caron, M. G. (1990) Specificity of receptor-G protein interactions. Discrimination of Gi subtypes by the D2 dopamine receptor in a reconstituted system. *J. Biol. Chem.* **265,** 4507–4514.
30. Negishi, M., Namba, T., Sugimoto, Y., Irie, A., Katada, T., Narumiya, S., and Ichikawa, A. (1993) Opposite coupling of prostaglandin E receptor EP3C with Gs and G(o). Stimulation of Gs and inhibition of G(o). *J. Biol. Chem.* **268,** 26,067–26,070.
31. Gierschik, P., Moghtader, R., Straub, C., Dieterich, K., and Jakobs, K. H. (1991) Signal amplification in HL-60 granulocytes. Evidence that the chemotactic peptide receptor catalytically activates guanine-nucleotide-binding regulatory proteins in native plasma membranes. *Eur. J. Biochem.* **197,** 725–732.
32. Chidiac, P. and Wells, J. W. (1992) Effects of adenyl nucleotides and carbachol on cooperative interactions among G proteins. *Biochemistry* **31,** 10,908–10,921.
33. Okamoto, T., Ikezu, T., Murayama, Y., Ogata, E., and Nishimoto, I. (1992) Measurement of GTP gamma S binding to specific G proteins in membranes using G-protein antibodies. *FEBS. Lett.* **305,** 125–128.
34. Gardner, B., Hall, D. A., and Strange, P. G. (1996) Pharmacological analysis of dopamine stimulation of [35S]-GTP gamma S binding via human D2short and D2long dopamine receptors expressed in recombinant cells. *Br. J. Pharmacol.* **118,** 1544–1550.
35. Ravindra, R. and Aronstam, R. S. (1991) Acetylcholine stimulates GTP binding to G proteins in rat striatum. *Neuroreport* **2,** 127–130.
36. Gachet, C., Cazenave, J. P., Ohlmann, P., Hilf, G., Wieland, T., and Jakobs, K. H. (1992) ADP receptor-induced activation of guanine-nucleotide-binding proteins in human platelet membranes. *Eur. J. Biochem.* **207,** 259–263.
37. Onaran, H. O., Costa, T., and Rodbard, D. (1993) Beta gamma subunits of guanine nucleotide-binding proteins and regulation of spontaneous receptor activity: thermodynamic model for the interaction between receptors and guanine nucleotide-binding protein subunits. *Mol. Pharmacol.* **43,** 245–256.
38. De Lean, A., Stadel, J. M., and Lefkowitz, R. J. (1980) A ternary complex model explains the agonist-specific binding properties of the adenylate cyclase-coupled beta-adrenergic receptor. *J. Biol. Chem.* **255,** 7108–7117.
39. Sim, L. J., Selley, D. E., Xiao, R., and Childers, S. R. (1996) Differences in G-protein activation by μ- and δ-opioid, and cannabinoid, receptors in rat striatum. *Eur. J. Biochem.* **307,** 97–105.
40. Asano, T., Pedersen, S. E., Scott, C. W., and Ross, E. M. (1984) Reconstitution of catecholamine-stimulated binding of guanosine 5'-O- (3-thiotriphosphate) to the

stimulatory GTP-binding protein of adenylate cyclase. *Biochemistry (USA)* **23,** 5460–5467.

41. Olianas, M. C. and Onali, P. (1996) Stimulation of guanosine 5'-O-(3-[35S] thiotriphosphate) binding by cholinergic muscarinic receptors in membranes of rat olfactory bulb. *J. Neurochem.* **67,** 2549–2556.
42. Abramson, S. B., Leszczynska Piziak, J., and Weissmann, G. (1991) Arachidonic acid as a second messenger. Interactions with a GTP-binding protein of human neutrophils. *J. Immunol.* **147,** 231–236.
43. Selley, D. E., Sim, L. J., Xiao, R., Liu, Q., and Childers, S. R. (1997) mu-Opioid receptor-stimulated guanosine-5'-O-(gamma-thio)-triphosphate binding in rat thalamus and cultured cell lines: Signal transduction mechanisms underlying agonist efficacy. *Mol. Pharmacol.* **51,** 87–96.

14

mRNA: Detection by *In Situ* and Northern Hybridization

Rachel M. C. Parker and Nicholas M. Barnes

1. Introduction

In situ hybridization histochemistry (ISHH), first described in 1969 by Gall and Pardue and John et al. *(1,2)* and northern hybridization, first described by Alwine et al. *(3)*, have become very powerful and now quite well established techniques in many research areas, including that of receptor research. Such applications include

1. direct assessment of the presence, distribution, and modulation of specific RNA species under different physiological conditions *(4,5)*;
2. molecular investigations of potential mRNA splice variants and region-specific heterogeneity in multimeric-receptor subunit expression *(6,7)*;
3. indirect identification of receptor-expression to add credence to the existence of that receptor when highly selective ligands are unavailable for receptor binding site localization studies *(8)*; and
4. investigation of molecular changes in pathological states and the possible modes of action of drugs used to treat such conditions *(9–11)*.

Changes at the molecular level to alter mRNA expression represent rapid changes within a cell; therefore, it can be envisaged that such studies on human biopsy and postmortem tissue will lead to an array of important diagnostic tools. Furthermore, the combination of *in situ* hybridization histochemistry and immunocytochemistry offers a powerful way to study the coexistence of mRNA and its peptide product *(12)*, or, alternatively, to study the colocalization of one mRNA species with a peptide/protein that is phenotypically characteristic of a certain cell type, allowing identification, and therefore the putative function, of that cell population to be investigated *(13,14)*.

From: *Methods in Molecular Biology, Vol. 106: Receptor Binding Techniques*
Edited by: Mary Keen © Humana Press Inc., Totowa, NJ

Both ISHH and Northern hybridization exploit the principle that single-stranded nucleic acid sequences anneal to their complementary nucleic acid sequence. When the single-stranded nucleic acid sequence is labeled (to produce a probe), the location of this hybridization can be detected. Northern hybridization is a relatively rapid method of detecting the presence, abundance, and size of specific RNA species within the population of cells from a given region: The RNA is first extracted from its source, fractionated by electrophoresis, immobilized onto a membrane phase, then hybridized with a labeled complementary nucleic acid probe ***(15,16)***. In comparison, ISHH allows a specific RNA species to be detected directly at its site of expression, revealing its cellular localization and relative abundance ***(15,16)***. Both methods basically comprise the following seven steps:

1. Probe labeling: the choice of probe and label depends on the requirements of the research being undertaken (*see* **Table 1** and **2**). (The cloning techniques needed to produce suitable vector templates for cDNA and riboprobe synthesis will not be covered in this chapter.)
2. RNA isolation: To minimize RNA degradation and maximize signal detection, it is critical that RNase-free conditions are maintained and tissue is collected, stored, and fixed correctly.
3. Prehybridization tissue treatment: The sensitivity of the method may be increased in several ways at this stage by employing one or a number of steps, depending on the nature of the tissue source, to
   a. maintain RNA integrity (e.g., tissue fixation and use of RNase inactivators),
   b. help reduce nonspecific background (e.g., delipidation, acetylation, and prehybridization with hybridization solution minus probe), and
   c. in the case of ISHH, improve probe access (e.g., wax removal and proteinase K treatment).
4. Hybridization: Optimal temperature for hybridization is, as a general rule, 20–25°C below the melting temperature (Tm) of the probe ***(16,25,26)***, where the Tm for DNA/DNA = $81.5 + 16.6 \times \log [Na^+] - 0.62 \times$ (% formamide) $+ 41 \times (G + C) - 500/$(probe length), RNA/RNA = $79.8 + 18.5 \times \log$ [Na+] - $0.35 \times$ (% formamide) $+ 58 \times (G + C) + 12 \times (G + C)^2 - 820/$(probe length), and DNA/RNA ≈ mean of Tm (DNA/DNA) and Tm (RNA/RNA). Therefore, the Tm value depends on the probe length, its base composition (GC pairs have a greater influence on overall duplex stability, as these form three hydrogen bond interactions vs AT pairs that form two hydrogen bonds) and homology to the target sequence, the ionic strength of the monovalent cations present, and the amount of denaturing agent (e.g., formamide) used.
5. Post-hybridization washing: This step is designed to remove nonspecific background caused by any unbound and loosely bound probe, that may be present after the hybridization step, because of weak homology with related RNA species or nonspecific interactions with other cellular components. Posthybridization wash stringency is directly proportional to temperature (where the most stringent

Table 1
Choice of Probe

Probe	Advantages to use	Disadvantages to use	Labeling methods	Reference
cDNA (200–500 bases)	Easy to generate	Need cloning expertise to generate	PCR	*15–20*
	Stable	Less efficient hybrids than with riboprobes	Nick translation	
	Long, giving high specific activity	Presence of both DNA strands may decrease sensitivity	Random primer	
Oligonucleotides (20–50 bases)	Easy to synthesis and label with no cloning Knowledge necessary Stable Short, therefore good tissue access and high specificity	Need knowledge on choosing a suitable sequence (*see* **Note 3**) and access to a synthesizer Relatively insensitive; may need a cocktail of oligomers to increase sensitivity Will tolerate only one or two mismatches before which hybridization is lost	Terminal deoxynucleotidyl transferase, or T4 polynucleotide kinase	*15,16,19–22*
Riboprobes (50–1000 bases)	Can generate long sense and antisense probes with high specific activity Very sensitive; good for detecting less abundant mRNA species or cross-species mRNA if the sequence from all species is unavailable, and RNase treatment after hybridization in ISHH further increases signal-to-noise ratio	Require cloning expertise to generate Difficult to generate and handle; require special protection against RNase degradation	In vitro transcription, using T3, T7, or SP6 specific RNA polymerase	*15,16,19,20,23*

Table 2
Choice of Label

Label	Advantages to use	Disadvantages to use
Nonradioactive[a] (e.g., fluorescein, digoxigenin, biotin)	No special safety precautions required Quick results (several d) Labeled probe is stable for up to 1 yr Provides cellular resolution in ISHH	Less sensitive than radioactive detection Tissue permeability is crucial Endogeneous biotin in some tissues may hinder accurate detection Nonquantitative with indirect detection (e.g., with conjugated polyclonal antibodies
Radioactive[b] (e.g., ^{3}H, ^{35}S ^{33}P, ^{32}P)	Sensitive Quick results obtained with high energy-emitting isotopes (e.g., ^{32}P) Cellular resolution obtained with low energy-emitting Isotopes (e.g., ^{3}H and ^{35}S) for ISHH Semi-quantitative	Special safety precautions required High energy emitters scatter signal, yielding low resolution, and are therefore only useful for Northern hybridization Low energy emitters need long exposure times, so are slow to yield results Labeled probes have short shelf-life

[a]*See* refs. ***16, 19, 20,*** and ***24*** for review.
[b]*See* refs. ***16, 19, 20*** for review.

wash is approx at 10–15°C below the Tm value) and inversely proportional to the salt concentration. Thus, optimal signal-to-noise ratio can be obtained by manipulating these two parameters at this stage.

6. Signal detection: Photographic emulsion, film, or nonradioactive detection methods are available, depending on the nature of the label used (*see* **Table 2**).
7. Controls: It is vital to include positive and negative controls to test the ability to obtain consistent, sensitive, and specific signal detection.

This chapter describes two highly sensitive, selective, and reproducible methods for analyzing mRNA expression, which are successfully employed in

our laboratory. **Subheading 3.1.** details two methods of *in situ* hybridization histochemistry; one uses radioactively-labeled 48 base antisense and sense oligonucleotide probes, corresponding to bases 862–909 of the rat prodynorphin (PPD) gene sequence *(27)* to identify PPD mRNA within rat brain (*see* **Fig. 1**) and spinal cord *(4)*. This probe was used to evaluate the modulation of a molecular marker to, in turn, assess the involvement of neurokinin receptors in models of long-term hyperalgesia *(4)*. The second method employs radioactively-labeled 750 base antisense and sense riboprobes, corresponding to amino acid residues 62–312 of a human 5-HT_3 receptor cDNA sequence (h5-HT_3R riboprobe *(28)* to identify specific 5-HT_3 receptor mRNA within the human central nervous system. The distribution of 5-HT_3 receptor binding sites has been characterized in the human brain, where it is suggested that they are involved in many important physiological roles, such as in memory and learning, anxiety, and emesis *(29)*. Therefore, it is relevant to phenotypically-determine which subpopulation of neurones express this receptor, to elucidate a role for this receptor subtype in such processes. **Subheading 3.2.** describes the application of Northern hybridization, which was employed to determine the selectivity of the various 5-HT_3R riboprobes used in our ISHH studies and to locate 5-HT_3 receptor mRNA within different nervous system regions of human and rat (*see* **Fig. 2**). These protocols should provide a framework from which to work and to adapt to other applications.

2. Materials

2.1. Chemicals and Solutions

It is important to take precautions against RNase contamination when making the following solutions (*see* **Note 1**).

1. 2-mercaptoethanol: e.g., Sigma (Dorset, UK; M3148).
2. ^{32}P-αUTP: (^{32}P-Uridine 5'-triphosphate, tetre(triethylammonium) salt; e.g., DuPont NEN (Boston, MA; NEG-507H) stored at –20°C; specific activity > 3000 Ci/mmol, 10 mCi/mL).
3. ^{35}S-αdATP: (deoxyadenosine 5'-(α-thio) triphosphate; e.g., DuPont NEN NEG-034H; stored at –20°C; specific activity > 1200 Ci/mmol, 12.5 mCi/mL).
4. ^{35}S-αUTP: (35S-Uridine 5'-(α-thio) triphosphate; e.g., DuPont NEN NEG-039C; stored at –20°C; specific activity > 1200 Ci/mmol, 40 mCi/mL).
5. Absolute ethanol.
6. Acetone.
7. Acid alcohol: add two to three drops of concentrated HCl to 70% ethanol solution.
8. Agarose: e.g., Ultrapure; Life Technologies (Renfrewshire, Scotland; BRL-540-5510UA).

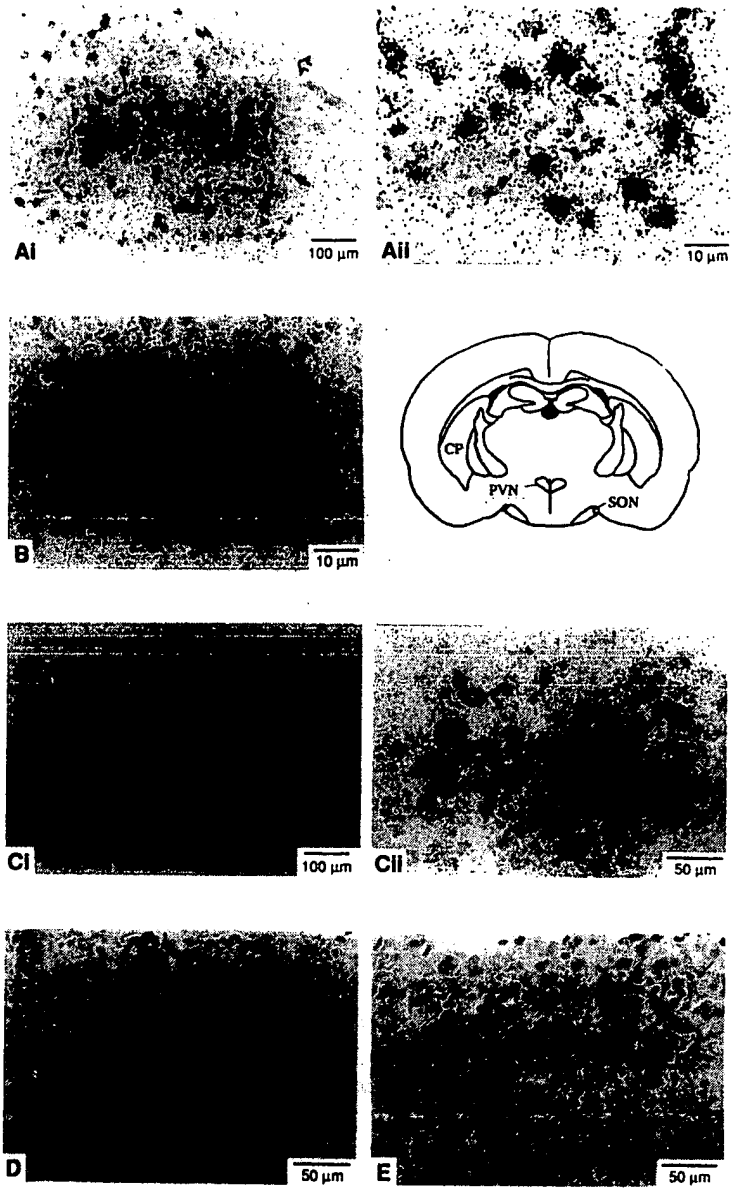

Fig. 1. Preprodynorphin mRNA expression in untreated rat brain, using *in situ* hybridization histochemistry. Low- and high-power light field photographs showing *in situ* hybridization histochemical identification of PPD mRNA expression, restricted to discrete areas within the brains of normal, untreated rats (see schematic diagram of a rat brain section). Positively-labeled neurones, as shown by a dense aggregation

9. Agarose (1%)/formaldehyde solution: for 100 mL, dissolve 1-g agarose in 72.1-mL DEPC-treated dH_2O, cool to approx 60°C, then add 10 mL of 10X MOPS running buffer. In a fume hood, add 17.7 mL of 37% solution of formaldehyde, to give a final concentration of 2.2*M*. Allow to cool before pouring the gel (agarose sets at approx 45°C).
10. Alkaline H_2O: add one drop of concentrated ammonia solution to 300 mL dH_2O; make fresh.
11. Chloroform.
12. Chloroform: Isoamylalcohol 49:1 mixture: mix in a fume cupboard, store at 4°C, wrapped in foil.
13. Chromic acid: dissolve 10% (w/v) potassium dichromate (e.g., BDH Poole, UK; 102024W) in autoclaved dH_2O, very slowly and carefully add 10% (v/v) concentrated sulfuric acid and mix with a glass rod. Handle this solution with care and store it at room temperature in a glass container with a tight-fitting lid, clearly labeled hazardous and corrosive. This solution can be used several times.
14. Cold sterilization solutions: 3% H_2O_2 in DEPC-treated dH_2O; 70% ethanol in DEPC-treated dH_2O; 0.1*N* NaOH containing 1-m*M* EDTA in DEPC-treated dH_2O.
15. Concentrated ammonia solution.
16. Concentrated HCl.
17. Decon.
18. Deionized formamide: mix 100-mL formamide per 10-g mixed-bed ion exchange resin 20–50 mesh (BioRad AG; Herts, UK; 501-X8) for 30–60 min at room temperature, in a fume cupboard; filter X2 through Whatman No. 1 filter paper, dispense into aliquots, store at –20°C.
19. Denhardt's solution (50X): 1% (w/v) Ficoll type 400 (e.g., Sigma F2637) 1% (w/v) PVP (polyvinylpyrrolidene; e.g., Sigma P5288), 1% (w/v) bovine serum albumin (BSA) (fraction V; e.g., Sigma A7030), made up in DEPC-treated dH_2O. Filter through a millipore 0.2-μm filter, store in 10-mL aliquots at –20°C.
20. DePX mounting medium.

Fig. 1. (*continued*) of silver grains around their nuclei (filled arrows), are present in **(A)**; the caudate putamen (CP) as seen at low power **(Ai)** and higher power **(Aii)**; **(B)** the paraventricular nuclei (PVN); and **(C)** two examples of labeling in the supraoptic nuclei (SON) at low power **(Ci)** and higher power **(Cii)**. Note in comparison, the low and evenly distributed background density of silver grains (approx 10 gr. per 10 μm^2) overlying nonexpressing nuclei (open arrows) and the cytoplasm of these regions and also in nonexpressing areas, such as surrounding the CP (Ai) and SON (Ci). Adjacent sections pretreated with RNaseA (1μg/μL) for 60 min at 37°C, before hybridization with the PPD oligonucleotide probe or hybridized with a similar concentration of the complementary sense probe to the PPD oligonucleotide, display a similar level of even background with no evidence of clustering characteristic of labeled cells, as shown for the SON region in **(D)** and **(E)**, respectively.

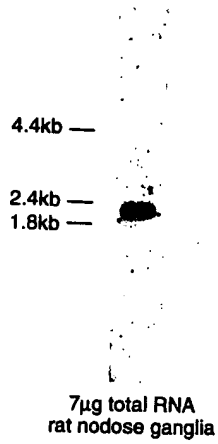

Fig. 2. Characterization of riboprobe selectivity by Northern hybridization. The selectivity of 5-HT_3R antisense riboprobes was tested by Northern hybridization. A Northern blot of total RNA, extracted from rat tissue known to highly express a 5-HT_3 receptor subtype, against a ^{32}P-mouse 5-HT_3R antisense riboprobe, clearly shows a single band of molecular weight corresponding to rat 5-HT_3 receptor mRNA *(28)*, using the protocol detailed in this chapter. The position of molecular weight markers are shown on the left. This result was also obtained when RNA extracted from a mouse neuroblastoma cell line, highly expressing native murine 5-HT_3 receptors, was probed with ^{32}P-mouse and ^{32}P-human 5-HT_3R antisense riboprobes, but no bands were detected when identical samples were probed with the equivalent sense riboprobes (data not shown).

21. Developer: e.g., Ilford Phenisol 1:4 dH_2O or Kodak D19 1:1 dH_2O (store in dark at room temperature, use until brown, which indicates that it has oxidized).
22. Diethyl pyrocarbonate (DEPC)-treated dH_2O (0.05%): in a fume hood, add 0.5-mL DEPC (e.g., Sigma D5758; stock stored at 4°C; very toxic) per liter dH_2O, shake well, then stand for 20 min, shake again, and leave standing at room temperature for 2–24, h then autoclave for 35–40 min to destroy excess DEPC. All of the solutions are made up with DEPC-treated water, unless otherwise stated.
23. Dithiothreitol (DTT; 1*M*): make a 1*M* solution of DTT (e.g., Sigma D9779) in DEPC-treated dH_2O, store at –20°C in autoclaved microcentrifuge tubes. (This solution degrades very quickly at room temperature.)
24. Dry ice.
25. EDTA (0.5*M*): add EDTA (ethylenediaminetetraacetic acid; e.g., Sigma E5134) to DEPC-treated dH_2O, stir with a magnetic flea, dissolve by adjusting to pH 8.0 with NaOH (10*M*), then autoclave.
26. Embedding medium: e.g., Cryo-M-bed or Tissue Tec.
27. Eosin Y (1%) in 80% ethanol: make 80% ethanol solution with dH_2O, dissolve

1% Eosin Y (e.g., Sigma E4382) in this, filter the solution twice through Whatman No.1 filter paper before use.

28. Ethanol solutions containing 0.3*M* ammonium acetate: Add freshly made 3*M* ammonium acetate solution (e.g., Sigma A1542 dissolved in DEPC-treated dH_2O) to 50%, 70%, 80%, and 90% ethanol solutions made up in DEPC-treated dH_2O, to give a final concentration of ethanol solutions containing 0.3*M* ammonium acetate.
29. Ethanol solutions for histological staining: make 95%, 80%, and 70% ethanol solutions with dH_2O, store at room temperature.
30. Ethanolamine solution: 0.15*M* NaCl (e.g., Sigma S3014), 0.1*M* triethanolamine (e.g., BDH 10370), 0.25% (v/v) acetic anhydride (e.g., BDH 100026Q). Make fresh.
31. Ethidium bromide solution (EtBr): make a 10-mg/mL solution of EtBr (e.g., Sigma E7637) in dH_2O; store at 4°C in a sealed, dark bottle, protected against light (very hazardous/carcinogen).
32. Fixer: e.g., Ilford Hypam fixer:dH_20 ratio of 1:4 or Kodak rapid fixer (e.g., Sigma P7542) (store in dark at room temperature, can reuse, but once diluted will last only approximately 1 wk).
33. Formaldehyde: 37% solution (12.3*M*); e.g., Sigma F8775; hazardous; store in chemical box.
34. GTC denaturing solution: at 65°C, dissolve 4*M* guanidine thiocyanite (GTC; e.g., Sigma G9277) (disrupts membranes and inhibits RNases) in a solution containing 25-m*M* sodium citrate solution (pH 7.0), 0.5% N-lauroylsarcosine (e.g., Sigma L9150) (disrupts nucleoprotein complexes) (prepare a 10% stock solution and store at 4°C; NB: may need to heat stock solution if it has precipitated), and 5-m*M* EDTA (pH 8.0) (RNase inhibitor); once dissolved add 0.8% (w/v) 2-mercaptoethanol (e.g., Sigma M3148) (RNase inhibitor), filter the final solution into an autoclaved bottle with 0.2-μm millipore filter and store at 4°C for up to 3 mo.
35. HCl (0.2*N*).
36. Histoclear.
37. Hybridization solution (2X) for ISHH: dissolve 20% (w/v) dextran sulphate (e.g., Sigma D8906; helps probe anneal) in DEPC-treated dH_2O, heated to 60°C, then add the following ingredients (final concentration); 1.2*M* NaCl (e.g., Sigma S3014), 20-m*M* Tris buffer pH 7.5, 2X Ficoll type 400 (0.04% w/v) (e.g., Sigma F2637), 2X polyvinylpyrrolidone (0.04% w/v) (e.g., Sigma P5288), 10X BSA (0.2% w/v) (96–99% albumin; e.g., Sigma A7030; store at 4°C), 2-m*M* EDTA (to chelate nuclease activating ions), 0.02% (200-μg/mL) salmon sperm sonicated ssDNA (e.g., Sigma D9156; store at –20°C), 0.001% (10-μg/mL) glycogen (e.g., Boehringer Mannheim Darmstadt, Mannheim, Germany; 901393; stock stored at –20°C), 0.01% (100-μg/mL) type X-SA baker's yeast tRNA (e.g., Sigma; R8759; stock stored at –20°C). (The last three stabilize the probe and are nonspecific hybridization blockers.) Mix the final solution well, taking care not to denature the BSA. (NB: solutions containing BSA cannot be autoclaved.) Store

0.5-mL aliquots in autoclaved microcentrifuge tubes at –20°C for up to 6 mo. When ready to use, thaw an aliquot and add an equal volume (i.e., 500 µL) of deionized formamide and mix well to give 1X hybridization solution containing 50% (v/v) deionized formamide. The final solution should be pH 7.0–7.5.

38. Isoamyl-alcohol (3 methyl-1 butanol).
39. Isopentane (2-methyl butane): e.g., BDH 103616V.
40. Isopropanol (2-propanol).
41. Linearized DNA template: approx 0.8 µg; store at –20°C (*see* **Note 7**).
42. Liquid nitrogen.
43. Mayer's Haematoxylin solution: e.g., Sigma MHS-16; filter twice through Whatman No. 1 filter paper before use.
44. MOPS running buffer (X10): for 1 L, dissolve 4.1-g sodium acetate (e.g., Sigma S2889) in 700-mL DEPC-treated dH_2O, add 41.9-g MOPS (e.g., Sigma M8899), pH to 7.0 with 10*M* NaOH, then add 10 mL of 0.5*M* EDTA (pH 8.0), make up volume with DEPC-treated dH_2O, autoclave, then store at 4°C.
45. NaOH (0.05*N*): make with DEPC-treated dH_2O.
46. Nuclear emulsion: e.g., Ilford K5 (Ilford Ltd, Cheshire, UK), store at 4°C in total darkness; lasts approx 2 mo; 20-mL diluted emulsion just sufficient for 35 slides.
47. Oligonucleotide: of known concentration (can be stable for years at –70°C) (*see* **Note 3**).
48. Paraformaldehyde (4% w/v) in 0.1*M* PBS: for 1 L, warm 500-mL DEPC-treated dH_2O to 65°C in a fume cupboard, slowly add 40 g paraformaldehyde (e.g., BDH 294474L). Add approx 200 µL NaOH (10*M*) and vigorously stir to facilitate dissolving of paraformaldehyde (takes < 1 h). Cool, add 500 mL of 0.2*M* PBS, pH to 7.5, will keep 1 mo at 4°C, after which it may polymerize (it will also polymerize if autoclaved); very hazardous chemical.
49. Phenol saturated with TE buffer: e.g., Sigma P4557; phenol is very hazardous; store at 4°C, always use in a fume hood and be extremely careful not to inhale fumes or expose to skin.
50. Phosphate buffered saline (PBS; 0.1*M*): 10-m*M* Na_2HPO_4 (e.g., Sigma S3264), 3-m*M* KCl (e.g., Sigma P9541), 1.8-m*M* KH_2PO_4 (e.g., Sigma P9791), 140-m*M* NaCl (e.g., Sigma S3014), pH to 7.4, autoclave. Will keep at 4°C for 2–3 wk.
51. Poly-L-lysine subbing solution: mix 100-mg poly-L-lysine (mol wt > 300,000, e.g., Sigma P1524; store at –20°C) in 500-mL DEPC-treated dH_2O in an autoclaved bottle (this is enough to generate approx 500 slides); make poly-L-lysine solution fresh.
52. RNA loading buffer: 0.4% bromophenol blue (e.g., Sigma B5525), 0.4% xylene cyanol (e.g., Sigma X4126),1-m*M* EDTA (pH 8.0), 50% glycerol (e.g., Sigma G5516). Store stock at 4°C. To minimize contaminations, aliquot 1-mL volumes into autoclaved microcentrifuge tubes.
53. RNA markers: 0.24–9.5 kb Ladder (e.g., GIBCO BRL 15626), store at –20°C.
54. RNA polymerases: supplied with 5X transcription buffer and 100-m*M* DTT; SP6 (e.g., Promega P1085), T7 (e.g., Promega P2075), or T3 (e.g., Promega, Southampton, UK; P2083); store –20°C or –70°C for long-term storage.

55. RNase-Free DNase: e.g., Promega M6101; store –20°C.
56. RNaseA solution buffer: 10 m*M* Tris-HCl, pH 7.6; 0.5 *M* NaCl (e.g., Sigma S3014); 1 m*M* EDTA (e.g., Sigma, E5134), pH to 8 and autoclave; will keep at 4°C.
57. RNaseA solution: dissolve ribonuclease A (RNase A; bovine pancreas; e.g., Sigma R5503; stock stored –20°C) in autoclaved dH_2O (which has not been DPEC-treated). Store aliquots at –20°C at a concentration of 12.5 mg/500 µL. When ready to use, boil aliquot for 1 min to remove DNase activity, then dilute this aliquot in RNaseA solution buffer to give a final concentration of 25-µg RNase/mL buffer.
58. rRNasin: Promega N2511; 20–40 units/µL; store at –20°C.
59. salmon sperm sonicated ssDNA: e.g., Sigma D9156; stored at –20°C; 10 mg/mL. Immediately before use, denature this solution at 100°C for 5 min, then rapidly cool on ice.
60. Scintillation fluid.
61. SDS: sodium dodecyl sulphate; 10% solution; e.g., Sigma L4522.
62. Sephadex slurry: equilibrate Sephadex G25 powder (e.g., Sigma G-25-80) in 1X TE buffer (pH 8.0) overnight, store slurry at 4°C.
63. Silica gel: 6–20 mesh, e.g., BDH 300634A.
64. Sodium acetate solution (2*M*): dissolve sodium acetate (e.g., Sigma S-2889) in DEPC-treated dH_2O, adjust to pH 4.0 with glacial acetic acid, autoclave, store solution at 4°C.
65. Sodium acetate solution (3*M*): dissolve sodium acetate (e.g., Sigma S-2889) in DEPC-treated dH_2O, adjust to pH 5.0 with glacial acetic acid, autoclave, store solution at 4°C.
66. SSPE (20X): 3*M* NaCl (e.g., Sigma S3014), 0.2*M* NaH_2PO_4 (e.g., Sigma S3139), 20-m*M* EDTA.
67. Standard sodium citrate solution (SSC; 20X): 3*M* sodium chloride (Sigma S3014), 0.3*M* tri-sodium citrate (Sigma C8532) in DEPC-treated dH_2O, adjust to pH 7.0, autoclave, will keep 2–3 wk at room temperature.
68. T4 DNA polymerase: e.g., Sigma D0410; 10 units/µL; store at –80°C.
69. terminal deoxynucleotidyl transferase enzyme: TdT supplied with 5X tailing buffer; e.g., GIBCO BRL; 18008-011; store at –20°C.
70. TE buffer (1X): 10-m*M* Tris, 1-m*M* EDTA, pH 8.0 with 10*M* NaOH, autoclave.
71. Tris (1*M*): add 6.35-g Trizma hydrochloride (Sigma T7149) to 1.18-g Trizma base (Sigma T8524) in 50 mL of autoclaved dH_2O, then autoclave to give a solution of pH 7.5 at 25°C. We do not use DEPC-treated dH_2O in case there is any residual DEPC present, which will react with Tris.
72. Unlabeled nucleotide mix: add 10 µl of each stock of 10-m*M* ATP, 10-m*M* GTP, 10-m*M* CTP (e.g., Promega; P1221; store at –80°C) to 10 µL of DEPC-treated dH_2O to give a final concentration of 2.5 m*M* of each base. Store the mix in aliquots of 2 µL at –20°C.
73. Xylene.

2.2. Equipment

1. Adequate radiation protection: perspex shielding, correct decontamination procedures, and methods of disposing radioactive waste.
2. Film cassettes and HyperFilm MP or βmax: e.g., Amersham International PLC, UK; 18 × 24 RPN6 or RPN9.
3. Gel apparatus and power pack.
4. Glass microfiber filter disks: e.g., Whatman 1822 025.
5. Hand-held beta counter.
6. Homogenator or sonicator.
7. Hybond-N+ membrane: e.g., Amersham RPN 203B.
8. Hybridization vials and mesh: (e.g., Hybaid; Hybaid, Middlesex, UK).
9. Image analysis system.
10. Intensifying screens: optional.
11. Light box.
12. Microscope.
13. Microscope cover slips (e.g., BDH 406/0188/42), slide mailers, and slides (e.g., BDH 406/0169/02 or BDH 406/0179/00).
14. Slide storage boxes: sealable (e.g., Kartell). Boxes that hold 25 slides are useful, as these will comfortably hold silica gel along with 20 slides (a manageable number to assay at one time).
15. UV spectrometer and 1-cm^2 quartz cuvet.
16. UV transilluminator.
17. Whatman chromatography paper (3MM).

3. Methods

3.1. Methods for In Situ Hybridization Histochemistry

It is important to take precautions against RNase contamination when carrying out the following protocols (*see* **Note 1**).

3.1.1. Probe Labeling

3.1.1.1. Spun Column Preparation

1. Plug a sterile 1-mL syringe barrel with glass microfiber filter paper, packing it in place with the syringe plunger.
2. Slowly pipet 1 mL of Sephadex slurry into the column, taking care to avoid air bubbles.
3. Place the column in a screw-capped microcentrifuge tube, and spin this setup in a 15-mL disposable centrifuge tube at > 1100*g* for 4 min, allowing the buffer to run through into the collecting microcentrifuge tube at the bottom.
4. Repeat the pipeting and spinning (**steps 2** and **3**) until the column contents stabilize at 1 mL of Sephadex G25.

5. Add a known volume (e.g., 100 µL) of 1X TE buffer to the top of the Sephadex bed, place the column in a fresh microcentrifuge tube, and repeat **step 3**. The volume recovered should be equal to that added to the top of the column.
6. Repeat **step 5** twice more.
7. Add 100 µL of 1X TE buffer to the top of the Sephadex bed, seal the column with Parafilm to prevent evaporation, and store upright at 4°C until ready to use (*see* **Note 2**).

3.1.1.2. 3' End-Labeling of Oligonucleotide Probes with ^{35}S

1. Set up the following reaction in autoclaved microcentrifuge in order:

Item	Amount	Final
Diluted PPD probe (*see* **Note 3**)	2 µL (~55 ng)	~50 n*M*
5X tailing buffer (supplied with the enzyme)	12 µL	1X
Autoclaved DEPC-treated dH_2O	*y* µL (to make up volume to 60 µL)	
^{35}S α-dATP (*see* **Notes 4** and **5**)	8 µL (~100 µCi)	~1.4 µ*M*
2. Equilibrate the aforementioned reaction mix to 37°C (takes ~5 min)		
3. Add TdT enzyme (15 U/µL)	6 µL	1.5 U/µL
Total Volume	60 µL	

4. Flick to gently mix, then microcentrifuge the reagents down for 2–3 s to remove air bubbles which may inhibit TdT enzyme activity.
5. Incubate the mixture for 1 h at 37°C. To obtain higher specific activity, add another 30 units TdT enzyme and incubate for a further hour at 37°C. (Meanwhile, let the spun column (as prepared in **Subheading 3.1.1.1.**) equilibrate to room temperature for approx 30 mins).
6. Stop the reaction by cooling the microcentrifuge tube on ice.
7. Prespin the spun column for 4 min at 1100*g* and discard the run through buffer.
8. Place the spun column in a fresh collecting microcentrifuge tube.
9. In duplicate, spot a 1 µL aliquot of prespun reaction mix (to measure total counts per minute [cpm]) onto a 0.5 cm^2 of filter paper in a scintillation vial, add scintillation fluid, and count with a suitable program on a beta counter.
10. Apply the rest of sample (approx 60 µL) to the center of the top of the spun column Sephadex bed, and spin the column for 4 mins at 1100*g*. The unincorporated label will remain in the column, while the probe runs through. The column can now be correctly disposed of as radioactive waste (*see* **Note 4**).
11. Retain the labeled probe in the collecting tube, measure the final volume (this should be of equal volume to that put on the column), and take duplicate 1-µL aliquots for scintillation counting (as **step 9**) to obtain a measure of incorporated

cpm/μL (dpm/μL can be calculated if the counting efficiency of the beta counter is known; it is usually approx 95% for ^{35}S isotopes). We obtain on average at least 1–1.5 × 10^6 dpm/μL (i.e., 1 X 10^8 dpm per ^{35}S-oligonucleotide labeling reaction).

12. The labeled probe can be stored at –20°C if it is to be used within the following few days. Alternatively, it can be kept up to 2 wk at –70°C, after which the level of disintegration necessitates repurification through a fresh Sephadex spun column. We usually label the oligonucleotide one day to use within 24 h.
13. From the scintillation readings, calculate:
    a. % incorporation = $\frac{\text{incorporated cpm (post-spin counts; **step 11**)}}{\text{total cpm (prespin counts; **step 9**)}}$ X 100

    The percent incorporation should average at least 70% and should not be below 50%.
    b. Specific activity (cpm [or dpm]/mol and cpm [or dpm]/μg) assuming 100% of the probe is labeled and recovered (we obtain on average 2.2–4.4 X 10^{18} dpm/mol, i.e., > 10^9 dpm/μg).

3.1.1.3. Riboprobe Labeling with ^{35}S by *In Vitro* Transcription

1. In an autoclaved microcentrifuge tube, at room temperature to avoid DNA precipitation, add in order:

Item	Amount	Final
5X transcription buffer	2 μL	1*x*
100-mM DTT (*see* **Note 6**)	1 μL	10 m*M*
rRNasin (20–40 units/μL)	1 μL	2–4 U/μL
linearized h5-HT_3R cDNA template (*see* **Note 7**)	1 μL	0.8 μg/reaction
unlabeled nucleotide mix (*see* **Note 8**)	2 μL	500 μ*M* of each base
^{35}S-αUTP (100 μCi) (*see* **Notes 4** and **9**)	2.5 μL	approx 10 μ*M*
RNA polymerase (20 U/μL) (*see* **Note 10**)	0.5 μL	1 unit/μL
	10 μL	

2. Flick to gently mix, then microcentrifuge the reagents down for 2–3 s to remove air bubbles that may inhibit enzyme activity.
3. Incubate at 37°C for 2 h (meanwhile let the spun column [as prepared in **Subheading 3.1.1.1.**) equilibrate to room temperature for approx 30 min].
4. After the 2-h incubation, add 1 unit of RNase-free DNase and incubate at 37°C for 15 min to destroy the DNA template (need 1 unit DNase/μg DNA).
5. Add 5 μL of 100-m*M* DTT stock and make the volume up to 80 μL with DEPC-treated dH_2O (*see* **Note 6**).

6. Purify the riboprobe through a spun column as **Subheading 3.1.1.2., steps 7–12.**
7. From the scintillation counter readings, calculate:
   a. cpm/μL (or dpm/μL, if the counting efficiency is known; it is usually approx 70% for ^{32}P and 95% for ^{35}S; for ^{35}S expect approx 10^7 dpm/μL) and the total cpm (or dpm), knowing the total volume (which should be equal to the volume added to the column);
   b. % incorporation = $\frac{\text{incorporated cpm (post-spin counts; Subheading 3.1.1.2., step 11)}}{\text{total cpm (pre-spin counts; Subheading 3.1.1.2, step 9)}} \times 100$
   (should obtain a value > 40%, < 90%);
   c. Total RNA made = % incorporation × theoretical maximum yield (assuming 1/4 of the total nucleotides are labeled-UTP); e.g., to calculate the theoretical maximum RNA yield, using 100-μCi ^{35}S-αUTP:

the maximum UTP incorporation	= 100 μCi/the specific activity of the radiolabel
	= 100 μCi/1200 nmol UTP
therefore maximum base incorporation	= 4 × 100/1200 nmol bases
molecular weight of RNA	= approx 330 ng/nmol
therefore the maximum yield of RNA	= approx 4 × 100/1200 × 330 ng

   d. Specific activity = total cpm/total RNA made, as calculated from the values obtained in a. and c. (this should be > 10^9 cpm/μg RNA for ^{32}P- and ^{35}S-αUTP).
8. Check the quality and molecular weight of the riboprobe on a RNA denaturing gel: Set up a denaturing gel as detailed in **Subheading 3.2.2.3., steps 1–10**, except load 0.5-μL riboprobe (or at least 5 X 10^5 cpm) in 4.5-μL loading solution with 1 μL of loading dye per well, and run the gel along with appropriate RNA size markers. Dry the gel (with the markers removed) on a gel drier, wrap in cling film and expose to autoradiography film at −70°C (as for membrane blot described in **Subheading 3.2.6.1.**) for up to 2 d. Develop the film as detailed in **Subheading 3.2.6.2.** and analyze it with reference to the markers, as described in **Subheading 3.2.8.** A good-quality probe will produce few bands of the expected length, indicating successful in vitro transcription. Poor-quality probes will yield a smear of smaller sized products as a result of degradation or poor-quality template cDNA or give bands of higher molecular weight than expected, indicating incomplete linearization of the template.

3.1.2. RNA Collection

3.1.2.1. Preparation of Clean, RNase-Free Microscope Slides

1. Taking precautions as set out in **Note 1**, stack slides in glass slide racks and wash them overnight in a sealed plastic container containing chromic acid (taking care, as the acid bath is very hazardous).
2. Rinse the slides in tap water, then wash in running water overnight.

3. Wash the slides in 2% warm Decon for 1/2 h before washing them in running water for 1/2–1 d.
4. Soak the slides for 15 min in DEPC-treated dH_2O, and repeat with fresh DEPC-treated dH_2O.
5. Soak the slides in absolute ethanol for 10–15 min to remove any remaining grease.
6. Dry the slides at 37°C, then immediately proceed to **Subheading 3.1.2.2.**

3.1.2.2. Subbing Microscope Slides

1. Dip the clean, RNase-free slides for 3 min each in 0.2*N* HCl, followed by DEPC-treated dH_2O, and finally acetone.
2. Dry the slides at 50–60°C for 15 min.
3. Dip the slides in freshly prepared poly-L-lysine subbing solution for 10 s, remove the slides, and then repeat dipping in the same solution for another 10 s.
4. Rinse the slides in DEPC-treated dH_2O for 10 min (this decreases static and dust attraction).
5. Dry slides overnight at 50–60°C, then store, sealed in dust-free slide boxes, at room temperature (the slides will keep for 6–8 mo; *see* **Note 11**).

3.1.2.3. Tissue Collection and Section Cutting

1. Immediately after death of the animal, isolate the tissue of interest, using sterile instruments and working as quickly as possible in order to reduce RNase activity and RNA degradation.
2. Mount the tissue in a minimal amount of embedding medium on a cryostat chuck. (Excess embedding medium can be trimmed off with a scalpel blade prior to cutting.)
3. Rapidly immerse the mounted sample in a beaker of isopentane, cooled to –45°C in a dry ice bath, and freeze rat spinal cord (1–1.5-cm-long segments) for 3 min and whole rat brain for 5 min. The temperature of the isopentane is critical; any lower than –45°C may cause the tissue to fracture when cut, any higher and the sample may not be rapidly frozen.
4. Wrap the frozen tissue in Parafilm, place in a sealed watertight container and store at –70°C.
5. Transfer the fresh frozen tissue from storage to the cryostat on dry ice, allowing the tissue to slowly equilibrate to the cryostat temperature (> 30 min). We find a chamber temperature of –20°C to –25°C works best for rat spinal cord and –16°C to –19°C for rat brain. (The optimal temperature will depend on the size of the tissue and on the cryostat.)
6. Trim tissue until intact, undamaged sections are obtained (*see* **Note 12**). Collect individual 10-µm thick sections by thaw mounting onto the poly-L-lysine subbed slides (*see* **Subheading 3.1.2.2.**), which have been kept at room temperature. (We usually mount two to three brain sections or five to ten spinal cord sections per slide.)
7. Periodically take sections for histological staining (*see* **Subheading 3.1.6.3.**) to check section quality.

8. Allow the sections to dry at room temperature for several minutes, then return them to the cryostat, until they can be transferred on dry ice to the −70°C freezer for storage in sealed slide boxes containing silica gel desiccant to prevent frost from building up on the slides. Sections should be used in *in situ* hybridization histochemistry as soon as possible.

3.1.3. Prehybridization

1. Sterilize all prehybridization containers and hybridization boxes (*see* **Note 1**).
2. Bring boxes containing the slides to room temperature (approx 10 min) before opening them, to prevent condensation from forming on the sections.
3. Stack the slides to be used in a slide rack. Return the remaining slides to the −70°C as soon as possible. We find 25–50 slides (enough to fill one to two slide racks) is a manageable number to assay at once.
4. Take the slides through the following steps, all carried out at room temperature:
   a. Fix with 4% paraformaldehyde in 0.1*M* PBS for 10 min (*see* **Note 13**).
   b. Wash in 1X PBS for 5 min.
   c. Repeat **step b** using fresh PBS.
   d. Acetylate with ethanolamine solution for 10 min (to reduce nonspecific binding of the negative probe to the positively charged glass slides and tissue) (*see* **Note 13**).
   e. Dehydrate through ascending 2-min steps of ethanol containing 0.3*M* ammonium acetate, from 70%, 80%, 90%, then 100% ethanol.
   f. Wash in chloroform for 2 min (to delipidate the sections, thus reducing nonspecific hybridization to white matter) (*see* **Note 13**).
   g. Wash in 100% ethanol followed by 90% ethanol containing 0.3*M* ammonium acetate.
5. Dry slides with a hair dryer (set to cold air).
6. Place slides (section side up!) in a sealable hybridization container containing thin foam or filter paper saturated with soaking solution (i.e., 1 part 4X SSC : 1 part deionized formamide). There should be sufficient soaking solution to keep the boxes saturated throughout overnight hybridization, but not so much that it spills onto the sections.
7. Hybridize immediately. (We have not found it necessary to prehybridize with hybridization solution minus probe before the hybridization step.)

3.1.4. Hybridization

1. Calculate the volume of labeled probe required to give 0.5–2.5 × 10^6 cpm/section (20,000–60,000 cpm/µL) (*see* **Note 14**).
2. Thoroughly mix 2X hybridization solution with an equal volume of deionized formamide (*see* **Note 15**) to give the required volume of hybridization buffer (final concentration of 1X hybridization solution, containing 50% [v/v] formamide).
3. Add the calculated amount of labeled probe to the hybridization buffer. Make sure the solution is well mixed and contains no air bubbles. Equilibrate this to

60–70°C for 10 min to denature the probe, then immediately cool it on ice for 2–3 min, to keep the probe single-stranded.

4. Add 10 µl of 1*M* DTT/mL of hybridization mixture, to give a final concentration of 10 m*M* DTT (*see* **Note 6**), mix well, and spin down to reduce air bubbles.
5. Pipet the determined aliquots of this hybridization buffer onto each section and, using forceps, gently coverslip with a piece of Parafilm cut to the size of the section, in order to prevent dehydration. It is important to cover the entire section with buffer (without scoring the section with the pipet tip or creating air bubbles, which are easily produced by excess pipeting because of the BSA in the solution) or by dropping the cover slip over the section.
6. Seal the hybridization chamber with tape, incubate overnight in an oven at the hybridization temperature. We successfully use 37°C for the PPD oligonucleotides and 60°C for the h5-HT_3 R riboprobes (*see* **Note 16**).

3.1.5. Posthybridization Washing

The temperature, wash durations, and SSC concentrations used at this stage depend on the properties of the specific oligonucleotides and riboprobes used (*see* **Note 17**). The conditions described below work well for the 48-base PPD oligonucleotides and the 750 base h5-HT_3 receptor riboprobes and can be used as a guide for other similar probes:

1. Dilute 20X SSC to the dilutions required below and equilibrate these wash solutions in a water bath to the necessary wash temperatures (takes approx 1 h). Sterile conditions do not need to be maintained at this stage (*see* **Note 1**). Make enough solution to completely immerse the slides. We use approximately 500 mL per 1 L beaker, containing 25 slides. For the riboprobe washes also equilibrate RNase solution (25 µg/mL) to 37°C.
2. After hybridization, stack the slides into slide racks and place them in slide boxes, containing 2X SSC at room temperature. Wash the slides for 5 min with slight agitation, and using forceps, carefully remove the Parafilm cover slips.
3. Meanwhile, rinse the used hybridization boxes, then soak them in Decon overnight to reduce radioactive contamination, remembering that everything that comes into contact with the hybridization solution is radioactive and should be handled accordingly (*see* **Note 4**).
4. Once all of the cover slips have been teased away from the sections, suspend slides in 1-L beakers and wash as follows:
   a. *For 48-base PPD oligonucleotide*: 2X SSC at 37°C for 120 min, followed by 1X SSC at 37°C for 120 min, and finally 0.5X SSC at 37°C for 120 min.
   b. *For h5-HT_3R riboprobe:* 2X SSC at 55°C for 30 min, followed by 25-µg/mL RNaseA solution at 37°C for 60 min (*see* **Note 18**), followed by 2X SSC at 50°C for 60 min, and finally 0.1X SSC, containing 14 m*M* of 2-mercaptoethanol at 50°C for 3 h, leaving them to cool to room temperature overnight (*see* **Note 19**).

5. Dehydrate the sections in 50% ethanol, containing 0.3*M* ammonium acetate for 4 min, then 70% ethanol, containing 0.3*M* ammonium acetate for 2 min, and finally in 90% ethanol, containing 0.3*M* ammonium acetate for 2 min (*see* **Note 20**).
6. Dry the slides overnight at room temperature under a paper towel to minimize dust, which may cause background problems if emulsion-dipping the sections.
7. Slides are now ready to expose to emulsion to obtain cellular resolution. Alternatively, slides can be exposed to film for rapid signal detection without cellular resolution for quick optimization of the assay parameters (*see* **Subheading 3.2.6.**).

3.1.6. Probe Detection

3.1.6.1. Emulsion Dipping

1. In the darkroom, equilibrate a water bath to 43°C and for accuracy measure out, in a separate measuring cylinder, the aliquot of dH_2O required to dilute the emulsion 1:2 water, knowing that 15 mL of diluted emulsion will coat approx 10 slides (*see* **Note 21**).
2. Under safelight conditions (e.g., using Ilford 902-904 safelight with a 15-W bulb): Let the emulsion reach room temperature before removing an aliquot with a clean metal spatula (*see* **Note 22**). Melt this aliquot at 43°C in a measuring cylinder (takes approx 1 h), and in this time also allow the premeasured dH_2O aliquot to reach 43°C.
3. Slowly add the water to the emulsion, pouring it carefully down the side of the measuring cylinder to prevent air bubbles forming in the emulsion, which will cause uneven coating. Gently pour the diluted emulsion into a slide mailer box (again avoiding air-bubble production). Support the mailer in the water bath at 43°C, and allow the emulsion to settle for a few minutes.
4. Dip each slide singly into the emulsion while holding the top, labeled end of the slide. Use a uniform dipping technique (e.g., hold each slide in the emulsion for 2 s and slowly extract) to obtain an even emulsion coating of similar thickness over the whole of each slide.
5. Blot the underside of the slide on a paper towel, lay the slides flat sections side up on a metal tray cooled on ice, or on a cold plate, for 2 h in total darkness to set the emulsion.
6. Once the emulsion has set, position the slides vertically and allow them to dry slowly overnight in total darkness.
7. The next morning, pack the dry slides in slide boxes containing silica gel desiccant, seal with electrical tape, wrap in foil, then a black plastic bag, and store the boxes at 4°C in the dark for required exposure time, away from any source of radiation or strong chemicals; this being 8–10 wk for the PPD oligonucleotide and h5-HT_3R riboprobe experiments. Initially, it is a good idea to prepare a number of similarly treated ISHH slides and develop these at different time points to ascertain the optimal exposure time for that specific probe (*see* **Note 23**).

3.1.6.2. Emulsion Developing

1. Remove the boxes of emulsion-coated slides from the cold room and equilibrate to room temperature (approx 30 min) before opening them to prevent condensation forming on the slides, which may wrinkle the emulsion coat. The slides should be treated gently at all times, as the emulsion coat is very prone to mechanical stress and is easily scratched.
2. Under safelight conditions (using Ilford 902-904 safelight with a 15-W bulb): Carefully remove the slides from their box, put them in slide racks, and process as follows, with gentle agitation (checking beforehand that the temperature of the following solutions is below 20°C, as silver grain size is proportional to temperature):
   a. developer (at 18°C): 4 min,
   b. dH_2O: rinse,
   c. fixer: 4 min (this being twice the time it takes for the emulsion to clear),
   d. fixer: 4 min, and
   e. dH_2O: 5 X 10 min (**Note 24**).
3. Stain and mount slides immediately.

3.1.6.3. Histological Staining of Slides using Haematoxylin/Eosin

Aim to obtain a light stain, so that the blue color does not interfere with image analysis (*see* **Note 25**). Stain the slides as follows:

1. Mayer's Haematoxylin: 20 s,
2. dH_2O: 5 s,
3. alkaline H_2O: 30 s,
4. dH_2O: 30 s,
5. 70% EtOH: 1 min (needed because alcohol-based eosin is used),
6. 1% eosin Y: approx 1 s (dilute if too "young"),
7. acid alcohol (70%): ≤ 15 s (this takes out excess eosin),
8. 95% EtOH: 2 X 1 min,
9. 100% EtOH: 2 X 1 min, and
10. Histoclear: 2 X 2min (clearing problems occur with "old" Histoclear).
11. Immediately mount the sections in DePX mounting medium and gently cover slip with the aid of forceps in order to avoid air bubbles (*see* **Note 26**).

3.1.7. Controls

3.1.7.1. Negative Controls

1. Antisense vs sense probes: Replace the antisense probe with a labeled sense probe, which has a complementary sequence to that of the antisense (i.e., an identical sequence to the mRNA under investigation) and therefore will have similar physical properties to the antisense probe but should not hybridize under identical assay conditions (*see* **Notes 3, 7** and **Fig. 1A–C** vs **1E**).
2. RNaseA pretreatment of tissue: After prehybridization (**Subheading 3.1.3.**) pipet 100 µL of RNase buffer containing RNaseA (1 µg/µL) onto each section and

3.2.1. Probe Labeling

Label probes for Northern blotting in exactly the same manner as described in **Subheading 3.1.1.2.** or **3.1.1.3.** Generally, cDNA and riboprobes are the probes of choice in Northern hybridization, as these are generally more sensitive than shorter oligonucleotides (*see* **Table 1**). Usually ^{32}P is the label of choice in Northern hybridization, where signal scatter and low resolution are not important (*see* **Table 2**). The following protocols describe the successful use of ^{32}P-labeled h5-HT_3R riboprobes. Standardly, the probe is labeled one morning and used that evening in overnight hybridization.

3.2.2. RNA Collection

3.2.2.1. Tissue Collection for RNA Isolation

1. Immediately after death of the animal, isolate the tissue of interest, using sterile instruments and working as quickly as possible in order to reduce RNase activity and RNA degradation.
2. Wrap the specimen in silver foil and snap freeze it for 5 min in liquid nitrogen.
3. Store the frozen tissue in sealed watertight containers at –70°C.

3.2.2.2. Rapid Extraction of Total RNA

This method is based on that by Chomczynski and Sacchi ***(30)***.

1. In a fume hood, wash a homogenizer or sonicator probe with 3% H_2O_2 solution, followed by 70% ethanol solution, then 0.1*N* NaOH solution containing 1 m*M* EDTA, and finally with at least seven changes of DEPC-treated dH_2O, to remove any possible RNase contamination.

The following procedures must be carried out in a cold room or on ice, using prechilled solutions:

2. Weigh out 30–40 mg tissue into autoclaved microcentrifuge tubes, using a sterile scalpel blade to cut samples from the frozen tissue block (*see* **Note 29**).
3. Immediately add 400 µL of GTC denaturing solution.
4. Homogenize the tissue on ice for approximately 4 s, washing the homogenizer as in **step 1** before each new sample.
5. Add 40-µL 2*M* sodium acetate (pH 4.0) and vortex well.
6. Add 400-µL TE saturated phenol and vortex. (The bubbles should disappear here.)
7. Add 80-µL chloroform:isoamyl alcohol mix (of ratio 49:1). (The presence of isoamyl alcohol gives a sharper and more hydrophobic interface, allowing better visualization and more efficient removal of the aqueous phase.)
8. Vortex for at least 10 s to obtain an emulsion, then cool on ice for 15 min.
9. Spin for 20 min at 4°C at 14,000*g* in a microcentrifuge.
10. Transfer the aqueous phase (i.e., the top, very clear layer of approximately 400 µL in volume) to a clean microcentrifuge tube, taking care not to contami-

nate this with any of the protein interface, which will result in impure RNA, or with the lower phenol-chloroform phase, which may prevent RNA precipitation.

11. Add 1 vol (i.e., approx 400 µL) of isopropanol and precipitate the RNA at −20°C for at least 1 h (overnight for maximum recovery).
12. Spin for 20 min at 4°C at 14,000*g* in a microcentrifuge.
13. Carefully remove and discard the supernatant with an autoclaved glass Pasteur pipet. A small opaque pellet of RNA should now be visible at the bottom of the microcentrifuge tube.
14. Flick resuspend the pellet in 120 µL of GTC denaturing solution.
15. Add 1 vol (i.e., 120 µL) of isopropanol and reprecipitate the RNA at −20°C for at least 1 h (overnight for maximum recovery).
16. Spin for 10 min at 4°C at 14,000*g* in a microcentrifuge.
17. Remove the supernatant with an autoclaved drawn out Pasteur pipet, taking care not to touch and therefore shear the RNA pellet.
18. Wash the pellet by flicking it in at least 400 µL of 75% ethanol made with DEPC-treated dH_2O.
19. Spin for 10 min at 4°C at 14,000*g* in a microcentrifuge, then pour off the ethanol.
20. Dry the pellet inverted on the bench at room temperature for approx 10 min; long enough to remove the ethanol but not too long that the overdried pellet will be difficult to resuspend.
21. Resuspend in 40-µL DEPC-treated dH_2O (i.e., 1-µL/mg starting tissue).
22. Store at −20°C, ready for Northern blotting (or for poly(A)+ RNA extraction; *see* **Note 30**).
23. Measure the absorbance values of the total RNA solution, using a quartz cuvet and a UV spectrometer at wavelengths of 230 nm (absorbance of guanidine thiocyanate), 260 nm (absorbance of nucleic acids), and 280 nm (absorbance of protein) to calculate:
    a. purity, where $Abs_{260/280}$ ratio = 2.0 represents 100% purity of RNA to protein and $Abs_{260/230}$ ratio >2.0 indicates successful removal of GTC and 2-mercaptoethanol and
    b. concentration, where (for a pathlength of 1 cm) 1 unit at Abs_{260} = 40-µg/mL RNA (expect a yield of 1–2 µg total RNA/mg starting tissue).
24. Measure the 28S:18S ratio on a denaturing gel to obtain a measure of the RNA integrity (*see* **Note 31**).

3.2.2.3. RNA Gel Fractionation

1. Soak a suitably sized gel tray, stops, and well molds that will hold 20-µL volumes, in DEPC-treated dH_2O for at least 1 h (*see* **Note 32**).
2. Make enough agarose (1%)/formaldehyde solution to give a gel no more than 0.5-cm thick.
3. Set up the gel case in a fume hood, pour the cooled gel into the RNase-free gel tray, allow this to set (15–30 min), then remove the stops and "age" the gel in 1X MOPS running buffer for at least 15 min.
4. Meanwhile, thaw the RNA samples and an aliquot of deionized formamide on ice.

5. Prepare fresh loading solution by mixing 100 µL of 10X MOPS running buffer with 175 µL of formaldehyde and 500 µl of deionized formamide.
6. For each RNA sample, dilute and gently mix (by flicking) up to 20 µg of RNA (at least 5 µg) in loading solution to give a final volume of 20 µL. Similarly prepare 20 µL of RNA marker solution, containing 3-µg RNA markers diluted in loading solution.
7. Incubate the diluted samples at 65°C for 15 min to denature the RNA, then rapidly cool them on ice to keep the RNA denatured.
8. Add 1 µL of loading dye to each 20 µL of diluted sample and carefully pipet the aliquots into separate wells of the "aged" gel, noting the order in which the samples and markers are loaded. Take care not to pierce the bottom of the gel or to expel the last drop of solution from the pipet tip, as this may cause air bubbles to push the solution out of the well. Work quickly to minimize sample diffusion.
9. Immediately run the gel at 100 V (approx 100 mA) from the anode to the cathode for 3 h or until the leading dye front is at least two-thirds down the gel.
10. Chop off the markers with a sterile scalpel blade and incubate these with ≤ 2-µg ethidium bromide/mL running buffer for 20 min, destain overnight in DEPC-treated dH_2O at 4°C to remove formaldehyde and excess ethidium bromide in order to visualize the RNA on a UV transilluminator and process as described in **Subheading 3.2.8.**
11. Trim off any excess gel from around the edges (to economize on blotting materials in later steps) and remove the top right corner so that the gel orientation can be identified.
12. Soak the gel containing the samples for 20 min in 0.05*N* sodium hydroxide, rinse in DEPC-treated dH_2O, soak for 45 min in 20X SSC, and immediately transfer the RNA to membrane by Northern blotting.

3.2.2.4. Northern Blotting by Capillary Transfer (see Fig. 3)

1. Cut a piece of nylon membrane (e.g., Amersham HybondN+) to the exact size as the gel, chop the top right corner to match the gel, and label the membrane. Handle the membrane very carefully, to avoid putting any pressure on it, or touching it without gloves, both of which will result in increased background levels.
2. Cut three pieces of Whatman 3MM chromatography paper to use as a wick.
3. Cut three pieces of Whatman 3MM chromatography paper to the exact size as the gel.
4. Pour 20X SSC (approx 1 L) into a plastic trough.
5. Wet the three paper wicks and place these over a plastic tray, bridging the trough so that each end of the wick is in the 20X SSC solution.
6. Roll out the wick, using a Pasteur pipet like a rolling pin, to remove any air bubbles that will cause uneven flow of solution.
7. Place the gel in the center of the wick-covered bridge.
8. Wet the nylon membrane for 1 min in 20X SSC, then place this to fit exactly on top of the gel, lining it up with the top of the wells. Roll out any air bubbles, using

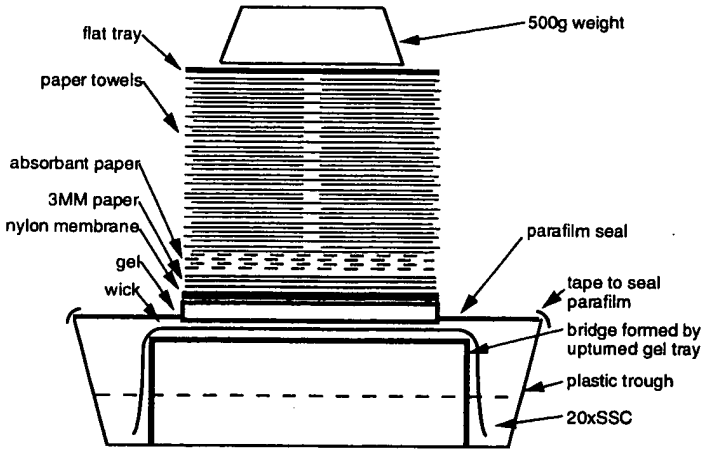

Fig. 3. Apparatus for Northern blotting by capillary transfer.

a Pasteur pipet as before, and finally mark the positions of the wells on the membrane (*see* **Note 33**).

9. Dip the three pieces of gel-sized Whatman 3MM paper for 1 min in 20X SSC, then place these to fit exactly over the membrane. Roll out any air bubbles, using a Pasteur pipet as described in **step 6**.
10. Surround the membrane with Parafilm to fully seal it, preventing solution flow from anywhere in the trough other than through the gel.
11. Cross four pieces of folded absorbent paper over the membrane set up at angles of 0°, 90°, 180°, and 270°.
12. Place a approx 5-cm thickness of paper towels over the absorbent roll, put a flat tray over these, and a 500-g weight on top of that (e.g., a 500-mL bottle of water) to aid consequential RNA transfer from the gel to the membrane with solution flow.
13. Leave this set up for at least 18 h at 4°C, replacing wet paper towels with fresh ones as necessary.
14. The next day, dismantle the setup and carefully lift the blotted membrane from the gel. Wash the membrane briefly in 2X SSC to remove any agarose and air dry for 30 min between filter paper (*see* **Note 34**).
15. Bake the membrane blot between two sheets of Whatman 3MM chromatography paper for 2 h at 80°C to permanently immobilize the RNA on the membrane (*see* **Note 35**).
16. Hybridize the membrane blot immediately or mount it on fresh filter paper, seal in cling film, then in foil, and keep at 4°C until hybridization. By doing the latter, a bank of membranes can be set up and stored for several weeks before hybridization.

Table 3
Choice of Prehybridization Solution

Prehybridization solution:	For 10 mL	Final concentration
Deionized formamide	5 mL	50%
20X SSPE	2.5 mL	5X
50X Denhardt's solution	1 mL	5X
10% SDS	500 µL	0.5%
0.5*M* EDTA	20 µL	1 m*M*
DEPC-treated dH_2O	880 µL	—
salmon sperm ssDNA	100 µL	100 µg/mL

3.2.3. Northern Prehybridization

Prehybridisation is an important step for reducing background levels in Northern hybridization.

1. Make the prehybridization solution (**Table 3**) in a sterile 15-ml vial and equilibrate this to the hybridization temperature, this being 55°C for the h5-HT_3R riboprobes (*see* **Note 36**).
2. Wet the mesh support in a trough of 2X SSPE at room temperature and lay the membrane blot over this, remembering to handle this carefully and only by the corners. Wet the membrane, roll it in the mesh, and place the whole roll in the 50-mL hybridization vial with enough (approx 15 mL) 2X SSPE to help roll out the mesh around the inside surface of the vial, avoiding all air bubbles (which, if not removed, will prevent even distribution of solution and cause hot spots of background radioactivity over the membrane).
3. When the membrane is in place, wrapped around the perimeter of the inside of the vial with no air pockets, replace the 2X SSPE with 5 mL of prewarmed prehybridization solution.
4. Prehybridize at 55°C for 1.5 h, with rotation.

3.2.4. Northern Hybridization Using ^{32}P-labeled Riboprobes

1. During prehybridization, prepare the hybridization solution in a sterile 15-mL vial (*see* **Table 4**).
2. We use all of the labeled product from one labeling reaction of 50 µCi ^{32}P (i.e., at least 16 ng of riboprobe of up to $1–2 \times 10^8$ dpm, **Subheading 3.1.1.3.**) for 5 mL of hybridization solution and one membrane blot, and perform one antisense and one sense reaction simultaneously in two separate vials. Denature the aliquot of ^{32}P-labeled riboprobe at 60–70°C for 10 min, then rapidly cool it on ice. Add this denatured probe to the hybridization solution, mix thoroughly, and equilibrate this mixture to the hybridization temperature in a water bath (*see* **Notes 4** and **36**).

Table 4
Choice of Prehybridization

Hybridization solution:	For 10 mL	Final concentration
Deionized formamide	5 mL	50%
20X SSPE	2.5 mL	5X
10% SDS	100 µL	0.1%
0.5*M* EDTA	20 µL	1 m*M*
DEPC-treated dH_2O	2.28 mL	—
salmon sperm ssDNA	100 µL	100 µg/mL

3. Immediately after prehybridization, replace the solution in the vial with the 5-mL aliquot of prewarmed hybridization solution.
4. Hybridize at 55°C, overnight with rotation.

3.2.5. Posthybridization Washing

1. Pre-equilibrate the washing solutions to their correct temperatures (*see* **Note 17**).
2. Pour off the radioactive hybridization solution (*see* **Note 4**).
3. Wash the membrane (50 mL/wash), with rotation, in:
   a. 2X SSC, containing 0.1% SDS for 15 min at room temperature;
   b. 2X SSC, containing 0.1% SDS for 15 min at 60°C;
   c. 2X SSC, containing 0.1% SDS for 15 min at 60°C;
   d. 0.1X SSC, containing 0.1% SDS for 15 min at 60°C; and
   e. 0.1X SSC, containing 0.1% SDS for 15 min at 60°C.
   Discard the wash solution and assess the amount of radioactivity left on the membrane with a hand-held beta counter, in order to adapt the stringency of the next wash accordingly, before adding the next solution (*see* **Note 37**).
4. Air dry the membrane on filter paper at room temperature behind protective shielding for 20–30 min.
5. Mount the membrane blot by the corners onto fresh filter paper, cutting the same corner of the filter paper as the membrane and label before covering with cling film, and then expose to autoradiography film.

3.2.6. Probe Detection

3.2.6.1. Exposing to Autoradiography Film

In the darkroom, using Ilford 902-904 safelight and 15-W bulb:

1. Cut one corner of the autoradiography film (usually the same corner as the membrane to avoid confusion!) to identify the orientation of the film after development. Arrange the film in a film cassette and fix securely in position with tape.

2. Securely, tape the mounted membrane blot to the film, avoiding creases in the cling film.
3. Mark the exact position of the wells on the film to enable accurate calculation of the size of the detected bands (*see* **Subheading 3.2.8.**).
4. Seal the cassette against light, label, date, and store it at −70°C. For the h5-HT_3R riboprobes, the film requires exposure for 4–5 d. The blot can be re-exposed to film if this time period is not sufficient, or intensifying screens may be used to decrease the exposure time.

3.2.6.2. Film Developing

1. Remove the film cassette from the −70°C freezer and allow it to equilibrate to room temperature for up to 1 h before opening the cassette under safelight conditions.
2. Develop the film as **step 2** of **Subheading 3.1.6.2.**
3. Hang the film up until dry, then visualize the silver grains on a light box (*see* **Note 38**).

3.2.7. Controls

3.2.7.1. Negative Controls

1. Antisense vs sense probes: Replace the antisense probe with a labeled sense probe, which has a complementary sequence to that of the antisense (i.e., identical sequence to the mRNA under investigation) and therefore will have similar physical properties to the antisense probe, but should not produce any bands under identical hybridization conditions (*see* **Notes 3** and **7**).
2. Assay RNA extracted from a source known to be devoid of the RNA species under investigation.

3.2.7.2. Positive Controls

1. The size, number of bands, and selectivity of the signal, as compared to the pattern obtained with the sense strand, give good indications of the validity of signal detection (*see* **Fig. 2**).
2. Assay RNA extracted from a cell line that highly expresses the mRNA of interest and/or from an area known to express the RNA species in abundance (*see* **Fig. 2**).
3. Rehybridize the stripped blot with a probe to a constitutive RNA species (such as β-actin mRNA), which is expressed in high and constant amounts independent of external influences, as an internal control to check the integrity and the amount of each RNA sample loaded on the gel. This also provides a method to quantify any changes in expression in the mRNA of interest under different conditions.

3.2.8. Analysis

1. Visualize the ethidium-bromide-stained markers on the destained gel (**Subheading 3.2.2.3., step 10**) on a UV transilluminator (taking the necessary precautions to protect one's eyes from UV light) and photograph these against a ruler.

2. Mark off the position of each molecular weight marker band on graph paper and plot the log of the molecular weight (given on the product data sheet) against band migration distance from the well (in millimeters) to obtain a linear standard molecular weight calibration graph.
3. After the film has been developed (**Subheading 3.2.6.2.**), measure the migration distance (in millimeters) of detected bands on the film from the top of the marked well position. Calculate the molecular weight of these bands, using the equation of the line for the linear standard molecular weight calibration graph obtained in **step 2**.

4. Notes

1. It is critical to maintain RNase-free conditions prior to and during hybridization. To minimize RNase contamination, bake glassware overnight at 200°C, autoclave pipet tips, microcentrifuge tubes and solutions, etc., where possible. If it is not possible to autoclave or bake items, these should be sterilized with 70% ethanol, then rinsed thoroughly with DEPC-treated dH_2O. Always wear gloves and avoid breathing directly on RNase-free items, as RNase is present on skin and in breath. Make solutions with DEPC-treated dH_2O where possible or autoclaved dH_2O if not (DEPC cannot be added directly to Tris-containing solutions, as primary amines will be produced). RNA/RNA and DNA/RNA hybrids are RNase-resistant, so non-RNase-free procedures can be carried out after hybridization.
2. RNase-free spun columns are commercially available (e.g., IBL, Cambridge, UK) Nuclean D25 columns; [store at 4°C] or Biospin 30 [Bio-Rad 732-6004] for DNA > 20 bp). However, it is cheap and quite straightforward to make them in-house, provided that RNase-free conditions can be maintained.
3. To design a suitable antisense oligonucleotide probe, select a complementary area within the transcribed sequence of interest of 20–50 bases that is selective for that sequence when compared with all other known gene sequences on a database, using, for example, a FASTA or BLAST search, and has a GC content of 50–60% (*see* **Subheading 1., step 4**). It is optimal to have 100% base-pair homology with the mRNA sequence, as only one mismatch in a short probe may be enough to lose signal. The PPD oligonucleotide antisense probe used here is complementary to a unique nucleotide sequence within the main exon of the rat prodynorphin gene, comprised of bases 862–909 *(27)*. The sense strand has the identical sequence to the mRNA in this region and therefore has similar physical properties to the antisense strand (i.e., a length of 48 bases, a GC content of 60%, Tm value under these conditions of 60°C, and a molecular weight of 18.23 g/mmol), yet should not hybridize. Shown below are the antisense and sense probe sequences, running left to right from the 5'-end to the 3'-end:

antisense: TATGGGGGCTTCCTGCGGCGCATTCGCCCCAAGCTTA AGTGGGACAAC

sense: GTTGTCCCACTTAAGCTTGGGGCGAATGCGCCGCA GGAAGCCCCCATA

Mol wt = (251 X nA) + (227 X nT) + (267 X nG) + (242 X nC) + (62 X n-1) + (54 X n) + (17 X n-1)

where: nA, nT, nG, nC = number of respective bases in the probe sequence
62 X n-1 = molecular weight of phosphate groups
54 X n = molecular weight of water molecules/nucleotide
17 X n-1 = mol wt of ammonium cations associated with the phosphate groups.

The stock concentration of antisense used in our case was 15.36 pmol/μL, from which aliquots were diluted with autoclaved dH_2O, ready to be used directly in the reaction mix.

4. Precautions should be stringently adhered to when working with radioactive isotopes such as ^{35}S and ^{32}P. These precautions include the use of protective acrylic plastic shielding in the case of ^{32}P isotopes, regular radiation level monitoring of persons and the designated working area, avoiding aerosol production, and disposal of radioactivity as required by the institute's regulations. Use only fresh radiolabel with a high specific activity. This will produce a probe of high specific activity and lower background.
5. Some oligonucleotides label better than others, and this appears to depend on their base composition. For good 3'-end labeling, we find a stoichiometry within the reaction mix of approximately 30 pmole of ^{35}S-αdATP to 1 pmol oligonucleotide probe and a TdT enzyme dilution of at least 1:10, works well. ^{32}P-labeled oligonucleotide probes can be generated by replacing ^{35}S-αdATP with a similar molar quantity of ^{32}P-αdATP in the labeling reaction and carrying out the procedure in the same way.
6. The reducing agent, DDT, is added to stabilize nucleic acid hybrids and also to prevent the formation of disulfide bridges in ^{35}S-labeled probes, keeping the probe single-stranded and thus available for hybridization.
7. A suitable antisense riboprobe can be 50–1000 bases long, depending on the tissue type and the way this tissue has been fixed and pretreated, all of which affect the degree of probe access to hybridization sites. When designing a suitable vector to generate a riboprobe, select from the restriction digest map an area within the transcribed sequence of interest that can be subcloned into an appropriate vector expression system for in vitro transcription and that has a high GC content (approximately 50%), but not too high that the probe will be very "sticky," causing background problems, and is selective for that sequence when compared with a database containing all other known gene sequences, using, for example, a FASTA or BLAST search. Once this selected cDNA sequence has been subcloned, the resulting vector is amplified and purified. Linearized cDNA template is then produced for in vitro transcription by cutting the vector containing the subcloned region of cDNA sequence with an appropriate restriction enzyme and purifying the product. An appropriate restriction enzyme is one that will cut the sequence either immediately downstream of the cDNA insert or within the insert, yet leave the promoter site intact, so that specific-sized transcripts are generated that contain minimal nonspecific vector sequence. **Fig. 4** shows a schematic representation of a vector, containing cDNA corresponding to amino acid residues 62–312 of the h5-HT_3 receptor sequence. The pBluescript II SK^+ plas-

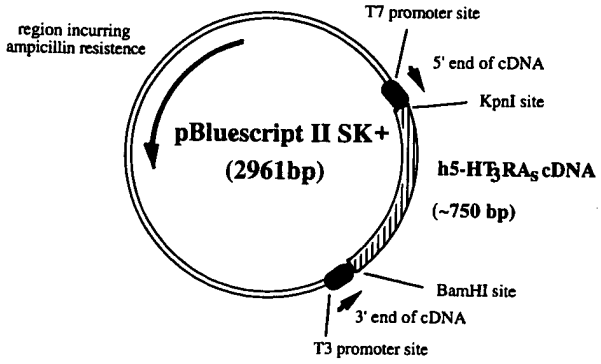

Fig. 4 Construct used to generate h5-HT_3R riboprobes.

mid vector is selectively amplified in *E. coli* XL1-Blue MRF′ competent cells (Stratagene, Cambridge, UK) in the presence of ampicillin. To generate antisense transcripts, the resulting purified plasmid is cut with KpnI and transcription performed from the T3 RNA polymerase site. To generate sense transcripts, the vector is linearized with BamHI and transcription performed from the T7 promoter site. For convenience, a stock of linearized cDNA template is stored at –70°C, and when necessary, an aliquot is diluted in DEPC-treated dH_2O to the required concentration for in vitro transcription. Aim to add 0.5–1 µg of template to the reaction set out in **Subheading 3.1.1.3.**

It is best to avoid using restriction enzymes that produce 3'-overhang ends on the cDNA template. These ends can act as promoters to initiate nonspecific or wraparound transcripts. If 3' sticky ends are unavoidable, such as when using KpnI to generate antisense h5-HT_3R riboprobes, it is necessary to blunt-end the cDNA with T4 DNA polymerase before in vitro transcription: Add 5 units of T4 DNA polymerase (i.e., 0.5 µL of 10-units/µL stock) per µg cDNA template to the reaction mix containing transcription buffer, DTT, rRNasin, and linearized DNA, as detailed in **Subheading 3.1.1.3., step 1**. Incubate at 22°C for 15 min, then add the remaining ingredients and proceed with in vitro transcription exactly as described.

8. Addition of cold UTP to the reaction mix should increase the amount of transcription, but will lower the specific activity of the resultant probe. We find that this also dramatically increases nonspecific binding; therefore, we avoid adding cold UTP.
9. ^{32}P-labeled riboprobes can be generated by substituting ^{35}S-αUTP for 50 µCi of ^{32}P-αUTP and proceeding as detailed.
10. RNA polymerases are very labile and should be kept on ice and returned to the freezer immediately after use. No more than 10-units/µg cDNA template is required, as promoter-specificity will be lost if excess polymerase is used; at high concentrations, T7 RNA polymerase may act at the T3 promoter site and vice versa.

11. It is possible to buy RNase-free subbed or positively charged slides (e.g., BDH superfrost plus microscope slides). These are very convenient to use and are competitively priced.
12. Throughout the cutting session, always wear gloves and avoid breathing on tissue, in order to avoid RNase contamination (*see* **Note 1**). Similarly, a new disposable blade should be used for each new sample. This blade is initially cleaned with xylene followed by ethanol, then frequently recleaned with ethanol throughout the cutting session.
13. The exact steps employed in prehybridization treatment may vary depending on the nature of the tissue: The length of the paraformaldehyde fixation step is critical, and times may need to be optimized to produce sufficient tissue fixation, without causing excessive cross-linkage that will inhibit probe penetration. We have acetylated then delipidated CNS sections with chloroform in a standard manner, but these steps may be ineffective in other situations and on other tissues.
14. We successfully use 20 µL of 1X hybridization buffer/rat spinal cord section, 50 µL of 1X hybridization buffer/rat coronal brain section, and 200 µL of hybridization buffer/human brain section (approx 4 cm^2). The volume of hybridization buffer used will obviously depend on the size of the section. Aim to have minimum volume, therefore maximum probe concentration, yet sufficient solution that the section is completely covered and will not dry out. The optimal probe concentration may differ between probes, therefore initially it may be necessary to try a range of probe concentrations to find which is best for the particular application.
15. Formamide is a hydrogen bond breaker, therefore it acts as a destabilizing agent reducing nonspecific binding. The signal-to-noise ratio can be manipulated by adjusting the percentage of formamide in the hybridization buffer (*see* **Subheading 1., step 4**).
16. The hybridization temperature is dependent on the properties of the probe used, as defined by the Tm equations (*see* **Subheading 1., step 4**). These equations reveal how hybrids formed between RNA and riboprobes are more stable than those formed with short DNA oligonucleotides, therefore formation of the former can withstand more stringent hybridization conditions.
17. The rate of hybridization increases with increasing salt concentration and decreasing temperature, therefore the ratio of hybridization to nonspecific background can be increased by adjusting the temperature and/or the salt concentration at the posthybridization wash stage. The wash conditions for oligonucleotides are usually much less stringent than when using a riboprobe, as DNA:RNA hybrids are less stable than RNA:RNA hybrids (*see* **Subheading 1., step 4**). However, if these conditions are too stringent, the probe will be stripped off completely, yielding no signal detection.
18. RNaseA destroys single-stranded RNA, leaving duplexed RNA intact. This is therefore an important step in removing any nonhybridized riboprobe and thus reducing background. Keep all containers and solutions containing RNaseA away from all materials that they may come in contact with prior and during subsequent hybridisation assays.

19. 2-mercaptoethanol (or DTT) is used to stabilize hybridized riboprobe, but also inhibits RNase activity; therefore it cannot be added to washes prior to the RNaseA step.
20. The ammonium acetate is added to reduce salt crystal formation, which will cause background problems if the slides are emulsion-coated.
21. Glassware used in emulsion dipping (e.g., measuring cylinders) should be washed in chromic acid before use to remove any emulsion remaining from the previous dipping session that may lead to increased background levels.
22. The emulsion has a short shelf life and should only be opened approximately five times before excessive background levels may become a problem. Mechanical stress will also increase background, so the melted emulsion and coated slides should be handled gently throughout the procedure.
23. As a control for the emulsion dipping procedure, it is useful to process a blank subbed slide through the dipping steps, along with the slides being assayed, and develop it the next day, when boxing the others. This "test" slide will reveal the evenness of the dipping technique and show if the slides have been exposed to any light/radiation source or excessive mechanical stress at any point during the procedure or dried too rapidly, all of which will increase background levels. Acceptable background, according to the manufacturers' instructions, is 10–25 grains/100X field. Histological staining (e.g., as **Subheading 3.1.6.3.**) will also highlight any streaking effects as a result of uneven emulsion coating.
24. It is important that the slides be washed for at least 30 min to remove excess chemicals before they are histologically stained. This can be done in tap water, but the final rinse should be in dH_2O.
25. Haematoxylin is a basic blue dye for nucleic acids, while eosin stains cytoplasm a pale pink/orange. Other examples of basic blue dyes are cresyl fast violet, toluidine blue, and thionin. In contrast, pyronin can also be used, this giving a pink stain. Preference will depend on which stain gives least interference to the computer-aided image analysis. It may be necessary to adjust the staining times set out here depending on the age of the stains and the condition of the tissue sections (eosin will be absorbed by the tissue very quickly if the sections are of good quality—so be careful!).
26. Glass cover slips can be removed from the sections at a later date by soaking the slides overnight in xylene to dissolve the DePX mounting medium. The slides should then be rehydrated through decreasing concentrations of ethanol, from 100% ethanol to dH_2O, and subsequently restained if necessary.
27. Other negative controls that may be employed to knock out specific hybridization include
    1. competition studies with 100-fold excess of unlabeled "cold" antisense probe co-applied with labeled antisense probe and
    2. using nonsense probes, such as scrambled oligonucleotides, which have the same base composition and, therefore, similar physical properties to the antisense probe, but no complementary sequences for possible hybridization.

    Other positive controls include

1. reconfirmation of the results when the experiments are repeated with another probe designed to a different region of the same mRNA (*see* **Notes 3** and **7** for design of probes) and
2. probing for a constitutive mRNA, e.g., β-actin, to verify the tissue RNA integrity.

28. Silver grain density is not linearly correlated with amount of RNA, therefore analysis can only really be considered semiquantitative at best. Furthermore, absence of detection may only reflect lack of sensitivity of the protocol and not absence of RNA expression. It may be necessary to use *in situ* PCR to detect very low expressing mRNA. Conversely, the presence of mRNA does not automatically demonstrate the presence of the translated peptide product.
29. RNA may be extracted from up to 1 g of starting tissue by proportionally scaling up the quantities in this protocol.
30. Protocols for poly(A)$^+$ RNA extraction are not covered in this chapter; however, it is possible to purchase kits to perform this procedure; for example, Promega PolyATtract mRNA Isolation Systems.
31. To measure the RNA integrity, run the samples on a denaturing gel, as described in **Subheading 3.2.2.3., steps 1–10**, except do not remove the marker lane. Instead, visualize all of the RNA by staining the whole gel with EtBr (**Subheading 3.2.2.3., step 10**). The total RNA should appear as a faint smear through the lane, with the most abundant RNA species (the 28S and 18S ribosomal RNA, which constitutes 80–85% total RNA) appearing as two strong and distinct bands, the 28S, being twice as abundant, should appear twice as strong as the 18S band (mRNA is estimated to make up 1–5% of total RNA). If the RNA has been degraded during isolation, it will run to the bottom of the gel with little or no indication of ribosomal banding.
32. If possible, it is better to dedicate a gel tray and wells purely to RNA work to minimize the risk of RNase contamination and therefore degradation of the RNA samples.
33. The membrane must exactly cover the gel to prevent gel dehydration and maximize solution flow through the gel, thus maximizing RNA transfer, and also so that the migration distance (and therefore the molecular weight of the detected bands) can be measured as accurately as possible.
34. The percentage transfer of RNA from gel to membrane can be checked by staining the gel with EtBr and visualizing any RNA remaining after blotting on a UV transilluminator. It is better to blot in the absence of EtBr and stain the gel afterward to check that transfer has been successful, as EtBr itself may affect RNA mobility.
35. Alternatively, the RNA can be efficiently cross-linked to the membrane with UV light exposure of up to 5 min. However, the exposure time in this method is critical and variable depending on the transilluminator used, so the optimal exposure time has to be calibrated accordingly.
36. High background will result if solutions are not equilibrated to the hybridization temperature, which is dependent on the properties of the probe used, as defined in the Tm equation (*see* **Subheading 1., step 4**).

37. The stringency of the next wash can be adapted appropriately, depending on the level of radioactivity measured on the hand-held counter. In this way, a more informed wash strategy can be applied in each experiment. A high level of radioactivity uniformly spread over the membrane is indicative that a high level of overall background still remains, requiring further washing steps. In contrast, the wash procedure should be terminated when membranes show only discrete patches of radioactivity, indicating only specific hybridization remains (or even no signal with the relatively insensitive hand-held counter).
38. The membrane can be stripped and reprobed after the film has been developed. To strip the blot, pour boiling 0.5% (w/v) SDS solution over the membrane and allow it to cool to room temperature. It is difficult to completely strip the probe from the membrane, but stripping should be sufficient to allow the membrane to be reprobed.

References

1. Gall, J. G. and Pardue, M. L. (1969) Formation and detection of RNA-DNA hybrid molecules in cytological preparations. *Proc. Natl. Acad Sci. USA* **63,** 378–383.
2. John, H. A., Birnstiel, M. L., and Jones, K. W. (1969) RNA-DNA hybrids at the cytological level. *Nature* **223,** 582–587.
3. Alwine J. C., Kemp, D. J., and Stark, G. R. (1977) Method for detection of specific RNAs in agarose gels by transfer to diazobenzyloxymethyl-paper and hybridization with DNA probes. *Proc. Natl. Acad. Sci. USA* **74,** 5350–5354.
4. Parker, R. M. C., Fleetwood-Walker, S. M., Rosie, R., Munro, F. E., and Mitchell, R. (1993) Inhibition by NK_2 but not NK_1 antagonists of carrageenan-induced preprodynorphin mRNA expression in rat dorsal horn lamina I neurons. *Neuropeptides* **25,** 213–222.
5. Rabadan-Diehl, C., Lolait, S. J., and Aguilera, G. (1995) Regulation of pituitary vasopressin V1b receptor mRNA during stress in the rat. *J. Neuroendocrinol.* **7,** 903–910.
6. Ciossek, T., Millauer, B., and Ullrich, A. (1995) Identification of alternatively spliced mRNAs encoding varients of MDK1, a novel receptor tyrosine kinase expressed in the murine nervous system. *Oncogene* **10,** 97–108.
7. Rigby, M., Le Bourdelles, B., Heavens, R. P., Kelly, S., Smith, D., Butler, A. et al. (1996) The messenger RNAs for the N-methyl-D-aspartate receptor subunits show region-specific expression of different subunit composition in the human brain. *Neuroscience* **73,** 429–447.
8. Gustafson, E. L., Durkin, M. M., Bard, J. A., Zgombick, J., and Branchek, T. A. (1996) A receptor autoradiographic and in situ hybridisation analysis of the distribution of the 5-HT7 receptor in rat brain. *Br. J. Pharmacol.* **117,** 657–666.
9. Taketazu, F., Kato, M., Gobl, A., Ichijo, H., ten Dijke, P., Itoh, J. et al. (1994) Enhanced expression of transforming growth factor-beta s and transforming growth factor-beta type II receptor in the synovial tissues of patients with rheumatoid arthritis. *Lab. Invest.* **70,** 620–630.

10. Harrington, K. A., Augood, S. J., Faull, R. l., McKenna, P. J., and Emson, P. C. (1995) Dopamine D1 receptor, D2 receptor, proenkephalin A and substance P gene expression in the caudate nucleus of control and schizophrenic tissue: a quantitative cellular in situ hybridisation study. *Brain Res. Mol. Br. Res.* **33,** 333–342.
11. Adcock, I. M., Peters, M., Gelder, C., Shirasaki, H., Brown, C. R., and Barnes, P. J. (1993) Increased tachykinin receptor gene expression in asthmatic lung and its modulation by steroids. *J. Mol. Endocrinol.* **11,** 1–7.
12. Kia, H. K., Miquel, M. C., McKernan, R. M., Laporte, A. M., Lombard, M. C., Bourgoin. S. et al. (1995) Localization of 5-HT_3 receptors in the rat spinal cord: immunohistochemistry and in situ hybridization. *Neuroreport.* **6,** 257–261.
13. Noguchi, K., Kawalski, K., Traub, R., Solodkin, A., Iadarola, M. J., and Ruda, M. A. (1991) Dynorphin expression and Fos-like immunoreactivity following inflamtion induced hyperalgesia are colocalised in spinal cord neurones. *Mol. Brain Res.* **10,** 227–233.
14. Morales, M. and Bloom, F. E. (1997) The 5-HT_3 receptor is present in different subpopulations of GABAergic neurons in the rat telencephalon. *J. Neurosci.* **17,** 3157–3167.
15. Sambrook, J., Fritsch, E. F., and Maniatis, T. (1989) *Molecular Cloning: A Laboratory Manual.* (2nd Ed.) Cold Spring Harbor Laboratory Press, Cold Spring Harbor, NY.
16. Hames, B. D. and Higgins, S. J. (eds.) (1987) *Nucleic Acid Hybridisation a Practical Approach.* IRL, Oxford University Press, Oxford, UK.
17. Rigby, P. W. T., Dieckmann, M., Rhodes, C., and Berg, P. (1977) Labelling deoxyribonucleic acid to high specific activity in vitro by nick translation with DNA polymerase I. *J. Mol. Biol.* **113,** 237–251.
18. Feinberg, A. P. and Vogelstein, B. (1983) A technique for radiolabelling DNA restriction endonuclease fragments to high specific activity. *Anal. Biochem.* **132,** 6–13.
19. Emson, P. C. (1993) In-situ hybridisation as a methodological tool for the neuroscientist. *TINS* **16,** 9–16.
20. Mitchell, B. S., Dhami, D., and Schumacher, U. (1992) Review article: in situ hybridisation: a review of methodologies and applications in the biomedical sciences. *Med. Lab. Sci.* **49,** 107–118.
21. Lewis, M. E., Sherman, T. G., and Watson, S. J. (1985) In situ hybridisation histochemistry with synthetic oligonucleotides: strategies and methods. *Peptides* **6(Suppl. 2),** 75–87.
22. Ratcliff, R. C. (1974) Terminal deoxynucleotydyl transferase, in *The Enzymes,* 3rd Ed. vol. XIV (Boyer, P.D., ed.), Academic, New York, pp. 105–118.
23. Angerer, L. M. and Angerer, R. C. (1992) In situ hybridisation to cellular RNA with radiolabelled RNA probes, in *In Situ Hybridization A Practical Approach* (Wilkinson, D. G., ed.) IRL, Oxford University Press, Oxford, U.K., pp. 15–32.
24. Höltke, H. J., Ankenbauer, W., Mühlegger, K., Rein, R., Sagner, G., Seibl, R. et al. (1995) The digoxigenin (DIG) system for non-radioactive labelling and detection of nucleic acids—an overview. *Cell. Mol. Biol.* **41,** 883–905.

25. Valentino, K. L., Eberwine, J. H., Barchas, J. D. (eds.) (1987) *In Situ Hybridisation: Applications to Neurobiology.* Oxford University Press, New York, pp. 57–58.
26. Wilkinson D. G. (ed.) (1993) *In Situ Hybridisation: A Practical Approach.* IRL, Oxford University Press, New York.
27. Civelli, O., Douglass, J., Goldstein, A., and Herbert, E. (1985) Sequence and expression of the rat prodynorphin gene. *Proc. Natl. Acad. Sci. USA* **82,** 4291–4295.
28. Belelli, D., Balcarek, J. M., Hope, A. G., Peters, J. A., Lambert, J. J., and Blackburn, T. P. (1995) Cloning and functional expression of a human 5-hydroxytryptamine type 3As receptor subunit. *Mol. Pharmacol.* **48,** 1054–1062.
29. Parker, R. M. C., Barnes, J. M., Ge, J., Barber, P. C., and Barnes, N. M. (1996) Autoradiographic distribution of [^{3}H]-(s)-zacopride-labelled 5-HT$_3$ receptors in human brain. *J. Neurol. Sci.* **144,** 119–127.
30. Chomczynski, P. and Sacchi, N. (1987) Single-step method of RNA isolation by acid guanidinium thiocyanate-phenol-chloroform extraction. Anal. Biochem. **162,** 156–159.

Index

Receptor Binding Techniques

Edited by

Mary Keen

The Medical School, University of Birmingham, Birmingham, UK

In *Receptor Binding Techniques*, detailed experimental protocols devised by expert practitioners demonstrate the power of radioligand binding for studying a wide variety of receptors. The methods can be applied to G protein–coupled receptors, receptors with integral ion channels, and sites other than receptors, such as guanine nucleotide binding proteins, enzymes, transporters, and mRNA. The individual protocols encompass many different preparations, ranging from solubilized receptors, through membrane preparations, intact cells, and autoradiography in tissue slices, to PET and SPECT analysis of binding in living human brain. Along with the detailed, easily reproducible instructions, the protocols also take into account the problems inherent in the basic binding technique, such as common experimental artifacts and the definition of receptor sites, as well as problems associated with the use of particular ligands and receptor preparations.

Receptor Binding Techniques shows clearly how these techniques can be adapted to many different applications and fully utilized in drug discovery programs. It will be of high value not only to researchers new to the field of receptor binding, but also to more experienced workers, serving as an authoritative bench manual replete with optimalized practical methods and protocols.

FEATURES

- **Covers a wide variety of systems for a broad range of receptor proteins**
- **Includes the use of binding techniques to study nonreceptor sites**
- **Explains in detail how to avoid the pitfalls inherent in the basic binding technique**
- **Reviews the problems associated with each ligand and receptor preparations**

CONTENTS

Methods in Molecular Biology™ • 106
RECEPTOR BINDING TECHNIQUES
ISBN: 0-89603-530-1